

## Countercurrent Heat Exchange Building Envelope Using Ceramic Components

Vollen, J.O.

**DOI**

[10.7480/abe.2020.05](https://doi.org/10.7480/abe.2020.05)

**Publication date**

2020

**Document Version**

Final published version

**Citation (APA)**

Vollen, J. O. (2020). *Countercurrent Heat Exchange Building Envelope Using Ceramic Components*. [Dissertation (TU Delft), Delft University of Technology]. A+BE | Architecture and the Built Environment. <https://doi.org/10.7480/abe.2020.05>

**Important note**

To cite this publication, please use the final published version (if applicable). Please check the document version above.

**Copyright**

Other than for strictly personal use, it is not permitted to download, forward or distribute the text or part of it, without the consent of the author(s) and/or copyright holder(s), unless the work is under an open content license such as Creative Commons.

**Takedown policy**

Please contact us and provide details if you believe this document breaches copyrights. We will remove access to the work immediately and investigate your claim.





# Countercurrent Heat Exchange Building Envelope Using Ceramic Components

---

Jason Oliver Vollen







# Countercurrent Heat Exchange Building Envelope Using Ceramic Components

---

Jason Oliver Vollen





**A+BE | Architecture and the Built Environment** | TU Delft BK

---

**20#05**

**Design** | Sirene Ontwerpers, Rotterdam

ISBN 978-94-6366-268-0

ISSN 2212-3202

© 2020 Jason Oliver Vollen

Digital version freely available at [abe.tudelft.nl](http://abe.tudelft.nl)

All rights reserved. No part of the material protected by this copyright notice may be reproduced or utilized in any form or by any means, electronic or mechanical, including photocopying, recording or by any information storage and retrieval system, without written permission from the author.

Unless otherwise specified, all the photographs in this thesis were taken by the author. For the use of illustrations effort has been made to ask permission for the legal owners as far as possible. We apologize for those cases in which we did not succeed. These legal owners are kindly requested to contact the publisher.



# Countercurrent Heat Exchange Building Envelope Using Ceramic Components

---

Dissertation

for the purpose of obtaining the degree of doctor  
at Delft University of Technology  
by the authority of the Rector Magnificus, prof.dr.ir. T.H.J.J. van der Hagen  
chair of the Board for Doctorates  
to be defended publicly on  
Monday, 6 April 2020 at 15:00 o'clock

by

Jason Oliver VOLLEN  
Master of Architecture, Cranbrook Academy of Art, United States of America  
born in Brooklyn, United States of America



This dissertation has been approved by the promotor.

### Composition of the doctoral committee:

---

Rector Magnificus,  
Prof.Dr.-Ing. U. Knaack  
Prof.Dr.-Ing. T. Klein

chairperson  
Delft University of Technology, promotor  
Delft University of Technology, promotor

### Independent members:

---

Dr. S.N.G. Lo  
Prof.Dr.-Ing. A.A.J.F. van den Dobbelsteen  
Prof.Dr. A. Beim  
  
Prof.Dr. U. Pottgiesser  
Prof.Dr. M. Perino

University of Bath  
Delft University of Technology  
Royal Danish Academy of Fine Arts  
School of Architecture  
Delft University of Technology  
Politecnico di Torino

---

This research was funded by the NEXUS-NY and the New York State Pollution Prevention Institute with in-kind support from Boston Valley Terra Cotta.

# Acknowledgements

---

This research would not have been possible without the significant contributions, influence, advisement, and support from many people and organizations.

Ulrich Knaack for your wisdom and encouragement and the opportunity. At our first meeting you asked if I had the fire in the belly to complete the journey - I did, as it turns out, and it was kept alight because you continued to stoke the flames year after year. Tillmann Klein for your influence, kindness and support. Your approach inspires me to be more thoughtful every day. You both have created the most incredible program within which to thrive and add knowledge to the world, better advisors one cannot have. A special note of acknowledgment, Stephen Lo, for your incredible in-depth review of the dissertation on every level, thank you for keeping the bar high. The Facade Research Group, who welcomed this American into the fray and whose feedback over the years was also ways insightful and influential.

Matt Gindlesparger, a better collaborator one cannot have, I am forever grateful and could not have done this dissertation without you. These journeys we take are never easy but they are always better because of your friendship.

Anna Dyson for your support at CASE and throughout the years, as a mentor, friend and researcher. Justin Shultz for your research support, collaboration and expert programming. Kelly Winn for all the years of collaborating and pushing forward the research. Shay Harrison for the years of developing EcoCeramics. Berardo Matalucci for your consults and attention to this area of inquiry. Xiaofei Shen for your support and unparalleled keen eye for data visualization.

John Krouse and Mitchell Bring and the Boston Valley Terra Cotta family, and Rigidized Metals, and United Architectural Metals for your support at the ACAW conferences and in fabricating the prototypes.

Álvaro Malo, for seeing in myself that which I did not, and teaching me how to lean in. Dale Clifford for starting the journey with me - long live Binary Design. Alfred, Sandra, Brad, Anders and Rob, my way of thinking and approach to the discipline has been formulated by our conversations over decades.



Max and Ginger Lily you have grown up alongside this work, and without your encouragement and most importantly your patience, it would never have been completed. If ever there were two delightful children who deserved a dissertation puppy, it's you. Karen, there are no words to express the gratitude I have for the sacrifice you have made all these years. Without your love and enduring support, this endeavor would have been impossible, but then again, you make the impossible possible every day for me.

# Contents

---

Acknowledgements	5
List of Tables	13
List of Figures	14
Summary	23
Samenvatting	25

---

## 1 Introduction 27

1.1	<b>Energy, Terra Cotta, and an Evolution of a Building Envelope</b>	27
1.1.1	Buildings, Energy Use and the Global Context	28
1.1.2	The Case for Expanding the Terra Cotta Building Envelope Products	29
1.1.3	Thermo Active Building System as a Building Envelope	30
1.2	<b>Project Overview</b>	35
1.2.1	Limitation of Thesis within the Larger Field of Inquiry	35
1.2.1.1	Concurrent Research Limitations	35
1.2.1.2	Climate Limitations	36
1.2.1.3	Building Typology Limitations	36
1.2.2	Hypothesis, Objectives, and Research Questions	37
1.2.3	Overview of Research Methodology	40
1.2.4	Research Platform	41
1.2.5	Societal and Scientific Relevance	42
1.3	<b>Dissertation Structure</b>	43
1.4	<b>Definitions and Abbreviations</b>	45

---

## 2 Critical Context 49

2.1	<b>Why is a New Approach Needed?</b>	49
2.1.1	Critical Context: Building Repositioning and Deep Energy Retrofits	50
2.1.2	Aging Building Stock of Commercial Buildings	51
2.1.2.1	Failing Building Envelopes and Outdated HVAC System	52

2.1.3	Increasing Building Energy Use Intensity Regulations	53
2.1.3.1	Architecture 2030 and the Roadmap to 80 x 50	54
2.1.3.2	ASHRAE, Greater Greener Buildings Plan	54
2.1.4	Energy Retrofits	55
2.1.4.1	Energy Conservation Measures	55
2.1.5	High Performance Office Buildings	56
2.2	<b>Critical Approach: Building Envelope as Energy Transfer Function</b>	57
2.3	<b>Effect of the Building Envelope on the Building Energy Profile</b>	57
2.3.1	Principles of Energy Transfer at the Building Envelope	58
2.3.1.1	Energy Resources and Demands	58
2.3.1.2	Latent and Sensible Heat	60
2.3.1.3	Conduction, Convection and Radiation	62
2.3.1.4	Dynamic Thermal Effects	63
2.3.1.5	Flow Rates, Surface Areas and Material Effects	64
2.3.1.6	Countercurrent Energy Exchange	64
2.4	<b>Summary</b>	65

---

### 3 Precedents 67

3.1	<b>Introduction</b>	67
3.2	<b>Literature Summary</b>	68
3.3	<b>Precedents</b>	71
3.3.1	Thermo Active Radiant Panels	77
3.3.2	Thermal Active Mullions	77
3.3.3	Active Insulation	79
3.3.4	Thermal Storage	83
3.4	<b>Summary: Literature and Precedents</b>	84

---

### 4 Module Design and Development 87

4.1	<b>Introduction</b>	87
-----	---------------------	----



4.2	<b>Thermal Adaptive Ceramic Envelope</b>	88
4.2.1	Concept Design of the TACE	89
4.2.1.1	Component Design of the TACE	93
4.2.1.1.1	Orientation and Morphology	97
4.2.1.1.2	Color: Reflection, Refraction, Absorption	97
4.2.1.1.3	Texture: Surface Area Ratios, Turbulence and Laminar Flows	98
4.2.1.1.4	Material: Thermal Mass and Conductivity	100
4.2.1.1.5	Thermal Exchange: Active Energy Vectoring	100
4.2.2	Design of the TACE MVP Prototype I	101
4.2.2.1	TACE Module Design	104
4.2.2.2	TACE System Design	106
4.2.3	Energy Transfer	109
4.2.3.1	Heat Exchangers	110
4.2.3.2	Energy Storage	110
4.2.3.3	Materials for TACE	112
4.3	<b>Prototype Design Iterations</b>	113
4.3.1	MVP Prototype I	114
4.3.2	POC Prototype II	116
4.3.3	ASI Prototype III	116
4.4	<b>Summary: Development of the TACE system</b>	118

---

## 5 Component Performance 119

5.1	<b>Introduction</b>	119
5.2	<b>Research Collaborations</b>	120
5.2.1	Research Methods	121
5.2.1.1	Modelling and Simulation	121
5.2.1.2	Design	121
5.2.1.3	Modelica	121
5.2.1.4	Dymola Interface	122
5.2.2	Model Calibration	122
5.2.2.1	CFD Model Experimental Validation	123
5.2.2.2	Results: CFD Model Experimental Validation	125
5.2.2.3	Physical Model Calibration	125
5.2.2.4	Results: Physical Model Experimental Validation	129

5.3	<b>Performance of Component Attributes</b>	133
5.3.1	Simulations	133
5.3.2	TACE Module Key Attributes	135
5.3.2.1	Mass	135
5.3.2.2	Assembly Techniques	139
5.3.2.3	Flowrates	141
5.3.2.4	Insulation	143
5.3.3	Results	145
5.3.3.1	Design Attributes and Energy Use Intensity Reduction	146
5.3.3.2	Impact of Mass on Energy Transfer	146
5.3.3.3	Impact of Geometry of Thermal Transfer Components on Energy Transfer	148
5.3.3.4	Impact of Assembling Components on Energy Transfer	151
5.3.3.5	Impact of Flowrate on Energy Transfer	151
5.3.3.6	Impact of Insulating Layer on Energy Transfer	153
5.4	<b>Summary: Energy Transfer Impacts of Design Attributes</b>	156

---

## 6 Performance and HVAC System Integration 159

6.1	<b>Introduction</b>	159
6.1.1	Case Study: Wesley J. Howe Center at Stevens Institute of Technology	160
6.2	<b>Research Collaborations</b>	162
6.3	<b>Research Methods</b>	162
6.3.1	Modelling and Simulation	163
6.3.1.1	Model and Simulation Design	164
6.3.1.1.1	Bay Model Design	166
6.3.1.1.2	Floor Model Design	167
6.3.1.2	Modelica and EnergyPlus Co-Simulation	169
6.4	<b>Model and Simulation of Envelope Types with Deep Energy Retrofit Scenarios</b>	170
6.4.1	Simulations	176
6.4.1.1	TACE 12 Module Array Simulations	176
6.4.1.2	Bay Zone Simulations	177
6.4.1.3	Floor Zone Simulations	180
6.4.1.3.1	Original Building Envelope with HVAC Scenario	184
6.4.1.3.2	Improved Building Envelope with HVAC Scenario	185
6.4.1.3.3	TACE with HVAC Scenario	186

6.4.2	Results using MVP Prototype I	187
6.4.2.1	Results of TACE 12 Module Array Simulations	187
6.4.2.1.1	Results of Inlet Temperature	188
6.4.2.1.2	Results of Heat and Coolth Harvesting by Flowrates	195
6.4.2.2	Analysis of HVAC Scenarios at Multiple Scales	198
6.4.2.3	Energy Use Intensity Reduction Potential MVP Prototype I: Bay Scale	198
6.4.2.4	Energy Use Intensity Reduction Potential MVP Prototype I: Floor Zone Scale	200
6.4.3	Results using ASI Prototype III	202
6.4.3.1	Results of TACE 12 Module Array Simulations Comparison	203
6.5	<b>Summary: Architectural Integration Impacts of HVAC Retrofit Scenarios with TACE</b>	207

## 7 Design Iterations 211

---

7.1	<b>Introduction</b>	212
7.2	<b>Methodology</b>	212
7.3	<b>Critical System Design Drivers</b>	213
7.3.1	TACE System Service Area	215
7.3.1.1	Minimum TACE Service Area	216
7.3.1.2	Exterior Surface Area	217
7.3.1.3	Window Wall Ratios	219
7.3.2	Fabrication Techniques	221
7.3.2.1	Current Fabrication Techniques	223
7.3.2.1.1	Pressing	224
7.3.2.1.2	Casting	225
7.3.2.1.3	Extruding	227
7.3.2.2	Future Fabrication Techniques	229
7.3.2.2.1	Computer Numerically Controlled Ceramic Additive Manufacturing	229
7.4	<b>TACE Module Options</b>	231
7.4.1	TACE Morphology Based on Cardinal and Ordinal Polar Coordinates	232
7.4.1.1	South Component Morphology	232
7.4.1.2	East and West Component Morphology	233
7.4.1.3	Southeast and Southwest Component Morphology	234
7.4.2	Design to Minimize System Loss	235
7.4.2.1	Surface to Working Fluid Ratio	236
7.4.3	Module Size Limitations	237



7.5	<b>TACE Assembly and Installation Options</b>	238
7.5.1	Rainscreen Assembly	239
7.5.2	Stick Build Rainscreen Curtain Wall	240
7.5.3	Unitized Curtain Wall	241
7.5.4	Assembly Limitations	241
7.6	<b>Results</b>	242
7.6.1	Deployment Potential	242
7.6.2	Deployment Limitations	245
7.7	<b>Summary: Design Limitations</b>	246
8	<b>Conclusions and Future Directions</b>	249

---

8.1	<b>Introduction</b>	249
8.1.1	Answers to the Research Questions	250
8.1.1.1	Review of the Hypothesis and Research Objectives	250
8.1.1.2	Review of the Research Questions	253
8.1.2	Review of the TACE Prototypes	263
8.1.2.1	MVP TACE Prototype I	263
8.1.2.2	POC TACE Prototype II	264
8.1.2.3	ASI TACE Prototype III	265
8.1.2.4	UCW TACE Prototype IV Design Proposal	266
8.1.2.5	Design Recommendations	267
8.1.2.5.1	Component and Module Design Recommendations	268
8.1.2.5.2	System Design Recommendations	272
8.1.2.5.3	Assembly Type Recommendations	275
8.1.2.5.4	Design Language Position	275
8.1.3	Valuation of the research proposition	275
8.1.3.1	Greenhouse Gas Emissions Reduction Potential	276
8.1.3.2	Comparison to Photovoltaic Systems	277
8.1.4	Propositions for Future Work	280
8.1.4.1	Testing Recommendations for TACE	280
8.1.4.2	Heat Balance and Advection	281
8.1.5	Potential Impact on the Discipline	281
8.2	<b>Reflections on the Research</b>	285
8.3	<b>Final Remarks</b>	285
	<b>Curriculum Vitae</b>	287

# List of Tables

---

- 1.1 Corresponding table of assembly types, drawbacks, and solutions to Fig. 1.4. [34](#)
- 1.2 Corresponding Objectives, Sub-research Questions, Methods and Dissertation Chapters, see Section 1.6 for the illustration and description of the dissertation structure. [38](#)
- 2.1 Table of the critical timeline showing an increased value of energy efficiency developed at the federal level. [53](#)
- 5.1 Results of the thermal transfer simulation before and after calibration. [125](#)
- 5.2 Comparison of Temperature Gradient at Various Flowrates, Offset Setup (Left) vs No Offset Setup (Right) [131](#)
- 5.3 Results are showing the impact of pin length and flowrate on temperature difference due to pin length and flowrates with and without glue layer, demonstrated graphically in Figure 5.24. [149](#)
- 5.4 Results showing impact of pin length and flowrate on heat flow due to pin length and flowrates with and without glue layer, demonstrated graphically in Figure 5.25. [150](#)
- 5.5 Results showing the negligible impact of the location of insulation within the TACE module assembly. [154](#)
- 6.1 Modelled building envelope U-value, Modelled building fenestration U-value, SHGC, and Visible Transmittance. [169](#)
- 6.2 Summary results showing the impact of system inlet temperatures on annual energy potential and maximum temperature flux for MVP Prototype I. [188](#)
- 6.3 MVP Prototype I EUI comparative simulation case results for a typical south facing bay installation in three cases: Simulation 1 Existing Envelope, Simulation 2 ASHRAE Curtain Wall, and Simulation 3 TACE System. [199](#)
- 6.4 MVP Prototype I EUI comparative simulation case results with TACE System contributing heating only for typical Floor Zone. [201](#)
- 8.1 Results comparing the performance of MVP Prototype I and ASI Prototype III. [251](#)
- 8.2 Annual CO<sub>2</sub> emissions based on US average electricity fuel mix. [277](#)
- 8.3 Annual CO<sub>2</sub> emissions based on New York State electricity fuel mix. [277](#)
- 8.4 Comparison using PV powering GSHP (COP 3 heating, 4.5 cooling) or WSHP (COP 2.5 heating, 3.5 cooling) and TACE ASI Prototype III at 2.5 l/min (0.66 gpm) and 22 °C inlet ground temperature. [279](#)

# List of Figures

---

- 1.1 Mike Davies' vision for the Polyvalent wall where each distinctive layer has a specific use . Redrawn (Davies, 1981). 31
- 1.2 The multivalent wall as envisioned by Ulrich Knaack where the layers have both specific uses and recombinant interactions. Redrawn (Knaack, 2007). 32
- 1.3 Installation of the Thermo Active Building System in the form of a radiant slab in the Balanced Office Building (BOB) engineered by VIKA Ingenieur GmbH in Aachen. (VIKA Ingenieur, 2005) 33
- 1.4 Taxonomy of wall assemblies showing the flows of energy across the building envelope and categorizing the drawbacks and potential solutions of the various broad categories of envelope types: Mono-Assembly (M), Layered-Assembly (L), Combined-Assembly (C). The area of focus of the dissertation is in the Layered-Assembly, Integrated, Adaptive Typology (A). 34
- 1.5 Overall structure of the dissertation. 44
- 2.1 Deep Energy Retrofit Strategy showing replacement of critical systems and façade. 51
- 2.2 Solar resource and demand profile of a typical office building annually and usage per hour. 59
- 2.3 New York City temperature, solar, wind, humidity availability and quantity of local climate derived loads and resources and volatility index of these available resources. 60
- 2.4 Thermal shifting of latent versus sensible heat. Capturing heat energy and storing it as latent energy for use later when the demands of the building require sensible heat is a key strategy to matching resources and demands in and around the building envelope. 61
- 2.5 Diagram of the forces of demands and the demarcation line separating the interior from the exterior of the building envelope that also illustrates the variables in the basic heat transfer equation. Developed from Klein (2013). 63
- 2.6 Diagram of counter vs concurrent flows. Countercurrent flows can exchange 50% more than concurrent flows 64
- 3.1 hypocaust (Hypocaust, 2019) image (1) and diagram (2) showing the flow of heat from the point source to radiant surfaces. 71
- 3.2 Radiant panel patent diagrams (1,2) from A.H. Baker. 72
- 3.3 Frank Lloyd Wright drawings and photographs of radiant systems in both residential in the Pope-Leighey House (1) (Komp, 2017) and commercial projects as shown as part of the heating and cooling systems for the Johnson Wax building (2,3,4) (Siry, 2013). 73
- 3.4 Modern Pex-Al-Pex piping used in almost all TABS radiant floor installations and products. Pex has less than 10% of the conductivity of comparable metal pipe, which, on the one hand, limits the thermal transfer rate, and on the other protects against sweating and as a flexible material protects against freezing as well. 74



- 3.5 Arrangements of the various TABS radiant flooring systems. Type A: with pipes embedded in the screed or concrete (“wet” system). Type B: with pipes embedded outside the screed (in the thermal insulation layer, “dry” system). Type C: with pipes embedded in the levelling layer, above which the second screed layer is placed. Type D: include plane section systems (extruded plastic/group of capillary grids). Type E: with pipes embedded in a massive concrete layer. Type F: with capillary pipes embedded in a layer at the inner ceiling or as a separate layer in gypsum. Type G: with pipes embedded in a wooden floor construction. Adapted from ISO 11855. 75
- 3.6 Flow conditions and thermal exchange for TABS radiant floor configuration. 76
- 3.7 Prevalence and relative performance of buildings that use radiant systems as a subset of high performing buildings. Redrawn (Higgins, 2017). 76
- 3.8 Radiant panels (2) as part of the net zero strategy in the EDGE office building (1). (SIG, 2016) 77
- 3.9 Diagram (2) of heating flow overlay on the north facade of the EMPAC building (1) (Fortmeyer & Linn, 2014), redrawn from Charles Linn. 78
- 3.10 TABS as an envelope configuration in the Zollverein School: (1) exterior mass envelope, (2) embedded thermo active building system (Mayer, 2012), (3) diagram of geothermal exchange, redrawn (Transsolar, 2006). 79
- 3.11 Diagrams showing a single fluid channel of air based BIST envelope assemblies. Air based BIST assemblies include the traditional Trombe wall configurations. Single Air Channel: 1) Glass Pane, air-filled glass tube, insulation, façade, 2) Glazing, absorber, insulation, façade, 3) Glazing, PV panel, insulation, façade, 4) Double glazing, air cavity, Venetian blind, internal glazing, 5) PV panel, air cavity, insulation, façade, 6) PV panel, air cavity, double glazing, 7) Transpired plate, air cavity, insulation, façade, 8) External sheet, air cavity, insulation, façade. Double Air Channel: 9) Glazing, outer air duct, PV panel, glazing, inner air duct, insulation, 10) Double glazing, 1st air cavity, Venetian blind, 2nd air cavity, internal glazing, 11) Glazing, colled PV Panel, insulation, façade, 12) Transpired Plate, plenum 1, high-porosity Sandtile. Redrawn (Zhang, 2015). 80
- 3.12 Diagrams showing various typologies of air and liquid based BIST envelope assemblies specifically as solar thermal collector designs. Solar Thermal Dsign: 1) Massive wall, water tube, massive wall, 2) Plaster, water tubes, insulation, façade, 3) bsorber, water tubes, insulation, façade. Photovoltaic Thermal Design: 4) Glass cover, air cavity, absorber, water tube, insulation, façade, 5) Bi-metallic water tube (Fe-Cu), copper plate, wooden plank, air cavity, insulation, façade, 6) Absorber, water tube, insulation, façade, 7) Glass cover, PV panel, absorber, water tube, insulation, façade, 8) Glass cover, PV panel, absorber, water tube, air cavity, insulation, façade. (Zhang, 2015). 81
- 3.13 Diagrams showing various typologies of combined PV and solar thermal based BIST envelope assemblies. Photovoltaic/Thermal Combination Design: 1) Absorber slat, PV panel, water tubing, double glazing, 2) PV panel, water tube, air cavity, absorber, insulation, façade, 3) PV panel, air cavity, water tube, insulation, façade, 4) PV panel, 1st air cavity, water tube, 2nd air cavity, insulation, façade. Redrawn (Zhang, 2015) 81

- 3.14 Dynamically breathing building envelope examples of the VDSI in CALA Hazledean (1,2,4) in comparison to traditional insulation (3). Photo and redrawn (Brown et al., 2004) 82
- 3.15 Example of liquid BIST system with seasonal storage (1, 2) in the ETA-Fabrik Factory Prototype and close up of exchange wall (2). Redrawn and photo (Maier et al., 2016). 83
- 4.1 Basic concept of countercurrent energy exchange leveraged in the TACE system. 89
- 4.2 The attributes that are part of the conceptual assembly of the TACE system are shown as separate and additive to illustrate the multifaceted approach to the prototype development. 90
- 4.3 Early TACE module studies showing from left to right: (1) surface texture for energy exchange; (2) orientation morphology; and (3) interior thermal transfer attribute component illustrating the increased surface area as intended to be in contact with the working fluid. 91
- 4.4 Early TACE module master positive fabricated using powder based rapid prototyping showing the advancement of the module design with articulated thermal transfer attribute components and a distinct front and back component. 92
- 4.5 Early TACE module full-scale mock-up and diagram illustrating purpose-based attribute components 93
- 4.6 The flows of energy across the building envelope connect the climate and human comfort from a series of critical variables, expressed above. Variables in red directly impact surface area. 94
- 4.7 Conceptual articulation of key attributes. 95
- 4.8 The diagram shows how the locally available resource – on both right and left side, can be intercepted by the envelope system to be made useful later. Modifying the variables that alter energy transfer, as shown in red in the principle expressions, modifies the flow of energy and support the capture transfer, store and redistribute strategy that underpins the TACE as a system. 95
- 4.9 The modified variables can be developed into a specific geometric and material response, in this case, the result is the TACE Module from MVP Prototype I, a combination of discrete components that have attributes that are leveraging the variable of the principle expressions.. 96
- 4.10 Further development of the conception of key element progression. 96
- 4.11 Comparison of colour according to the wavelength of available sunlight (top) to projected performance load (bottom) showing: white, IrO<sub>2</sub>, typical brick, green, blue, and black for a ceramic flat panel envelope. 98
- 4.12 Impact of surface morphology showing exposure and shading percentages over the calendar year that may be used as both a morphology and colour patterning guide. This analysis conducted shows an exposure reduction due to self-shading, significantly more in the summer than in the winter (Vollen & Winn, 2013). While this optimization of the self-shading is not directly explored in this dissertation, it is a crucial attribute to integrate as part of future work. 99
- 4.13 Diagram showing an early version of the TACE system proposal where multiple forms of energy transfer are delineated. While the development of the TACE System in this research focuses on thermal energy storage and reuse, Stirling Engine and Thermoelectric energy transfer were explored as standalone prototypes in 2011 and 2012 as part of initial proof on concept physical models. Redrawn (Vollen & CASE, 2011) 101

- 4.14 Examples of forged aluminium thermal transfer components. The geometry of the cast aluminium oxide thermal transfer component of the MVP Prototype I has a similar geometry (Forged Heat Sink, 2019). [103](#)
- 4.15 Ashby material properties chart of thermal expansion and thermal activity showing an overlap of properties between metals and technical ceramics. The alumina formulation used for MVP Prototype I and the subsequent simulations used 97% industrial grade alumina (Al<sub>2</sub>O<sub>3</sub>), with minor constituents like SiO<sub>2</sub> and MgO from added materials. Recycled glass was added to increase silica content (SiO<sub>2</sub>) up to 10%. Redrawn (Granta, 2020). [103](#)
- 4.16 Early proposed TACE solar absorption tile basic geometry (left), and TACE solar absorption tile with cutaway (right) showing: 1. Moulded tile geometry for optimal winter solar collection, 2. Textured solar collection surface for improved solar heat gain. 3. Overlapping geometry for rainscreen water shedding. 4. Ceramic fins on interior tile surface for improved heat transfer to phase change cavity. 5. Working fluid cavity. 6. Lapping tile geometry for clipping to modular track cladding system. 7. Heat transfer loop for conduction to thermal storage bank. 8. Thermal storage bank. 9. Thermal transfer switching connection to thermal storage bank for seasonal performance control. [105](#)
- 4.17 Evolution of the full-scale development of the TACE module that was used for testing in Chapter 5. [106](#)
- 4.18 Early proposed TACE system assembly includes the following components follows: 1. A moulded ceramic rainscreen tile tuned for a specific time range of solar exposures. 2. Lapping tile geometries for rain shedding. 3. A solar collection surface to generate heat energy for building systems. 4. An integrated heat transfer loop system to collect and redistribute heat energy, 5. A thermal storage sink to hold collected thermal energy for transfer. 6. Integrated plumbing system to move heat transfer fluid quickly around the architectural envelope. 7. Typical aluminium track façade system for the easy installation, maintenance, and replacement of modular components. 8. Typical insulation and vapour barrier layers to limit heat transfer between interior and exterior as a semi-active integrated system. 9. The aluminium track allows for easy integration with typical architectural structures. 10. Similar track system for supporting interior tile system. 11. Modular supporting interior tile system. 12. Interior tile radiation geometry tuned for thermal performance, lighting, ergonomics, and other interior design criteria. 13. Heat exchanger for building systems, domestic hot water, heating, heat exchange cooling, etc. 14. Chill beam or other radiation, or convection or other suitable environmental conditioning systems. 15. Typical ceiling geometry to conceal systems. 16. Typical building floor structure. [108](#)
- 4.19 Delineation of the MVP Prototype I that was used for fabrication and testing. [109](#)
- 4.20 Typical flat plate heat exchangers showing counter current flow energy exchange. [110](#)
- 4.21 Solar resource (as one type of energetic resource) availability by climate type and ceiling relative to heating and cooling degree days (Vollen & CASE, 2010). [111](#)
- 4.22 SunAmp heat battery is an example of a small form factor high capacity thermal storage device that can be used in conjunction with the TACE system. (Sunamp, 2016) [112](#)

- 4.23 Delineation of four evolutions of the prototype design: 1) upper right is the MVP TACE Prototype, 2) lower right is the as simulated MVP TACE Prototype, 3) lower left is the POC TACE Prototype, 4) upper left is the ASI TACE Prototype. 114
- 4.24 Photographs of MVP Prototype. 1) CNC router cutting face tile positive. 2) CNC positive of rear tile. 3) Assembled CNC positive. 4) CNC positive with mould piece. 5) CNC positive and mould piece detail. 6) CNC Positive rear tile and mould. 7) Alumina slip-cast TACE face tile. 8) Multiple TACE modules tiles with varying pin lengths. 9) TACE module testing stock. 115
- 4.25 Photographs of POC Prototype II with workshop participants (1), exterior tile detail (2) and interior tile and working TACE System POC (3). 116
- 4.26 Photographs of ASI Prototype III from the 3<sup>rd</sup> Annual ACAW conference showing exterior module and tubing matrix (1) and interior radiator/absorber (2). 117
- 4.27 Reconfigured ASI Prototype III rainscreen developed for the ACAW III into a Curtain Wall frame. 117
- 5.1 Diagram of the testing process showing the integration of physical results with simulations.. 123
- 5.2 Acusolve CFD Model of Temperature and Velocity Difference Between Comparing the .33 and .66 gpm flowrates. 124
- 5.3 Hotbox rig showing centre module mounting are and interior and exterior environmental chambers. 126
- 5.4 Schematic of TACE module testing chamber. 128
- 5.5 Module showing the different locations, (1) parallel, and (2) offset, of the inlet and outlet ports. 130
- 5.6 Results visualization illustrating heat temperature distribution for parallel (Left) and offset (Right). 131
- 5.7 Comparison of fluid temperatures (1) and tile face temperatures (2) showing measured and modelled results. 132
- 5.8 Diagram of Modelica model components. 134
- 5.9 Variables isolated to develop the scientific comparison. 134
- 5.10 Key attributes used to manipulate the energy flows within the Modelica model: model nodes above attributes are external to the TACE module; model nodes below the attributes are internal to the TACE module. 135
- 5.11 Diagram of pin connection showing variable mass. The simulation was run with several different masses for the pin plate to determine how much impact increased mass would have on the overall performance. 136
- 5.12 The thickness of the plate, and thus the mass, was adjusted by the circled attribute. 137
- 5.13 Geometries of plate types initially identified for CFD simulation. 138
- 5.14 Diagram of pin plates used for quantitative testing and simulations. 138
- 5.15 1.75 inch hexagonal pins, staggered arrangement (Left) and parallel arrangement (Right) 139
- 5.16 Diagram of conductive epoxy layer modelled. The simulation was run with and without the glued connection. 140
- 5.17 The simulation used the following parameters for the conductive epoxy: conductivity of 0.2 W/m<sup>2</sup>/K; surface area of 0.0249 m<sup>2</sup>, based on the area of the exterior top panel that comes into contact with the thermal energy component; thickness of 0.001m, assuming a 1mm thick layer of conductive epoxy. 141
- 5.18 Diagram showing pin length location. The simulations were run for multiple cases. 142
- 5.19 Diagram of systems model showing flowrate and pin length components. 143



- 5.20 Diagram of the location of the insulating layer. 144
- 5.21 Diagram showing the location of the insulation component. 145
- 5.22 Results graph showing the negligible impact of changing the mass of the collecting surface. 147
- 5.23 Results graph showing the negligible impact of changing the mass of the collecting surface. 148
- 5.24 Results graph illustrating the temperature difference due to pin length and flowrates with and without glue layer. 149
- 5.25 Results graph illustrating the heat flow due to pin length and flowrates with and without glue layer. 150
- 5.26 Diagram series and parallel arrangement. Results indicate that series may support the increased performance of the system as a whole. 153
- 5.27 Results showing the negligible impact of the insulation layer on the interior side of the MVP I module. 155
- 5.28 Results showing the negligible impact of the insulation layer on the interior side of the MVP I module. 156
- 6.1 The Wesley Howe Center at Stevens Institute of Technology is an example of first generation curtain walls buildings that need significant building systems upgrades. 161
- 6.2 Diagram of scalar relationships studied in this chapter. The components, or module, modelling in Chapter 5 was developed into a model for a typical Bay, Zone and extrapolated to represent the impact of the TACE system on a whole building EUI in this chapter. 163
- 6.3 Model in simulation workflow showing the flow of input and outputs of data to arrive at performance results. 164
- 6.4 Diagram of the Howe Center showing general orientation, geolocation and analemma. 165
- 6.5 Bay-scale energy model geometry in Google SketchUp and OpenStudio model showing ASHRAE Recommended VAV with reheat. 167
- 6.6 Howe Center floor building energy model geometry created in Google SketchUp. 168
- 6.7 Diagram of visual programming interface in Dymola showing working fluid integration. 171
- 6.8 OpenStudio Diagram of Hot Water Circuit. 172
- 6.9 Diagram of visual programming interface in Dymola showing weather and climate data integration and fuif inlet. 173
- 6.10 Module array in Dymola interface highlighting the multiplier node that creates a simulation of the module in series. 174
- 6.11 Diagram of Modules in Stacks on a typical Bay. 175
- 6.12 Existing Assembly of the Howe Center building envelope as typical of office buildings of this vintage. 178
- 6.13 Example Assembly of ASHRAE Recommended Standard for Climate Zone 4 179
- 6.14 Example TACE building envelope applied at the spandrel panel. 180
- 6.15 Representative model of Floor Zone used for the EnergyPlus model. The model was divided into thermal zones and most closely reflects the modern office space where there was the complexity of having multiple zones open to one another where at times some zones may be in heating and other in cooling modes. 181
- 6.16 Pipe Fan Coil in the current Howe Center using a seasonal switch with return and potential connection to DOAS. 182
- 6.17 Variable Air Volume (VAV) with Reheat (ASHRAE Baseline). 182
- 6.18 4-Pipe Fan Coil with DOAS. 183

- 6.19 Direct Radiant System decoupled from the primary heating and cooling system. [183](#)
- 6.20 Alignment of existing heating and cooling type with existing façade. [185](#)
- 6.21 Alignment of ASHRAE recommended heating and cooling type with recommended façade. [186](#)
- 6.22 Alignment of the initially proposed TACE system and heating and cooling system, and diagram of system design modified based on simulation results that were used for final EUI studies for Prototypes I and III. [187](#)
- 6.23 MVP Prototype I comparison of normalized annual energy with 2.50 l/min (0.66 gpm) using system inlet temperatures of: groundwater temperature; 22° C (71.6° F) temperature; average between indoor and outdoor temperatures. [189](#)
- 6.24 MVP Prototype I comparison of normalized annual energy with 0.625 l/min (0.165 gpm) using system inlet temperatures of: groundwater temperature; 22° C (71.6° F) temperature; average between indoor and outdoor temperatures. [190](#)
- 6.25 MVP Prototype I comparison of normalized annual energy using 2.50 l/min (0.66 gpm) vs 0.625 l/min (0.165 gpm) using the system inlet temperature of an average between indoor and outdoor temperatures. [191](#)
- 6.26 MVP Prototype I comparison of normalized annual energy using 2.50 l/min (0.66 gpm) vs 0.625 l/min (0.165 gpm) compared to Photovoltaic and Solar Thermal outputs. [192](#)
- 6.27 MVP Prototype I comparison of temperature flux at 2.50 l/min (0.66 gpm) flowrate using ground temperature and 22°C (71.6° F) as inlet temperatures. [193](#)
- 6.28 MVP Prototype I comparison of temperature flux at 0.625 l/min (0.165 gpm) flowrate using ground temperature and 22°C (71.6° F) as inlet temperatures. [194](#)
- 6.29 MVP Prototype I comparison of power per area at 0.625 l/min (0.165 gpm) flowrate using ground temperature and 22°C (71.6° F) as inlet temperatures. [196](#)
- 6.30 MVP Prototype I comparison of power per area at 2.50 l/min (0.66 gpm) flowrate using ground temperature and 22°C (71.6° F) as inlet temperatures. [197](#)
- 6.31 Normalized cumulative energy comparison for MVP Prototype I and ASI Prototype III showing MVP Prototype I outperforming ASI Prototype III in coolth, where ASI Prototype III outperforms MVP Prototype I in heating. [203](#)
- 6.32 Normalized thermal energy comparison for New York climate (40.7° Collector Inclination Angle). MVP Prototype I outperforms ASI Prototype III in coolth, where ASI Prototype III outperforms MVP Prototype I in heating. [204](#)
- 6.33 Average monthly fluid temperature rise per stack using 22° C inlet temperature and 0.63 l/min flow rate for NY. ASI Prototype III outperforms MVP Prototype I in both average high and low temperatures. [204](#)
- 6.34 Normalized thermal energy comparison for the Netherlands climate (50.2° Collector Inclination Angle). MVP Prototype I outperforms ASI Prototype III in coolth, where ASI Prototype III outperforms MVP Prototype I in heating. [205](#)
- 6.35 Average monthly fluid temperature rise per stack using 22° C inlet temperature and 0.63 l/min flow rate for NL. ASI Prototype III outperforms MVP Prototype I in both average high and low temperatures. [205](#)
- 6.36 Normalized thermal energy comparison for Phoenix climate (33.4° Collector Inclination Angle). MVP Prototype I outperforms ASI Prototype III in coolth. ASI Prototype III outperforms MVP Prototype I in heating in only 22°C inlet temperature and 0.66 gpm, in all other cases I outperforms III. [206](#)

- 6.37 Average monthly fluid temperature rise per stack using 22 °C inlet temperature and 0.63 l/min flow rate for Phoenix. ASI Prototype III outperforms MVP Prototype I in both average high and low temperatures. 206
- 6.38 Volume identified required to house the integrated system components. 208
- 7.1 Critical drivers as part of the TACE module and system. 215
- 7.2 Diagram of typical bay showing surface area to volume ratio. 216
- 7.3 Surface areas at multiple scales showing the proportion of actual collection surface to total façade surface to the service area. 218
- 7.4 Relationships of critical metrics of the façade design and energy impacts. Multiple scenarios can privilege most energy reduction to no loss in energy efficiency while increasing daylight and access to view-sheds. 221
- 7.5 Taxonomy of shape logics based on manufacturing methods. 223
- 7.6 Process diagram of RAM pressing manufacturing steps. 225
- 7.7 Process diagram of Pressure Cast (above) and Slip Cast (below) manufacturing steps. 227
- 7.8 Process diagram of Extrusion manufacturing steps. 228
- 7.9 Process diagram of Digital Fabrication manufacturing steps. 230
- 7.10 Diagram of typical unit size limitation and increased limitations with robotic lifting support. 231
- 7.11 Diagram of South facing component geometries for prototype POC Prototype II (above) and ASI Prototype III (below). 233
- 7.12 Diagram of East and West facing component geometries for Prototype POC II (above) and Prototype ASI III (below). 234
- 7.13 Diagram of Southeast and Southwest facing geometries for POC Prototype II (above) and ASI Prototype III (below). 235
- 7.14 Comparison of Prototypes I and III by working fluid volume, surface areas and power output. 237
- 7.15 Assembly methods diagram for: masonry cavity or traditional rainscreen (top); stick build rainscreen curtain wall (middle); unitized curtain wall (bottom). 239
- 7.16 Diagram of the component parts showing rainscreen attachment system integrated with Unitized Curtain Wall components. 243
- 7.17 Example of Unitized Curtain Wall assembly options. 243
- 7.18 Example of potential facades with corresponding WWR and TCS areas. 244
- 7.19 Example of typical bays showing UCW examples from Figure 7.17. 245
- 8.1 Rainscreen and punched window deployment for the TACE system. 257
- 8.2 Stick Built curtain wall deployment of the TACE system. 257
- 8.3 Unitized Curtain Wall deployment of the system. 258
- 8.4 Energy Information Administration 2019 Outlook and Trends for Commercial Energy Cost in USD ("Annual Energy Outlook 2019," 2019). 260
- 8.5 Comparison of Amsterdam showing projected energy reduction impact due to TACE system. The graph is defined by correlating ASI Prototype III simulation data applied on the South, East, and West facades at 40% WWW with the modelled energy use of a 300,000 m<sup>2</sup> office tower. 261
- 8.6 Comparison of Phoenix showing projected energy reduction impact due to TACE system. The graph is defined by correlating ASI Prototype III simulation data applied on the South, East, and West facades at 40% WWW with the modelled energy use of a 300,000 m<sup>2</sup> office tower. 262

- 8.7** Comparison of New York showing projected energy reduction impact due to TACE system. The graph is defined by correlating ASI Prototype III simulation data applied on the South, East, and West facades at 40% WWW with the modelled energy use of a 300,000 m<sup>2</sup> office tower. [262](#)
- 8.8** Analytique of UCW Prototype IV Design. [267](#)
- 8.9** UCW Prototype IV developed for the 4<sup>th</sup> annual ACAW in August of 2019. The prototype was developed with direct support from United Architectural Metals, Rigidized Metals, and Boston Valley Terra Cotta. [268](#)
- 8.10** Reduction of connections as developed from prototype III to IV. [269](#)
- 8.11** Diagram of radiant panel locations for future work. [270](#)
- 8.12** Endcaps required for extrusion design. This assembly as the prototyped and modelled current version either must capture or offload thermal energy, restricting the adaptive potential of the TACE system. [271](#)
- 8.13** Diagrams of thermally improved prototype proposals for future study. The left arrangement separated cold and hot loops, and the right arrangement separated the tiles into a cold loop tile and a hot loop tile creating 1) a thermally broken assembly, and 2) the ability to simultaneously capture and offload thermal energy in that same assembly. [272](#)
- 8.14** Climate diagrams showcase available resources and should play a role in determining how the TACE system should function to be most effective in local conditions [273](#)
- 8.15** Multizone TACE system array showing TACE module arrays biased for heating on the south, cooling on the north, or in combination on the East and West faces of the floorplate. This diagram also shows a connection to a geo-exchange loop. This arrangement, when deploying the TACE modules in Figure 8.12, can heat, cool, and store thermal potential simultaneously. [274](#)
- 8.16** Diagram of the First Law and Second Law of Thermodynamics in relation to the building envelope. The First Law approach encourages disciplinary segregation, whereas the Second Law may encourage disciplinary cooperation. Adapted (Vollen & Shen, 2015). [284](#)

# Summary

---

Of myriad systems that comprise the building systems matrix, the building envelope represents the greatest singular potential for energy gain or loss - as much as 50% in the commercial building sector - and thus offers the greatest opportunity to influence the overall energy profile of the building. Traditionally building technologists have tended towards envelope designs that mitigate energy flows by separating the energy flows derived from climate on the exterior from the occupancy derived loads on the interior. Over the past few decades, the coupled pressures of the societal goal of reducing the overall carbon footprint while providing for high quality office space of both new and existing building stock has placed significant attention on increased energy efficiency to lower building energy profiles. To meet this goal, new building systems would be required to manage the energy in and around the building more effectively. Two systems types, Thermo-Active Building Systems and Adaptive Building Envelopes, have been developing in response to this critical context.

Over the past several decades, research and development in building envelope design have promoted the convergence of Thermo-Active Building Systems and Adaptive Building Envelopes that re-conceptualize the envelope as a distributed energy transfer function that captures, transforms, stores, and even re-distributes energy resources.

The widespread deployment of Thermo-Active Building Systems as a building envelope will depend on several factors. These factors include the value of the design attributes that impact energy transfer in relation to the performance of the building envelope assembly and the return on investment that these attributes individually or in the aggregate can provide as a reduction in Energy Use Intensity. The research objectives were developed to focus on the design development, testing, and energy reduction potential of a Thermo-Active Building System as an adaptive countercurrent energy exchange envelope system using ceramic components: the Thermal Adaptive Ceramic Envelope.

A series of prototypes were developed alongside a numerical model throughout the research in an iterative process. The first prototype was designed for a south facing wall of a typical commercial building in the New York City metro region. Using this geographical region and solar orientation as a constant defined the isolation of

the specific design attributes to be investigated and evaluated for their impacts on the energy capture, and ultimately the impact on building energy use intensity in a climate region with both heating and cooling needs.

To understand the impact of the design attributes that distinguish the Thermal Adaptive Ceramic Envelope, simulations at the component, bay, zone and building scales were conducted, and the building scale simulations were evaluated for energy savings. Based on the simulation results and an analysis of the impacts of architectural integration, three additional designs and prototypes were developed as part of an iterative process.

The conclusion of the research discussed the results of the simulations which definitely showed a progressive saving in energy use for both heating and cooling and proposes future work, including further testing, modelling, simulation and design explorations for improvements in performance at the module and system integration scales.



# Samenvatting

---

Van de talloze systemen waaruit de bouwsysteemmatrix bestaat, heeft de bouwschil zonder twijfel het grootste potentieel voor het besparen of verliezen van energie – soms tot wel 50% voor commerciële gebouwen – en het biedt dus de grootste mogelijkheid om het complete energieprofiel van een gebouw te beïnvloeden. Van oudsher hebben bouwtechnici geneigd naar bouwschilontwerpen die de energiestromen inperken door de energiestromen van het klimaat aan de buitenkant te scheiden van de energiebelasting aan de binnenkant die het gevolg is van het gebruik.

In de afgelopen decennia heeft de gezamenlijke druk van de maatschappelijke doelstelling voor het verminderen van onze CO<sub>2</sub>-voetafdruk samen met de vraag naar kantoorruimtes van hoge kwaliteit in reeds bestaande oude en nieuwe gebouwen, ervoor gezorgd dat er veel aandacht is voor een hogere energie efficiëntie en dus voor gebouwen met een lager energieprofiel. Om dit doel te bereiken moet van nieuwe bouwsystemen vereist worden dat ze de energie in en rondom het gebouw effectiever beheren. Als reactie op deze dringende context zijn twee soorten systemen ontwikkeld, namelijk Thermo-Actieve Bouwsystemen en Adaptieve Bouwschillen.

In de laatste paar decennia heeft onderzoek en ontwikkeling in het ontwerp van bouwschillen de samenvoeging van Thermo-Actieve Bouwsystemen en Adaptieve Bouwschillen naar voren gebracht waarbij de bouwschil heruitgevonden is als een functie van energieoverdracht en -distributie door het opvangen, transformeren, opslaan en zelfs herverdelen van energiebronnen.

Of de toepassing van Thermo-Actieve Bouwsystemen in de vorm van bouwschillen zich wijd zal verbreiden, zal afhangen van verschillende factoren. Deze factoren zijn onder andere hoe de waarde van de ontwerpeigenschappen die de energieoverdracht beïnvloeden zich verhouden tot de prestatie van de bouwschilmontage en het investeringsrendement wat deze eigenschappen individueel of gezamenlijk kunnen opleveren in de vorm van een vermindering van Intensiteit van het Energieverbruik. De onderzoeksdoelstellingen zijn ontwikkeld om te focussen op de ontwikkeling van het ontwerp, het toetsen en het energiereductie potentieel van een Thermo-Actief Bouwsysteem als een adaptieve tegenstroom van energie-uitwisseling in het bouwschilsysteem, gebruik makend van keramische componenten: de Thermisch Adaptieve Keramische Bouwschil.

Een reeks prototypes werd ontwikkeld naast een wiskundig model gedurende het onderzoek in een verbeteringsproces. Het eerste prototype werd ontworpen voor een zuidelijke muur van een typisch commercieel gebouw in het grootstedelijk gebied van New York City. Gebruik makend van deze geografische regio en zonneoriëntatie als een constante, bepaalde de isolatie van de specifieke ontwerpeigenschappen die onderzocht en geëvalueerd moesten worden op hun effect op de energieopvang, en uiteindelijk het effect op de energiegebruiksintensiteit van het gebouw in een klimaatzone waar zowel verwarming als koeling nodig is.

Om het effect van de ontwerpeigenschappen die de Thermisch Adaptieve Keramische Bouwschil uniek maken te weten te komen, werden simulaties uitgevoerd op de schaal van het onderdeel, het compartiment, een deel van het gebouw en het hele gebouw, en de simulaties op de schaal van het hele gebouw werden geëvalueerd op basis van hun energiebesparing. Op basis van de resultaten van de simulaties en een analyse van de effecten van de architecturale integratie werden drie extra ontwerpen en prototypes ontwikkeld als onderdeel van het verbeteringsproces.

In de conclusie van het onderzoek werden de resultaten van de simulaties besproken die definitief aantoonde dat er een progressieve besparing was in het energieverbruik met betrekking tot zowel de verwarming als de koeling en werd voorgesteld wat nog meer gedaan moet worden, inclusief meer toetsing, modellering, simulatie en ontwerpverkenningen voor verbeteringen in prestatie op de schaal van de module en de systeemintegratie.

# 1 Introduction

---

The purpose of this research is to determine how much energy reduction may be attributed to a countercurrent energy exchanging building envelope using ceramic components in support of the reintroduction of architectural ceramics as an adaptive energy exchanging building envelope product. The use of ceramics as a building technology has been around for thousands of years. Reimagining this useful material as an energy exchanging system is both pragmatic and extremely important; now more than ever, as energy conservation is a necessity in the preservation of our environment.

## 1.1 Energy, Terra Cotta, and an Evolution of a Building Envelope

---

High-performance building envelope design has been moving in recent years towards the development of adaptive building envelopes. The impetus for this trifold focus is explained by three key drivers:

- diminishing returns of the performance of non-adaptive envelopes
- increasing costs and availability of energy and material resources
- an overall concern of our industry for the localized impact of buildings on the climate

These drivers combined the pressures of increased performance-based regulations and the increasing need to provide modern office space to create an atmosphere that supports the development of new building systems technologies – where the most substantial impact may also be in the improvement of the performance of the building envelope as a system.

### 1.1.1 Buildings, Energy Use and the Global Context

---

Buildings use 40% of raw materials globally, or 3 billion tons annually (Roodman, et al., 1995). Most striking is the pace at which our global society is exceeding the Earth's biocapacity, by some estimates 40% since 1980 (WWF, 2016). We are the producers, consumers, and decomposers of an entirely distinctive and relatively new built ecology with which natural ecologic systems, both local and global, must contend.

Globally, final energy consumption attributed by sector is 30% Transportation, 31% Industry, and 35% Buildings, with the remaining 4% split across other various sectors. (IEA, 2013). It is widely accepted that buildings are one of the most massive consumers of natural resources and account for 40% of the greenhouse gas emissions that affect climate change.

Coinciding with the increasing energy usage, the global population continues to grow, with currently 54% of the world's population living in a built ecology that can be classified as an urban condition; steady growth is projected for at least the next century (United Nations, 2014). By global comparison, the U.S. is a leading consumer of energy per capita. In particular, buildings represent 38.9% of US primary energy use, including fuel for construction, again with Industry and Transportation sectors accounted for the remaining usage. Based on global trends of energy use per capita, the US was surpassed only by a handful of Middle East oil producing states and Iceland (DataBank, 2019). In the United States (US) buildings account for 38% of all CO<sub>2</sub> emissions and by some measures, buildings represent 72% of all US consumption. Within building types in the US, residential and commercial energy consumption is split; within commercial buildings, accounting for 30% of total commercial building energy use, consumption is split between very low density uses, (i.e., dry cleaners, gas stations, etc.) and high density uses (i.e., multi-floor office buildings) (EIA, 2020).

At a state level, New York State has one of the largest total comparable energy footprints when compared directly to total energy use to that of other states. However, whilst energy use per capita in New York State is actually the lowest of all US States, the cost of energy is amongst the highest, twice the national US average; trends predict that energy use per geographical area and energy costs per unit consumed will continue to rise due to the pressures of increased growth. The New York State Metro Region is the region of interest to explore new building systems because of the growth of new buildings, the focus on energy efficiency, and the age of the current building stock where the building envelope is past its useful life. Ultimately, the effects of growth on local, regional, and global energy resources and

the subsequent long-term effects on the corresponding ecosystems have significant ramifications for the design and construction industries.

Sustainable planning in preparation for the inevitable future population, especially in the US, and the corresponding growth of built ecologies has focused attention on the energy efficiency of buildings since the energy crisis of 1973 (Alliance Commission, 2013). Some 40 years later, it is easy to deduce that the global goal of reducing the overall carbon footprint of the built environment has placed increased attention on the potential to lower building energy use profiles, with increased emphasis on the development of building technologies that impact energy use.

### 1.1.2 **The Case for Expanding the Terra Cotta Building Envelope Products**

---

At the turn of the 20th century, the zeitgeist of building technology in the US was utilizing handcrafted terracotta ceramic tiles mounted on structural steel framing. There were dozens of companies in the United States alone employing thousands of workers making each tile from custom built moulds interpreted from architects' drawings. As pressure on the architecture, engineering and construction industry increased the size and speed of how buildings were built, building technology evolved to meet the needs of the changing market, and handcrafted time-intensive building systems fell by the wayside of the mainstream industry. Today, few such terra cotta companies remain, and most are primarily involved in the historic preservation of old buildings. Yet, the natural process of erosion of the Earth's crust likely produces clay faster than we could ever hope to use it. While terracotta has many desirable properties as a building material; durable vitrified (glazed) finishes, thermal mass characteristics (energy efficiency), humidity controlling properties (environmental control), and plasticity of form (structural stability), modern building techniques require an efficient and resilient construction system with a streamlined design and manufacturing process. While modern terra cotta products are by-and-large globally available and developed from a mature and efficient industry, the bridge between the energy manipulation of the material and the product types available has not been built.

To be of significant value, a new building industry product must contribute to energy efficiency, utilize abundant or recyclable materials and encourage local economic development through appropriate available technologies. Ceramic building materials meet these requirements. To reintroduce architectural ceramics more widely to the high performance design and construction industry, traditional terracotta must be

expanded. In this time of diminishing energy resources, it is desirable to use the properties of ceramics to support the thermal management of energy transfer across the building envelope.

### 1.1.3 Thermo Active Building System as a Building Envelope

---

When considering the active transfer of energy across the building envelope, there are two broad categories of systems: active and adaptive. Mike Davies' characterization of the polyvalent wall, as shown in Figure 1.1 is the cornerstone of the development of Adaptive Building Envelopes and paved the way as the primary instigation towards the development of multiple functioning building envelope systems. The contemporary work being developed at TU Delft in the Architectural Engineering + Technology Department and specifically the development of the integrated wall strategy by Professor Ulrich Knaack, as illustrated in Figure 1.2, has been used to inform advances in the characterization of Adaptive Building Envelopes as a multivalent wall that engages the building envelope construction with bioclimatic forces lowering reliance on energy intensive mechanical systems (Knaack, 2007). The research in this dissertation focuses on the thermal adaptability of the building envelope because this is the most extensive system that has yet to widely develop any paradigm shifting advances in the state of the art and that also has the most opportunity to have the most substantial impact on energy use in the building sector.

The ability to control energy transfer rates for heat loss and heat gain through the building envelope can be developed by storing and releasing sensible heat as latent heat. This effect has traditionally been accomplished with the application of thermal mass as a building system. As illustrated in Figure 1.4 and Table 1.1, the drawback of using these types of systems (e.g., terra cotta, clay brick, concrete, etc.) in simple terms (detailed in Section 1.4) are: 1) the unmanageable time lags of energy transfer; 2) the significant mass required to store the quantities of energy; 3) requirements of modern building envelopes largely isolate mass systems to either the interior (i.e., passive thermal or Trombe type) or exterior (i.e., rainscreen type) of the weather barrier which is the demarcation of the building envelope as either interior or exterior. One solution that makes the qualities of thermal mass more effective in modern building operation is to integrate a controllable countercurrent energy exchanger design into a thermal mass building system.

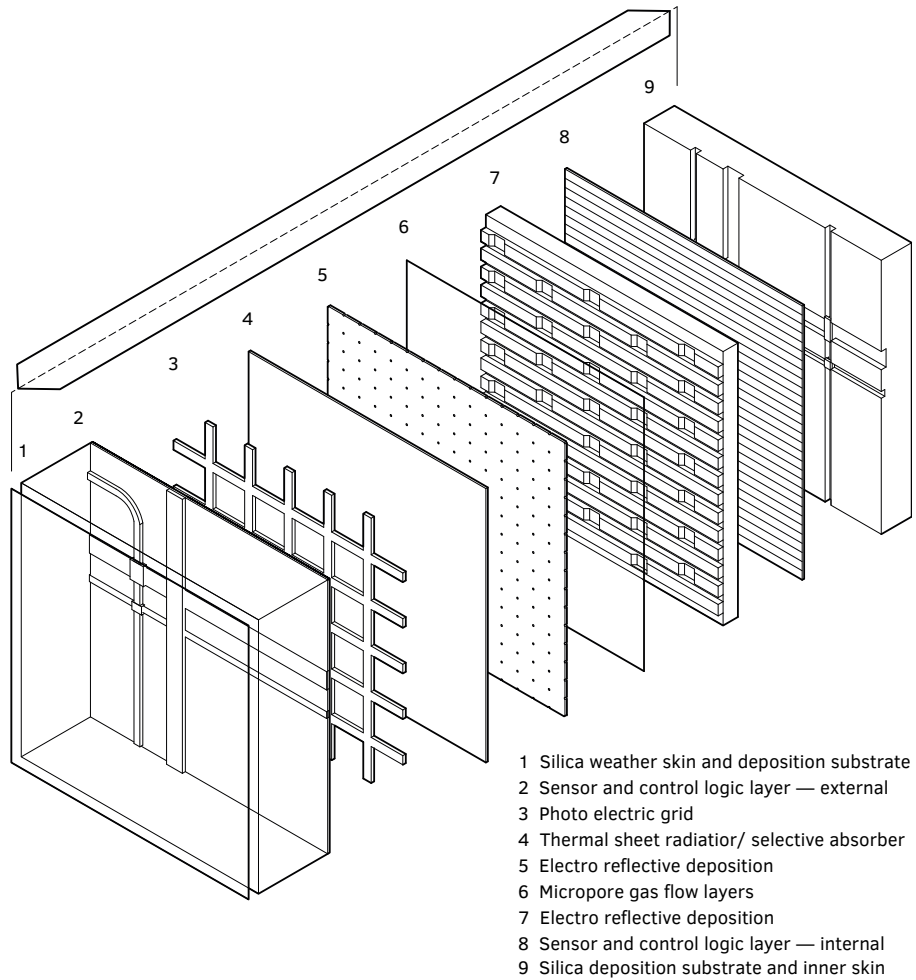


**FIG. 1.1** Mike Davies' vision for the Polyvalent wall where each distinctive layer has a specific use . Redrawn (Davies, 1981).

In modern building envelopes, this could allow the capacitive storage of mass systems to transgress the weather barrier demarcation line if the exchange systems are deployed as an array to move energy between the inside and outside. By controlling the transfer, storage and release of thermal energy across the building envelope, a thermal mass-based system can achieve the same balancing effects, without the unmanageable time lag and the required quantities of materials used in traditional thermal mass strategies.



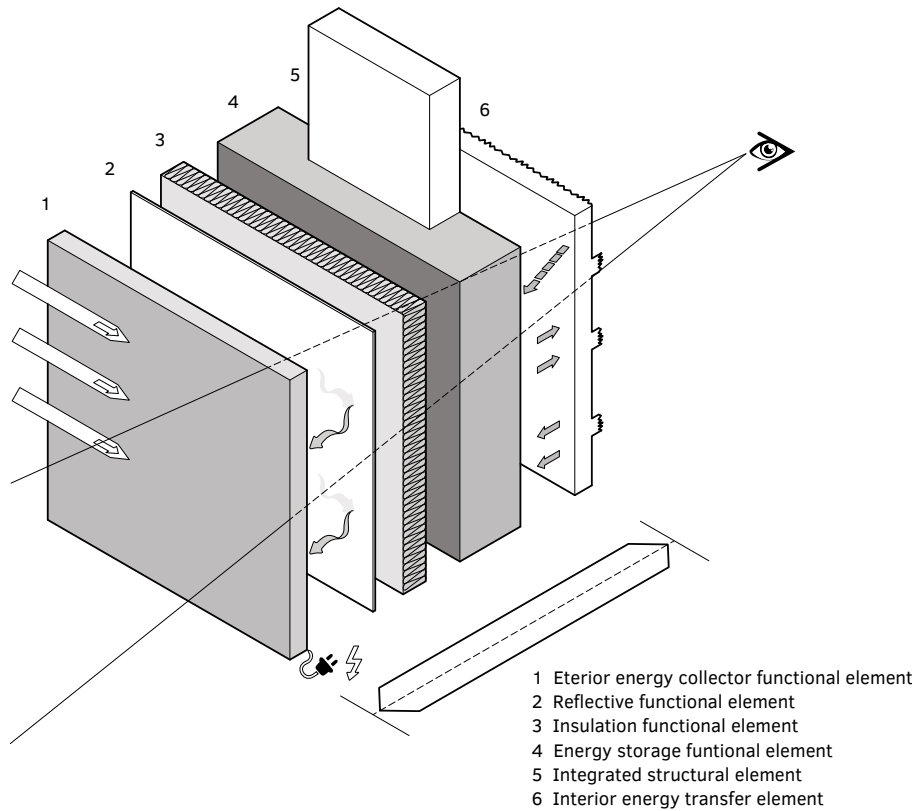


**FIG. 1.2** The multivalent wall as envisioned by Ulrich Knaack where the layers have both specific uses and recombinant interactions. Redrawn (Knaack, 2007).

Thermo-Active Building Systems (TABS), as exemplified in Figure 1.3, are considered to be active systems where a working fluid is used to heat or cool the thermal mass, typically an interior floor slab or mass based wall, through integrated piping (Olesen, 2012). TABS have typically, though not exclusively, relied on an active energy source (e.g., boiler, chiller, etc.) to charge the mass. An alternative to using an active energy source is to use locally available energy sources (e.g., ground or water temperature, ambient air temperature, insolation, etc.). While not a high quality of power, a system relying on locally available energy resources uses significantly less input energy. Unlike systems that use energy intensive energy sources, this approach is not a brute force system. Available resources are often low grade or fluctuate and may not be able to be used based on weather, climate and building energy demand profiles; the system ‘adapts’ to the conditions to best use the resources available at the times where this is effective.



**FIG. 1.3** Installation of the Thermo Active Building System in the form of a radiant slab in the Balanced Office Building (BOB) engineered by VIKA Ingenieur GmbH in Aachen. (VIKA Ingenieur, 2005)

Developed as the main body of the research of this dissertation, the Thermal Adaptive Ceramic Envelope (TACE) is one instance within the broader typology of TABS. The TACE system integrates a working fluid to assist in the heating and cooling of the interior of the building using a scalable form of countercurrent energy exchange. It operates by adapting its thermal characteristics, depending on the local energy resource and demand conditions, that are being managed (e.g., heating vs cooling, night time radiation, diurnal energy storage, etc.). The system is active because it deliberately and mechanically transfers energy to achieve desired results. The differentiating quality, however, is that the system adapts to the local conditions of energy resource and demand with minimal external energy inputs.

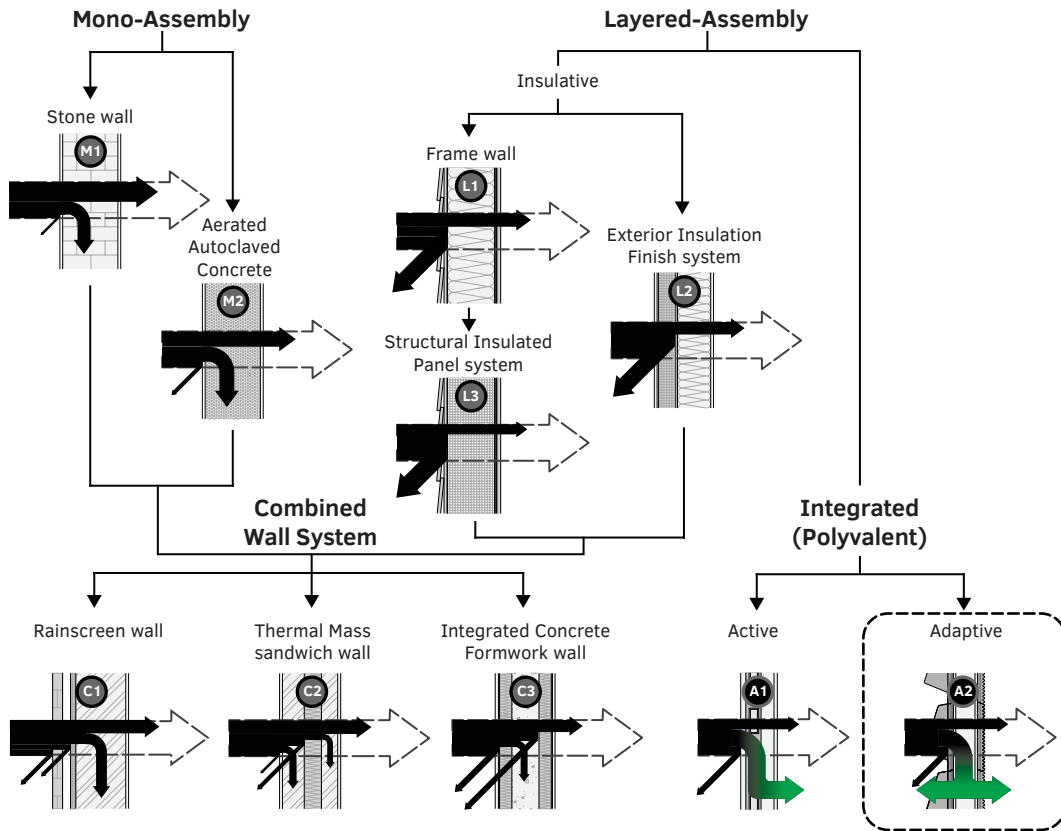


FIG. 1.4 Taxonomy of wall assemblies showing the flows of energy across the building envelope and categorizing the drawbacks and potential solutions of the various broad categories of envelope types: Mono-Assembly (M), Layered-Assembly (L), Combined-Assembly (C). The area of focus of the dissertation is in the Layered-Assembly, Integrated, Adaptive Typology (A).

TABLE 1.1 Corresponding table of assembly types, drawbacks, and solutions to Fig. 1.4.

Assembly Type	Drawbacks of Energy Transfer Control	Assembly Type	Potential Design Solution
(M), (L), (C)	Various Envelope Assemblies	(A)	Active/Adaptive Envelope
M1 M2 C1 C2	Lag Time: useful energy release is out of sync with demand or does not adjust to dynamic space needs	A1 A2	Active circulation with adjustable flowrate moving energy held in both material, working fluid and storage bank
MI M2 L1 L2 L3 C1 C2 C3	Flow Direction: lack of control strategy for useful energy flow in or out of space	A2	Bi-directional active energy flows for heating and cooling of space
L1 L2 L3 C1 C2 C3	Interior/Exterior Separation: useful energy is relegated to inside or outside.9 cm	A1 A2	Energy is captured transformed, stored and redistributed across the building envelop demarcation line

## 1.2 Project Overview

---

The focus of the research is to determine how much energy reduction, if any, can be attributed to a countercurrent energy exchanging building envelope using ceramic components of the Thermal Adaptive Ceramic Envelope system. To make this determination, modelling of the TACE system design was conducted on multiple scales; the module (i.e., the basic unit of the building envelope); bay (i.e., the space delineated between columns on a building floor plate); thermal zone (i.e., the area of the floor plate subject to similar energy thermal demands); and building (i.e., the aggregation of the all the thermal zones that combine to make the building as a whole). The modelling at the building scale used a commercial repositioning case study as a basis for comparison. Modelling at the module scale was used to calibrate and to test the efficacy of the specific design attributes of the system. Modelling at the module scale was used f calibrate and test the efficacy of the specific design attributes of the system against the ASHRAE Standard 90.1 recommended building envelope and HVAC systems. To validate the modelling studies, a series of three physical ceramic prototypes were developed throughout the research and supported by a series of design studies that were informed by both the modelling results. The prototype development was conducted to determine the impacts of architectural integration of different system morphologies. Finally, the recommendations for future research and design opportunities for the TACE system was developed and a further system design and integration strategy proposed as future work.

### 1.2.1 Limitation of Thesis within the Larger Field of Inquiry

---

The research is limited to investigating the TACE as one example of TABS and countercurrent energy exchanging building systems.

#### 1.2.1.1 Concurrent Research Limitations

---

Within the TACE research platform, this investigation falls within two areas of recent and ongoing research by Winn (2013) and Matalucci (2017), initiated by, and under the supervision of the author. The overall component morphology and external surface texture of the TACE system prototype was limited by the previous investigation by Winn and Vollen and will not be further investigated in this research

(Vollen & Winn, 2013) with the exception of the development of the new prototypes where advances were made. Radiant panels to deliver thermal comfort as the end use of the energy transported from building envelope is currently being investigated by Matalucci as a thermoelectric system and was not explicitly addressed in detail by this research, although an interior radiant panel was developed and demonstrated directly as part of this research (Matalucci, 2017; Vollen & Winn, 2013). The focus remained on radiant panels as a thermal system to directly gauge the impact the primary mechanical heating and cooling building system.

---

### 1.2.1.2 Climate Limitations

The research was focused primarily on a single climate zone. The New York Metro Region provides a base climate for systems development that straddles Humid Subtropical and Humid Continental on the Köppen climate classification and provides an overall limiting focus for the development of the TACE system. This climate has a distinct heating and cooling season and two mixed diurnal seasons, thus providing a range for performance simulation. This region also provides a growing market example for deep energy retrofits and façade replacements while still having a robust market for Class A Office space, with progressive energy targets for new constructions. As a test of system efficacy as linked to a geoclimatic region, performance comparisons for the TACE system were conducted in Phoenix Arizona, USA and Amsterdam, the Netherlands.

---

### 1.2.1.3 Building Typology Limitations

While other building types beyond offices are relevant for the application of the design principles investigated in this research, including new constructions, the ownership model of an asset has more determination and impetus of whether a building technology gets deployed on a particular project (Vollen & Harrison, 2014-2015). There are three types of developer-owner models relevant to this study: 1) the property is developed and sold; 2) the property is developed and leased; 3) the property is developed and occupied. In the business case either of the first two models, there is less incentive to integrate voluntary measures for integrating new building systems that support a reduction in operating costs due to lower energy use, unless energy use is highly regulated by region (Cobb, 2018). Where the property is developed and sold, the interest by the developer extends insofar as the purchase price may be augmented based on the market value of the

inclusion of novel building systems or an advanced degree of sustainable features that come with it, including reduced operating costs. Developer-owners, who are developing or choosing to reposition their assets with an eye on getting a higher market value at sale fall into this category as they do not have a long-term interest in the performance of the asset beyond the aforementioned sales price boost that may adjoin a higher performing building. In the developer-owner lease model, the tenant fit out is almost always the responsibility tenant, and as in the example of triple net leases, any efficiency gains are seen by the tenant as they are responsible for energy costs of their space as well as the mechanical system efficiency. Thus, while energy costs and mechanical system efficacy is essential to the lessor, there is a fractured stakeholder model at best to coordinate and realize gains of novel and high-performance building systems. Developer-owners who are operators, relating to either new or repositioned assets, who occupy their own space or are responsible for fitting out and/or operating costs, have a vested interest in the long-term energy profile of their building assets. These stakeholders were identified as the most likely early adopters of a Thermal Adaptive Ceramic Envelope that can take advantage of potential gains during a deep energy retrofit or new construction and thus provide the limiting model for the research (Vollen & Harrison, 2014-2015).

## 1.2.2 Hypothesis, Objectives, and Research Questions

---

As discussed in Section 1.1, rising energy consumption and the global trend to mitigate greenhouse gas levels have forced the construction industry to identify and to develop energy effective building systems as alternatives. Concurrently, there is increased pressure to both develop new and revitalize existing commercial building stock to keep up with market demand. To be truly effective, these new systems must be multifunctional, responsive, and developed from abundant natural resources. Thermo Active Building Systems act as a buffer against the energy loads from outside sources and energy demands from inside sources. These systems, when deployed in the form of the building envelope, directly address the energy that transfers through the envelope that ultimately amounts to an Energy Use Intensity (EUI) measured in kWh/m<sup>2</sup>/yr (kBtu/ft<sup>2</sup>/yr). It can be hypothesized that:

**Countercurrent Heat Exchange Building Envelope using ceramic components reduces the peak energy loads that contribute to the Energy Use Intensity of commercial buildings.**

Thus, the prime research question developed to test the hypothesis is stated:

**What is the energy use intensity reduction potential of the Thermal Adaptive Ceramic Envelope system using ceramic components for commercial office projects?**

**TABLE 1.2** Corresponding Objectives, Sub-research Questions, Methods and Dissertation Chapters, see Section 1.6 for the illustration and description of the dissertation structure.

METHODOLOGY MATRIX	Primary Research Question	Method	Tool	Chapter
	What is the energy use intensity reduction potential of the Thermal Adaptive Ceramic Envelope system using ceramic components for commercial office projects?	• Architectural Theoretical Framework	Literature Review Discussion	2, 3, 8
<i>Objectives</i>	<i>Sub Research Questions</i>			
To evaluate Energy Use Intensity reduction using a counter current heat exchanging envelope with ceramic components	How much does the Thermal Adaptive Ceramic Envelope system impact Energy Use Intensity?	• Quantitative and Qualitative • Evaluation Framework	• Energy Simulations • Evaluation Frameworks	5, 6
To test various combinations of design attributes including surface area, flow rate and flow direction of the Thermal Adaptive Ceramic Envelope prototype for the most effective performance	What are the impacts of the Thermal Adaptive Ceramic Envelope on building systems?	• Quantitative Physical Testing • Building Envelope Design • Quantitative Dimensional Analysis	• Prototype Designs • Experimental Inputs • Energy Simulations	4, 5, 6
To assess architecture integration and design impacts for the Thermal Adaptive Ceramic Envelope	What are the potential design limitations for the TACE system?	• Building Envelope Design • Quantitative Dimensional Analysis • Quantitative and Qualitative Evaluation Framework	• Design Iterations • Evaluation Frameworks	7, 8

The following objectives are derived from the hypothesis and prime research question and form the framework for the sub research questions:

- Evaluate Energy Use Intensity reduction using a countercurrent heat exchanging envelope with ceramic components.
- Test various combinations of design attributes including surface area, flow rate and flow direction of the Thermal Adaptive Ceramic Envelope prototype for the most effective performance.

- Assess architecture integration and design impacts for the Thermal Adaptive Ceramic Envelope.

The following sub research questions are asked to answer the prime research question.

### 1 **How much does the Thermal Adaptive Ceramic Envelope system effect Energy Use Intensity?**

To answer this question, the following investigative question was discussed:

- What design attributes of the Thermal Adaptive Ceramic Envelope impact the Energy Use Intensity reduction?

The following investigative questions support the performance of the design attributes:

- How much impact does the amount of mass of the ceramic have on the energy transfer rate?
- How much impact does the length, mass, and geometry of the thermal transfer components have on the heat transfer rate?
- How much impact does the adhesive used to assemble the ceramic components have on the transfer rate?
- How much impact does the flowrate of the working fluid have on the energy transfer rate?
- How much impact does adding an insulating layer have on the heat transfer rate?

### 2 **What are the impacts of the Thermal Adaptive Ceramic Envelope on building systems?**

To answer this question, multiple system configurations were explored, and the following investigative questions were discussed:

- What building systems are impacted by the Thermal Adaptive Ceramic Envelope?
- What is the impact of Thermal Adaptive Ceramic Envelopes on the sizing of HVAC systems?
- What are the most effective HVAC systems to combine with a Thermal Adaptive Ceramic Envelope?

### 3 **What are the potential design limitations for the Thermal Adaptive Ceramic Envelope system?**



To answer this question, various designs and assemblies will be explored, and the following investigative questions will be discussed:

- What are the possible forming techniques of the Thermal Adaptive Ceramic Envelope components, and how would these forming techniques affect the component design?
- What are the design limitations for the Thermal Adaptive Ceramic Envelope module based on the forming techniques and method of assembly?
- What are the potential envelope system configurations to assemble the Thermal Adaptive Ceramic Envelope system?

### 1.2.3 Overview of Research Methodology

---

The research methodologies addressing the research objectives and research questions were constructed as three parallel approaches.

**System Development:** The research methodology was employed to develop the Thermal Adaptive Ceramic Envelope for testing. The system development serves the purpose of providing an integrated building system where the building envelope acts as a transfer function for thermal energy. The system was used to evaluate the effects of a set of interrelated design attributes and their effect on Energy Use Intensity.

**Applicability:** The research methodology was employed to establish the relationship between energy sources, design attributes and Energy Use Intensity. Applicability includes a dimensional analysis for the quantification of resources utilized for heating and cooling at the module, bay, zone, and building scale. This method is used to study the integration and applicability of the design attributes of the Thermo Adaptive Building Envelope, the heating and cooling system, and Energy Use Intensity.

**Valuation:** The research methodology was employed to interpolate the impact of the performance characteristics of the Thermal Adaptive Ceramic Envelope operational expenses and the potential return on investment. The valuation methodology looked holistically at the relationship of Energy Use Intensity and value as delineated by energy reduction and associated energy costs, greenhouse gas emissions, and comparable technologies.

The following methods were used to deploy the research methodologies.

Architectural Theoretical Framework was used to connect and contextualize an array of aspects relating to the theoretical and historical development of the relationship between energy flows and envelope design. This framework characterized the problematique.

Building Envelope Design was used to develop the Thermal Adaptive Ceramic Envelope as an architecturally integrated system that serves as a research platform to conduct dimensional analysis. The design delineates the integration of the envelope components with energy transport, storage and distribution to heating and cooling systems.

Quantitative Physical Testing was used to calibrate the quantitative dimensional analysis. The physical prototype and hotbox testing apparatus and a Computational Fluid Dynamics simulation were used to calibrate the results of a simulation model to scale the dimensional analysis to physical performance.

Quantitative Dimensional Analysis was conducted using a parametric modelling environment to establish performance benchmarks using a case study commercial building. Performance at multiple scales was measured against standard benchmarks to assess the impact of the system on Energy Use Intensity. The results of the simulations were used to evaluate the effectiveness of the research to alter the building energy profile and form the basis of the valuation.

Quantitative and Qualitative Evaluation Framework used the simulation results to evaluate and propose recommendations for the design of the individual components, the combination of components, and further architectural integration strategies for thermos adaptive building envelopes.

---

#### 1.2.4 **Research Platform**

To answer the research questions, two interconnected the research platforms were developed: 1) a comparison framework was developed using a case study commercial building, 2) sequential physical prototypes were developed. The case study was examined for three scenarios: the existing building envelope and mechanical system; the ASHRAE recommended building envelope and mechanical system; the TACE system as a deep energy retrofit. The case study also served as a model to compare the potential performance of the TACE system in different geographies which is used to evaluate the system for different climate zones. The prototypes were developed to: calibrate the quantitative model for use in simulating

the performance of the system used ultimately to model the and simulate case study; proof of concept showcasing working components and as an architecture and systems integration. Taken together, the case study and the prototype provided a design platform to explore the development of the TACE system through architectural impacts.

## 1.2.5 **Societal and Scientific Relevance**

---

### **Socio-Behavioral Contribution: Towards Interdisciplinary Co-Development**

---

The research investigates the potential reduction in mechanical systems energy use based on the performance of the building envelope, coupling the architect as facade designer and the mechanical engineer in a collaborative, interdisciplinary trajectory to reduce energy usage in buildings. Energy transported through the building envelope to match real time demand will decrease dependence on external energy sources, meeting societal goals of reducing the overall carbon footprint and associated emissions of the built environment. Further, Thermo-Active Building Systems contribute to economic valuation strategies for green building innovations that are based on managing entropy. These innovations have policy and regulatory implications that may significantly contribute to changing how the next generations of buildings utilize energy within the larger built ecology.

### **Scientific and Environmental Contribution: New Strategies for Building Envelope Design**

---

Currently accepted standards for energy modelling have a limited range and ability to quantify the complex interactions of the energy flows around the building envelope. The focus on individual measures to increase energy efficiency has contributed to policies and incentives around the potential reduction in building energy profiles based on energy mitigation rather than management, privileging the current direction of design standards and policies. Using the more robust modelling protocol of physics based modelling environment and co-simulation that allows for the design of specific attributes of the building envelope that help manage the energy flows are more easily explored as the art is advanced, supporting more exploration and potential innovations of Thermo Active Building Systems.

The Building Research Establishment Environmental Assessment Method (BREEAM) was first launched in 1990 to assess the performance of the environmental footprint

of a building. Following BREEAM the Leadership in Energy and Environmental Design (LEED) was deployed in 1998 and is the metric that is the accepted standard in the United States, and together with BREEAM has formed the basis for other green building standards globally. BREEAM and LEED certification require predictive energy simulation and commissioning that do not require instrumented operational post occupancy validation, even though, for example, LEED buildings have been shown typically to underperform in terms of energy efficiency. At the same time, BREEAM assessment allows for multiple types of energy models allowing for the general possibility of inconsistency in the predictive energy simulations (Lianjun et al, 2012). Due to the design of the rating systems, there are often incentives for the design team to make low cost choices (e.g., including a LEED Accredited Professional on the design team, inclusion of bicycle racks, etc.) to achieve certification instead of striving for Zero Net Energy (ZNE) Capable status – although this is currently changing with the introduction of the LEED Zero verification process. Further, achieving compliance certifications are often used by municipalities which are giving incentives (e.g., reduced taxes, low interest loan support, waiving of fees, etc.) as policy in building codes as noted as becoming common in the United States (USGBC, 2009). The results of the research will provide a design and evaluation framework for Thermo-Active Building Systems to improve the potential of adaptive building envelopes to help buildings achieve ZNE status.

### Socio-Economic Contribution: Impact of Novel Strategies to Incentivize Policy and Increase Deployment Potential

---

The Thermal Adaptive Ceramic Envelope addresses multiple interacting demand factors, coupling the building envelope with thermal resources for heating and cooling while adopting the distributed and systems-integrated approach of Thermo Active Building Systems. The research will contribute to the discussion of the broader potential system impacts (e.g., valuation strategy, asset management, policy, regulatory and societal impacts) of Thermo-Active Building Systems. In addition, the advent of radiant systems has the potential to improve occupant comfort and wellbeing.

## 1.3 Dissertation Structure

---

The dissertation structures follow three interrelated paths; prototype development, physical and numerical testing and simulation, and design explorations.

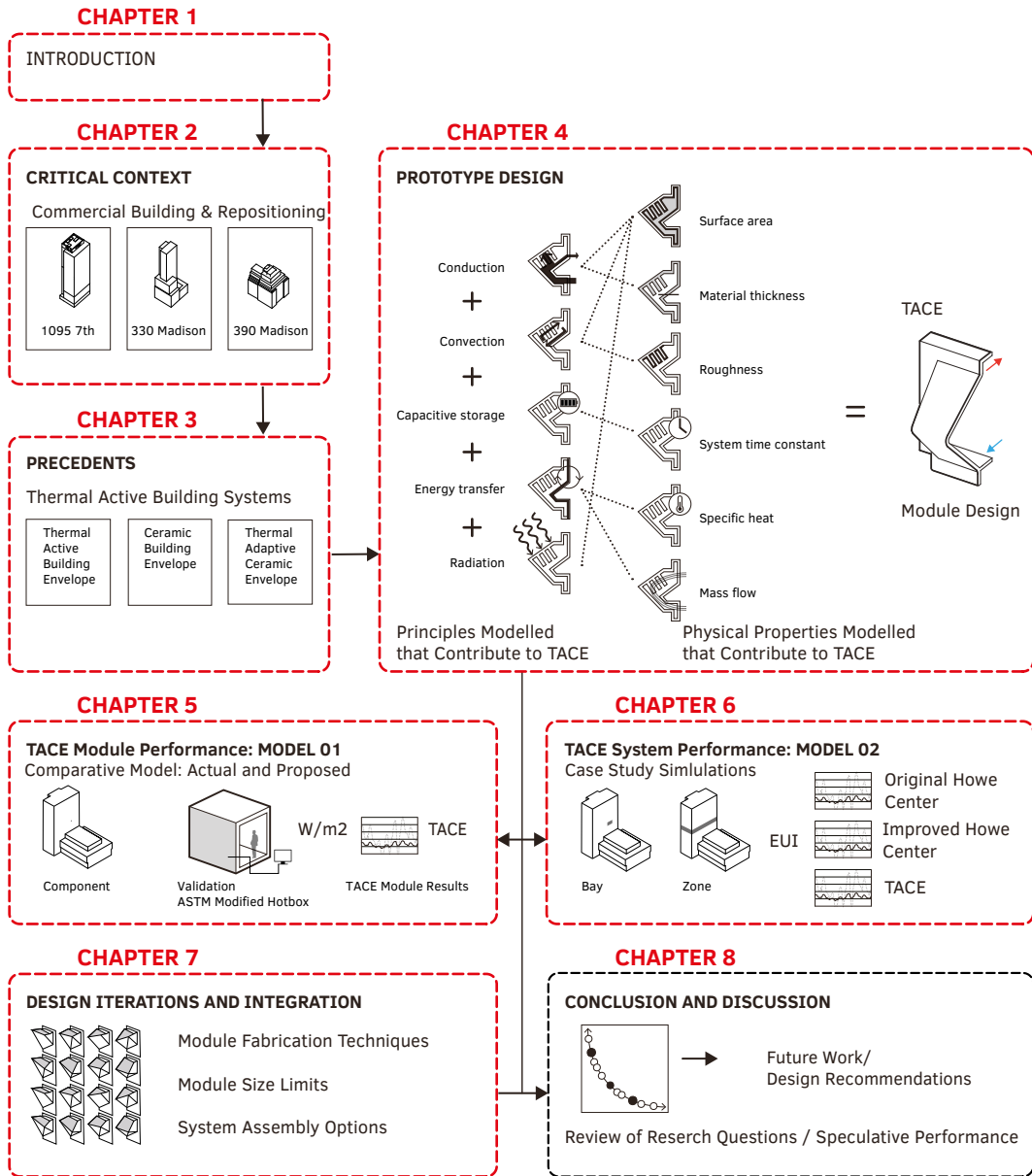


FIG. 1.5 Overall structure of the dissertation.

## Specifically

---

- **Chapter 1 Introduction:** introduces the objectives, research questions and motivations.
- **Chapter 2 Critical Context:** discusses the critical context.
- **Chapter 3 Thermal Adaptive Envelope Precedents:** reviews the primary influencing literature and case studies that support the design development.
- **Chapter 4 Thermal Adaptive Ceramic Envelope Module Design and Development:** delineates the development of a countercurrent energy exchanging building envelope using ceramic components as prototypes I, II, and III.
- **Chapter 5 Thermal Adaptive Ceramic Envelope Component Performance:** quantifies the potential thermal transfer impact of the countercurrent energy exchanging building envelope components using physical calibration and energy modelling and simulation.
- **Chapter 6 Thermal Adaptive Ceramic Envelope Performance and HVAC System Integration:** delineates the countercurrent energy exchanging building envelope as a system and quantifies system performance using energy modelling and simulation
- **Chapter 7 Thermal Adaptive Ceramic Envelope Design Iterations:** uses design explorations of the countercurrent energy exchanging building envelope using ceramic components to delineate an integrated building envelop system.
- **Chapter 8 Conclusions and Future Directions:** discusses the results and proposes future work, including further testing, modelling, simulation and design explorations.

## 1.4 Definitions and Abbreviations

---

The following definitions and abbreviations are used to provide specificity to the terminology used in the dissertation.

- **Active Thermal Insulation (ATI)** – Insulation system that actively reduces heat loss or gain at the building envelope by moving or adding thermal energy to the system.
- **American Society for Testing and Materials (ASTM, ASTM International)**– International standards organization that publishes technical standards.
- **American Society of Heating, Refrigerating and Air–Conditioning Engineers (ASHRAE)** – American professional society that publishes industry standard guidelines.
- **Architecture and Systems Integration (ASI)** – Prototype that integrates systems components into an architectural assembly.

- **Building Envelope Demarcation Line** – The conceptual plane that separates the interior of the building envelope from the exterior of the building envelope.
- **Building Integrated Solar Thermal (BIST)** – Insulation system that integrates solar thermal in the building envelope assembly.
- **Building Research Establishment Environmental Assessment Method (BREEAM)** – First established method for assessing rating and certifying sustainable performance for buildings.
- **Center for Architecture Science and Ecology (CASE)** – Academic / Industrial alliance founded by Anna Dyson focused on next generation building systems design and development.
- **Class A Office Space** – Category of office space that is significant in size, typically centrally located, and is designed to high standards for workplace organization, finishes, and mechanical systems.
- **Cross-linked Polyethylene (PEX)** – Flexible material when in pipe form used for hydronic heating and cooling.
- **Energy Use Intensity (EUI)** – The standard measure per area of energy use over time, typically one calendar year.
- **Functional Mock-Up Interface (FMI)** – Defined standard interface that allows for interplatform use of complex physical simulations.
- **Input Data File (IDF)** – A text based editable file used that describes the building and building systems for energy modelling.
- **Integrated Concentrating Solar Facade (ICSF)** – Combined heat and power system integrated into the building envelope developed by Dyson, et al.
- **International Organization for Standardization (ISO)** – Independent worldwide standards organization.
- **Lawrence Berkeley National Laboratory (LBNL)** – United States national laboratory with multiple research areas of inquiry including building energy use.
- **Leadership in Energy and Environmental Design (LEED)** – Green building certification standard developed in the United States by the US Green Building Council.
- **Minimum Viable Product (MVP)** – Level of product development that allows for testing the basic features for performance in the market and where market and initial performance feedback is used for further product development.
- **Phase Change Material (PCM)** – Material that absorbs and releases thermal energy as sensible or latent heat during the transition of the state of matter, (e.i., liquid to solid transition).
- **Proof of Concept (POC)** – Level of product development that proves the functional working premise of the product for real work operation.
- **Thermal Adaptive Ceramic Envelope (TACE)** – Countercurrent thermal envelope that adapts to heating and cooling needs based on resource availability and demand

- **TACE Assembly** – Array of modules functionally linked together and connected to a system
- **TACE Attribute** – Physical quality that affects TACE performance.
- **TACE Component** – Single object that may have, part or, one or more TACE attributes.
- **TACE Module** – Single unit that is assembled of multiple TACE components.
- **TACE System** – Complete combination of all parts including the assembly, thermal storage, and all mechanical, electrical and plumbing components required for TACE operation.
- **Unitized Curtain Wall (UCW)** – Type of building envelope facade assembly that utilizes factory fabrication and reduces on site installation.
- **Void Space Dynamic Insulation (VSDI)** – Insulation system that uses the void space in the wall assembly to reduce heat loss or gain.
- **Zero Net Energy (ZNE)** – Building with zero energy consumption, typically on an annual basis.

## References

- Alliance Commission on National Energy Efficiency Policy. (2013). The History of Energy Efficiency. Retrieved from [https://www.ase.org/sites/ase.org/files/resources/Media%20browser/ee\\_commission\\_history\\_report\\_2-1-13.pdf](https://www.ase.org/sites/ase.org/files/resources/Media%20browser/ee_commission_history_report_2-1-13.pdf)
- Balanced Office Building, [Digital Image] VIKA Ingenieur GmbH (2005). [http://www.bine.info/fileadmin/content/Publikationen/Englische\\_Infos/themeninfo\\_I07\\_engl\\_internetx.pdf](http://www.bine.info/fileadmin/content/Publikationen/Englische_Infos/themeninfo_I07_engl_internetx.pdf)
- Cobb, M. (2018). 3 Different Types of Commercial Real Estate Leases. Retrieved from <https://42floors.com/edu/basics/types-of-commercial-real-estate-leases>
- DataBank. (2019, July 10th 2019). 2015 Energy use (kg of oil equivalent per capita). Retrieved from <https://databank.worldbank.org/reports.aspx?source=2&series=EG.USE.PCAP.KG.OE&country=>
- Davis, M. (1981). "A wall for all seasons." RIBA Journal, 88(2), 55–57.
- Energy Information Association (EIA) Consumption & Efficiency. (2020). Retrieved from <https://www.eia.gov/consumption/>
- International Energy Agency (IEA), Directorate of Sustainable Energy, Policy & Technology. (2013). Transition to sustainable buildings: strategies and opportunities to 2050. International Energy Agency. Paris, France.
- Knaack, U. (2007). Façades: Principles of Construction: Birkhäuser.
- Lianjun, A., Young, Chae, T., & Young, L. (2012). Estimation of Thermal Parameters of Buildings Through Inverse Modelling and Clustering for a Portfolio of Buildings. Retrieved from Yorktown Heights, New York 10598, USA.
- Matalucci, B. (2017). Modular Indoor Micro–Climate: Investigation on Solid-State Heating and Cooling for a Sustainable Personalization of the Thermal Environment. (Doctorate), Rensselaer Polytechnic Institute, Troy, New York.
- Olesen, B. (2012). Thermo Active Building Systems Using Building Mass To Heat and Cool. ASHRAE, 52(2), 44-52.
- Roodman, D., Lenssen, N., Peterson, J. (1995). A building revolution: how ecology and health concerns are transforming construction. Washington, DC: Worldwatch Institute.
- United Nations, (2014). World Urbanization Prospects: The 2014 Revision, Highlights.
- Vollen, J., Harrison, S. (2014-2015). High Performance Masonry System (Vol. \$45,000). Rensselaer Polytechnic Institute NEXUS-NY Technology Accelerator.



Vollen, J. O., Winn, K. (2013). Climate camouflage: advection based adaptive building envelopes. Paper presented at the 8th Energy Forum Conference Proceedings, Advanced Building Skins, Bressanone, Italy.

World Wildlife Fund (WWF). (2016). Living Planet Report 2016. Retrieved from Gland, Switzerland. Retrieved from: [https://c402277.ssl.cf1.rackcdn.com/publications/964/files/original/lpr\\_living\\_planet\\_report\\_2016.pdf?1477582118&\\_ga=1.148678772.2122160181.1464121326](https://c402277.ssl.cf1.rackcdn.com/publications/964/files/original/lpr_living_planet_report_2016.pdf?1477582118&_ga=1.148678772.2122160181.1464121326)

# 2 Critical Context

---

The critical context that supports the research and development of the TACE system requires a characterization of the opportunity for a Counter Current Thermo Active Building Envelope. This Chapter focuses on the critical context with a discussion of the building typologies, enabling policies, and the energy transfer characteristics that describe energy flows and opportunities at the building envelope that form the foundation for the design of the TACE component, module, and system design as described in Chapter 4.

## 2.1 Why is a New Approach Needed?

---

Current roadmaps for lowering the building energy profile are centred on energy efficiency at the building envelope through reducing heat loss by focusing on insulation, air sealing, and reflective surfaces and improvements in mechanical system efficiency which have been mostly incremental (IEA, 2013). The traditional envelope and the mechanical systems are considered separate and distinct by the design and construction industry, yet they both contend with the same energy flows. There is only so much improvement that the current strategies for envelope development and high-performance mechanical system equipment can provide when seen as separate systems.

A new approach is needed that takes advantage of the available energy in and around the building envelope to offset loads and boost efficiencies of the mechanical systems used for heating and cooling. The proposed thermally active systems that engage both the building envelope and mechanical system must be deployable for new construction and be able to be retrofitted into the existing built ecology to extend the usefulness of existing building stock.

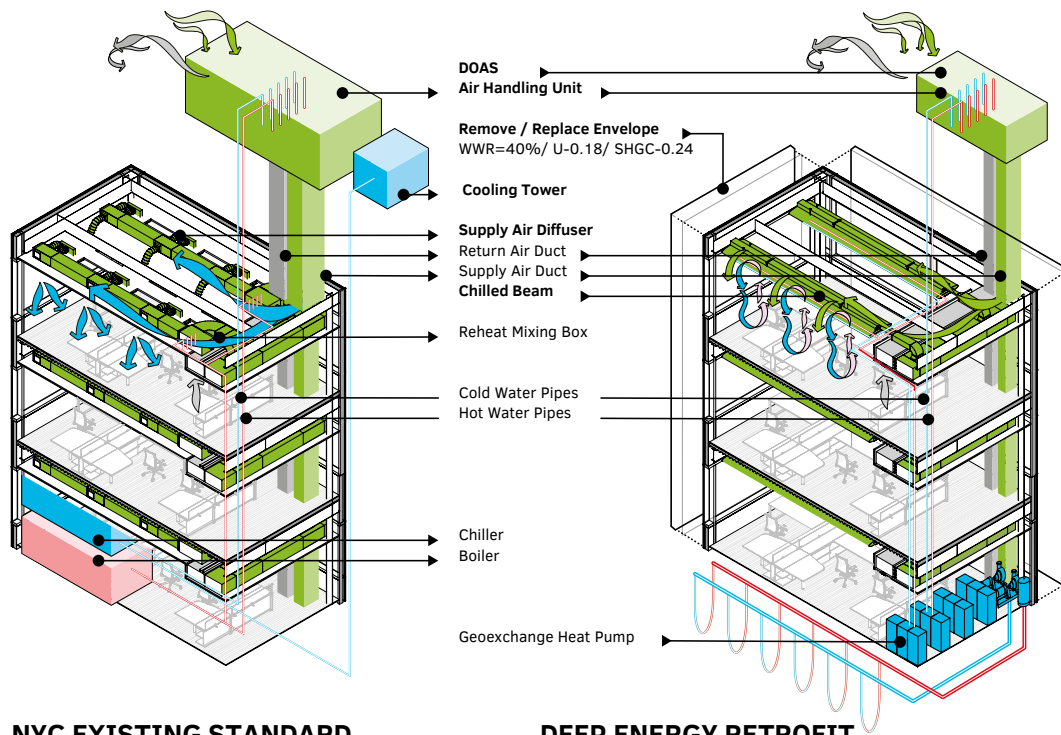
## 2.1.1 Critical Context: Building Repositioning and Deep Energy Retrofits

---

Since 1979, the number of commercial buildings in the United States has increased from 3.8 million to 5.9 million. The total amount of commercial lettable area has increased from 51 billion to 87 billion m<sup>2</sup> (EIA, 2015). These statistics highlight two notable trends: 1) most of the commercial building stock was designed and constructed prior to the initiation of global energy efficiency goals, and 2) there continues to be sustained growth in commercial building sector. The pressures on the real estate market and the changing workplace combined with the capital costs of building new commercial space has created a significant market for commercial building repositioning. Buildings are repositioned for a variety of reasons, including maximizing financial returns by increasing net operating income (NOI) through raising rents, decreasing vacancy rates, reducing operating expenditures, lowering tax liability, and attracting premium tenants (McArthur et al, 2015).

Additionally, High-Growth Industries (HGI) that include technology companies and industry disruptors, such as WeWork, have very different requirements for space (including locations in live/work/play neighbourhoods, a communication and collaboration layout, daylight, and ambience) than traditional office users. HGI's are forecasted to make up 60% of the total NYC office demand between 2013 and 2025, for example, and precipitate a need to provide more of this type of building space (Alvarez & Marsal, 2013).

The opportunity to reposition existing assets, as shown in Figure 2.1, at reduced cost and increased speed to meet demand in densifying urban centres is becoming attractive to a variety of owner types. For owners to make a repositioning investment, they must believe that material increases in rental rates will be achieved, and the building will be leased more quickly or more fully. By linking together repositioning with an energy retrofit strategy that includes building envelope replacement and mechanical system upgrades, operational expenses can be reduced, and the building lifecycle clock may be reset. Including sustainability and resiliency as a core component of building repositioning not only reduces operating expenses and increases rental and occupancy rates, but also mitigates the cost of compliance with evolving regulations and mandates.



**NYC EXISTING STANDARD**

**DEEP ENERGY RETROFIT**

FIG. 2.1 Deep Energy Retrofit Strategy showing replacement of critical systems and façade.

With a commercial real estate market in New York City of approximately 74.3 m<sup>2</sup> (800,000,000 ft<sup>2</sup>), energy retrofits in the commercial sector are projected to be €36.196 billion (\$40 billion) (Sinreich et al., 2010). In the United States alone, the commercial building market represents over a €65.153 billion (\$72 billion) opportunity, and currently, deep energy retrofits account for about €18.098 billion (\$20 billion) annually (Hart, 2013). In 2014, the industry expectation was that the retrofit market for commercial buildings would continue to grow for ten years or longer (Flanagan, 2014).

2.1.2 **Aging Building Stock of Commercial Buildings**

Buildings consist of integrated systems have a multitier service lives. Typically, major mechanical systems last an average of 20-30 years; building envelopes average a lifespan of 30-60 years; major structural components average 60-120 years. In

the United States, most buildings have outlived at least one typical lifecycle, and these are considered old buildings (Alvarez & Marsal, 2013). 82% of Class A office buildings in U. S. Central Business Districts were constructed before 1990, and 53% were built before 1980. By the lifecycle metric, 90% of all the buildings in the New York City metro region are considered old buildings by 2020.

Recent construction activity renovating the older building stock into updated commercial building space supports the current and projected growth of the building repositioning market sector. During 2013 and 2014 in New York City, 24 buildings totalling 770,000 m<sup>2</sup> (8,300,000 ft<sup>2</sup>) were being renovated compared to 9 new build construction projects totalling 697,000 m<sup>2</sup> (7,500,000 ft<sup>2</sup>) (Flanagan, 2014).

### 2.1.2.1 Failing Building Envelopes and Outdated HVAC System

---

While many old buildings have a useful remaining life to their structural systems, they often have outdated mechanical systems and failing envelopes. The building envelope fails for a variety of reasons, both natural and human-made. Exposure to the elements (e.g., solar exposure, rain, pollution, etc.), structural movements (e.g., thermal expansion and contraction, foundation settlement, etc.), and defects in materials, manufacturing, design, construction and routine maintenance (e.g., exposure of material during construction, climate appropriate design, etc.), all reduce or extend the average useful life of the building envelope (Schoen, 2010) (Sanders, 2003).

The widespread use of building-scale heating and air-conditioning systems that are not tuned to the climates in which they are located has contributed to under performing or failing mechanical systems. The HVAC systems of buildings in Oslo, New York, Miami or Phoenix, for example, were thought of often as interchangeable between climates, despite vast differences between those cities in daily and annual temperature fluctuations, relative humidity levels and exposure to sunlight. As a result of this widespread distribution of similar systems, these HVAC systems must work harder and consume more energy to cool or heat the interior, especially when considering the modern demand profile of occupant energy use due to increased equipment loads and occupant density that is demanded by market forces.

With the average age of commercial buildings being over 80 years in New York City, much of the old building stock is due for a mechanical and envelope retrofit. When considering that tenant refits in commercial spaces currently average around ten years, many of these old buildings are well positioned for a deep energy retrofit that

realigns the performance of the office space for increased productivity, occupant comfort, reduced operational costs, ultimately resulting in increased revenues for property owners.

### 2.1.3 Increasing Building Energy Use Intensity Regulations

Concurrent, the growth pressures of competitive commercial real estate markets in an ageing building stock are both the increase in regulations as well as greater demand for these regulations governing building performance. Energy regulations in the building sector grew as a direct result of the energy challenges faced in the 1970s. Led by federal efforts in the form of the Energy Policy and Conservation Act of 1975, state efforts by California and New York leveraged the federal laws and created statewide conservation policies.

From a historical perspective of federal policies as shown in the timeline in Table 2.1, the National Energy Act of 1978, specifically the National Energy Conservation Policy, created energy efficiency tax credits. The Energy Policy Act of 1992 created commercial office equipment efficiency standards. The Energy Policy Act of 2005 created efficiency standards for commercial equipment. The Energy Independence and Security Act of 2007 created institutional grants and loans and set new standards for equipment, the project result of which will reduce energy consumption by 7% and greenhouse gas emissions by 9% by the year 2030. These policies, developed over the last four decades, have created effects ranging from baseline building energy codes to long term energy reduction targets (Alliance Commission, 2013).

**TABLE 2.1** Table of the critical timeline showing an increased value of energy efficiency developed at the federal level.

1975	Energy Policy and Conservation Act	POLICY - Established state conservation
1978	National Energy Act & National Energy Conservation Policy	POLICY - Established national conservation
1992	Energy Policy Act	STANDARD - Established office equipment efficiency
2005	Energy Policy Act	STANDARD - Updated office equipment efficiency
2007	Energy Independence and Security Act	FUNDING - Created to grow impact and support
2030	Target referenced as goal for energy and emissions reduction	TARGET - Major milestone for buildings sector

### 2.1.3.1 Architecture 2030 and the Roadmap to 80 x 50

---

Established in 2002, the Architecture 2030 Challenge is a target-based voluntary commitment that frames a goal to make buildings carbon neutral by the year 2030. Focused on the global architecture, engineering and construction community, targets are adopted for both new buildings and renovations. The federal government, the U.S. Council of Mayors, the American Institute of Architects (AIA), the American Society of Heating, Refrigerating and Air-Conditioning Engineers (ASHRAE), and many other organizations have committed to achieving these targets. The framework recognizes that the most reduction can be achieved through design innovation and onsite renewable energy systems (Architecture 2030, 2017).

Published in 2007, PlaNYC is proposed roadmap to secure a longer term sustainability plan for New York City. PlaNYC is aligned with Architecture 2030 and has aggressive targets coinciding with the challenge. The plan, which updates every few years, focuses on practical solutions to achieve the 80% reduction of greenhouse gas emissions from 2005 by the year 2050. In 2014, New York City committed to achieving the 80 x 50 targets in alignment with the Paris Agreement as part of the revised PlaNYC. While the plan focused on all sectors to achieve the target, including waste reduction transportation reform, and power generation, the most substantial opportunity is in the improvement of energy efficiency in the New York City building stock. This outlook acknowledges that much of the building stock is likely to remain beyond 2050, so energy efficiency investments in this sector have long lasting effects tied directly to the long-term targets (Shorris, 2014).

### 2.1.3.2 ASHRAE, Greater Greener Buildings Plan

---

ASHRAE started developing energy standards for buildings in response to the energy crisis of the 1970s. The ASHRAE Standard 90.1 Energy Standard for Buildings Except Low-Rise Residential Buildings has formed the basis for energy performance since 1975. The standard was updated in 1989, 1999, 2007, 2010, 2013 and 2016 and increased performance metrics by over 50% since its inception. It is referenced by LEED and is considered a baseline for energy modelling across multiple energy modelling platforms. Standard 90.1 is the measure by which performance is measured. The effects of this standard on the design of commercial buildings have been the driving force in aligning commercial buildings to the targets of Architecture 2030 and 80 x 50. In 2009 ASHRAE released Standard 189.1 Standard for the Design of High-Performance Green Buildings. Standard 189.1 expands upon

Standard 90.1 to include the guidelines for whole building design including siting, resource utilization efficiency, indoor air quality and greenhouse gas emissions.

Focused on New York's existing building stock, the 2009 Greener, Greater Buildings Plan enacted four local laws effecting all buildings larger than 50,000 square feet: Local Law 85 New York a New York City Energy Conservation Code; Local Law 84 Energy Benchmarking; Local Law 87 Energy Audit & Retro Commissioning; Local Law 88 Lighting Upgrades (Shorris, 2014). The result of implementing this plan was a robust database of baseline information from which to refine and implement the roadmap and achieve the targets set out by the Architecture 2030 and 80 x 50.

---

#### 2.1.4 **Energy Retrofits**

In the commercial building market energy retrofits often accompany the change in lease, use or program, or coincide with other critical building infrastructure upgrades or repairs. Since 2012, Green Retrofits have transformed from a green marketing tool into a business case for owner-operators of commercial buildings. These owner-operators were seeing increased revenues and lowered long term costs of their assets. In 2015 New York City instituted a Retrofit Accelerator to push forward the deployment of energy conservation measures. The goal is to make significant progress on municipal-owned building stock towards cleaner primary fuel sources (e.g., from number 6 heating oil to number 4 heating oil) and reduce greenhouse gas emissions by improving energy efficiency and deploying energy conservation measures.

---

##### 2.1.4.1 **Energy Conservation Measures**

Lighting upgrades (e.g., from incandescent to compact fluorescent to LED), heating and cooling upgrades (e.g., increased boiler efficiencies through replacement, installing variable refrigerant flow systems, etc.), replacement windows (e.g., replace window seals, replace single glazed windows, etc.) and upgraded insulation each contribute to increasing energy efficiencies in buildings. As an energy retrofit strategy, Energy Conservation Measures are often deployed as standalone upgrades even when multiple systems are upgraded for the same location.



#### 2.1.4.2 Deep Energy Retrofits

---

Deep energy retrofits are a holistic approach to Energy Conservation Measures, viewing each system as part of a broader interdependent and parametric building systems matrix. A deep energy retrofit ideally looks at the interaction of systems and their impact on system sizing, associated cost and operations and maintenance costs throughout the useful life of the building systems matrix. Target savings of 30% in annual energy costs are expected for Deep Energy Retrofits. There is an increased focus on evidence-based improvements in occupant productivity, health and wellbeing and the value that this brings to both owners and occupants. In deep energy retrofits, as differentiated from energy retrofits, thermal management at the building envelope is considered holistically alongside the mechanical heating and cooling systems as part of the interrelated whole.

#### 2.1.5 High Performance Office Buildings

---

At the same time as building repositioning is growing as an essential market sector for commercial office buildings, new high performance Zero Net Energy (ZNE) buildings are showcasing the future of building technology at the nexus of environmental sustainability and the workplace of the future. Recent ZNE office buildings like The Edge, Deloitte's headquarters in Amsterdam, Bloomberg Headquarters in London, and The Tower at PNC Plaza in Pittsburgh, each took a decisive and distinct approach to both the building envelope and mechanical heating and cooling. While there is an enormous focus on upgrading existing building stock and existing portfolios, these new buildings represent contemporary values and showcase the very best in advancements in building technology. These types of showcase projects offer a halo effect for new technologies to develop and trickle down to other building typologies in other sectors as well as drive innovations that may be applicable to building repositioning. While all ZNE buildings are high-performance, not all high-performance buildings are ZNE; however, they share many similar system choices, such as radiant systems for mechanical heating and cooling.

## 2.2 Critical Approach: Building Envelope as Energy Transfer Function

---

Contemporary approaches to thermal management design of the building envelope tend to address thermal loads through the resistance or transmittance (e.g., reflection, absorption, transmission) of convection, conduction, and radiation (Olgyay et al., 2015). Such building envelope systems (e.g., terra cotta rainscreen, double glazed curtain walls, etc.) either absorb excessive heat or reject useful heat into the local environment using a combined strategy of insulation and natural or mechanical heating, ventilating and air conditioning. Since conventional envelopes do not adapt to the dynamic diurnal and seasonal shifts in solar radiation or the cyclical energy loads generated by programmed use and occupancy patterns, to maintain acceptable levels of human comfort, buildings depend heavily on mechanical systems, leading to high-energy consumption and inefficient building energy profiles.

Recent commercially deployable state-of-the-art building envelopes that modulate thermal energy primarily include; automated louvres as external shading devices, automated mechanical ventilation strategies usually coupled with double skin facades, integrated blinds within the building fenestration, and thermochromic or similar glazing technologies (Dyson, 2008). Widespread adoption of these commercially deployable systems has been met with limited success and currently do not provide significant impact on building energy profiles of energy usage in the building sector due to a variety of factors including: lack of integration with complementary building systems, and both real and perceived initial costs with unfavorable cost payback periods (WBCSD, 2015).

## 2.3 Effect of the Building Envelope on the Building Energy Profile

---

Within the context of the building energy use profiles, the building envelope represents the greatest singular potential energetic gain or loss - as much as 50% in the commercial building sector - and thus offers the greatest opportunity to address

overall energy effectiveness within the built environment (International Energy, Directorate of Sustainable Energy, & Technology, 2013). The building envelope, in one way or another, impacts every building system that seeks to maintain thermal comfort. As space heating, cooling and ventilation have the largest amount of associated energy use, each of these systems has a significant portion of their associated energy expenditure parametrically linked to the performance of the building envelope. Therefore, a change in energy flows through the building envelope has a significant impact on the building energy profile, the costs of buildings systems and the cost to operate the building over its lifecycle.

### 2.3.1 Principles of Energy Transfer at the Building Envelope

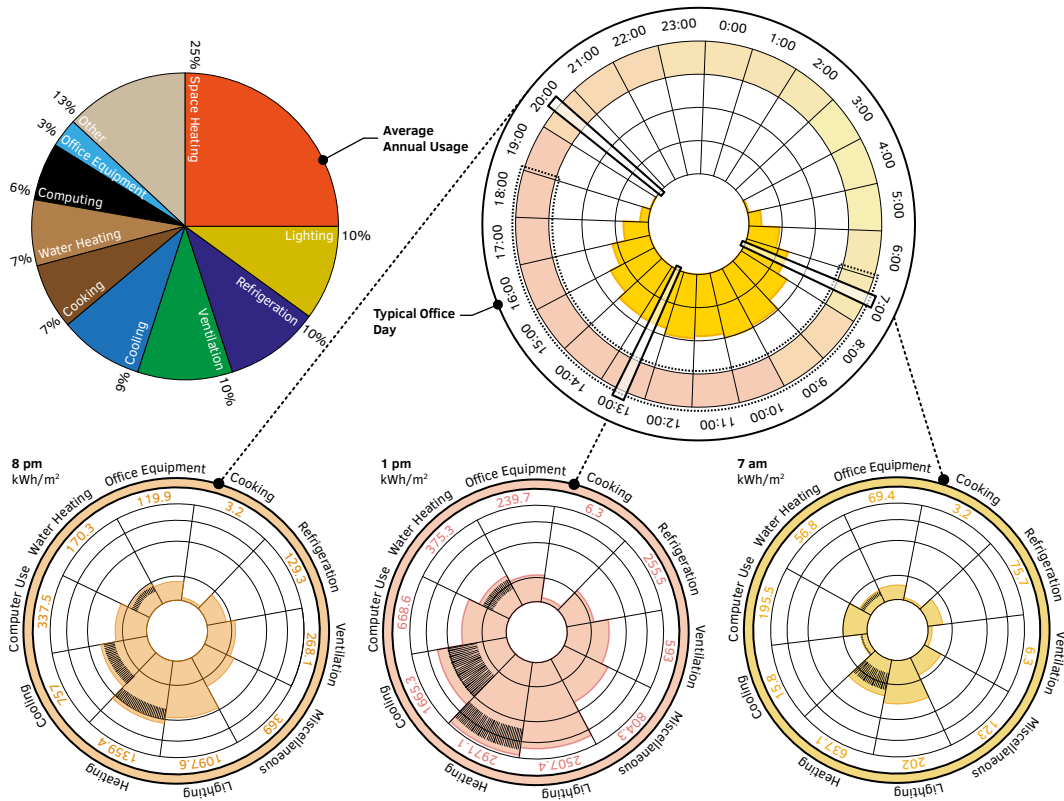
---

Thermal transfer at the building envelope is governed primarily by Conduction, Convection, Radiation considered as first principles and Advection and Diffusion in the form of Mass/Energy Transfer and Capacitive Storage as secondary principles. Energy transfer is guided by several critical variables: surface area, flowrate and capacitive storage.

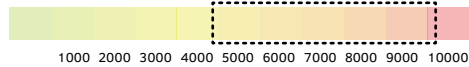
#### 2.3.1.1 Energy Resources and Demands

---

Energy demands have been typically characterized as the energy loads required to operate a building. Specifically, in commercial buildings energy demands have been accounted for by, space heating, cooling, ventilation, water heating, lighting; refrigeration, office equipment, and computing, etc. The demand profile of a building is regular and predictable, and ultimately the annual demand profile must be met by energy resources. In New York State, for example, those resources come predominantly in the form of electricity, produced primarily from natural gas, nuclear power and hydroelectricity, that accounts for about 90% of the electrical generation, with renewable resources other than hydroelectric rounding out the rest. These renewables consist primarily of wind power, biomass, and photovoltaic generation. When developing Zero Net Energy approaches to building design, reducing the reliance on non-renewable resources is a crucial strategy. When further trying to utilize locally available resources to reduce transmission losses, the renewable resource strategy to meet the energy demands refocuses, therefore on wind power and photovoltaic generation (Administration, 2015).



Spectrum of Avg Energy Usage for New York City



Fluctuating User Preferences + Building Demand Loads

Building Load for 3,716 m<sup>2</sup> Commercial Office Space  
(kWh/m<sup>2</sup> Value Relative to Radial Area)



FIG. 2.2 Solar resource and demand profile of a typical office building annually and usage per hour.

The typical energy demand profile, as shown in Figure 2.2, shows energy use in a typical commercial building of one day with the superimposition of available solar resources. Figure 2.3 shows: 1) how often the local resources of wind and solar are available on an annual scale using the Typical Meteorological Year 3 (TMY3) data for New York City and, 2) shows when on an annualized hour by hour basis when local resources are available to address the demand profile. Perhaps most importantly, Figure 006 shows the volatility index of the available resources. Taken altogether, this tells a story of a fluctuating resource and rhythmic demand. The TACE system has been developed to match the locally available resources with the demand profile rhythm.

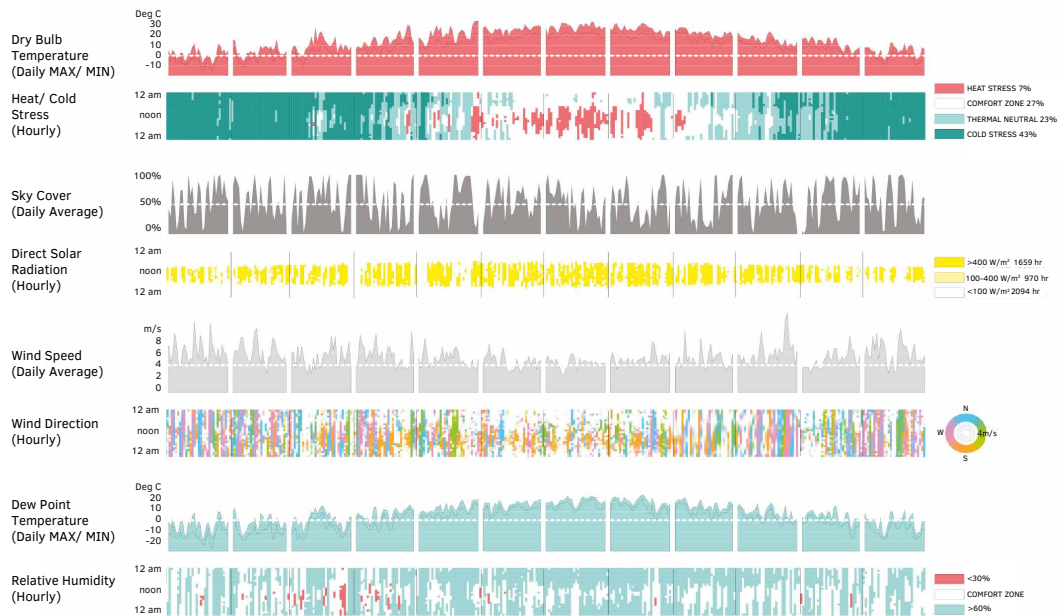
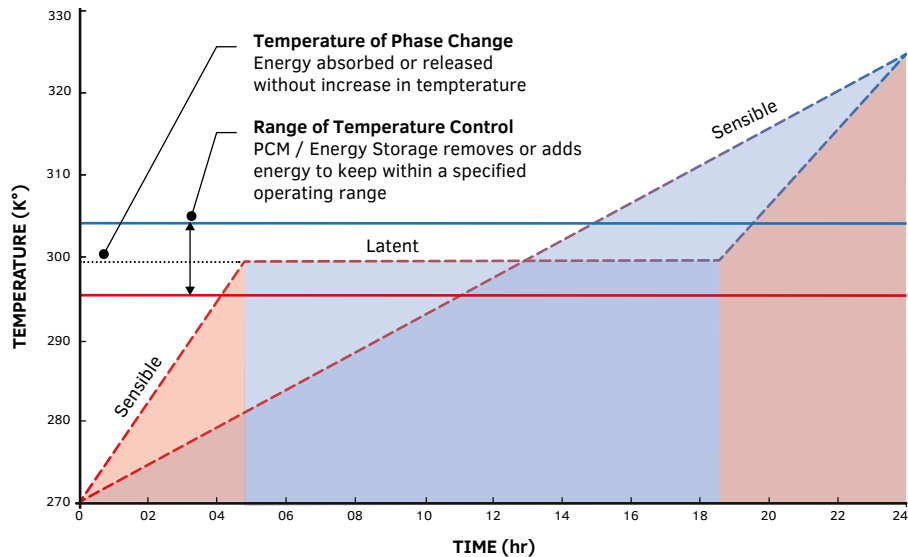


FIG. 2.3 New York City temperature, solar, wind, humidity availability and quantity of local climate derived loads and resources and volatility index of these available resources.

### 2.3.1.2 Latent and Sensible Heat

Sensible heat is heat energy that changes the temperature of a thermodynamic system, whereas latent heat is heat energy stored within that system without raising the temperature. The ability of materials to absorb sensible or latent heat as a thermal mass is a stabilizing agent against the peaks and valleys of typical energy loads transferred through the building envelope. Common brick, for example, has a specific heat capacity ( $C_p$ ) of  $921.1 \text{ J/kg}^\circ\text{C}$   $.22 \text{ Btu/lb}^\circ\text{F}$ . This relatively high  $C_p$  allows more sensible heat to be absorbed before effecting the surrounding environment, including the building occupants (Lechner, 2015). Thermal mass has traditionally been used to buffer temperatures by aligning the specific heat capacity of a material with a material quantity and material location (e.g., exposure to solar insolation) to balance high diurnal temperature fluctuations. Functionally, a design that incorporates a phase change material allows the absorption of sensible heat in one part of a two part dynamic cycle and then releasing that heat as latent energy during the other part of the cycle as shown in Figure 2.4.



**FIG. 2.4** Thermal shifting of latent versus sensible heat. Capturing heat energy and storing it as latent energy for use later when the demands of the building require sensible heat is a key strategy to matching resources and demands in and around the building envelope.

The primary drawbacks of using traditional thermal mass as a primary building envelope strategy are: the limits of available climates with the proper characteristics to take advantage of passive thermal mass; the difficulties in controlling the rate of energy flow in and out of the mass to adjust to dynamically fluctuating internal and external loads; the requirements of extremely dense, and thus heavy, material located at or near the building envelope; the modern requirements for a stabilized and predictable interior temperature that contributes to acceptable thermal comfort. Therefore, contemporary envelopes have, at best, utilized passive thermal mass as a secondary and mostly internal strategy for thermal management (e.g., the transmission of energy through fenestration to be absorbed in concrete floors, brick walls, etc.). Materials with thermal mass characteristics (e.g., concrete block and panels, brick, terra cotta tiles and rainscreens, etc.) used as part of the envelope assembly are more often chosen for aesthetic considerations. This decision basis has led to conventional building envelope strategies that rely upon insulation to resist energy transfer across the building envelope demarcation line and typical mechanical heating and cooling that has been disengaged from the energy transfer occurring at the building envelope. The TACE system is developed to merge the attributes of mass-based building materials with the dynamic performance of adaptive facades providing a more dynamic envelope system than typical mass-based assemblies.

Thermo Active Building Systems (TABS) are a mass based thermal management system that uses a working fluid to charge or release the mass of thermal energy by moving heat. Typically, TABS use thermal loops to move energy from a source (i.e., water boiler source, ground source, geothermal source, etc.) to a terminal (i.e., radiant slab, ceiling panel, wall panel, etc.) for thermal delivery. Countercurrent energy exchange as proposed in this dissertation assumes the loops move energy between interior and exterior spaces, using both terminals as sensible heat on the exterior of the building envelope and the interior of the building envelope. This process is coupled with latent energy storage within the building envelope to create a matrix of countercurrent relationships. The dynamic ability of the TACE system allows for the qualities of mass-based material assemblies applied to a broader range of climate profiles and regions.

### 2.3.1.3 Conduction, Convection and Radiation

---

The heat transfer at the building envelope is characterized by the equation (in W/m<sup>2</sup>K):

$$\dot{Q} = AU(T_{inside} - T_{outside})$$

Heat is transported through the building envelope generally by three means; Conduction, Convection and Radiation. Conduction is the heat flow on the molecular scale. More heat energy flows via conduction as a material gets more conductive, as the surface area increases, and the temperature differential is greater. Convection is the heat conveyed as the thermal energy of a mass that is displaced. Radiation is heat transfer by electromagnetic waves. Heat also moves from higher temperature to lower temperature (Lechner, 2015). Building envelope design has developed to mitigate Conduction, Convection and Radiation wherever possible through the building envelope, resisting the natural flow from hot to cold. Driving the building envelope design is the demarcation between the exterior and the interior, as illustrated in Figure 2.5, and most approaches try to resist thermal transfer, measured as a U, G or R-values across the demarcation line.

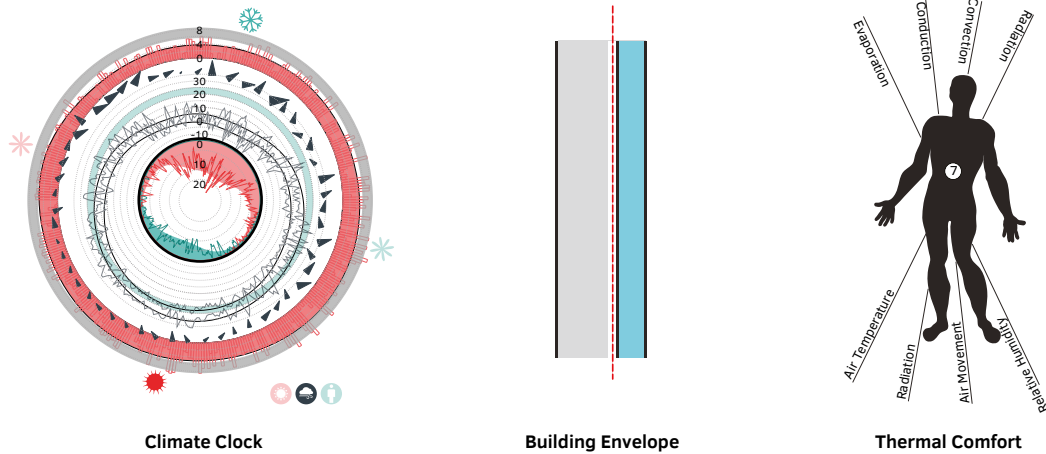


**FIG. 2.5** Diagram of the forces of demands and the demarcation line separating the interior from the exterior of the building envelope that also illustrates the variables in the basic heat transfer equation. Developed from Klein (2013).

### 2.3.1.4 Dynamic Thermal Effects

The ability to control energy transfer rates through the building envelope can be developed by storing and releasing sensible heat as latent heat in a controllable countercurrent heat exchanger arrangement, effectively creating Active Thermal Mass. By controlling both the storage and release of heat energy, Active Thermal Mass can achieve the same balancing effects, without the required quantities of materials used in passive thermal mass strategies. Dynamic thermal effects can be developed by modulating the relationship between the sensible thermal conductors and latent heat storage. Phase Change Material (PCM), for example, stores large quantities of thermal energy as latent heat; up to 14 times more heat can be stored by PCM's than stored in a sensible solution (Lechner, 2015). Furthermore, PCMs hold a set melting temperature and transitions between phases when environmental temperatures fluctuate, absorbing or releasing thermal energy dynamically and adaptively. An appropriately selected set melting temperature can be used as a reliable switch for temperature stabilization by converting sensible heat to latent heat, without increasing temperature. When coupled with an advective working fluid to augment thermal transfer with varying flow rates, the rate of energy exchange and direction of energy flow can be controlled to create the active mass property for energy vectoring.



### 2.3.1.5 Flow Rates, Surface Areas and Material Effects

The manipulation of localized geometry has the potential for building envelopes to move away from planar components and take advantage of available energy flows, creating optimized forms for absorbing, reflecting or offloading energy. Energy transfer through the building envelope can be manipulated using localized geometries of the building envelope components. Variations in component geometry take advantage of multiple energy flows through the building envelope where the manipulation of the aspect and surface ratio of geometries can switch component performance from absorbing to offloading and slow or speed up the rate of energy transfer. These geometries can be further refined to fit specific climatic performance needs (Vollen, 2008).

### 2.3.1.6 Countercurrent Energy Exchange

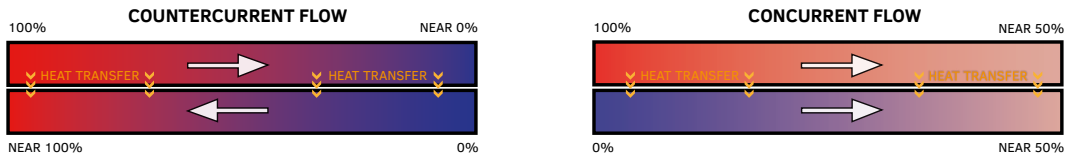


FIG. 2.6 Diagram of counter vs concurrent flows. Countercurrent flows can exchange 50% more than concurrent flows

Countercurrent energy exchange is an effect where two fluids are placed in opposing flows as compared to concurrent flows. The impact of this flow arrangement is that energy exchanged can be increased by 50%, as illustrated in Figure 2.6. While countercurrent energy exchange is found commonly in natural systems (e.g., the skin of lamnid sharks, the feet of ducks, limbs of mammals), it has been used successfully in building system for decades as enabling principles for heat recovery and heat exchangers in mechanical heating, cooling and ventilating systems. As discussed in more detail in this Chapter, countercurrent energy exchange can also be used across the building envelope demarcation line in several ways. Countercurrent is the primary method of energy exchange in the TACE System, as shown in Chapter 4.

## 2.4 Summary

---

The development of the Thermal Adaptive Ceramic Envelope (TACE) system was based on several key factors:

- The role of the building envelope in the changing landscape of policy, commercial market and socio-economic pressures
- The reframing of the building envelope as part of the heating and cooling system as an active and adaptive system
- Leveraging the fundamental principles that govern thermal flows in, around, and through the building envelope

The critical context provides a real work scenario to develop the research as a response towards functioning prototypes, systems design and real-world performance metrics. This approach to system development using the guidance of multifaceted - and seemingly disparate conditions - is a way to develop new systems in a complex context and frames an architectural approach to research. Chapter 3 was developed as a response to this critical context with a focus on real world scenarios and drives the structure of the overall literature review to focus on the development of:

- key pieces of literature in the last 40 years which delineate design approaches and envelope systems developed to influence thermal transfer at the building envelope in nontraditional ways
- key precedents that highlight the design and development of thermal systems as Thermo-Active Building System (TABS), and ultimately position the transition of TABS as an adaptive thermal envelope strategy

To address the breadth of the critical context, both a historical and technical look at the literature and precedents was developed within sequencing of the Chapter 3.

## References

- Alliance Commission on National Energy Efficiency Policy. (2013). The History of Energy Efficiency. Retrieved from [https://www.ase.org/sites/ase.org/files/resources/Media%20browser/ee\\_commission\\_history\\_report\\_2-1-13.pdf](https://www.ase.org/sites/ase.org/files/resources/Media%20browser/ee_commission_history_report_2-1-13.pdf)
- Architecture 2030. (2017). The 2030 Challenge. Retrieved from [http://architecture2030.org/2030\\_challenges/2030-challenge/](http://architecture2030.org/2030_challenges/2030-challenge/)
- Dyson, A. & Vollen, J. (2008, 2016). The Center for Architecture Science and Ecology (CASE). Retrieved from <https://www.case.rpi.edu/>
- Sinreich, E., Leifer, D., North, R. & Bobker, M. (2010). Energy Efficiency Retrofitting For NYC Commercial Buildings. Retrieved from New York <http://www.baruch.cuny.edu/realestate/pdf/Evolving-Landscape.pdf>
- Flanagan, T. (April 15th, 2014). Smart Repositioning Strategies for Real Estate. Home & Architecture. Retrieved from <http://marketsmedia.com/smart-repositioning-strategies-real-estate/>
- International Energy Agency (IEA), Directorate of Sustainable Energy, Policy & Technology. (2013). Transition to sustainable buildings: strategies and opportunities to 2050. International Energy Agency. Paris, France.
- Lechner, N. (2015). Heating, cooling, lighting: sustainable design methods for architects. Fourth Edition. John Wiley & Sons. Hoboken, New Jersey.
- Alvarez & Marsal. (2013). Commercial Real Estate Competitiveness Study. Retrieved from [https://edc.nyc/sites/default/files/filemanager/Resources/Studies/Commercial\\_Real\\_Estate\\_Competitiveness\\_Study.pdf](https://edc.nyc/sites/default/files/filemanager/Resources/Studies/Commercial_Real_Estate_Competitiveness_Study.pdf)
- McArthur, J., Jofeh, C., & Aguilar, A. (2015). Improving Occupant Wellness in Commercial Office Buildings through Energy Conservation Retrofits. Buildings, 5(4).
- Olgay, V., Olgay, A., Lyndon, D., Reynolds, J., & Yeang, K. (2015). Design with Climate: Bioclimatic Approach to Architectural Regionalism - New and expanded Edition (Revised ed.): Princeton University Press.
- Sanders, A. & Sanders, R. (2003). Forecasting Building Envelope Reliability and Preparing for Inevitable Deterioration. Hoffman Architects Journal, 21(1).
- Schoen, L. (2010). Preventive Maintenance Guidebook: Best Practices to Maintain Efficient and Sustainable Buildings Third Edition. BOMA International. Washington, D.C.
- Shorris, A. (2014). New York City's Roadmap to 80 x 50. Retrieved from [www.nyc.gov/onenyc](http://www.nyc.gov/onenyc)
- United States Energy Information Administration (EIA). (2015). Commercial Buildings Energy Consumption Survey (CBECS). Retrieved from <https://www.eia.gov/consumption/commercial/>
- Vollen, J., Winn, K., Laver, J., & Clifford, D. (2008). Digital Material: Ecological Response in Parametric Modeling. Architecture in the Age of Digital Reproduction. Paper presented at the ACSA West Central Fall Conference.
- World Business Council For Sustainable Development (WBCSD). (2015). Energy Efficiency in Buildings: Action Plan. Retrieved from 115 Fifth Ave, 6th Floor, New York, NY 10003.
- Hart, Z., McClintock, M., Olgay, V., Jackaway, A. & Bendewald, Michael. (2013). Deep Energy Retrofits: An Emerging Opportunity. Retrieved from <http://www.aia.org/aiaucmp/groups/aia/documents/pdf/aia099241.pdf>

# 3 Precedents

---

Conventional approaches to building envelope system designs typically mitigate thermal transfer through the resistance or transmittance (e.g., reflection, absorption, transmission) of convection, conduction, and radiation, as discussed in Chapter 2, Section 2.3.1. An alternative approach is to enhance and control thermal transfer by the capture, transformation, storage, and distribution of thermal energy across the building envelope as the thermal transfer strategy as opposed to one that relies on mitigation.

The nature of the critical context as delineated in Chapter 2 was broadly defined within three buckets as *policy*, *market*, and *technique*, as well as creating a real world scenario. Therefore the approach to precedents in this chapter are focused on design led initiatives that resulted in prototypes or evolutionary thinking within the field. Through this lens the Chapter 3 discusses the key supporting literature, significant precedents in both research and architecture projects, and a survey of various energy transfer focused building envelope types to place the research in both the historical and critical contexts.

## 3.1 Introduction

---

TACE was developed to be part of a class of thermal management systems known conventionally as Thermo-Active Building Systems (TABS) (found also in the literature as 'Thermo Active Building Systems' and 'Thermally Active Building Systems') (Schmelas et al., 2015). TABS typically use a working fluid to distribute energy and mass to deliver energy. These systems traditionally are interior systems as described in Section 3.3 with several notable exceptions. The following literature summary and precedents are used to illustrate both history and current state-of-the-art systems, as well as a timeline for the development of major evolutionary milestones. These influences were used to inform the development of the proposed TABS configuration options and ultimately to the TACE system as explored in this dissertation.

## 3.2 Literature Summary

---

The literature review summary was focused on the prior research and designs instrumental in the development of thermal management through adaptive building envelopes. Those referenced systems and seminal figures in the field have been the driving and enabling influences for the development of the TACE system.

The multifunctional wall system was described succinctly as the Polyvalent Wall in Mike Davies' seminal text *A Wall for All Seasons* (Davies, 1981), described in Figure 001. From a lineage perspective, the most direct link to the Polyvalent wall as a design evolution is the integrated or liquid façade I and II as described by Knaack (2007) and Knaack and Klein in *Imagine No 1: Facades* (Knaack et al, 2008), as shown in Figure 002. In addition, presenting the foundation for TACE design as an integrated system is the book by Knaack, Klein, Bilow, and Auer *Facades: Principles of Construction* (Knaack et al., 2007) which frames the landscape as a whole of integrated facades. Of particular note was the framing of a new purpose for the building envelope: as an active and critical participant that navigates between the energy resources and energy demands as shown by Klein in *Integral Façade Construction* (Klein, 2013) and which the diagrams in Figure 2.5 and its derivatives in Figures 4.6 and 4.8 are based on.

From the perspective of high-performance facades in office buildings, Selkowitz and the work of Lawrence Berkeley National Laboratory (LBNL) has driven both technology development and design tool development. Many works from Selkowitz and LBNL - going back decades - can be considered seminal to the field. High-performance commercial building façade (Lee, Selkowitz, Bazjanac, Inkarojrit, & Kohler, 2002), captures a broad view of the territory and discusses, in a preliminary way, the demand/response for active façades moving forward. While this is not the first publication to do so, it is both a culmination of the-state-of-the-art in high-performance facades. The trend at the time was focused predominately on glass, and a transition to the active and ultimately the adaptive facades that have been developing since.

The Integrated Concentrating Solar Façade (ICSF) by Dyson was developed in the early 2000s and was initially published as a manuscript *Integrated Concentrating Solar Façade System* (Dyson et al., 2007). This system leverages the building envelope for structural support that houses a Fresnel lens integrated tracking solar photovoltaic system. In order to keep the system cool and to operate at peak efficiency, an active working fluid cooling system was integrated into the back of

each module. This heat was then captured and repurposed for building systems. One of the key aspects that made the ICSF unique was its function as a transparent shading device. While the system does not transfer energy from the inside of a building, it did showcase an example of a façade integrated combined heat and power system in a unitized curtain wall format that has been hugely influential in the context of next generation façade integrated building systems. Perhaps most importantly, the development of the ICSF led to the founding of The Center for Architecture Science and Ecology (Dyson & Vollen, 2008) (CASE). CASE, at the time of its founding, was a radical collaboration model, combining the academic and research world of Rensselaer Polytechnic Institute (RPI) with professional architects, urban planners, interior designers, and engineers of multiple industrial collaborators, including founding partner, Skidmore, Owings & Merrill LLP (SOM). Through this partnership, the boundaries of environmental performance in urban building systems on a global scale were being tested both in the research laboratory and in actual building projects as testbeds. The parallel process of tracking architectural research as part of the development of architectural projects provided a direct model for the development of the TACE system. CASE, in many ways, was structured similarly to the Façade Research Group (now Architecture Façades and Products Research Group founded by Knaack and Klein) at TU Delft.

Also developed at RPI, concurrent with the development of the ICSF and the founding of CASE, Xu, Dessel, and Messac, advanced a thermoelectric façade module published as Study of the performance of thermoelectric modules for use in active building envelopes (Xu et al., 2007). Unlike ICSF, this system proposed to utilize energy flows in two directions across the building envelop demarcation line to power a thermoelectric generator. In many regards, this system was similar to and falls in between both Davies' Polyvalent Wall and Knaack's Integrated Wall as an example of active façade typologies.

While radiant heating and cooling have been around for thousands of years in one form or another, Olesen in Thermo Active Building Systems Using Building Mass To Heat and Cool (Olesen, 2012) succinctly characterized the active mass using a mechanically driven working fluid as a modern building integrated system; this directly supported advancing energy use policies in the built environment and overall high performance design strategies. The descriptions of TABS in Olesen's works provided a robust platform to discuss TABS as an envelope system, an evolutionary step in the development of adaptive building envelope systems.

The specific landscape of adaptivity in facades was described Loonen in Climate adaptive building shells: State-of-the-art and future challenges (Loonen et al., 2013). TACE, as a form of TABS, was classified as a Climate Adaptive Building Shell

(CABS). Loonen makes a case for the need for multifunction building envelopes that could combine the advantages of passive and active systems into adaptive systems that are more easily able to address the challenges of sustainability and environmental stewardship.

Co-simulation, as a modelling technique discussed and utilized in 6, was developed by Wetter in A View on Future Building System Modeling and Simulation (Wetter, 2011) and discussed in more detail in Functional mock-up unit for co-simulation import in EnergyPlus (Nouidui et al., 2014). Wetter, also associated with LBNL, pioneered co-simulation which forms the foundation for Shultz's dissertation A Framework for Modeling Complex Integrated Building Systems at Whole-Building Scale with Co-Simulation: Applied to a Coupled Simulation Between a Facade System Model and a Whole Building Energy Model (Shultz, 2018). Shultz conducted his dissertation on co-simulation, which was done concurrently with the research of this dissertation and directly supported the modelling and simulation of the TACE System in Chapters 5 and 6.

Extemporaneous sources include the broad summary by Zhang A Review of Building Integrated Solar Thermal (BIST) Technologies and their Applications (Zhang, 2015) as redrawn in Figure 3.11-3.13 in Section 3.3.3. This review further refined the territory that the TACE System inhabit. The research in this dissertation concludes that there is a need to advance control systems in developing state of the art adaptive building envelopes, as discussed in Chapter 8. Schmelas discussed this same need for TABS in Adaptive predictive control of thermo active building systems (TABS) based on a multiple regression algorithm (Schmelas et al., 2015). The use of algorithms to support CABS – and the TACE system – was an evolutionary step in the development of these same systems described for use by TABS (Schmelas, 2015).

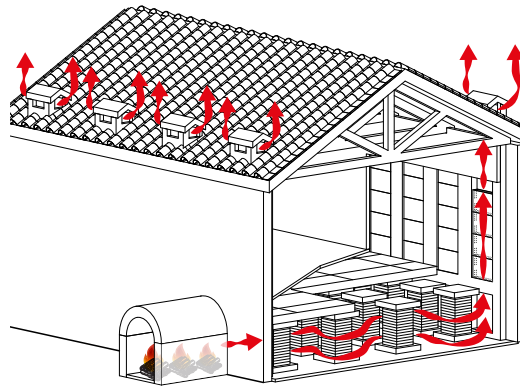
The key findings of the literature review show: 1) there has been growing development in systems that transfer rather than mitigate energy at the building envelope over the last half century, 2) significant need has been demonstrated for developing alternative approaches to how energy is treated at the building envelope, and 3) and significant advances in alternative systems have been developed over the last two decades as shown in several examples the precedents in Section 3.3. While this literature summary is not exhaustive, it highlights the lineage of influence on this research and shows similar precedent systems as a basis for the development of a new system.

### 3.3 Precedents

The sophisticated use of charging a thermal mass with a working fluid to heat a space can be traced back to the Roman hypocaust as shown in Figure 3.1; in the 1st century B.C. Vitruvius described the hypocaust in book X of *de architectura* (Pollio & Morgan, 1914). The hypocaust used heat from a source, wood burning fire, distributed using a working fluid, (air), to a thermal mass to charge and radiate, ceramic brick and tile. Similar systems have appeared in myriad cultures for thousands of years. Modern thermal Thermo Active Building Systems behave in remarkably similar ways; energy from a point source is distributed through a working fluid to charge a mass.



1

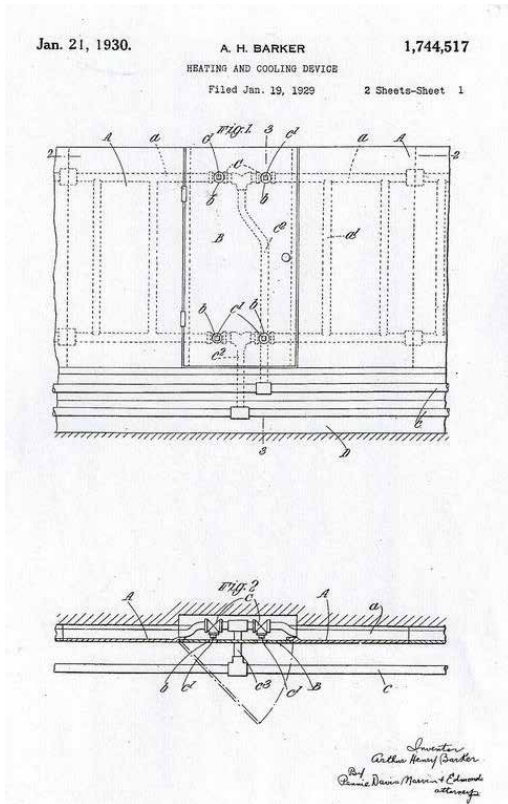


2

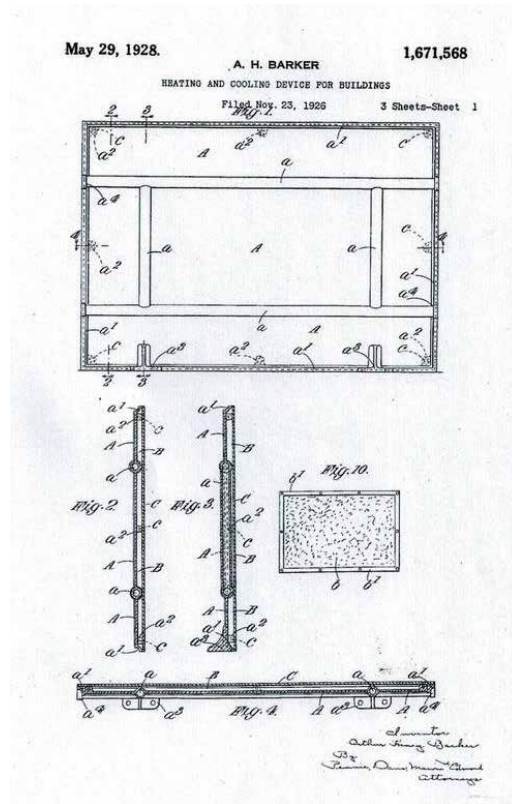
**FIG. 3.1** hypocaust (Hypocaust, 2019) image (1) and diagram (2) showing the flow of heat from the point source to radiant surfaces.

Radiant slabs are the most ubiquitous deployment of TABS. Modern types of mass embedded radiant systems have been used for over a century. In 1907 A.H. Baker developed the first radiant panel, similar to what is shown in the 1930 US Patent drawing as shown in Figure 3.2 that used small pipe arrays for energy transport and large building surfaces as the delivery of heat. He was granted U.K. Patent No. 28477 with rights assigned to the R. Crittall and Company which installed these systems in both residential and commercial developments.





1



2

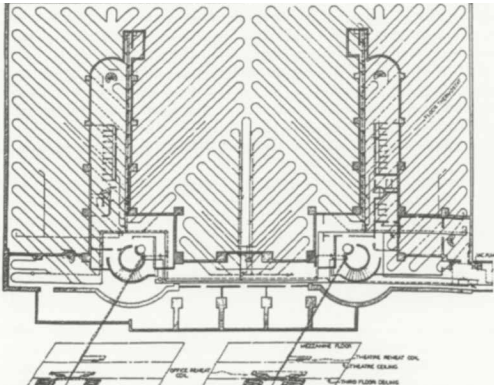
FIG. 3.2 Radiant panel patent diagrams (1,2) from A.H. Baker.

Structural Engineer Oscar Faber, along with mechanical specialist Robert Kell, as part of the redesign of the Bank of England building project in 1924-1933, deployed radiant heating and cooling using embedded pipes in reinforced concrete (Bean, 2010). Eventually, Oscar Faber & Partners would join with G. Maunsell & Partners to become Faber Maunsell. In 2009, Faber Maunsell was acquired by AECOM Technology Corporation.

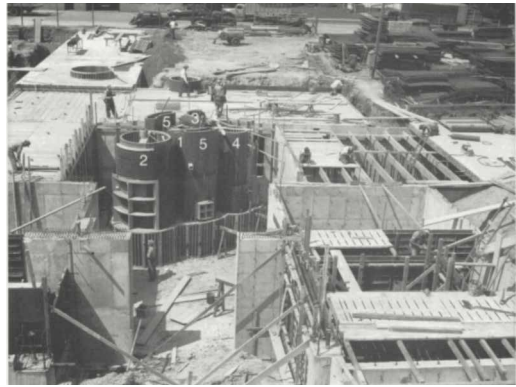
Architect Frank Lloyd Wright used radiant floor heating in the Johnson Wax Building in 1937 and his Usonian houses such as the Pope-Leighey House in 1939, as shown in Figure 3.3. The housing boom in the United States following World War II led to innovations that sped up homebuilding to comply with the demand. Levitt and Sons built thousands of homes that removed the traditional basement in lieu of a slab on grade which allowed deploying radiant heating on a mass scale.



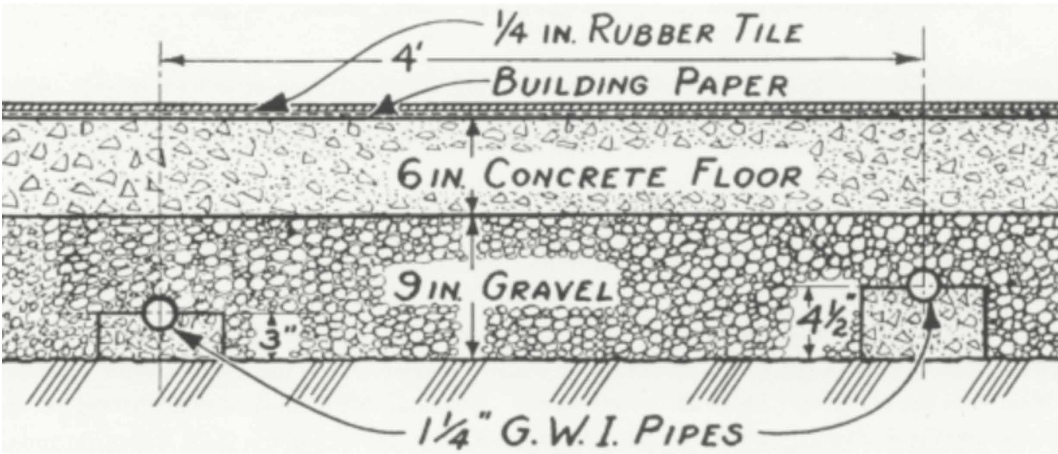
1



2



3



4

**FIG. 3.3** Frank Lloyd Wright drawings and photographs of radiant systems in both residential in the Pope-Leighey House (1) (Komp, 2017) and commercial projects as shown as part of the heating and cooling systems for the Johnson Wax building (2,3,4) (Siry, 2013).

These prior mentioned deployments made use of steel or copper pipes embedded in concrete; an arrangement that had a limited useful lifespan. German inventor Thomas Engel is primarily credited with inventing modern Cross Linked Polyethylene (PEX) tubing in 1967 to apply radiant heat to livestock areas. Engel licensed the technology process to Wirsbo, now Uponor, who become a global manufacturer and distributor of PEX tubing for various applications. PEX had the advantage of the flexibility and lower cost than copper and steel, and while susceptible to degradation by UV light, this was seen as an advantage for embedding this piping in radiant applications creating a recombinant system between the PEX and the concrete mass, as shown in Figure 3.4. PEX tubing, much advanced in its current form, is the standard piping for radiant hydronic systems.

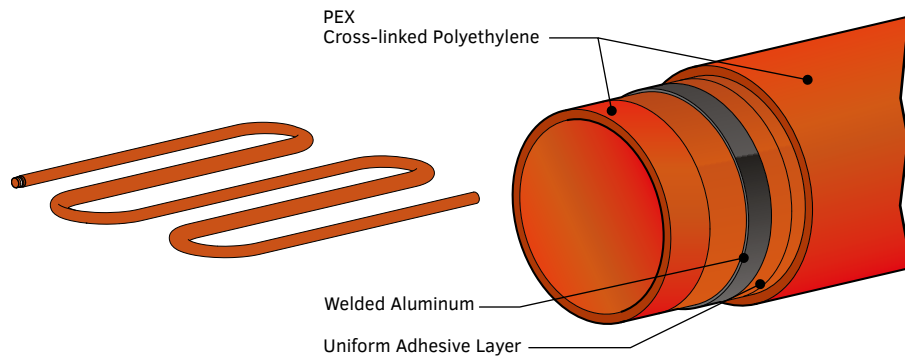


**FIG. 3.4** Modern Pex-Al-Pex piping used in almost all TABS radiant floor installations and products. Pex has less than 10% of the conductivity of comparable metal pipe, which, on the one hand, limits the thermal transfer rate, and on the other protects against sweating and as a flexible material protects against freezing as well.

Since 2012, the International Standards Organization (ISO) has produced ISO 11855 Building environment design - Design, dimensioning, installation and control of embedded radiant heating and cooling systems that describe seven types of radiant systems as shown in Figure 3.5.

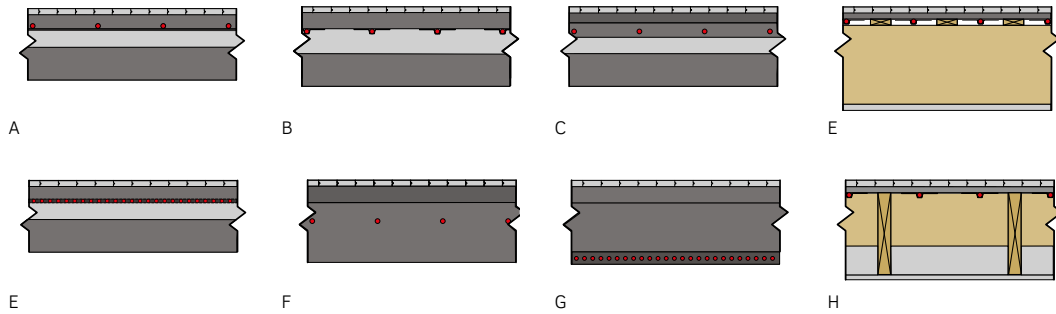


**FIG. 3.5** Arrangements of the various TABS radiant flooring systems. Type A: with pipes embedded in the screed or concrete (“wet” system). Type B: with pipes embedded outside the screed (in the thermal insulation layer, “dry” system). Type C: with pipes embedded in the levelling layer, above which the second screed layer is placed. Type D: include plane section systems (extruded plastic/group of capillary grids). Type E: with pipes embedded in a massive concrete layer. Type F: with capillary pipes embedded in a layer at the inner ceiling or as a separate layer in gypsum. Type G: with pipes embedded in a wooden floor construction. Adapted from ISO 11855.

While all of these variations are radiant systems, the configurations that are more commonly discussed as TABS are those where the mass component of the system has a recombinant effect to the heat and coolth energy of the working fluid. A typical deployment of a radiant slab that uses this mass in commercial buildings is Type A and C where a zone loop is embedded into the concrete slab for use as a floor or ceiling. The benefit of these configurations is that it can be charged over time with a low temperature gradient and hold that temperature stabilizing the adjacent spaces through the force of thermal inertia as a function of the thermal capacity of the mass. It can be charged to different levels depending on the demand, and the capacitive storage of the system can be considered to be dynamic. Countercurrent flow occurs between the working fluid (fluid 1) loop and the air (fluid 2) moving across through the slab mass. This arrangement differs from two flows in counter-currency as the airflow is chaotic, as shown in Figure 3.6 and is only for direct concurrent flow state coincidentally when the airflow aligns in the opposite direction of flow with the working fluid within the mass.

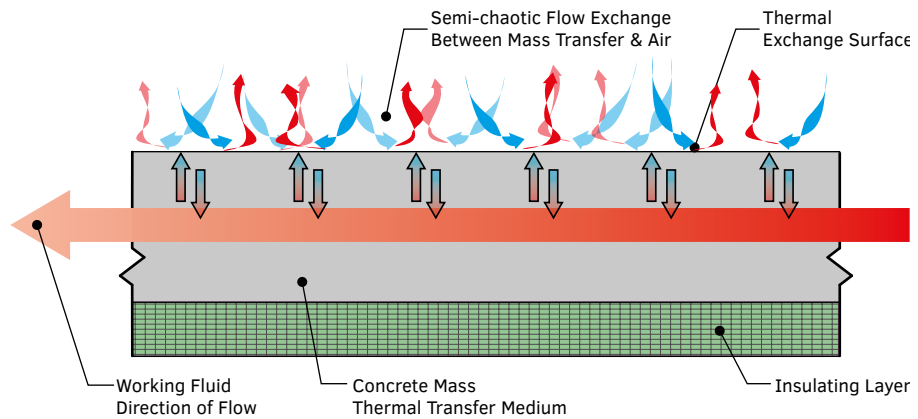


FIG. 3.6 Flow conditions and thermal exchange for TABS radiant floor configuration.

In the 2017 report, Energy Performance of Commercial Buildings with Radiant Heating and Cooling benchmarks buildings with radiant systems against the national averages for their respective building types. Commercial buildings with radiant slabs have been shown to have an average of 22%-27% lower Energy Use Intensity (EUI) than comparative buildings, as shown in Figure 3.7, and as a group approach the highest performing buildings that are known as Zero Net Energy (ZNE) or Net Zero Energy Capable (Higgins, 2017).

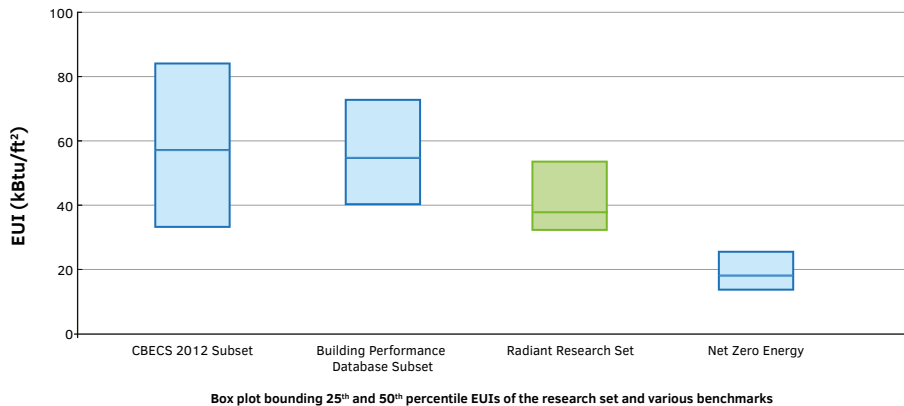
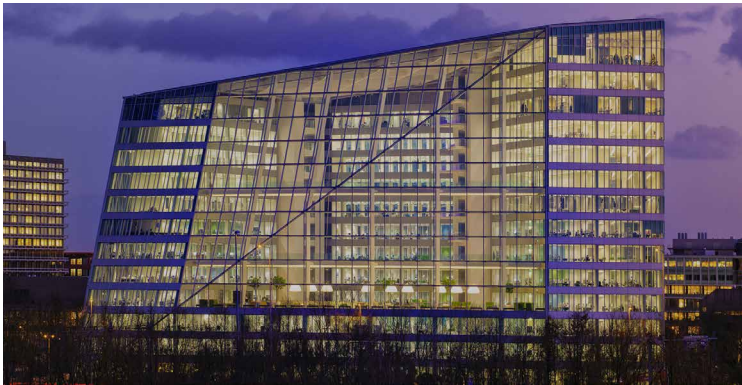


FIG. 3.7 Prevalence and relative performance of buildings that use radiant systems as a subset of high performing buildings. Redrawn (Higgins, 2017).



### 3.3.1 Thermo Active Radiant Panels

A derivative of the radiant slab is the radiant panel. Rather than using the mass of the concrete as a heat sink or source, the radiant panel uses countercurrent flow either directly exchanging energy with the air (fluid 2) or transferring energy to a metal (radiant) panel that exchanges with fluid 2, as shown in Figure 3.8, to exchange thermal energy. The SIG Air Handling Company, for example, has developed several versions of the radiant panel in the form of the Climate Ceiling and the Climate Island. This system has been installed in several projects developed by OVG Real Estate, including their headquarters in Las Palmas, Rotterdam (SIG, 2016). The Climate Ceilings were showcased prominently in The EDGE, Deloitte's headquarters in Amsterdam and was considered the most sustainable office building in the world for several years with a sustainability score for the building of 98.36% (BREEAM-NL). In 2017, the Bloomberg Headquarters by Fosters + Partners was completed and took the lead with a sustainability score of 98.5% which also uses an active ceiling panel to aid in heating and cooling, (BREEAM-UK).



1



2

FIG. 3.8 Radiant panels (2) as part of the net zero strategy in the EDGE office building (1). (SIG, 2016)

### 3.3.2 Thermal Active Mullions

In 1968 Joseph Gartner, now part of the Permasteelisa Group, integrated heating and cooling into the mullion system as the Integrated Façade System Gartner. Using a working fluid, heat or coolth was sent through curtain wall mullions to provide additional heating or cooling (Gartner). This arrangement had the advantage of

reducing perimeter heat and cooling augmentation generally required in traditional curtain wall constructed buildings, but the limitation of being confined to a point source with little mass effect. Still considered to be a radical approach, Gartner's Integrated façade system has had limited deployment both globally and in the United States. Yet, this system does illustrate a countercurrent heat exchange with one closed loop through the mullions, and two open loops as the fluid of the air on the interior and exterior sides of the building envelope directly adjacent to the mullions.

Among many deployed examples, Carnegie Mellon University tested this system for over two decades in the Intelligence Workplace as part of The Center for Building Performance and Diagnostics led by Dr. Volker Hartkopf. Opening in 2008, Rensselaer Polytechnic Institute's EMPAC Center designed by Grimshaw Partners used a Joseph Gartner curtain wall design that integrated heated water to reduce condensation and increase the overall insulation of the large North facing curtain wall. As shown in Figure 3.9, both horizontal and vertical mullions were used to add heat to the curtain wall system with a working fluid, specifically propylene glycol and water. The system uses a flow pattern intended to reheat or recharge the working fluid as it travels across the façade. These systems were principally interior heating and cooling systems using a point source for energy generation and thermal exchange on the interior of the building; fundamentally a modern, if sophisticated configuration of the hypocaust model.

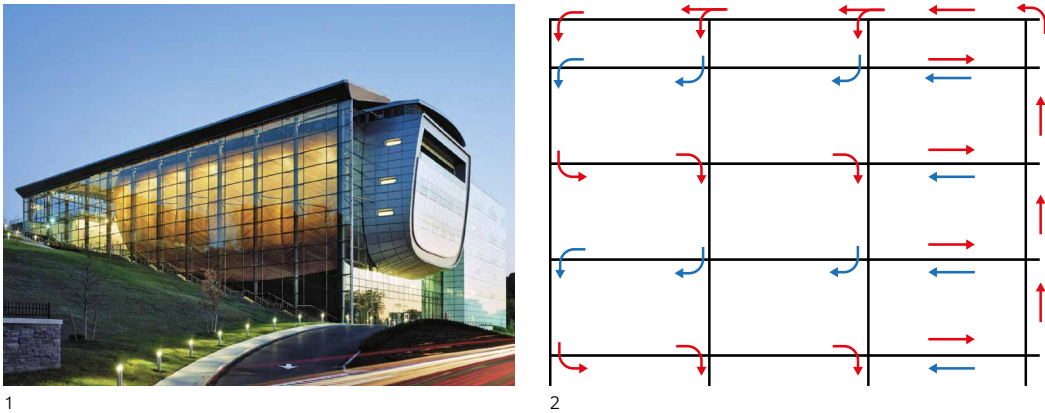


FIG. 3.9 Diagram (2) of heating flow overlay on the north facade of the EMPAC building (1) (Fortmeyer & Linn, 2014), redrawn from Charles Linn.

### 3.3.3 Active Insulation

A critical variation on the TABS configuration was the integration of the system into large surfaces of the exterior envelope. This type of configuration provides a direct mechanical function of heating or cooling the parts or whole surfaces of the building envelope directly, either reducing the need for insulation or reducing the usage of internal mechanical systems by providing heat or coolth directly at the surfaces where energy flows.

The Zollverein School Building, as shown in Figure 3.10, by SANNA Architects, completed in 2006, transformed the traditional radiant slab configuration of TABS into such an exterior configuration. The principle behind this active envelope, which is closely related to ISO 11588 Type E, has been referred to as Active Thermal Insulation (ATI). The Zollverein project used a water source heat pump that leverages geothermal thermal energy from a site adjacent mineshaft as the locally available energy source. The thermal energy is distributed through the cast-in-place monolithic concrete walls and floors to provide energy to balance the load and demand on the building from both external (e.g., climate, weather) and internal sources (e.g. equipment, occupation). The energy pushed in to and out of the exterior wall created an effective dynamic and controllable R-Value.



**FIG. 3.10** TABS as an envelope configuration in the Zollverein School: (1) exterior mass envelope, (2) embedded thermo active building system (Mayer, 2012), (3) diagram of geothermal exchange, redrawn (Transsolar, 2006).

Another variation of the TABS configuration was the Building Integrated Solar Thermal (BIST) system that integrated the functions of the solar thermal collection into the building envelope components and assembly. BIST systems function as a form of countercurrent heat exchanger and can take on multiple configurations with both water and air as the working fluid. Void Space Dynamic Insulation (VSDI) is a configuration of a BIST that uses air as the working fluid to transfer energy between the interior and exterior of the building envelope. VSDIs can either be passive or



active configurations. The critical difference between the VSDI configuration and the thermally active mullions described in Section 3.3.2 is that the thermal source is a locally available resource (i.e. geothermal heat pump from local defunct mine shaft) and not a highly concentrated source using added fuel for production.

TACE is a variation and natural evolutionary progression of the liquid based BIST typologies that advance the state-of-the-art by balancing a two-way energy exchange between exterior and interior energy resources and needs where illustrated BIST assemblies focus on the usefulness of the solar thermal source energy.

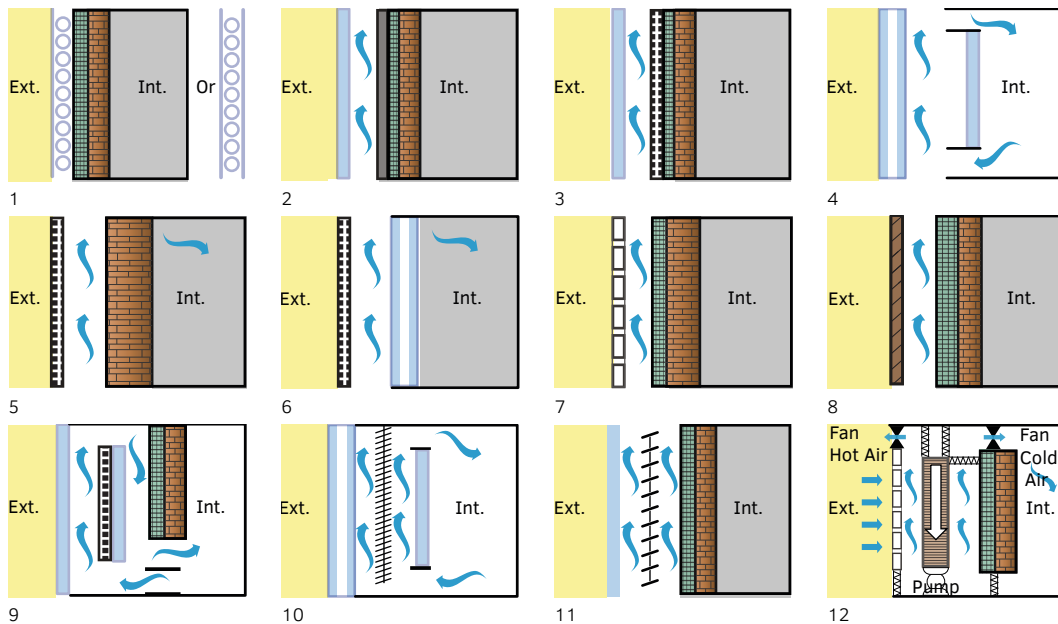


**FIG. 3.11** Diagrams showing a single fluid channel of air based BIST envelope assemblies. Air based BIST assemblies include the traditional Trombe wall configurations. Single Air Channel: 1) Glass Pane, air-filled glass tube, insulation, façade, 2) Glazing, absorber, insulation, façade, 3) Glazing, PV panel, insulation, façade, 4) Double glazing, air cavity, Venetian blind, internal glazing, 5) PV panel, air cavity, insulation, façade, 6) PV panel, air cavity, double glazing, 7) Transpired plate, air cavity, insulation, façade, 8) External sheet, air cavity, insulation, façade. Double Air Channel: 9) Glazing, outer air duct, PV panel, glazing, inner air duct, insulation, 10) Double glazing, 1st air cavity, Venetian blind, 2nd air cavity, internal glazing, 11) Glazing, collated PV Panel, insulation, façade, 12) Transpired Plate, plenum 1, high-porosity Sandtile. Redrawn (Zhang, 2015).

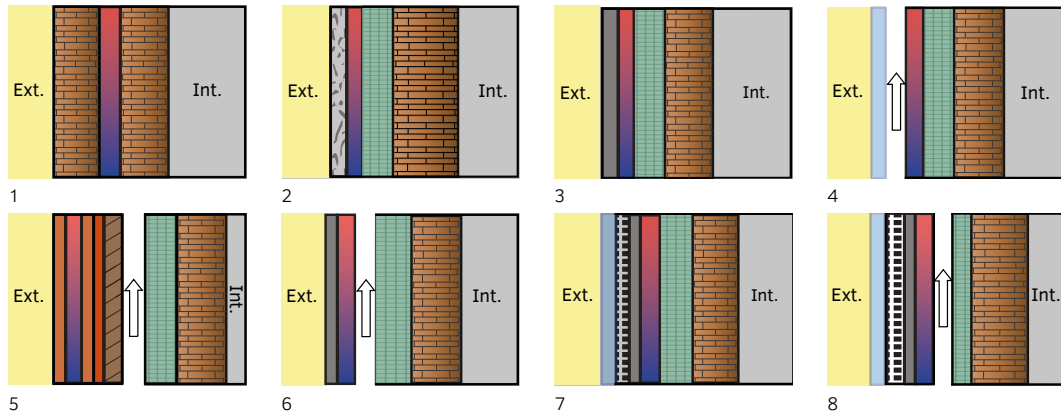


**FIG. 3.12** Diagrams showing various typologies of air and liquid based BIST envelope assemblies specifically as solar thermal collector designs. Solar Thermal Design: 1) Massive wall, water tube, massive wall, 2) Plaster, water tubes, insulation, façade, 3) absorber, water tubes, insulation, façade. Photovoltaic Thermal Design: 4) Glass cover, air cavity, absorber, water tube, insulation, façade, 5) Bi-metallic water tube (Fe-Cu), copper plate, wooden plank, air cavity, insulation, façade, 6) Absorber, water tube, insulation, façade, 7) Glass cover, PV panel, absorber, water tube, insulation, façade, 8) Glass cover, PV panel, absorber, water tube, air cavity, insulation, façade. (Zhang, 2015).

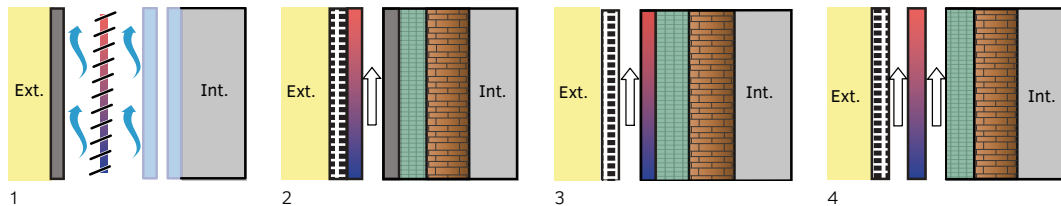


**FIG. 3.13** Diagrams showing various typologies of combined PV and solar thermal based BIST envelope assemblies. Photovoltaic/Thermal Combination Design: 1) Absorber slat, PV panel, water tubing, double glazing, 2) PV panel, water tube, air cavity, absorber, insulation, façade, 3) PV panel, air cavity, water tube, insulation, façade, 4) PV panel, 1st air cavity, water tube, 2nd air cavity, insulation, façade. Redrawn (Zhang, 2015)

The CALA Hazledean house in Balerno, City of Edinburgh, shown in Figure 3.14, is a modern prototype deployment of VSDI. This version of VSDI was developed by Dr. Mohammed Salah-Eldin Imbabi at the University of Aberdeen and completed full-scale deployment for testing in 2006. Initial post-occupancy results showed an average winter saving on heating energy of 5-7% and possible shoulder month savings up to 18% compared to a standard residence. What is notable with VSDI, as opposed most BIST systems and other ATI systems, is the use of local diffuse sources of energy to effectively transfer, store and distribute that energy locally through the envelope. This arrangement is a significant departure from using point

energy sources and extensively associated distribution networks, thus representing a paradigm shift in thinking (Brown et al., 2008).

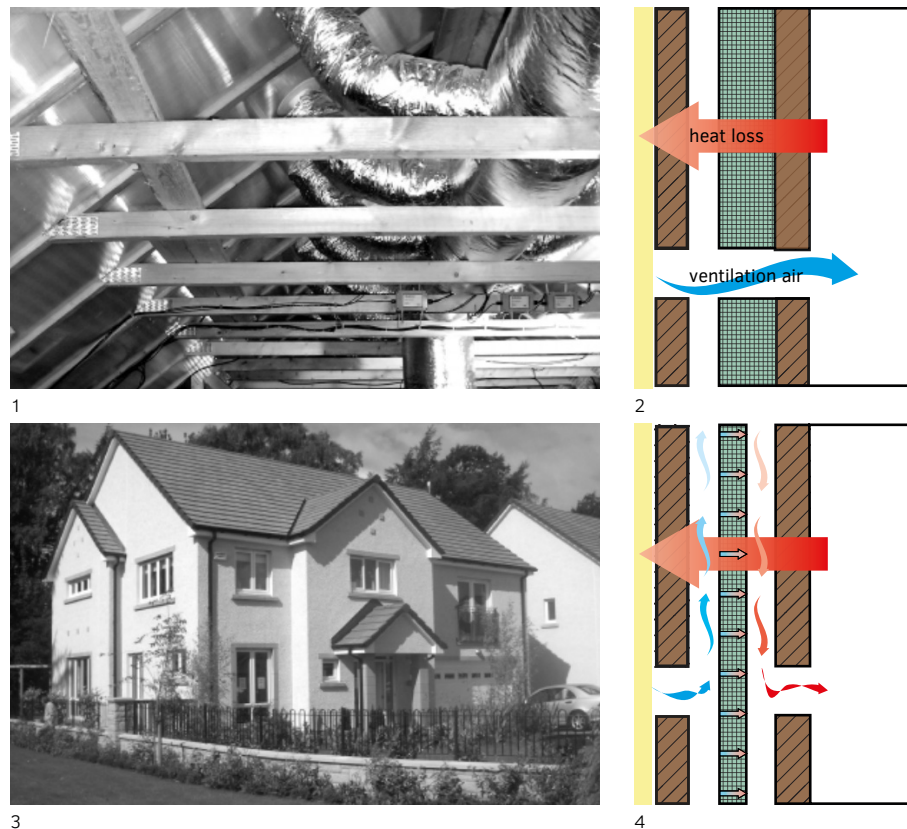


**FIG. 3.14** Dynamically breathing building envelope examples of the VSDI in CALA Hazledean (1,2,4) in comparison to traditional insulation (3). Photo and redrawn (Brown et al., 2004)

The VSDI concept proposed that the heat recovery function of the mechanical system is transferred to the building envelope. This function has several distinct advantages, the surface area is significant, and is already part of a required building system – the envelope – and the energy exchange takes place directly where the primary energy flows take place. A VSDI system may reduce the fan energy needed to provide fresh air required in most building types and when coupled with a water side heating and cooling system may significantly reduce the overall impact of the HVAC system on the building energy profile.

The ETA-Fabrik Factory Prototype, as shown in Figure 3.15, was developed at the Technical University of Darmstadt and was conceived as a net zero capable learning laboratory. The exterior wall is arranged as a concrete sandwich panel system that serves as a type of BIST. A capillary network is embedded in an external high-performance concrete panel and another in an internal structural panel. A mineralized concrete layer sits between the two capillary embedded panels providing additional R-Value while maintaining some thermal mass characteristics. The heating and cooling system of the ETA factory prototype building works in a fundamentally different way than VSDI where the energy from the surfaces of the envelope is captured and stored before distribution. The system manages the entropy generation to become highly efficient rather than focused on energy recovery and ventilation (Maier et al., 2016).



**FIG. 3.15** Example of liquid BIST system with seasonal storage (1, 2) in the ETA-Fabrik Factory Prototype and close up of exchange wall (2). Redrawn and photo (Maier et al., 2016).

### 3.3.4 Thermal Storage

Thermal storage in TABS has typically relied on the mass as a recombinant material that often has another primary function: floors, structural walls, etc. To balance energy expenditures with thermal comfort needs, a secondary thermal storage system that adds thermal capacity, time controls, and distribution options, has advantages over systems without them. The ETA-Fabrik, for example, uses two primary storage methods; distributed passive thermal storage within the TABS assembly as the mass of the structural envelope, and remote active thermal storage of the working fluid tank that charges the passive mass.

The thermal storage component of any TABS system is critical to the system efficiently. Rarely is energy available precisely at the time or the form that it is

needed in today's buildings. Therefore, the ability to store energy for later use is critical to the overall effectiveness of any TABS system; specifically, when used in an envelope configuration, and particularly when attempting to shave the peaks and fill the valleys of the building energy use profile. Summary: Development of the TACE system.

## 3.4 Summary: Literature and Precedents

---

Building Integrated Solar Thermal (BIST) systems, including Void Space Dynamic Insulation (VSDI) systems, have been focused on the harvesting of solar thermal energy to augment heating, and in some cases cooling, of the occupied space. Generally, the systems are not modular and are limited in their adaptability, and some cases their scalability. Typically, they have been deployed specifically by solar orientation to maximize thermal energy collection. Active Thermal Insulation (ATI), on the other hand, often uses alternative sources, such as geothermal, to mitigate heat or coolth loads on the building envelope; and can function regardless of orientation as the focus is on temperature that does not need to be linked to insolation. ATI systems are also not modular or scalable, with the notable exception of the ETA- Fabrik Factory Prototype.

TACE shares an overlap with both BIST and ATI systems, bridging the gap between solar thermal heat collection and active insulation in a dynamic adaptive system. Through the TACE system, the external and internal loads are both considered as resources. While the ETA-Fabrik uses seasonal storage, TACE is designed to work predominately on diurnal cycles reducing the daily peaks and valleys of energy usage; thus the speed and quantity of thermal exchange is the driver for developing the design of the components of the system, as these attributes define how the TACE system is differentiated from other BIST and ATI systems. It is in this way that the development process of the prototypes provided critical insights into how the idea of a countercurrent energy exchanging building envelope based on the principles of building physics could ultimately transfer into a utilized object developed from an iterative research and design process.

This chapter illustrates the historical lineage and conceptual alignment to inform the development of the TACE system in Chapter 4 and place it within the broader context of thermo active building systems. Specifically, the following key performance

indicators (KPI) are derived from the literature and precedents that formed the basis of design for the TACE System:

- Modularity and scalability – for the application on multiple building forms and sizes
- Bi-directional energy flows – to take advantage of exterior and interior energy flows
- Dynamic thermal storage – to address the availability of energy and the demand response profile of the building program

Chapter 4 addresses these KPIs by manipulating specific design principles.

## References

- Bean, R., Olesen, B., Kim, K. (2010). History of Radiant Heating and Cooling Systems - Part 2. ASHRAE Journal, January.
- Brown, A. Imbabi, M., & Peacock, A. (2004). The Balerno Project. Paper presented at the Proceedings of the 8th World Renewable Energy Congress (WREC VIII), Glasgow, UK.
- Davis, M. (1981). "A wall for all seasons." RIBA Journal, 88(2), 55–57.
- Dyson, A., & Vollen, J. (2008, 2016). The Center for Architecture Science and Ecology (CASE). Retrieved from <https://www.case.rpi.edu/>
- Dyson, A., Starck, P., & Jensen, M. (2007). Integrated Concentrating Solar Facade System. Prototype Development Report.
- Fortmeyer, R., & Linn, C. (2014). Kinetic architecture: designs for active envelopes.
- Gartner, J. Retrieved from <https://josef-gartner.permasteelisagroup.com/about-gartner/products-services/integrated-steel-fa%C3%A7ades/>
- Higgins, C. (2017). Energy Performance of Commercial Buildings with Radiant Heating and Cooling. Retrieved from: <https://newbuildings.org/wp-content/uploads/2017/08/Radiant.pdf>
- Hypocaust [digital image]. (2019) <https://gw4.ac.uk/news/gw4-alliance-and-national-trust-announce-new-research-partnership/nt-chedworth-roman-villa-baths/>
- Klein, T. (2013). Integral Facade Construction: Towards a new product architecture for curtain walls. TU Delft.
- Knaack, U., Klein, T., & Bilow, M. (2008). Imagine No. 01: Facades. nai010 Publishers. Rotterdam, Netherlands.
- Knaack, U., Klein, T., Bilow, M., & Auer, T. (2007). Façades: Principles of Construction. Birkhäuser. Basel, Switzerland.
- Komp, C., [digital image] (2017). <https://vpm.org/news/articles/2680/as-frank-lloyd-wright-turns-150-a-small-jewel-in-virginia-shares-lessons-in>
- Lee, E., Selkowitz, S., Bazjanac, V., Inkarojrit, V., & Kohler, C. (2002). High-performance commercial building facade.
- Loonen, R., Trčka, M., Cóstola, D., & Hensen, J. (2013). Climate adaptive building shells: State-of-the-art and future challenges. Renewable and Sustainable Energy Reviews, 25, 483–493.
- Maier, A., Gilka-Böttzow, A., & Schneider, J. (2016). An energy-active facade element from mineralized foam (MF) and micro-reinforced, ultra-high-performance concrete (mrUHPC). DOI:10.7480/jfde.2015.3-4.984
- Mayer, T., [photographs]. (2012) Retrieved from [https://thomasmayerarchive.de/categories.php?cat\\_id=813&l=english#&gid=1&pid=31](https://thomasmayerarchive.de/categories.php?cat_id=813&l=english#&gid=1&pid=31)
- Nouidui, T., Wetter, M., & Zuo, W. (2014). Functional mock-up unit for co-simulation import in EnergyPlus. Journal of Building Performance Simulation, 7(3), 192–202.
- Olesen, B. (2012). Thermo Active Building Systems Using Building Mass to Heat and Cool. ASHRAE, 52(2), 44–52.
- Pollio, V., & Morgan, M. (1914). Vitruvius: Dover Publications.

- Schmelas, M., Feldmann, T., & Bollin, E. (2015). Adaptive predictive control of thermo-active building systems (TABS) based on a multiple regression algorithm. *Energy and Buildings*, 103, 14-28.
- Shultz, J. (2018). A Framework for Modeling Complex Integrated Building Systems at Whole-Building Scale with Co-Simulation: Applied to a Coupled Simulation Between a Facade System Model and a Whole Building Energy Model. (A Dissertation Submitted to the Graduate Faculty of Rensselaer Polytechnic Institute.), Rensselaer Polytechnic Institute, ProQuest, LLC.
- SIG. (2016). HC Group completes the world's most sustainable office building. Retrieved from <https://pveuk.com/hc-group-complete-the-worlds-most-sustainable-office-building/>
- Siry, J. (2013). Frank Lloyd Wright's innovative approach to environmental control in his buildings for the S. C. Johnson Company. *Construction History*, 28(1), 141-164. Retrieved from <http://www.jstor.org/stable/43856032>
- Transsolar [digital image]. (2006). [https://www.cyclifier.org/wp-content/uploads/Geothermie030728\\_mitF-1.jpeg-jpeg](https://www.cyclifier.org/wp-content/uploads/Geothermie030728_mitF-1.jpeg-jpeg)
- Wetter, M. (2011). Building Performance Simulation for Design and Operation. J. Hensen & R. Lamberts.
- Xu, X., Dessel, S., & Messac, A. (2007). Study of the performance of thermoelectric modules for use in active building envelopes. *Building and Environment*, 42(3), 1489-1502.
- Zhang X., Hong Z., Wang L., & Yang T. (2015). A Review of Building Integrated Solar Thermal (BIST) Technologies and their Applications. *Journal of Fundamentals of Renewable Energy and Applications*, 5(182).

# 4 Module Design and Development

---

The development of the TACE system is based on the fundamental principles as discussed in Chapter 2 and developed upon the precedent context and key performance indicators as described in Chapter 3. The goal of the system is to transfer energy usefully across the building envelope demarcation line while leveraging several specific principles that articulate the TACE module as part of a countercurrent energy exchange system.

This chapter discusses: 1) the design principles that create the energy transfer functionality, 2) the process of developing a TABS as a module and an envelope system, and 3) discusses the material and morphological choices made in designing the system.

## 4.1 Introduction

---

The aim of the Prototype Design and Development of the TACE system was to develop a research platform in the form of physical and computational prototypes that were used to test the hypothesis and answer the research questions. The prototype design development was divided into three broad categories: the components required to create the envelope system; the components required to transfer energy; and the components as part of a complete countercurrent energy exchange system.

The approach to the prototype design development was to create a Minimum Viable Product (MVP Prototype I) to test the conceptual design and functional principles in support of the hypothesis detailed in Chapter 1. The outcome of the design and testing of MVP Prototype I led to the development of two additional prototypes: Proof of Concept (POC) Prototype II explored both manufacturing



techniques of components and demonstrates energy exchange between the inside and outside of the envelope; Architectural and Systems Integrated (ASI) Prototype III explored the real world architectural integration and performance of the TACE system at the component and system scales and investigated the architectural impacts of deploying the system. The focus of Chapter 4 is on the development of the MVP Prototype I; Prototypes II and III were delineated as part of the results as design iterations, with Prototype III forming the basis for investigating installation assemblies in Chapter 7 as well as for developing the Unified Curtain Wall Prototype IV discussed in Chapters 7 and 8.

The TACE MVP Prototype I module was developed as an active, modular ceramic façade tile assembly that captures and distributes thermal energy from the exterior environment. These TACE modules were designed to connect to an active working fluid loop where the exterior tile component was intended to transfer energy into a working fluid via interior thermal transfer component in the form of a pin plate, not unlike a typical heat sink. The working fluid was circulated in and out of the TACE module and into an insulated thermal energy reservoir where it could be exploited for space heating or cooling.

## 4.2 Thermal Adaptive Ceramic Envelope

---

Similar to the VSDI concept discussed in Chapter 3, the TACE system is designed to operate using locally available energy sources across the building envelope demarcation line. Unlike the VSDI, the TACE uses thermal storage as a buffer before distribution in the local heating and cooling of envelope adjunct spaces. Like the ETA-Fabrik Factory Prototype, the TACE is designed to use a distributed fluid network to capture heat and coolth around the building envelope, and unlike ETA-Fabrik, the TACE is designed to regulate flows in a modular distributed system in spaces directly adjacent to the exterior wall.

The precedents in Chapter 3 showed: 1) that the building envelope can play a critical role in the energy performance for the building as a whole and 2) that it is feasible to use locally available resources that can be harnessed for a building envelope assembly as a passive, active or combined system to support the reduction in energy use. While the TACE system functions partially like several of its precedents, there is no existing system that assembles the specific design functionalities described in

this section. The following design, developed as the main body of this research fills a niche in the landscape of adaptive building envelopes. The ability to store energy locally in a modular and scalable system is one unique instance in the evolutionary process of developing TABS as building envelope systems.

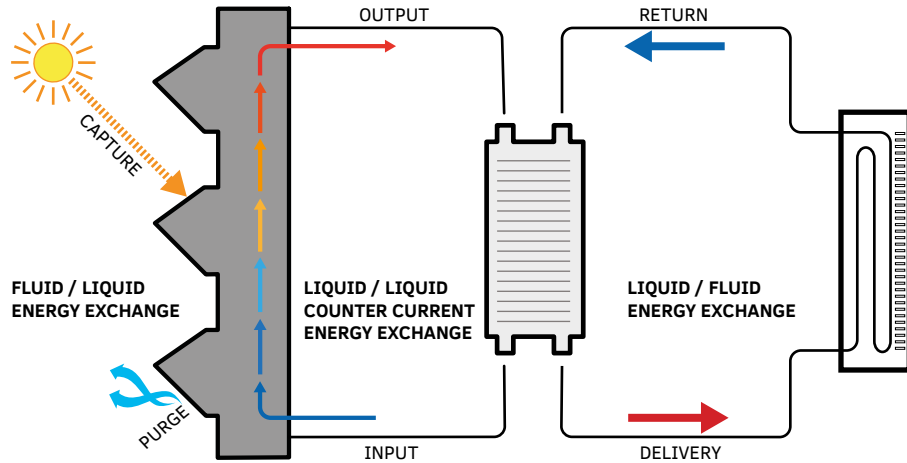
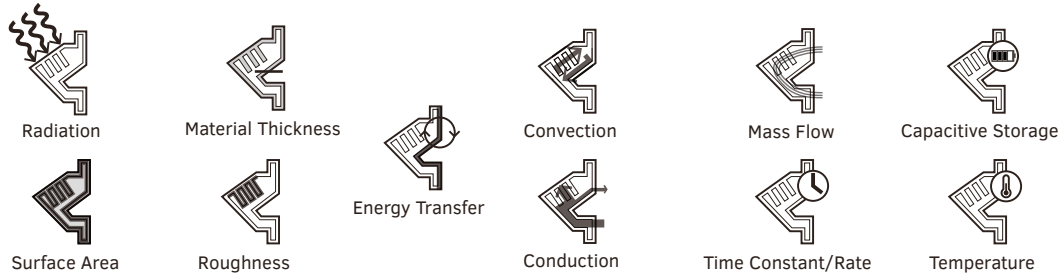


FIG. 4.1 Basic concept of countercurrent energy exchange leveraged in the TACE system.

#### 4.2.1 Concept Design of the TACE

The concept design of the TACE system, as shown conceptually in Figure 4.1, was developed as a reimagining of traditional terra cotta cladding systems whose design was optimized to work with local climate conditions by absorbing or rejecting locally available thermal and solar energy by manipulating a set of component attributes that make up the TACE module and system (e.g., surface textures, colours, etc.) as shown in Figure 4.2. These purpose-formed components work together in an assembly comprised of modules that vector energy using a working fluid across the building envelope demarcation line.

## Fundamental Attribute Principles



**FIG. 4.2** The attributes that are part of the conceptual assembly of the TACE system are shown as separate and additive to illustrate the multifaceted approach to the prototype development.

The TACE system uses this multivalent strategy to absorb, release, and redirect heat or coolth to conserve energy by managing entropy production. By managing entropy production at the building envelope, it was expected that there would be reduced mechanical system energy expenditures to maintain indoor thermal comfort than if entropy was generated solely from the primary mechanical heating and cooling system.

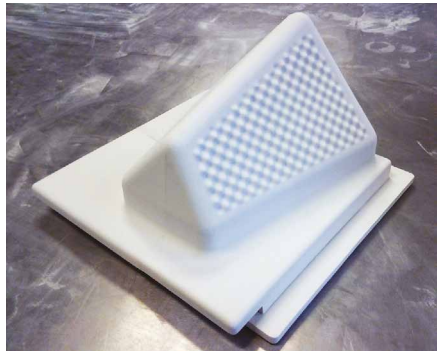
By developing an integrated system of multiple components, the proposed system can be recombined in multiple arrangements as required for an architectural integration in specific locations (e.g., geolocation, azimuth orientation, programmed demands). As a conceptual proposal, the TACE system uses this module-based framework to embed oriented geometries, material technologies, and semi-active heat transfer systems to enhance thermal and energy performance of opaque architectural facades. Rather than using the architectural envelope purely as a sealed barrier to prevent the free and unwanted transfer of energy, this system was designed to intercept and direct the flow of energy for thermal storage, redistribution, or redirection to support thermoelectric systems. The implementation of such a system would be highly specific to intended or potential applications in order to maximize the potential benefit from the system. The need for specificity also required a level of modularity, such that modules could be exchanged in an installed envelope, in order to meet changing programmatic needs of the building over time (Vollen, 2011).

Along these lines, the TACE has been developed for this dissertation based on the integration of heat transfer principles and commonly used construction methods that are necessary to develop a system accessible to the manufacturing, design and construction industry. The TACE module, as shown in Figure 4.3 as an early version of MVP Prototype I, is comprised of a component each with attributes that can be

manipulated by a range of variables as identified in Section 4.2.1.1. The TACE as a system is an array of the TACE module in series that is connected to a thermal storage bank that in turn is connected to a heating or cooling exchange with the interior environment as shown in Figure 4.1.



**FIG. 4.3** Early TACE module studies showing from left to right: (1) surface texture for energy exchange; (2) orientation morphology; and (3) interior thermal transfer attribute component illustrating the increased surface area as intended to be in contact with the working fluid.



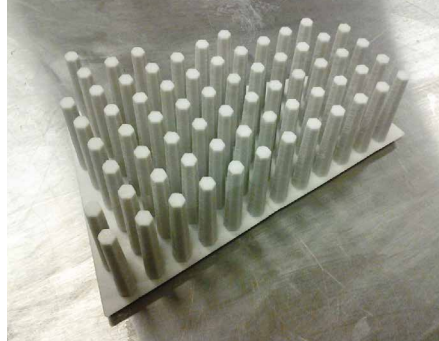
1



2



3



4

**FIG. 4.4** Early TACE module master positive fabricated using powder based rapid prototyping showing the advancement of the module design with articulated thermal transfer attribute components and a distinct front and back component.

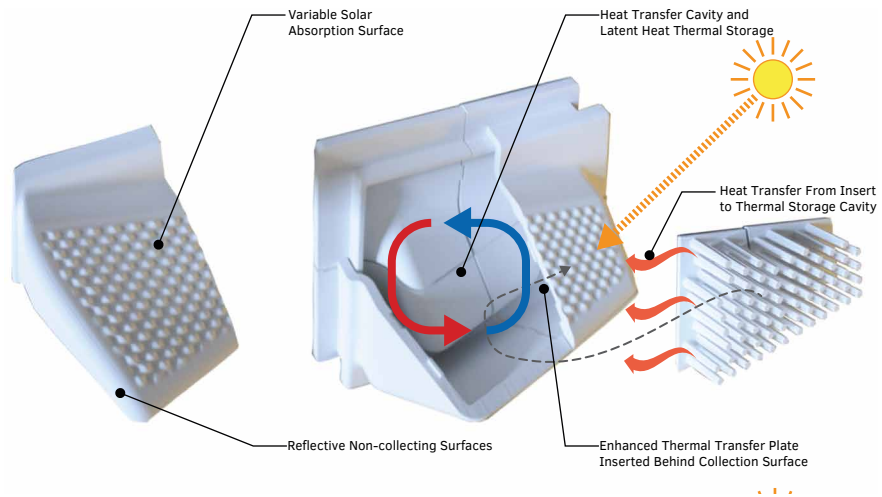


FIG. 4.5 Early TACE module full-scale mock-up and diagram illustrating purpose-based attribute components

#### 4.2.1.1 Component Design of the TACE

In order to develop the ability to modulate energy flows through a specific object, the results of which were demonstrated by the early prototypes as shown in Figure 4.5, it is important to understand the general flows of energy across the building envelope as shown in Figure 4.6, how the building envelope assembly addressed these flows, and which operating principles are engaged.

The principles that govern these energy flows at the building envelope are:

- Conduction: energy flowing through direct contact
- Convection: energy transfer due to bulk movement in fluids
- Capacitive Storage: energy storage in relation to temperature rise
- Mass/Energy Transfer: energy transfer from one location to another
- Radiation: electromagnetic energy transfer
- Refraction/Reflection: energy vector change
- Human Thermal Comfort: balance of factors that results in the perception of satisfaction of the surrounding thermal environment

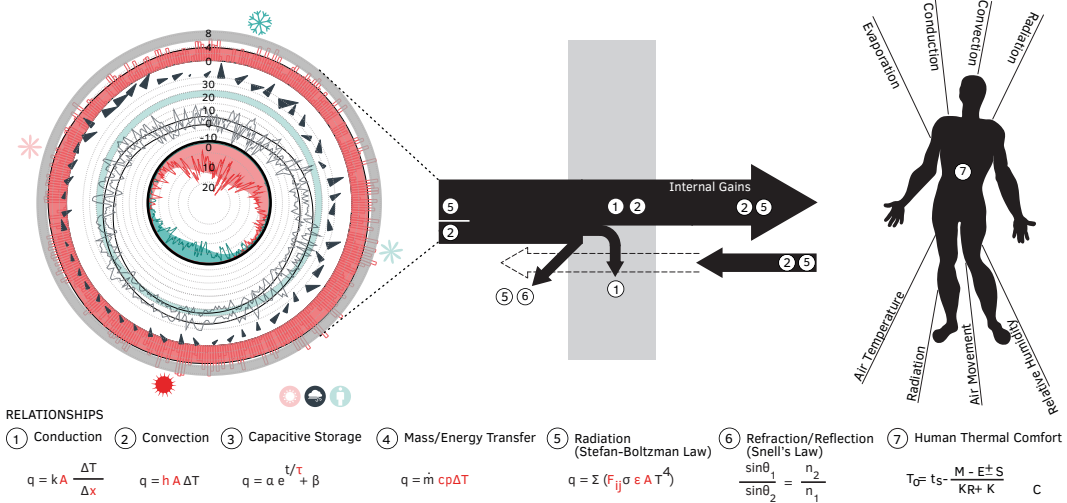


**FIG. 4.6** The flows of energy across the building envelope connect the climate and human comfort from a series of critical variables, expressed above. Variables in red directly impact surface area.

These principles function in the fluctuating conditions of the local climate and the fluctuating demands of the occupied program of the building. As stated in Section 2.3.1.3 previously, these fluctuating conditions are almost always out of alignment, making thermal comfort difficult to achieve without adding external point energy sources into the system. The TACE system was designed to leverage these principles to lower the external point energy sources needed to maintain thermal comfort. The components of TACE used the following variables to manipulate the principles that govern the energy flows. The following manipulations shown in Figure 4.7 were used to leverage the principles that govern energy flows from Figure 4.6:

- Orientation And Morphology – Radiation
- Color – Refraction/Reflection
- Material – Capacitive Storage, Conduction
- Texture - Convection
- Thermal Exchange – Mass/Energy Flow, Human Thermal Comfort

### Attribute Assembly Characterization

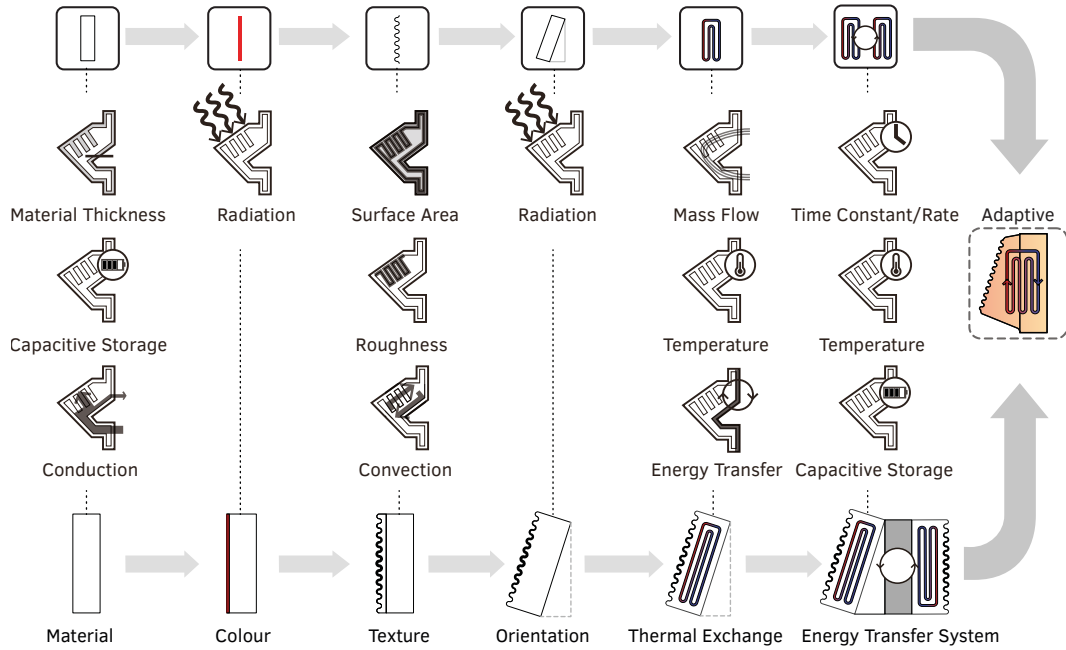


FIG. 4.7 Conceptual articulation of key attributes.

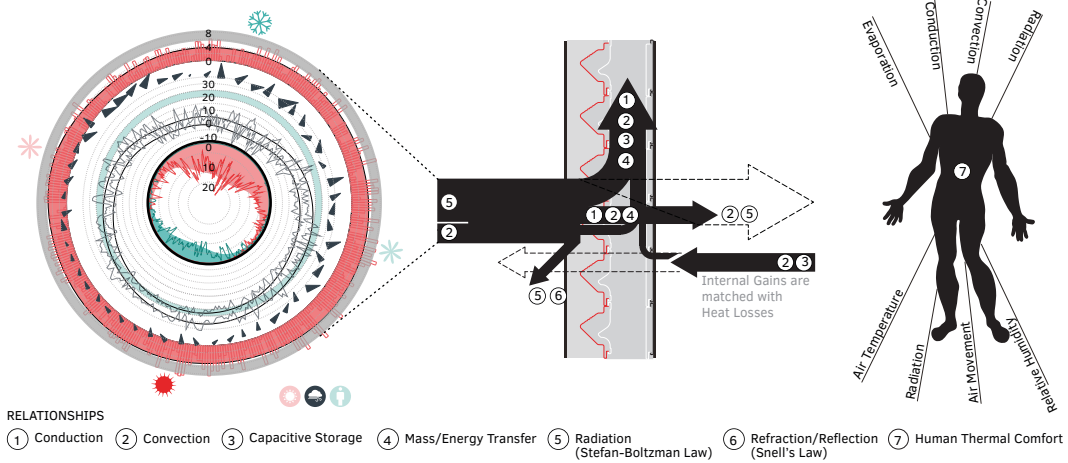


FIG. 4.8 The diagram shows how the locally available resource – on both right and left side, can be intercepted by the envelope system to be made useful later. Modifying the variables that alter energy transfer, as shown in red in the principle expressions, modifies the flow of energy and support the capture transfer, store and redistribute strategy that underpins the TACE as a system.



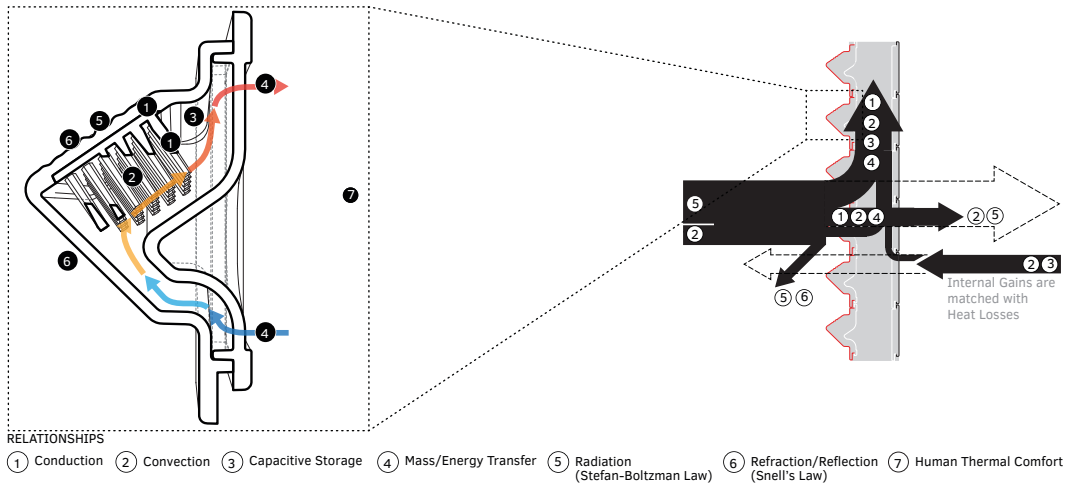


FIG. 4.9 The modified variables can be developed into a specific geometric and material response, in this case, the result is the TACE Module from MVP Prototype I, a combination of discrete components that have attributes that are leveraging the variable of the principle expressions..

Figure 4.8 shows how the principles were altered in concept as part of the envelope system. The individual components, as shown in concept in Figure 4.9, were designed to each shape the flow of energy at the building envelope to reduce the reliance on external energy resources to heat and cool the building.

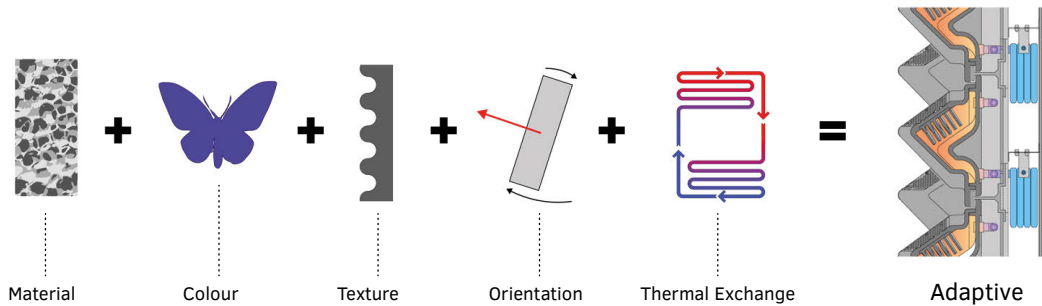


FIG. 4.10 Further development of the conception of key element progression.

#### 4.2.1.1.1 Orientation and Morphology

---

The manipulation of component geometry was designed to optimize the building envelope to take advantage of available energy flows by creating forms tuned for absorbing or reflecting energy based on diurnal and season shifts in insolation. Due to the mass of the ceramic module, the ambient environment was considered and modelled in Chapter 5 as an additional factor. Variations in component geometry were thought of to be biased to take advantage of multiple energy flows at the envelope where the manipulation of the aspect ratio of tilted geometries can switch component performance from self-shading to solar collection. These geometries could be further refined to fit specific climatic performance needs or specific orientations on the building face. An eastern or western facing façade, would, for example, have a more vertically oriented face to capture lower angle solar energy from the earlier morning and later afternoon. For the investigation of this thesis, a southern oriented morphology optimized for the southern New York latitude is chosen as the baseline and served as the criteria for MVP Prototype I. The combination of all of these attributes are shown in in Figure 4.10.

#### 4.2.1.1.2 Color: Reflection, Refraction, Absorption

---

The use of colour enhances the performance of the modulation of thermal flows at the surface of the building envelope. Variations in surfaces by colour, that which is located in the visible electromagnetic spectrum, as well as through changes in reflection, absorption, and transmission values, allow for greater control of the surface performance. Selective absorptance and emittance characteristics, exemplified by colour ranges, of the external solar facing component, prevent or encourages heat capture for energy production or domestic hot water supply. Empirical quantitative studies, as shown in Figure 4.11, explore the impact of colour on the exterior component of the TACE module (Vollen, 2010; Winn, 2014). Further opportunities also not explored in this thesis but were part of the initial concept were selective finishes that could be used to prevent heat loss to the environment, and similar to glass curtain walls, switchable thin films could be applied to ceramic components to manipulate colour or surface reflectance.

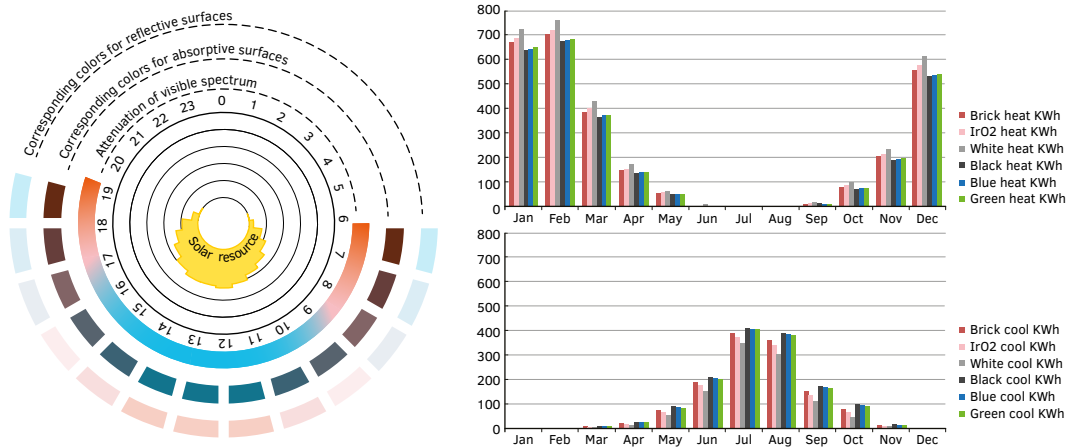
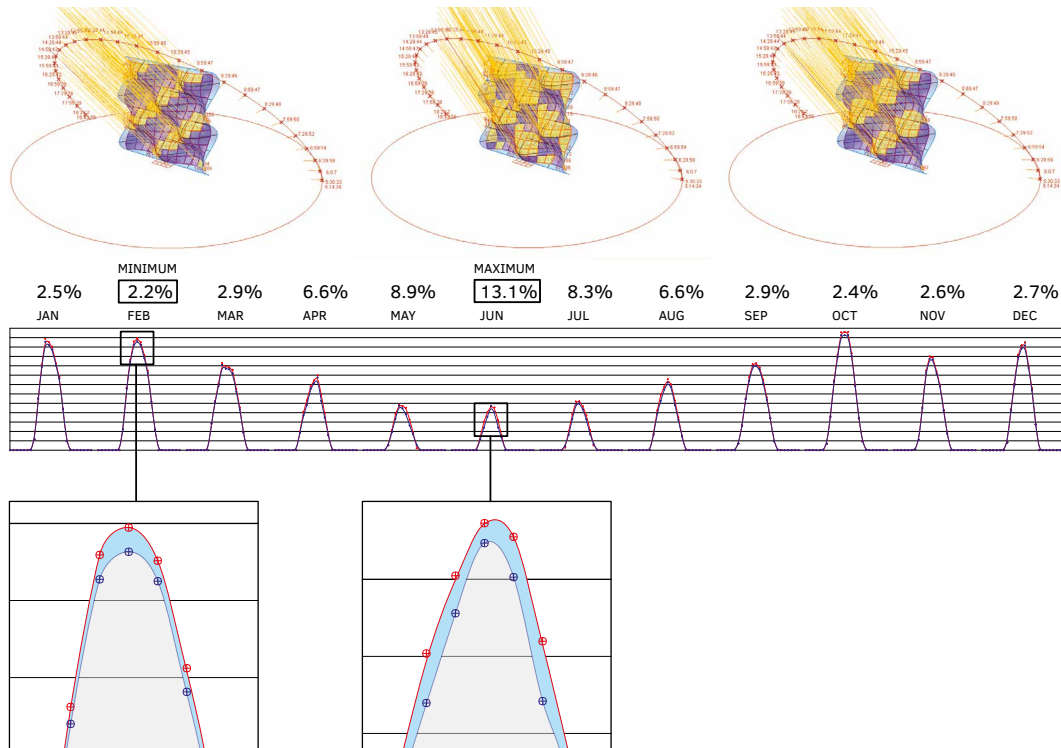


FIG. 4.11 Comparison of colour according to the wavelength of available sunlight (top) to projected performance load (bottom) showing: white, IrO<sub>2</sub>, typical brick, green, blue, and black for a ceramic flat panel envelope.

The Orientation and Morphology and the impacts of the surface characteristics as demonstrated by colour has been previously explored in 2004–2008 and were not further explored in this thesis (Vollen, et al, 2008). The research focus of this dissertation was on the impacts of the texture, the material, and the thermal exchange, and how components designed to manipulate these characteristics impact the EUI of the building.

#### 4.2.1.1.3 Texture: Surface Area Ratios, Turbulence and Laminar Flows

Texture manipulation at the surface of the building envelope component takes advantage of the thermal, luminous, and fluid environment at the milli-, centi- and deci- scales. Texture at multiple scales presents a range of novel possibilities for architectural surfaces that can modify the performance of envelopes through the localized manipulation of the boundary layer towards laminar or turbulent flows, where laminar flows provide added insulation value and turbulent flows encourage heat transfer (Vollen, 2010; Vollen & Winn, 2013). The study in Figure 4.12 study shows that the average exposure values based on the surface morphology can be manipulated to modulate the amount of exposure. Further examination in the principle of laminar and turbulent flows based on the surface morphology have been explored in 2006–2009 (Vollen, 2010; Vollen et al., 2008).



**FIG. 4.12** Impact of surface morphology showing exposure and shading percentages over the calendar year that may be used as both a morphology and colour patterning guide. This analysis conducted shows an exposure reduction due to self-shading, significantly more in the summer than in the winter (Vollen & Winn, 2013). While this optimization of the self-shading is not directly explored in this dissertation, it is a crucial attribute to integrate as part of future work.

The focus on texture in this dissertation was limited to the surface area manipulations of the energy transfer component located inside the TACE module, referred to as pins, pin plates, or thermal transfer pipe, depending on the prototype, as described below in Section 4.2.2.1. The function of this component is to increase energy transfer as a quantity, rate, or both, from the ceramic component to the working fluid and as per the system design, back to a ceramic component again.

#### 4.2.1.1.4 Material: Thermal Mass and Conductivity

---

The ability of thermal mass to absorb latent heat provides a stabilizing agent acting against the peaks and valleys of typical energy flows on the building envelope. The conductivity and specific heat of the primary material that makes up the components has a direct effect on the energy absorption and carrying capacity of the model and the system. A high alumina oxide content ceramic was proposed as the primary material for forming the components.

While not explored in detail in this dissertation, the incorporation of Phase Change Material (PCM) (e.g., BioPCM, a commercially available PCM for use in building systems from provider Phase Change Energy Solutions) could facilitate large quantities of thermal energy can be stored as latent heat. The PCM transitions between phases (i.e., solids, liquids, gasses) when environmental temperatures fluctuate. As they change state, they hold to a set melting temperature that can be used as a reliable method of temperature stabilization by converting thermal gain to latent thermal energy storage without increasing temperature. Commercial PCM based energy solutions, such as the SunAmp Heat Battery that was used in the design for UCW Prototype IV are under development and discussed in Section 7.1.2.6.

#### 4.2.1.1.5 Thermal Exchange: Active Energy Vectoring

---

Ultimately, the approach of linking together the morphology, colour (and surface effects), texture, and material becomes most effective when the thermal momentum is vectored towards usefully balancing the energy profile of the building as a whole over time as shown in Figure 4.13. In the form of simple countercurrent exchanging plumbing loops, a working fluid can transport the latent heat energy to a heating application or a heat exchanger and used for building heat or coolth. In this way, thermal loads can be collected and stored during the day rather than removed mechanically and then transferred to supplement night-time heating, or coolth, allowing the system to recharge, as modelled in Chapter 6. The ability to manage the entropy production locally via active energy vectoring through a working fluid defines the TACE system as adaptive and distinguishes the system from other TABS.

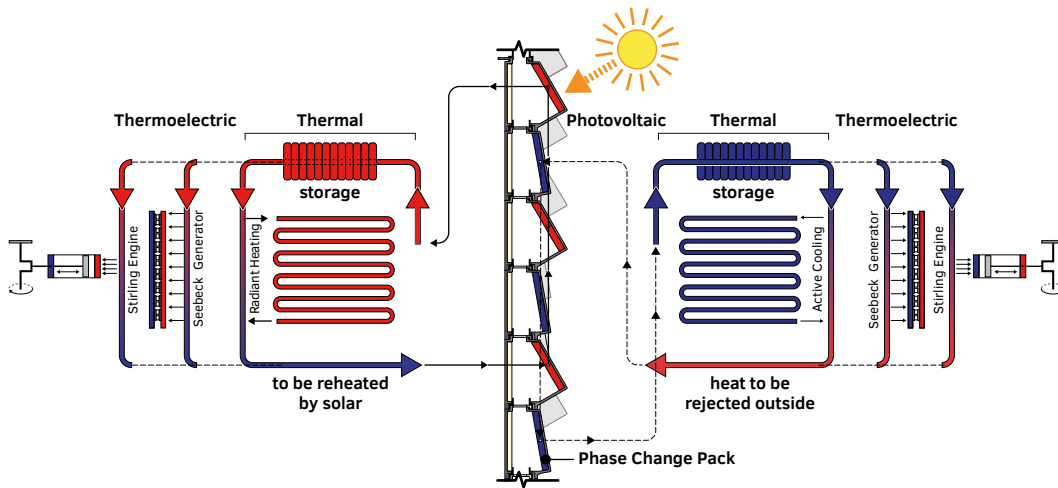


**FIG. 4.13** Diagram showing an early version of the TACE system proposal where multiple forms of energy transfer are delineated. While the development of the TACE System in this research focuses on thermal energy storage and reuse, Stirling Engine and Thermoelectric energy transfer were explored as standalone prototypes in 2011 and 2012 as part of initial proof of concept physical models. Redrawn (Vollen & CASE, 2011)

In concept, countercurrent flow would occur in the TACE system in multiple stages, as both direct and indirect transfer. Indirect countercurrent flow would occur similar to the radiant slab energy exchange; energy would be exchanged between fluid 1 (air) that exhibits natural flows around the exterior of the envelope, and fluid 2 (working fluid in a closed loop) that would be able to control fluid flow and direction, through the mass of the TACE exterior module. Direct countercurrent exchange would occur between the closed fluid 2 loop through a heat exchanger (i.e. flat plate heat exchanger such as delineated in Section 4.2.2.1) into thermal storage. This flow was demonstrated by POC Prototype II and ASI Prototype III, as described in Section 4.3.

#### 4.2.2 Design of the TACE MVP Prototype I

The morphology of TACE was derived from design constraints at three scales: the azimuth orientation of the tile, the inclined altitude of the tile face, and the surface texture of the inclined face as shown in Figure 4.12. Azimuth orientation, inclined altitude, and surface texture were not explored explicitly in this dissertation. These characteristics were explored previously (Vollen & Winn, 2013; Winn, 2014). However, in the developed of the system as a whole, it was imperative to have a

starting point from where to depart in the research of developing the TACE into a countercurrent energy exchange system. The morphology of the TACE module as explored in this dissertation as MVP Prototype I was derived from the optimization of a south facing tile adjusted for the NYC grid, inclined at latitude, 40° degrees. The face was rotated toward the south west 29° degrees. While Prototypes II and III were true 180° degree south facing geometries, Prototype I was intended to approximate potential real-world conditions of an urban setting where the constraints of the city grid would drive the limitation of the tile morphology. Prototypes II and III were developed to be greenfield examples showcasing the cardinal South direction morphology, and a version of Prototype I with a cardinal South direction as shown in Section 4.3 as a frame of reference for the MVP Prototype I. The energy modelling delineated in Chapters 5 and 6 assumed a cardinal South orientation.

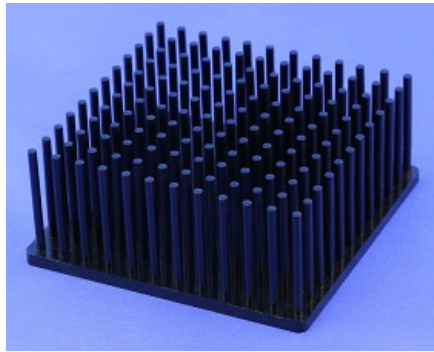
#### 4.2.2.1 Energy Transfer Components of the TACE

---

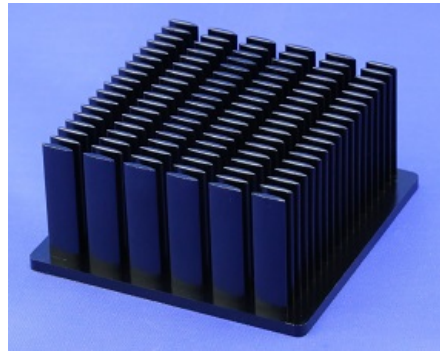
In its purest form, the TACE module is comprised of an exterior surface component (and in the MVP Prototype I, an interior surface component), an energy transfer component, and an insulation layer. The component identified for energy transfer in MVP Prototype I was an array of ceramic pins as you would find in an omnidirectional heatsink as shown Figure 4.14, heatsinks, in simple terms, transfer heat to a surrounding fluid from a conductor as heat moved from one end to the other away from the source. Since the heat transfers to the fluid, the heat in the conductor continues to flow along the conductor to the fluid; as hot moves to cold, this can also be reversed.

The primary design factors for heat sinks are thermal resistance of the material and fin efficiency. While metals such as copper and aluminium alloys perform well as conductors, MVP Prototype I is comprised of a high performance ceramic body described in Section 4.2.3.3 that is predominately alumina oxide, and thus performs well as a conductor. The Ashby chart, as shown in Figure 4.15, shows the relationship of the ceramic body performance in relationship to metal families in terms of thermal conductivity, thermal diffusivity and cost (Granta, 2020).

Fin efficiency is the ratio of heat transferred by the fin, divided by the total heat transfer was the fin (i.e., pins, plats, or others morphology used as the dissipating surface to transfer energy from one medium to another) to be isothermal (Lienhard, 2018). Thermal conductivity and the morphology of the fin both contribute to the fin efficiency, thus the thermal transfer component for MVP prototype I was a convergence of material properties, geometry and flow, where the flow was both the rate of flow and the mixing of the working fluid in the pin field.



1



2

FIG. 4.14 Examples of forged aluminium thermal transfer components. The geometry of the cast aluminium oxide thermal transfer component of the MVP Prototype I has a similar geometry (Forged Heat Sink, 2019).

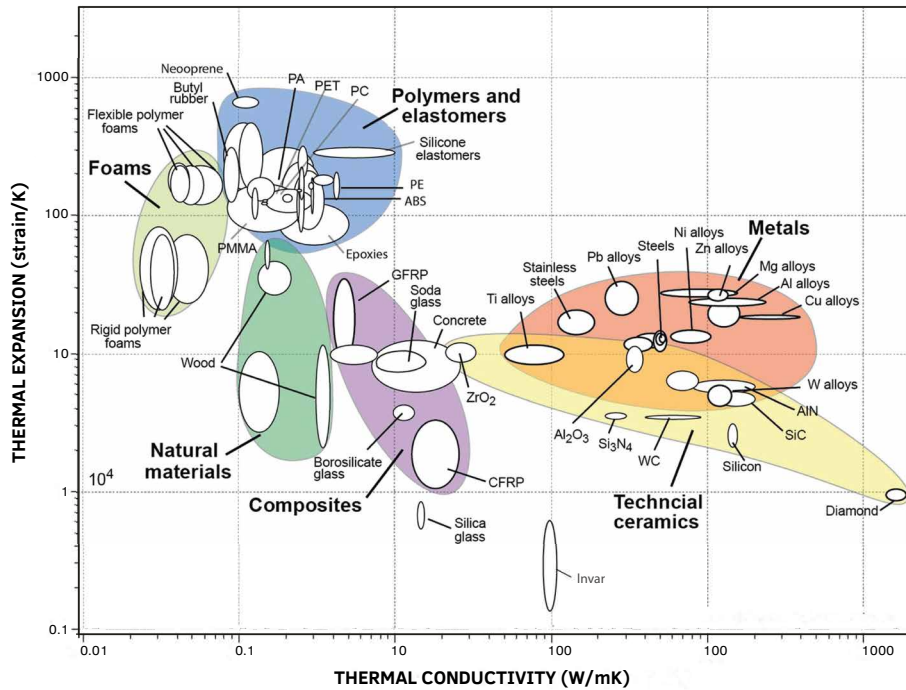


FIG. 4.15 Ashby material properties chart of thermal expansion and thermal activity showing an overlap of properties between metals and technical ceramics. The alumina formulation used for MVP Prototype I and the subsequent simulations used 97% industrial grade alumina (Al<sub>2</sub>O<sub>3</sub>), with minor constituents like SiO<sub>2</sub> and MgO from added materials. Recycled glass was added to increase silica content (SiO<sub>2</sub>) up to 10%. Redrawn (Granta, 2020).



#### 4.2.2.2 TACE Module Design

---

The development of the TACE system began in 2004. The concepts discussed in Section 4.2.1 were developed to various degrees as conceptual designs and a range of material and physical studies. The focus of the module design for this dissertation was determined by the gaps in the research as discussed in Chapter 3, but predominantly the gaps in the design resolution of the TACE system from the previous work that when filled would allow for significant advancement in the system design.

Conceptually, the TACE module design was developed to be able to array the thermal transfer variables, as shown in Figure 4.9 as physical attributes. Ceramics offered both a supportive framework to form and arrange the attributes as well as being a robust architectural façade material with desirable thermal transfer properties. The design development of the module prototype was intended to test both the thermal performance as well as the technical detailing necessary to adapt the TACE system to a building envelope assembly. The TACE module is formed by the assembly of the three primary components: 1) the outer tile face which is the primary solar absorber surface; 2) the thermal transfer component; 3) the interior cavity enclosure surface. These three primary components were bonded together to create a hollow cavity within the assembly lined with the thermal transfer component that was filled with the working fluid that performed the heat transfer operation. The primary absorbing surface was angled to maximize exposure – which can be tailored depending on the cardinal orientation or to maximize annual seasonal or daily collection, and support the potential applications of additional texture and colour as described in Sections 4.2.1.1.2-4.2.1.1.3.

The design of the edge details of the module was formed to solve two critical detailing issues: water shedding by overlapping adjacent modules and a geometry that accepted the attachment system to the rainscreen support as part of the building envelope assembly. The key driver developing the geometry of edges for overlapping modules was to keep the modules in plane when in the array of the envelope assembly. These edges were also designed to use standard terra cotta rainscreen attachments, in this case, specifically those used by Boston Valley Terra Cotta's TerraClad System. The TerraClad support system allows for multiple types of installations discussed later in Chapter 7 and holds the modules away from the weather barrier allowing for space for the connections required by the working fluid.

Perhaps more importantly, by having developed the MVP Prototype I to include the other functions of a building envelope alongside the thermal performance, we gained an understanding of how much façade real estate could be realistically

dedicated to adaptive thermal transfer and how much must be dedicated to baseline building facade detailing and performance. By simultaneously including both sets of attributes, thermal performance related, and façade detail related, more useful knowledge of both their potential interaction and the real per area performance that is used to extrapolate and to gauge the impact on a whole bay or building was gained, as discussed in Chapter 6.

Figure 4.16 shows an early stage patent application drawing for the TACE module delineating the purpose-built components amassed to encompass the attributes for the key principles for controlling thermal transfer. This early stage diagram shows, with some evolutions for production, the same basic arrangement as MVP Prototype I as shown in Figure 4.17.

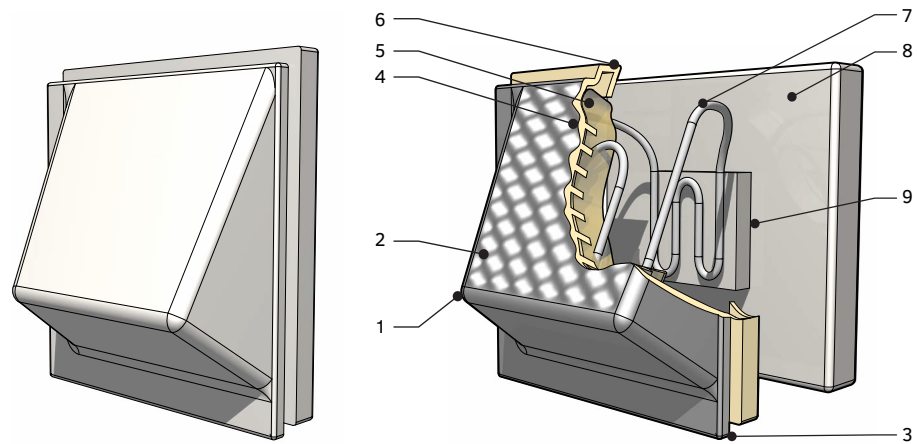


**FIG. 4.16** Early proposed TACE solar absorption tile basic geometry (left), and TACE solar absorption tile with cutaway (right) showing: 1. Moulded tile geometry for optimal winter solar collection, 2. Textured solar collection surface for improved solar heat gain. 3. Overlapping geometry for rainscreen water shedding. 4. Ceramic fins on interior tile surface for improved heat transfer to phase change cavity. 5. Working fluid cavity. 6. Lapping tile geometry for clipping to modular track cladding system. 7. Heat transfer loop for conduction to thermal storage bank. 8. Thermal storage bank. 9. Thermal transfer switching connection to thermal storage bank for seasonal performance control.

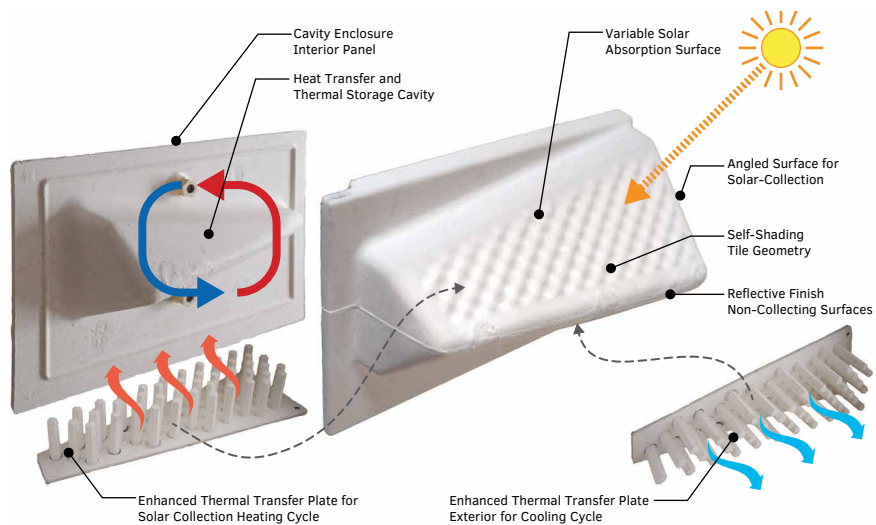


FIG. 4.17 Evolution of the full-scale development of the TACE module that was used for testing in Chapter 5.

#### 4.2.2.3 TACE System Design

The design of the TACE as a system, conceptually, was focused on viewing the building envelope as an energy transfer function. The variables of the function were arranged to serve the effective transfer of energy – and the system was developed to hold these variables within the architectural context. With the ceramic module as the starting point, the system was developed to support the primary function of transferring energy across the building envelope demarcation line – the conceptual line that determines where the building envelope is considered exterior and where it is considered the interior. The primary components of the system are: 1) exterior thermal transfer module developed as the TACE module; 2) thermal storage battery module; 3) the interior thermal transfer module. These three primary components were linked as a system through a series of working fluid loops: exterior to the thermal battery, and thermal battery to the interior. As the system design developed, each loop was bifurcated by a countercurrent heat exchanger so that energy alone was exchanged between the modules. In the ASI Prototype III, the heat exchangers are similar to those as described in Sections 4.2.31.

While all three modules play a critical role in the operation of the TACE system, the TACE module, as described previously is the critical component of the system and the focus of this research. As this module was developed to take advantage of

the qualities of ceramics as previously described, the first system design as shown in the patent drawing in Figure 4.18, focused around a rainscreen terra cotta enveloped system.

The challenges of trading energy across the building envelope are multiple. While the envelope assembly includes the TACE module, both the thermal storage module and the interior thermal exchange module must be both linked to the building envelope but also integrated with the existing architecture as part of a systems integration strategy.

By developing the TACE as an integrated building system, the realities of engaging within the architectural construct of multiple building assemblies were confronted. While the method of integration was not the primary focus of this research, the impact of linking together the three primary system modules across the building envelope was a driver for the prototype development and design possibilities as described in Section 4.2.1 and as discussed in Chapter 7. In this way, by making sure the system integration was always present for the scientific inquiry, the research maintained a close relationship within the a priori context of actual buildings rather than remaining part of a conceptual context. This approach becomes important in Chapter 6, where the potential integration for the system is contemplated, the results of which drove the system design in an unexpected direction that is discussed in Chapters 6 and 7.

Figure 4.18 shows a version of the TACE system assembly designed to replace the terra cotta components of a rainscreen cladding system; however, the system can potentially be integrated with different types of enclosure typologies as investigated in Chapter 7.

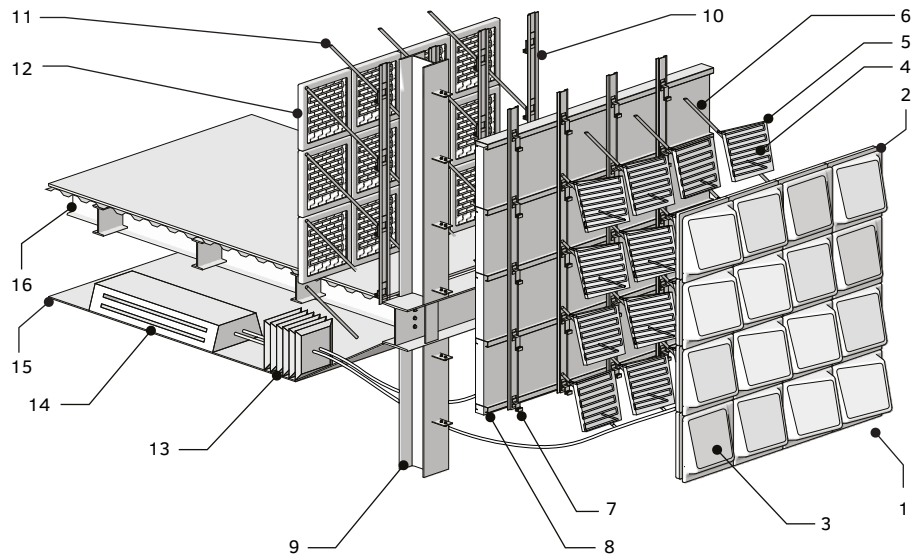


**FIG. 4.18** Early proposed TACE system assembly includes the following components follows: 1. A moulded ceramic rainscreen tile tuned for a specific time range of solar exposures. 2. Lapping tile geometries for rain shedding. 3. A solar collection surface to generate heat energy for building systems. 4. An integrated heat transfer loop system to collect and redistribute heat energy. 5. A thermal storage sink to hold collected thermal energy for transfer. 6. Integrated plumbing system to move heat transfer fluid quickly around the architectural envelope. 7. Typical aluminium track façade system for the easy installation, maintenance, and replacement of modular components. 8. Typical insulation and vapour barrier layers to limit heat transfer between interior and exterior as a semi-active integrated system. 9. The aluminium track allows for easy integration with typical architectural structures. 10. Similar track system for supporting interior tile system. 11. Modular supporting interior tile system. 12. Interior tile radiation geometry tuned for thermal performance, lighting, ergonomics, and other interior design criteria. 13. Heat exchanger for building systems, domestic hot water, heating, heat exchange cooling, etc. 14. Chill beam or other radiation, or convection or other suitable environmental conditioning systems. 15. Typical ceiling geometry to conceal systems. 16. Typical building floor structure.

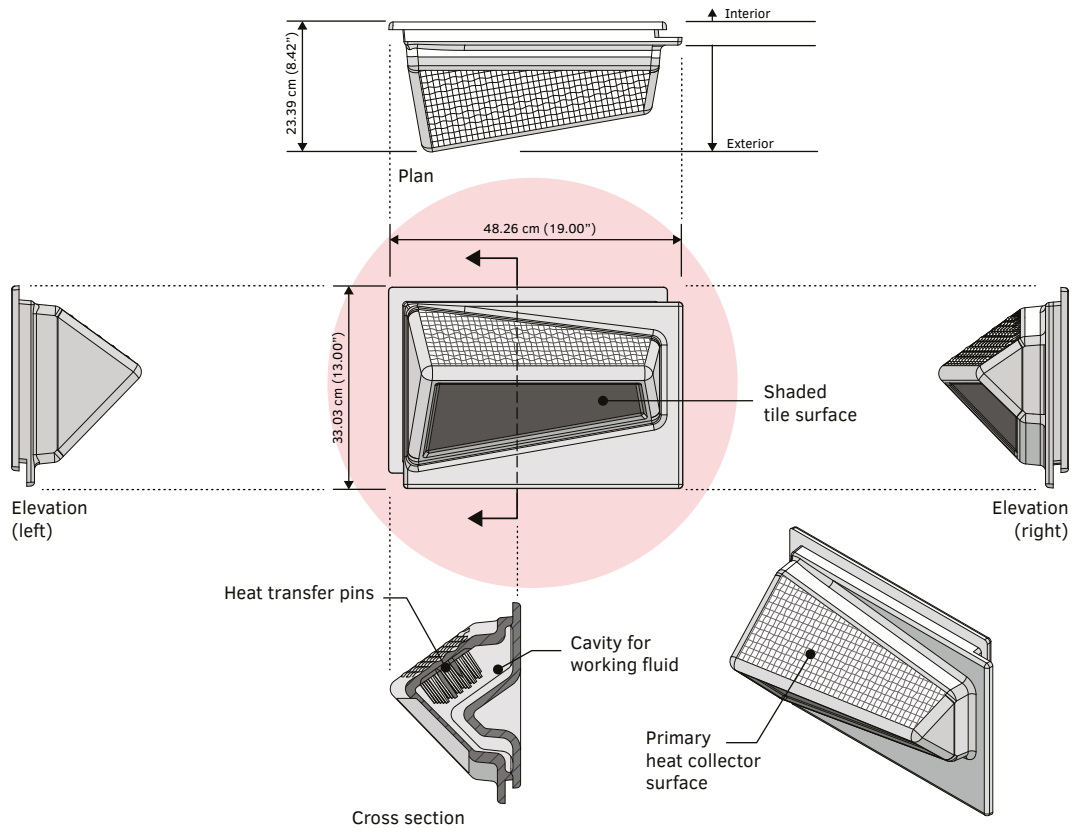


FIG. 4.19 Delineation of the MVP Prototype I that was used for fabrication and testing.

### 4.2.3 Energy Transfer

As described in Section 2.3.1 energy transfer, often referred to as heat exchange, thermal exchange or thermal transfer is the exchange of energy from one medium to another. As shown in Figure 2.6. The TACE system uses both a form of concurrent and countercurrent heat exchange. Supporting the process of capture, transform, store, and distribute are several components and material properties.

### 4.2.3.1 Heat Exchangers

Heat exchangers are typically configured to allow counter current flows. The primary types of heat exchangers at the building equipment scale are bell and tube and flat plate type, as shown in Figure 4.20. Flat plate exchangers such as the Bell & Gossett type offer several distinct advantages over the bell and tube type. Flat plate exchangers are 1/6 the size, 1/5 the weight, 1/8 the liquid volume and 1/3 to 1/5 the surface area for comparable thermal transfer performance (“Brazed Plate Heat Exchangers,” 2019). With comparable performance and a significantly reduced form factor make the flat plate heat exchanger type attractive choice as a key system component and was utilized in the TACE system design and on ASI Prototype III.

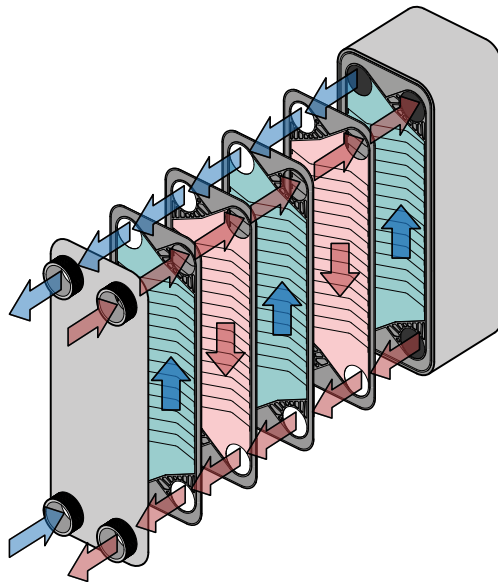
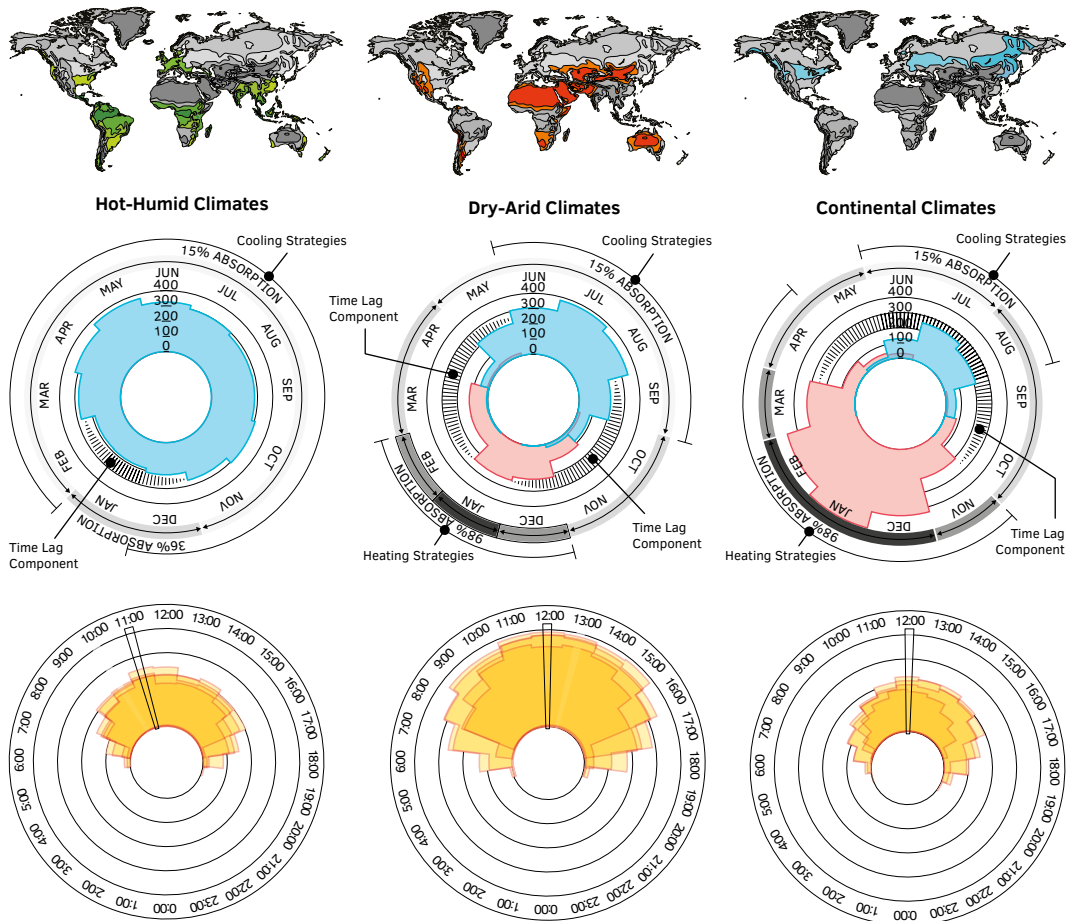


FIG. 4.20 Typical flat plate heat exchangers showing counter current flow energy exchange.

### 4.2.3.2 Energy Storage

Based on the diagram in Figure 2.2, much of the year energy in and around the building envelope needs to be stored before being used. By climate type, the diagram shows the proportion of heating and cooling and the annual percentage where a time lag is needed to move energy from the inside and the outside to maintain thermal comfort for occupants. Energy storage is a component that helps the locally available thermal resources be vectored to be useful.



**FIG. 4.21** Solar resource (as one type of energetic resource) availability by climate type and ceiling relative to heating and cooling degree days (Vollen & CASE, 2010).

Once energy is harvested from the environment, the working fluid moves the energy to a storage module. To be shown in Chapter 5 with MVP Prototype I and POC Prototype II and in Chapter 6 with ASI Prototype III, a simplified water tank storage was used for both quantitative and proof of concept testing. The tight spaces required in integrating the required system components make PCM an appealing material solution due to the power density and tunability of PCM solutions for thermal storage. Thus, the TACE system was developed to take advantage of the compactness of PCM storage systems and was explored in Chapter 7 as part of the system integration design where to explore architectural integration, the SunAmp Heat Battery, as shown in Figure 4.22, was modelled for heat and coolth storage.



SunAmp uses PCM to hold heat or coolth in a compact form factor (500mm X 460mm X 115mm). The basic SunAmp thermal battery is rated at 2.25 kWh, 35kW, with PCM 58°C, 130Wh/LPCM, operating ranges between a 5-80°C: it was designed for use in buildings with a small form factor and adequate storage capacity (Sunamp, 2016).



FIG. 4.22 SunAmp heat battery is an example of a small form factor high capacity thermal storage device that can be used in conjunction with the TACE system. (Sunamp, 2016)

### 4.2.3.3 Materials for TACE

---

The TACE clay body and material properties used for the MVP Prototype I and the simulations were as follows:

#### Material Formulation

---

The ceramic body was predominantly an Alumina formulation, starting with 97% industrial grade alumina ( $\text{Al}_2\text{O}_3$ ), with minor constituents like  $\text{SiO}_2$  and  $\text{MgO}$  from added materials. Recycled glass was added to increase the silica content ( $\text{SiO}_2$ ) up to 10%. Mixes were varied to control flowability and conductance between the starting formulation and a formulation with, for example, 87% industrial grade alumina, 11% silica, and a mixture of  $\text{MgO}$ ,  $\text{Na}_2\text{O}$ , etc. as the additional minor constituents.

#### Basic Material Properties

---

- Compressive Strength about 1,090 kg/cm<sup>2</sup> (15,500 psi)
- Freeze/thaw for 80 cycles, 0.02 weight % loss
- Shrinkage less than .1%

Prototypes II and III shared a common foundation as commercially available terra cotta clay bodies developed by Boston Valley Terra Cotta. While there were some differences based on how each Prototype was produced, they generally both exhibit the following characteristics:

### Material Formulation

The tan ceramic body was predominantly an Alumina and Silica formulation, with 31% alumina ( $\text{Al}_2\text{O}_3$ ) from Aluminum Silicate, and 65.7% Silicon Dioxide ( $\text{SiO}_2$ ) with addition constituents of Potassium Oxide ( $\text{K}_2\text{O}$ ), Calcium Oxide ( $\text{CaO}$ ), Sodium Oxide ( $\text{Na}_2\text{O}$ ), Titanium Oxide ( $\text{TiO}_2$ ), and Iron Oxide ( $\text{Fe}_2\text{O}_3$ ). This formulation was used with various amount of Kaolin, Aluminum silicate, Calcium silicate, Feldspar, Barium Carbonate, and deflocculants as the raw materials and to control flowability. The critical difference is in the varied raw materials and of each formula.

### Material Properties

- Compressive Strength about 422 kg/cm<sup>2</sup> (6000 psi)
- Freeze/thaw resistance, 300 cycles without degradation
- Shrinkage 7-14% depending on pressed, slipped or extruded

## 4.3 **Prototype Design Iterations**

---

Multiple prototypes of the TACE system ceramic components were developed throughout the dissertation research: MVP Prototype I, the development of which is delineated above, and POC Prototype II, ASI Prototype III, and UCW Prototype IV. Figure 4.23 shows the first three prototypes and distinguishes between MVP as designed and as simulated. The design evolution between the prototypes was based on two primary drivers: 1) the results of the research questions regarding the method and quality of energy transfer the TACE module and system is capable of; 2) the integration potential of the system in the architectural and buildings system context. While each prototype addressed a specific phase of TACE component and module design and system development, the design of the module evolved in each prototype as a direct response from three criteria: 1) the results and observations of the physical testing; 2) the quantitative results of the simulations. Similar to the discussion in Section 4.2.2.2, the evolution of the three prototypes used the scientific inquiry as the critical driver of design development. This process of

increasing the role of functional or engineering design and detailing with each prototype was another variable of testing and acted as an additional context within which the scientific inquiry resided.

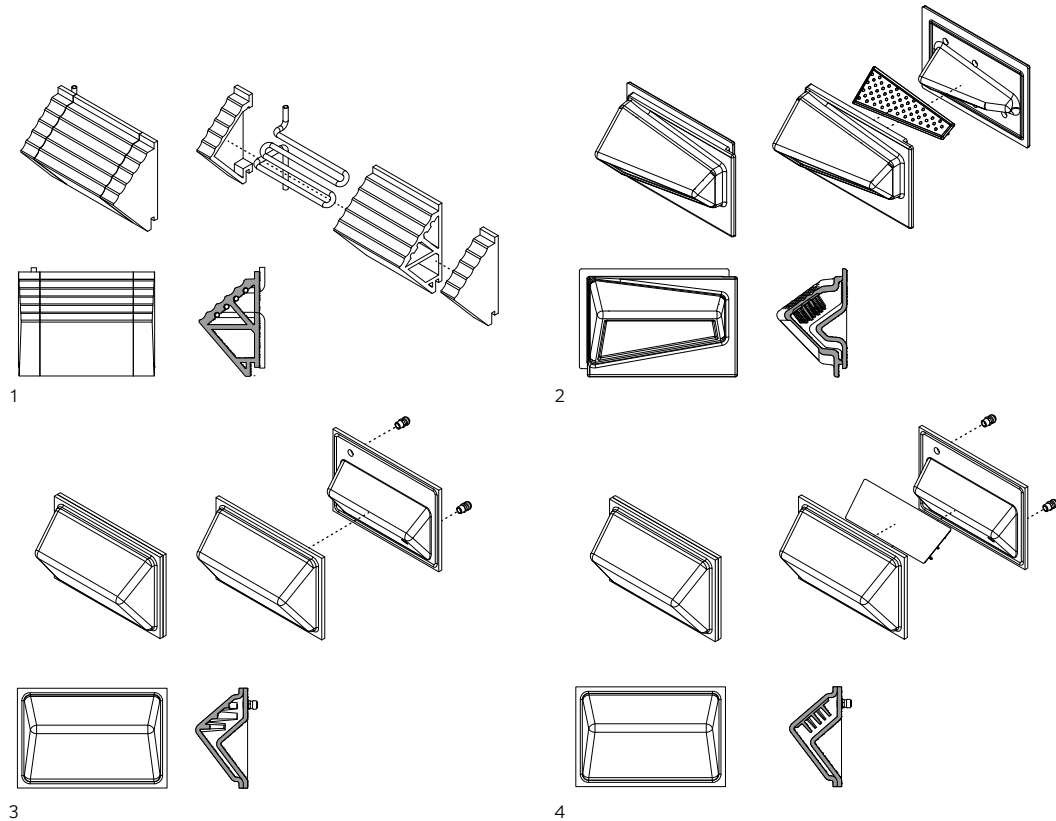


**FIG. 4.23** Delineation of four evolutions of the prototype design: 1) upper right is the MVP TACE Prototype, 2) lower right is the as simulated MVP TACE Prototype, 3) lower left is the POC TACE Prototype, 4) upper left is the ASI TACE Prototype.

### 4.3.1 MVP Prototype I

The MVP Prototype I was developed based on initial conceptual ideation and quantitative testing and computational simulation. This prototype was used to develop the quantitative testing protocols delineated in Chapter 5 and 6. Based on both the experience in developing this prototype and the results of the simulations,

two more prototypes were developed as part of the Advanced Ceramics Assemblies Workshop (ACAW) sponsored by Boston Valley Terra Cotta, in 2017 and 2018. MVP Prototype I was manufactured using a slip-casting process described in Section 7.3.2.1.2, the process of which is summarized in Figure 4.24.

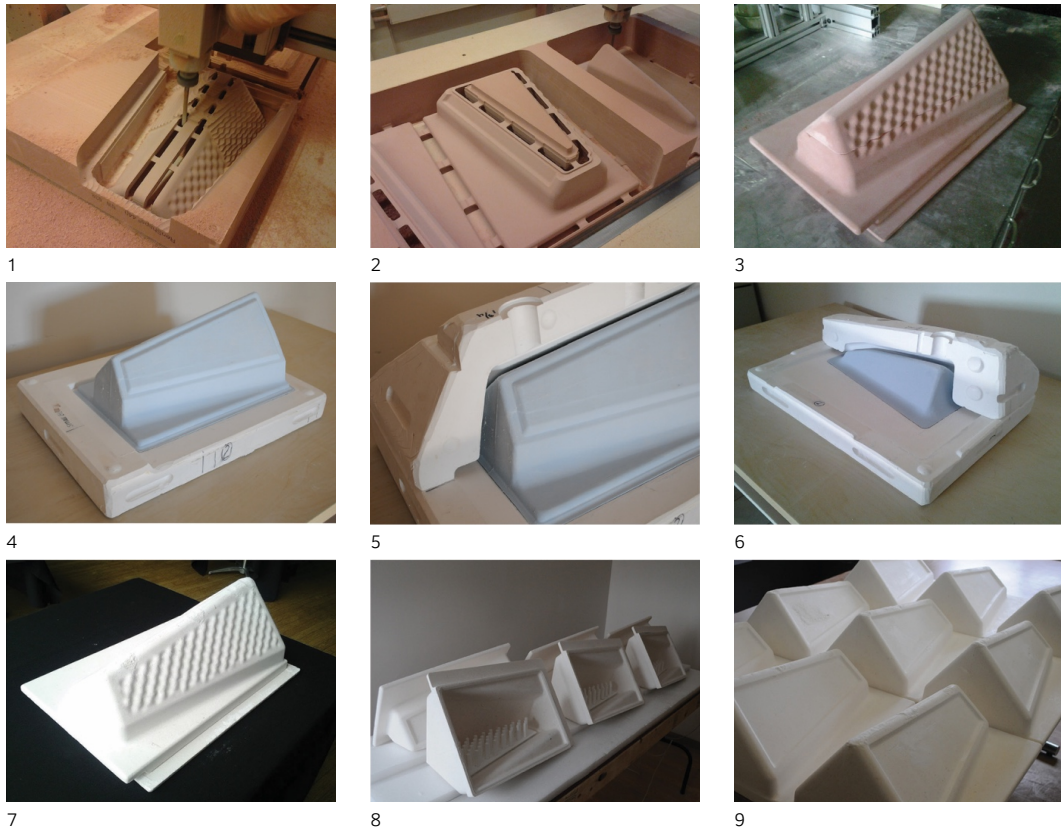


**FIG. 4.24** Photographs of MVP Prototype. 1) CNC router cutting face tile positive. 2) CNC positive of rear tile. 3) Assembled CNC positive. 4) CNC positive with mould piece. 5) CNC positive and mould piece detail. 6) CNC Positive rear tile and mould. 7) Alumina slip-cast TACE face tile. 8) Multiple TACE modules tiles with varying pin lengths. 9) TACE module testing stock.

### 4.3.2 POC Prototype II

Proof of Concept (POC) Prototype II was developed alongside and assembled at the 2nd ACAW conference to demonstrate the viability of thermal transfer and the viability of using industry standard manufacturing processes, shown in Figure 4.25. POC Prototype II was manufactured using a RAM pressing process, as described in Section 7.3.2.1.1. The development and observations from POC Prototype II are discussed in Chapter 8. This prototype aimed to both demonstrate the basic working TACE System which advancing the integrating of the thermal transfer component into the exterior component and connects the interior with the exterior by adding an interior module to receive the energy from the exterior module.



**FIG. 4.25** Photographs of POC Prototype II with workshop participants (1), exterior tile detail (2) and interior tile and working TACE System POC (3).

### 4.3.3 ASI Prototype III

Architectural System Integration (ASI) Prototype III, shown in Figures 4.26 and 4.27, was developed alongside and assembled at the 3rd ACAW conference to demonstrate the production capable strategy that modelled representative system components. ASI Prototype III was manufactured using the extruding process as described in Section 7.3.2.1.3. The development and observations from ASI Prototype III are discussed in Chapter 8. This prototype focused on developing the TACE as an integrated and scaled system, for the first time linking multiple TACE modules together in an array.



1



2

**FIG. 4.26** Photographs of ASI Prototype III from the 3<sup>rd</sup> Annual ACAW conference showing exterior module and tubing matrix (1) and interior radiator/absorber (2).

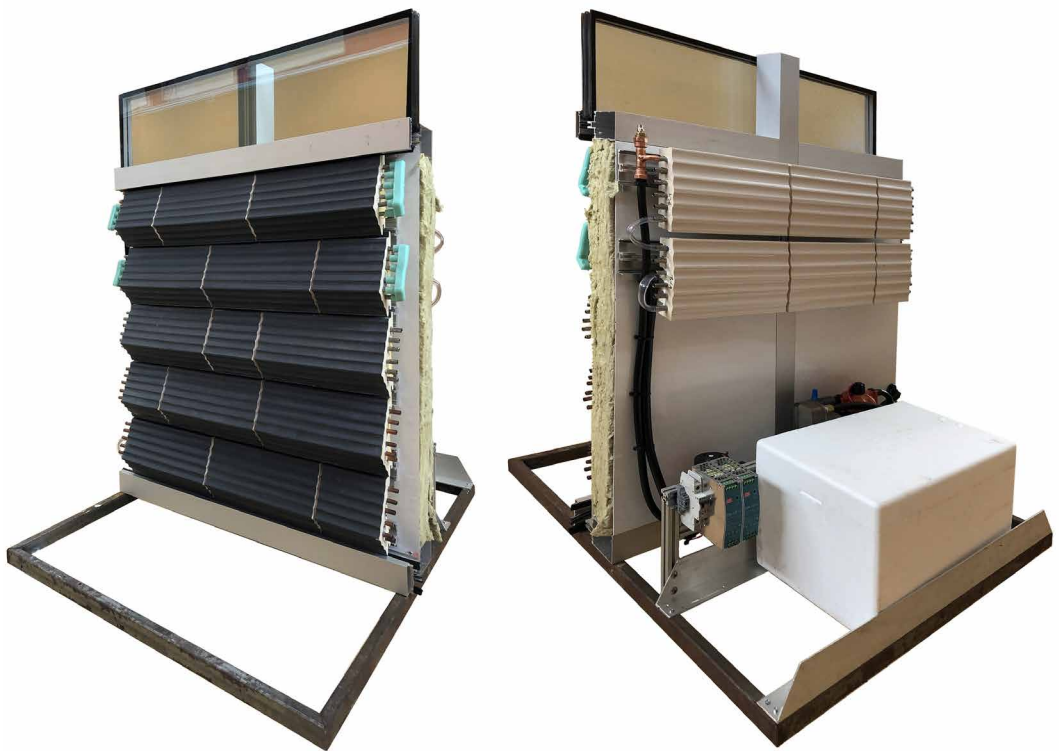


**FIG. 4.27** Reconfigured ASI Prototype III rainscreen developed for the ACAW III into a Curtain Wall frame.

A final UCW Prototype IV was proposed as a future design and is detailed in Chapter 8.

## 4.4 Summary: Development of the TACE system

---

The critical sections for the research inquiry are 4.2.1 and 4.2.1.1 as they identify and locate within the system the variables and constants which are used in the simulations in subsequent Chapters 5 and 6. Conduction, convection, capacitive storage and mass/energy transfer are isolated to test the impact of modulating flow rates and surface areas, as these components are directly related to the speed and quantity of thermal exchange, while reflection, refraction and human thermal comfort remain as constants.

These variables are ultimately what was tested to answer the research questions that lead directly to the iterative evolution of the system, the results of which were shown in Section 4.3.

### References

---

- Brazed Plate Heat Exchangers. (2019). Retrieved from <http://bellgossett.com/heat-exchangers/brazed-plate-heat-exchanger/>
- Forged Heat Sink [Digital Image]. (2019). <https://myheatsinks.com/products/round-pin-heat-sinks/>
- Granta Thermoconductivity Materials Chart, [Digital Image] (2020), <https://grantadesign.com/education/students/charts/>
- Lienhard IV, J., Lienhard V, J. (2018). A Heat Transfer Textbook (4th ed.). Cambridge, MA: Phlogiston Press.
- Sunamp Thermal Battery Storage. (2016). Retrieved from <https://www.sunamp.com/>
- Vollen, J. (2010). Climate Camouflage awarded Special Mention. Integrate: Innovate Competition. New York Center for Architecture.
- Vollen, J., Winn, K. (2013). Climate Camouflage: Advection Based Adaptive Building Envelopes. Paper presented at the 8th Energy Forum Conference Proceedings, Advanced Building Skins, Bressanone, Italy.
- Vollen, J., Winn, K., Dyson, A., & Ngai, T. (2011). US Patent No. US20130340969A1. <https://patents.google.com/patent/US20130340969A1/en>: USPTO.
- Vollen, J., Winn, K., Laver, J., & Clifford, D. (2008). Digital Material: Ecological Response in Parametric Modeling. Architecture in the Age of Digital Reproduction. Paper presented at the ACSA West Central Fall Conference.
- Winn, K. (2014). Inter-scalar Multivariable Decision Making Framework for the Architectural Envelope. (Ph.D.), Rensselaer Polytechnic Institute, ProQuest LLC.



# 5 Component Performance

---

The Minimum Viable Product (MVP) of the Thermal Adaptive Ceramic Envelope (TACE) as delineated in Chapter 3 as the MVP Prototype I was developed to leverage specific design attributes that are hypothesized to impact the energy performance of specific TACE components. In order to have an accurate evaluation of the performance of the TACE system, a comprehensive and highly resolute energy model using industry standard metrics needed was developed. This model was calibrated to physical testing data developed from a modified ASTM C1363-11 Standard Test Method for Thermal Performance of Building Materials and Envelope Assemblies by Means of a Hot Box Apparatus. Without this model and testing data, it was difficult to: 1) understand which design attributes are contributing to the performance of the TACE system, and thus; 2) which future directions for refinement should the TACE be developing in order to gauge the potential impact of the system on Energy Use Intensity (EUI) reduction.

## 5.1 Introduction

---

Chapter 4 focused on the performance of the design attributes of TACE: surface areas, flowrates, and material properties. The objective of this chapter was to test the performance of design attributes to determine how much impact, if any, did they have in isolation or combination, on the overall performance of the TACE. In support of answering the primary research question that was focused on overall Energy Use Intensity reduction of the TACE system, Chapter 5 aims to answer the following research sub question:

**What design attributes of the Thermal Adaptive Ceramic Envelope impact Energy Use Intensity reduction?**



In order to answer this question, the following dependent questions were investigated in this chapter:

- How much impact does the thermal mass of the ceramic have on the energy transfer rate?
- How much impact does the length, mass, and geometry of the thermal transfer components have on the heat transfer rate?
- How much impact does the adhesive used to assemble the ceramic components have on the transfer rate?
- How much impact does the flowrate of the working fluid have on the energy transfer rate?
- How much impact does adding an insulating layer have on the heat transfer rate?

## 5.2 Research Collaborations

---

Modelling in support of this chapter was funded by a \$44,000 grant from the Green Technology Accelerator Center (GTAC) as part of a program administered by the New York State Pollution Prevention Institute (NYSP2I). The funds were distributed to the Center for Architecture Science and Ecology (CASE) at Rensselaer Polytechnic Institute (RPI) to support research assistant Justin Shultz, and the class project for MANE 4140 given at RPI in the Spring Semester of 2017. The focus of the class was to develop a numeric translation of the TACE module to be used in designated model scenarios in support of the objective of this chapter. Through the GTAC funding, Matt Gindlesparger at Jefferson University in Philadelphia collaborated on the physical testing and model calibration. The author designed the experiments and methodology in this chapter and with Shultz and Gindlesparger worked collaboratively to execute the experiments. The contents of this chapter have been peer-reviewed and published and presented in part in the 2018 ARCC-EAAE International Conference Architectural Research for a Global Community proceedings as Design Optimization Workflow for a Dynamic Mass Envelope System Using Complementary Digital and Physical Testing Methods by Gindlesparger, Harrison, Shultz and Vollen (Gindlesparger et al., 2018).

## 5.2.1 Research Methods

---

The primary method used in Chapter 4 was a computational framework. A discrete numeric model of the performance of the individual components of the TACE module was taken into a broader simulation framework that evaluates the performance of the component as part of the assembly. The computational model was calibrated using a physical quantitative test and further refined using a CFD model.

### 5.2.1.1 Modelling and Simulation

---

Current standards for modelling the performance of buildings in the United States is the EnergyPlus building energy model engine (“Energy Plus,”). The use of EnergyPlus in support of the research was to develop an apples-to-apples comparison in terms of Energy Use Intensity (EUI) - a direct output of the model. For EnergyPlus to accurately reflect the performance of the TACE system, the TACE module was modelled in a building physics simulation environment: Modelica.

### 5.2.1.2 Design

---

The design of the model and simulations was based on isolating key variables that were developed into the design attributes of the TACE module delineated in Chapter 4. While EnergyPlus does not have the capability to include the performance of design attributes at the component scale, other modelling environments do. To answer the primary research question, the model and simulations were required to span multiple scales, from the attribute to the building, therefore requiring that several modelling environments work together as a co-simulation. Chapter 5 is focused on the modelling of the design attributes into the Modelica modelling environment framework that provided the basis for integration into the co-simulation environment.

### 5.2.1.3 Modelica

---

Modelica is an open source modelling language that uses equations in object-based assemblies to solve for a variety of physics based problems (Modelica). It was therefore useful in simulating complex building physics scenarios like fluid dynamics

and mass transfer at the building envelope. While Modelica was essential to solving the physics based problems of the TACE, the components were arranged as a series of interacting physics objects. Modelica then output these interactions into a broader building simulation environment.

#### 5.2.1.4 Dymola Interface

---

Dymola is the Modelica modelling environment developed by Dassault Systèmes. Since Modelica is object oriented, it allows the development of specific performance components and links them together to run simulations. Dymola can also package the model as a defined object. This object is called a Functional Mock-up Unit (FMU). The FMU was exported from Dymola as a code object that was compatible with an IDF file; the same file type that comes from Energy Plus when exported from Open Studio as will be utilized in Chapter 5 (Dessault Systèmes, 2018).

### 5.2.2 Model Calibration

---

The simulation framework, as shown in Figure 5.1, was designed to explore a wide range of tile and system designs. Calibrating the computational model that was the basis for the simulation framework was essential to developing results that could be extrapolated to the building scale simulations. To calibrate the simulation framework a two phase process using both a Computational Fluid Dynamics (CFD) model using Altair AcuSolve and quantitative physical testing was used to compare temperature profiles across the MVP Prototype I TACE module. AcuSolve is industry proven and was chosen as the CFD simulation environment as it allows for simultaneous fluid and heat transfer interactions of conduction and convection; critical to characterizing how the TACE system was intended to operate (“Acusolve,” 2019). The Modelica MVP Prototype I module model was adjusted to develop a curve fit that approximates the quantitative testing data. The quantitative testing was conducted using several TACE modules inserted within a calibrated and modified hotbox based on the ASTM C1363 Standard Test Method for the Thermal Performance of Building Assemblies by Means of a Hot Box Apparatus. A modified standard hot box design was used instead of a guarded hot box design as the TACE module fitted completely within the hot box chamber; therefore, the metered chamber was used when the testing subject could not completely fit within the testing chamber.

### 5.2.2.1 CFD Model Experimental Validation

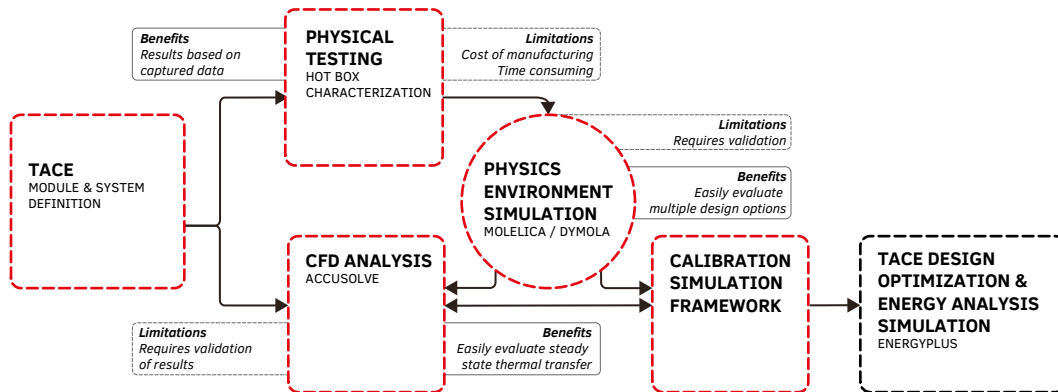
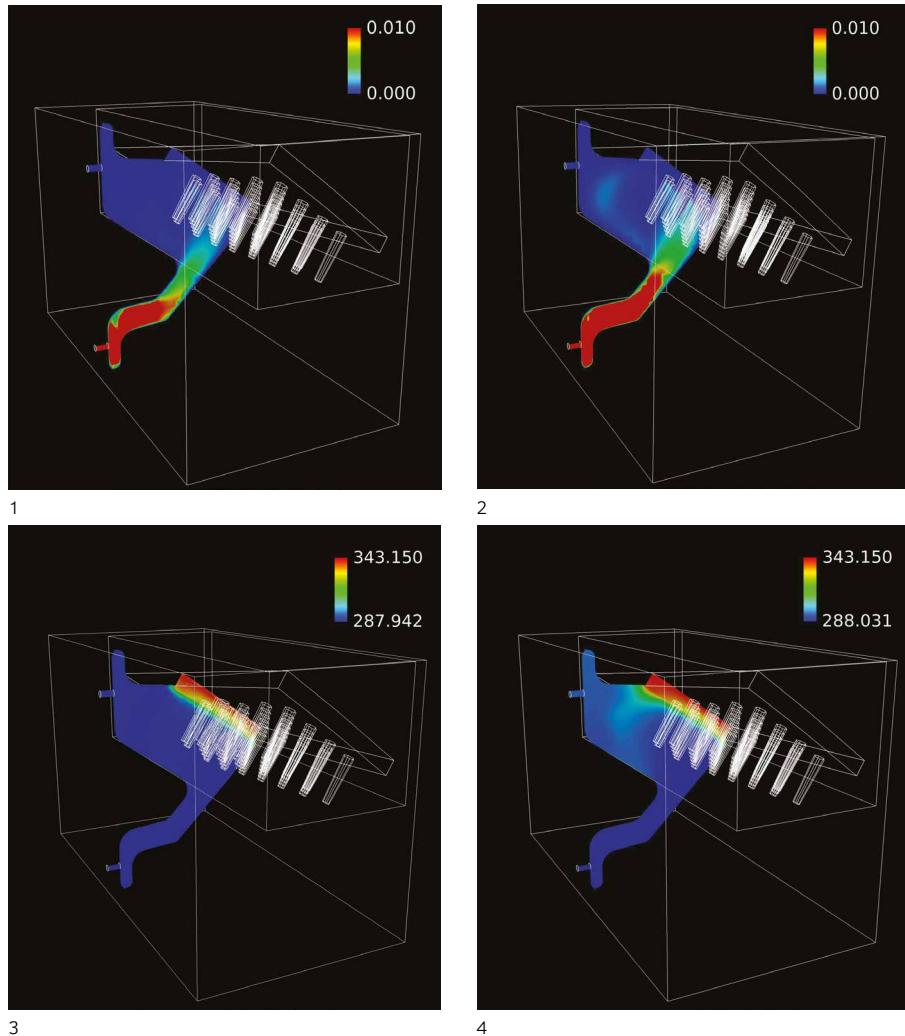


FIG. 5.1 Diagram of the testing process showing the integration of physical results with simulations..

The CFD model, as shown in Figure 5.2, and an MVP Prototype I Modelica model was produced with corresponding boundary conditions. A 70°C surface temperature was introduced to the top of the exterior TACE component in both models; 70°C was the assumed max temperature of a black roof in summer conditions. Simulations were run for 0.625, 1.250, and 2.500 liters per minute (l/min) (0.165, 0.33, and 0.66 gallons per minute (gpm)) flowrates and the energy transfer component with pin lengths specified of 0, 1.1, 2.9, and 4.4 cm (0.4375, 1.155, and 1.75 in). These pins lengths reflect the actual physically tested pin lengths, the specific sizes were limited by the longest possible pin array that fit within the module geometry, which was limited by the fabrication technique, with medium and small lengths chosen to demonstrate a range of lengths, and thus surface areas, in a nonlinear progression. The flowrates were determined by using the upper range of the small circulator pump which was similar to the low range of a radiator circulator pump, then stepping down in thirds. Both the flowrates and lengths listed above are consistent through the experiments. Each configuration was run within the CFD model and Modelica model for the duration required to achieve a steady state; with 1 minute of preconditioning, steady state was achieved between 20 and 60 minutes. The Modelica model was observed to be overestimating the temperature increase for each of the flowrates by about 2°C (3.6°F) in comparison to the CFD model.



**FIG. 5.2** Acusolve CFD Model of Temperature and Velocity Difference Between Comparing the .33 and .66 gpm flowrates.

To adjust for the trending 2°C (3.6°F) increase in temperature from the Modelica model as observed by the CFD model, the pin convection coefficient was reduced in scale by 30%, resulting in an overall efficiency of 70% in the Modelica model. As shown in the CFD image in Figure 5.2, and results in Figure 5.6 and Table 5.2, not all the pins transfer heat to the working fluid at the same rate. To account for this uneven thermal transfer rate, a flowrate contingent function was applied. This function was included in the Modelica model that modulates the efficiency factor

from 67% for 2.5 l/min (0.66 gpm) of flow up to 72% for 0.625 l/min (0.165 gpm) flow. While it was difficult to validate the efficiency factor and flow dependent applied above without significantly more study, cross-referencing the results between the physical model, the CFD simulation, and the Modelica simulation creates a conservative case as a baseline.

### 5.2.2.2 Results: CFD Model Experimental Validation

After applying the efficiency factor and the flow dependent factor, the average temperature difference between the Modelica calibration model and CFD model did not exceed more than 0.41°C (0.738°F) for each tested flowrate; a 4.04% disparity as shown in Table 5.1. The energy transfer component that has medium pin length pins were used in the subsequent building energy modelling that had the highest temperature divergence of 0.18°C (0.234°F); a 2.37% disparity, the more conservative approach was used (Gindlesparger et al., 2018).

TABLE 5.1 Results of the thermal transfer simulation before and after calibration.

Pin Length	Temperature Difference (°C) Before CFD Calibration			Temperature Difference (°C) After CFD Calibration		
	0.625 l/min (0.165 gpm)	1.25 l/min (0.33 gpm)	2.5 l/min (0.66 gpm)	0.625 l/min (0.165 gpm)	1.25 l/min (0.33 gpm)	2.5 l/min (0.66 gpm)
1.1 cm (0.4375 in)	13.06	9.57	7.17	9.83	7.46	5.37
2.9 cm (1.155 in)	13.15	9.78	7.23	10.29	7.64	5.42
4.4. cm (1.75 in)	13.19	9.79	7.14	10.3	7.64	5.42
Average	13.13	9.71	7.18	10.14	7.58	5.40
CFD Results	10.55	7.76	5.48	10.55	7.76	5.48
Difference Between Modelica and CFD (°C)	-2.58	-1.95	-1.70	0.41	0.18	0.08
Percentage Change Between Modelica and CFD	-19.67%	-20.11%	-23.68%	4.04%	2.37%	1.42%

### 5.2.2.3 Physical Model Calibration

The second phase of model calibration used experimentally quantified data gathered from physical testing to adjust the transient energy flow rates in the Modelica MVP Prototype I module model. The calibration assembly includes four primary

components: 1) the testing chambers; 2) instrumentations; 3) the TACE MVP Prototype I modules; 4) a mass transfer working fluid loop.

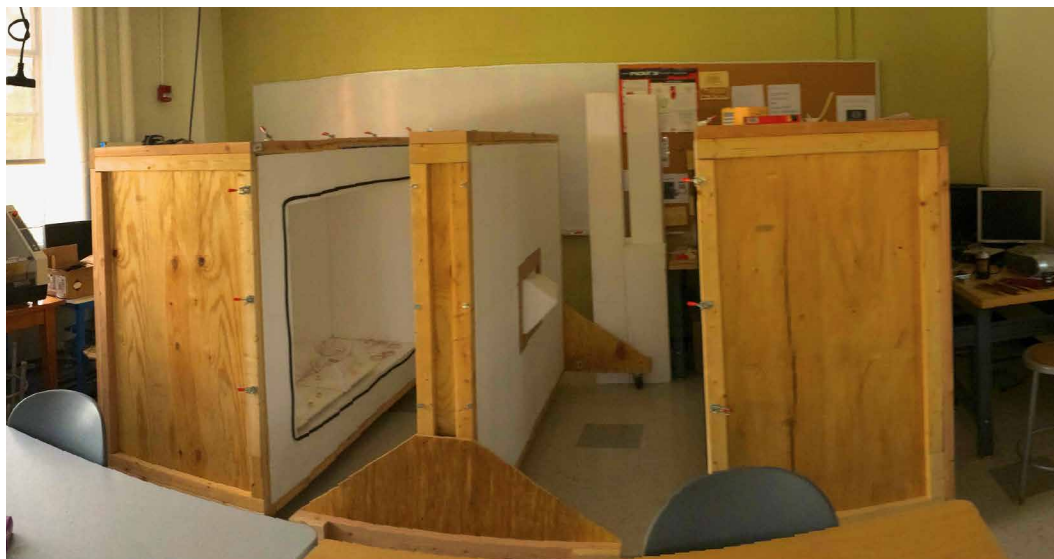


FIG. 5.3 Hotbox rig showing centre module mounting area and interior and exterior environmental chambers.

The chamber wall construction was comprised of 8" thick 2lb per cubic foot polystyrene foam insulation designed and constructed using a modified hotbox test chamber, based on ASTM C1363 Standard Test Method for Thermal Performance of Building Materials and Envelope Assemblies by Means of a Hot Box Apparatus. The fundamental hotbox arrangement consists of two same sized thermal chambers (ASTM, 2012), as shown in Figure 5.3 and 5.4.

A 950w enclosure heater was placed within the exterior chamber, which provided the thermal load. The thermal conditions in the hotbox enclosure were observed and recorded with a 32 total channel Data Acquisition system. The individual thermocouples were located at varying positions which provided an understanding of the thermal profile and conditions with the hotbox. The measurement of values was averaged with focus on looking for rates of change, rather than absolute values; thus, a broader array was used, creating an extensive network within the chamber. The averaging was also used to account for the accuracy of the T-type thermocouple, which can vary as much as 1°C (1.8°F).

The data sample rate was set for one measurement per second per thermocouple. The Ambient Temperature was monitored by a single thermocouple positioned on the exterior face of the experimental setup used as a control to monitor the environment that the experiment took place. The Exterior Chamber used an array of 8 thermocouples, with two on the back surface, two on the top surface, and one on each side surface, to develop an average temperature within the exterior chamber. The exterior face of the TACE MVP Prototype I module was monitored using two thermocouples on the upper and two on the lower faces. The working fluid was monitored with one thermocouple submersed in-line on the water inlet side of the TACE module, one submersed within the fluid of the TACE module, and one submersed in-line on the water outlet side of the TACE module. The thermocouples used for the inline data acquisition were immersion type stainless steel designed for insertion in pipes to monitor fluid temperatures. The interior face of the module used three thermocouples positioned on the component surface within the interior chamber. In a direct correlation with Exterior Chamber, the Interior Chamber also used eight thermocouples positioned on all interior surfaces in order to characterize the difference and rate of change in the environments and monitor the amount of energy through temperature change that was transmitted through the TACE MVP Prototype I module. Energy capture was also monitored with one thermocouple submersed in the storage tank ((NYSP2I), 2017).

The modules used for testing have ports on the interior component of the module for inlet and outlet of the working fluid and additional ports which serve as openings for the thermocouples. The inlet and outlet ports of the module were fitted with ball valves that modulate the flowrate. The working fluid was circulated at specific flow rates through the insulated piping into the insulated storage tank. The tank was filled 9.46 litres (2.5 gallons) of water. The amount in working fluid in the module was 4.73 litres (1.25 gallons)



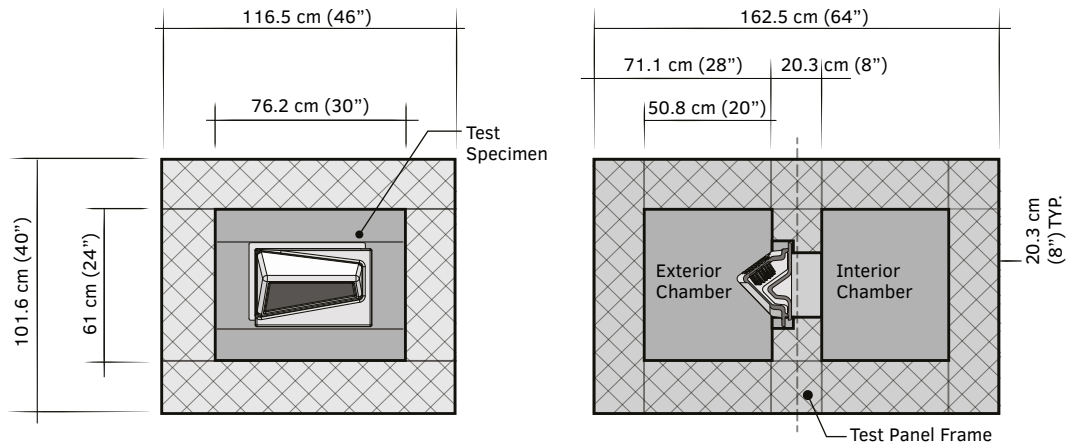


FIG. 5.4 Schematic of TACE module testing chamber.

The outside of the TACE module was exposed to the Exterior Chamber, and the inside was exposed to the Interior Chamber. In this configuration, the only non-insulated connection between the two chambers was the module and the working fluid. Because the module was the only direct connection, thermal energy must pass through the module, and the flow could be measured and characterized via the temperature differential in the chambers and the inlet and outlet temperatures.

A minimum of three 20 minute testing runs for each set up was conducted with the purpose to observe the consistency in temperature rise in the chamber and flow while using a consistent flowrate. Following preconditioning and once each the set up was observed to work consistently, three final testing rounds were conducted and logged for comparison with the simulation framework. Throughout each run, relative starting temperature, set-point temperature, ramp time, soak time, and fluid volume was maintained as consistent. The only variable used to create the ramp profiles was the flowrate of the working fluid: 1) 0 l/min/gpm, static or no flow; 2) 0.625 l/min (0.165 gpm), low flow; 2.5 l/min (0.66 gpm), high flow.

The scheduling and steps for each of the experimental rounds were as follows:

- 00:00 / Verify TC Temperatures: enclosure and fluid temperatures in the TACE MVP Prototype I module and storage tank were at ambient temperature
- 00:00 / Test Run Start: begin data-logging, and initiate fluid flow, no heat

- 02:00 / Ramp Profile:  
Turn on heater (set point at 60°C (140°F))
- 40:00 / Soak Profile:  
Turn off heater, continue water flow
- 120:00 / End Test:  
discontinue data-logging

With a starting temperature of 23°C for both chambers, the preconditioning between experimental setups took about 60 minutes to reach the starting temperature, the approximate time for the apparatus to return to ambient temperatures. The water temperature was also returned to ambient temperatures during the preconditioning period. Thus at the start of the experiments, both chambers were at a steady state near equilibrium temperature with no discernible flow. The pre-defined ramp temperature and soak temperature profile began with heat coming from the enclosure heater. The temperature for the hot side of the chamber was set at 60°C (140°F); ramp time was 38 minutes; the soak time was an additional 80 minutes. Once the ramp time was achieved, the heater was turned off. The thermocouples continued to take readings during the soak period until both sides of the chamber reached a new steady state, based on how much energy was put into the test chamber. As noted, following reaching a new steady state condition, the experiment was re-prepped with preconditioning and repeated.

The Modelica calibration model was configured to the same parameters as the hotbox chamber set up. The temperature of the working fluid in the storage tank was used as the baseline fluid inlet temperature. A convection heat transfer coefficient was calibrated in the model for the hot side of the TACE exterior component to match the surface temperature as seen in the experiment. This convection heat transfer coefficient was assumed to be 100 W/m<sup>2</sup> K (17.62 btu/hr/ft<sup>2</sup>/F) do to the hotbox chambers being small encapsulated spaces. This size resulted in a more considerable amount of air movement from the heating unit and the large temperature difference observed between the air in the exterior chamber and the exterior face of the module.

#### 5.2.2.4 Results: Physical Model Experimental Validation

---

The MVP Prototype I module was designed to have an offset inlet and outlet ports. The inlet port was on the lower left side of the interior components when viewed from inside; the outlet was placed on the upper right when viewed from inside, as shown in Figure 5.5. The Modelica model and the CFD model were initially set up with the

same outlet configuration. An alternative was tested in the CFD model that aligned the inlet and outlet ports in the centre of the time, top and bottom respectively. It was observed that the model with the parallel central port configuration had a more even spread of heat transfer between the pins with limited short circuiting, thereby delivering more heat transfer from the pin components to the working fluid as more fluid was forced across more pins more evenly. The offset ports performed at a decrease of about 75% from the parallel pins. Therefore, an additional 75% efficiency factor was added to the Modelica model to simulate the use of parallel pins in the building energy simulations.

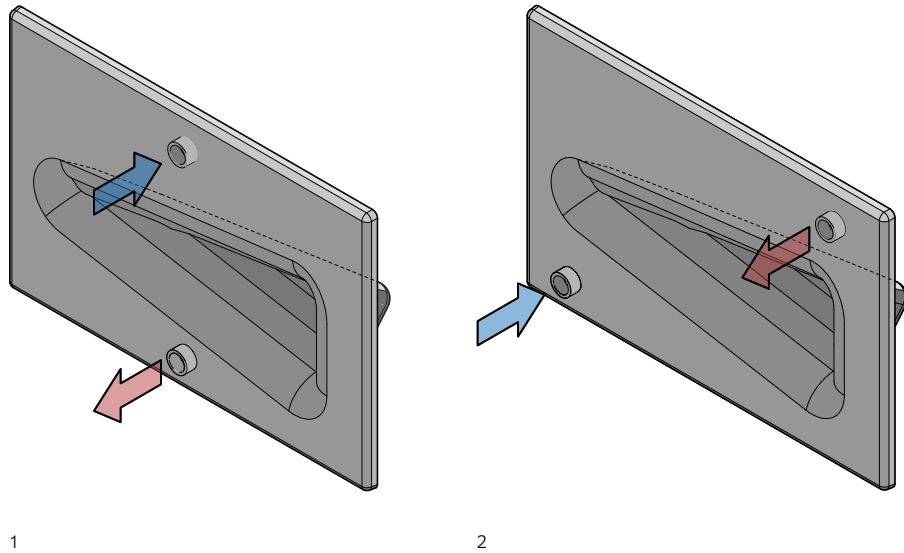


**FIG. 5.5** Module showing the different locations, (1) parallel, and (2) offset, of the inlet and outlet ports.

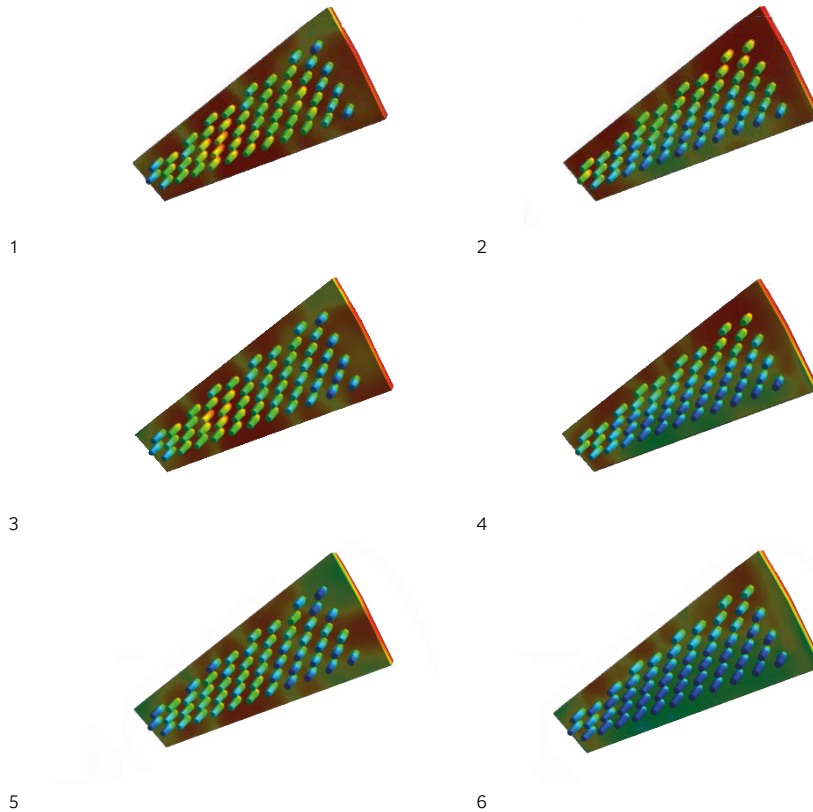


FIG. 5.6 Results visualization illustrating heat temperature distribution for parallel (Left) and offset (Right).

TABLE 5.2 Comparison of Temperature Gradient at Various Flowrates, Offset Setup (Left) vs No Offset Setup (Right)

Flowrate l/min (gpm)	Medium Pin: 2.921 cm (1.15 in)	Medium Pin: 2.921 cm (1.15 in) w/ offset
0	-54.8966	-54.8623
0.625 (0.165)	-10.4834	-7.8287
1.261 (0.333)	-7.3455	-4.8695
2.521 (0.666)	-5.50717	-3.3865

The data that was logged from the hotbox enclosure with MVP Prototype I and energy transfer component medium pin length 29.34mm (1.155 in) with the .625 litres per minutes (0.165 US gpm) flowrate was compared to the Modelica experimental validation model that was modified with the data from the CFD and steady state model. The medium pin length was determined in early physical testing

to have the equivalent of the long pin length, this was confirmed in subsequent simulations. The temperatures of the outward facing surfaces of the Modelica systems model of the exterior and interior components were compared to the measured data logged from the hotbox chamber experiment. These temperature ranges appear to match in quantity and ramp profile, as shown in Figure 5.7.

The working fluid temperatures were measured at the inlet and outlet ports of the MVP Prototype I module in the modified hotbox chamber experiment to the Modelica Module Model results. The working fluid outlet temperature of the Modelica Module Model shows more movement due to the high temperature peaks in the surface on the exterior component temperature than the hotbox chamber experiment. As expected, the higher peaks of the outlet port working fluid temperature for the model corresponds to the temperature peaks on the surface of the exterior component. While a significant amount of noise was recorded in the working fluid temperature as shown in Figure 5.7 the peaks in temperature should be noted, though not to the quantity or clarity of the Modelica Module Model results. Modifications (e.g., adding more mass to the model, changing surface areas, etc.) to the Modelica Module Model were implemented in an attempt to better align with the lower peaks of the experiment results. No modification developed a better fit curve than the one shown in Figure 5.7. To develop a more accurate fit curve to the experimental ramp profile, additional comparisons are suggested that examine more discreet and isolated areas of the MVP Prototype I Module.

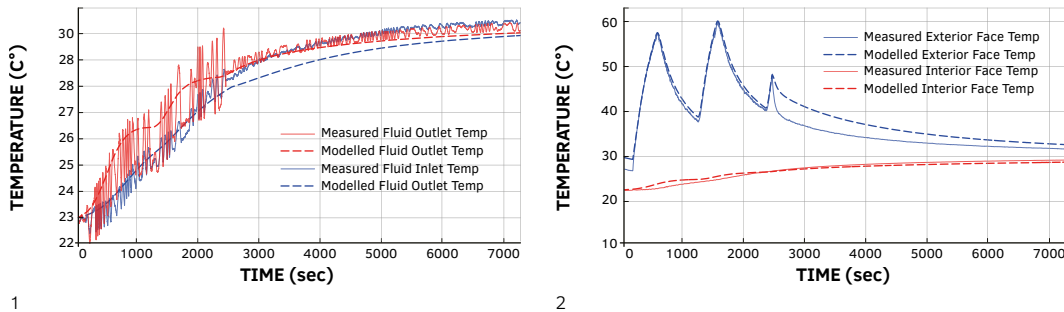


FIG. 5.7 Comparison of fluid temperatures (1) and tile face temperatures (2) showing measured and modelled results.

Results from quantitative testing were used to calibrate the Modelica Module that was used in the co-simulations that were developed as the basis for the energy models in Chapter 6. This calibration process supported the quantitative comparison between the TACE system and baseline systems.

A parallel simulation experiment was created with the same variables and the results adjusted to align with the physical testing.

## 5.3 Performance of Component Attributes

---

As discussed in Chapter 3, the MVP Prototype I module was developed as a set of components. The attributes of these components were then adjusted to an attempt to modify the energy flows across the building envelop. A Modelica Module Model was developed to test the efficacy of a range of key attributes; Mass, Thermal Transfer Geometry, Joining Techniques, Flowrates, and Insulation. Variables associated with these attributes were simulated to understand what, if any, effect they would have on the flow of energy across the TACE module as a whole. The overarching investigation asked in this section is – what is the difference that makes a difference.

### 5.3.1 Simulations

---

The simulations to investigate the design attributes of the components of the MVP Prototype I module was conducted from a Modelica model developed in Dymola. The model was run as a steady state and developed in two scales; the physical attributes of the MVP Prototype I module, as shown in Figure 5.10, that was contained within a simulated physics environment, as shown in Figure 5.8. Figure 5.9 shows the variables that are being isolated and modulated to answer the supporting research questions investigated in this chapter.

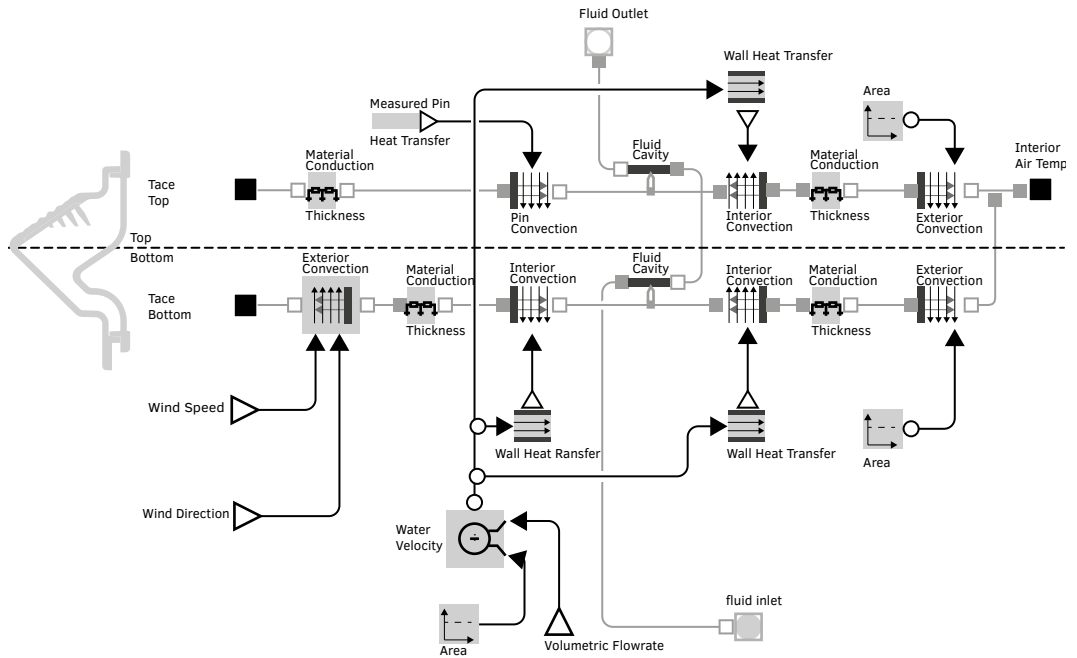


FIG. 5.8 Diagram of Modelica model components.

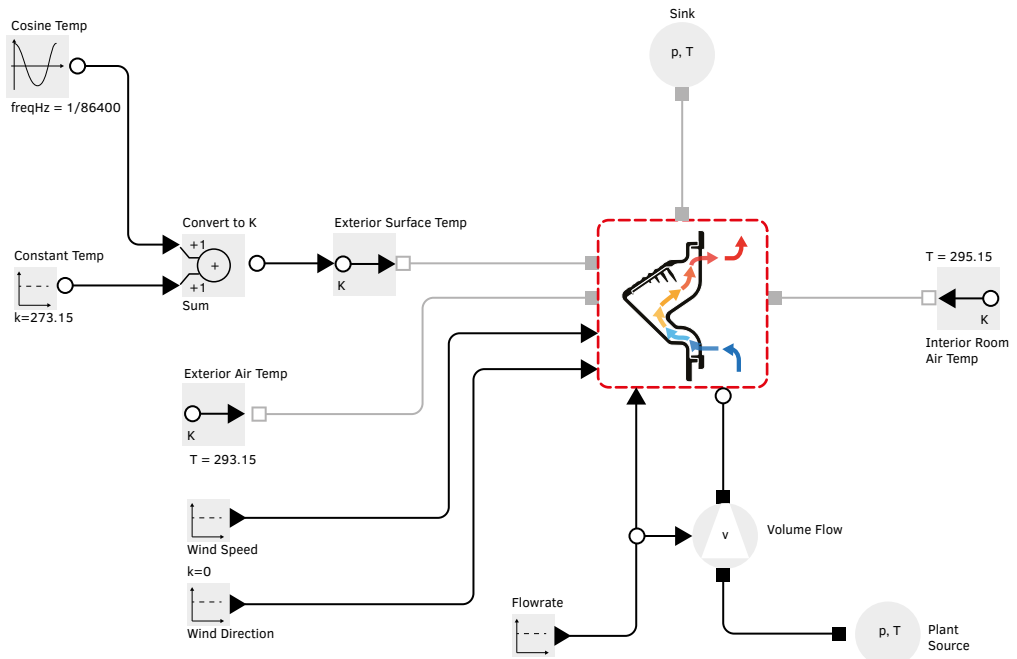


FIG. 5.9 Variables isolated to develop the scientific comparison.

## 5.3.2 TACE Module Key Attributes

The attributes of the physical TACE module as delineated in the conceptual design in Chapter 4 were developed into building physics components in the Dymola environment for simulation.

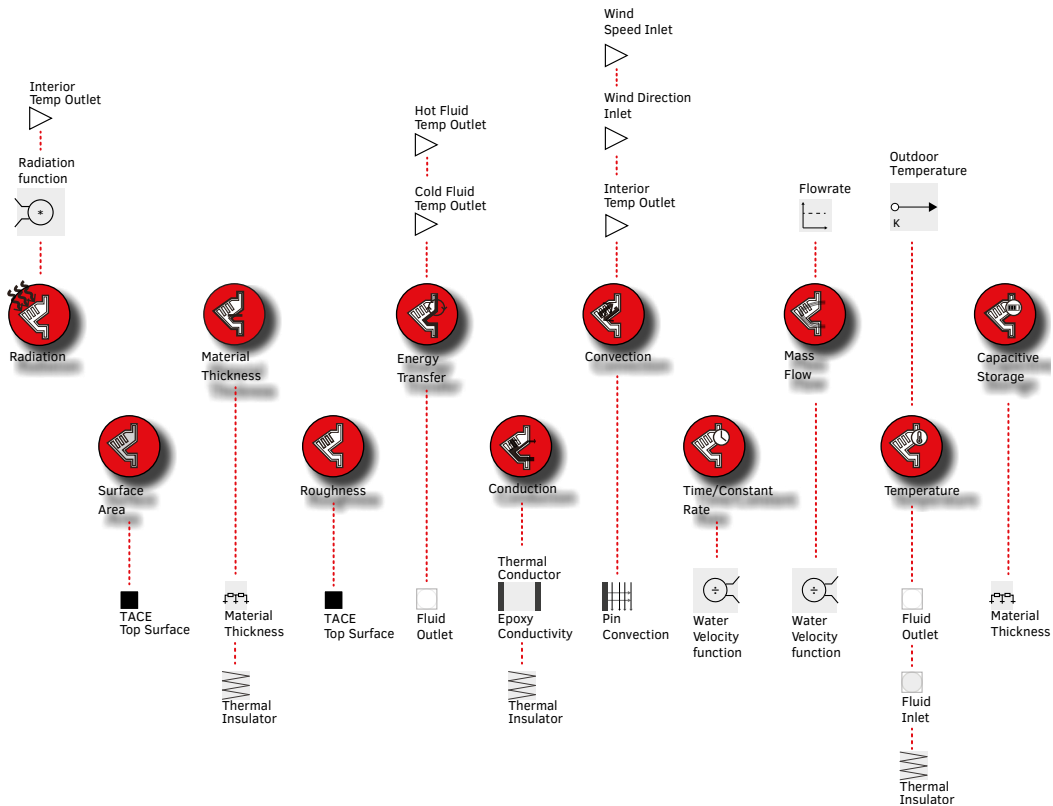


FIG. 5.10 Key attributes used to manipulate the energy flows within the Modelica model: model nodes above attributes are external to the TACE module; model nodes below the attributes are internal to the TACE module.

### 5.3.2.1 Mass

The energy transfer component of the MVP Prototype I was modelled and tested using the differing lengths of pins. Testing one size pin against another, the module mass as a whole was also changing in proportion to the changing mass of the pins.



The pin length of 1.1 cm (0.4375 in), for example, has a mass of 13.86 grams (0.49 ounces), where a pin length of 2.9 cm (1.155 in) has a mass of 16.79 grams (0.59 ounces) using 3.5 g/cm<sup>3</sup> (2.02 oz/in<sup>3</sup>). With greater mass, we would expect higher heat capacity as thermal capacity was dependent and in proportion the amount of material. In order to understand how much the change in module mass could impact operative thermal capacity, it was critical to test if the amount of component mass had any effect on the mass transfer of the module as a whole as illustrated in Figure 5.11.

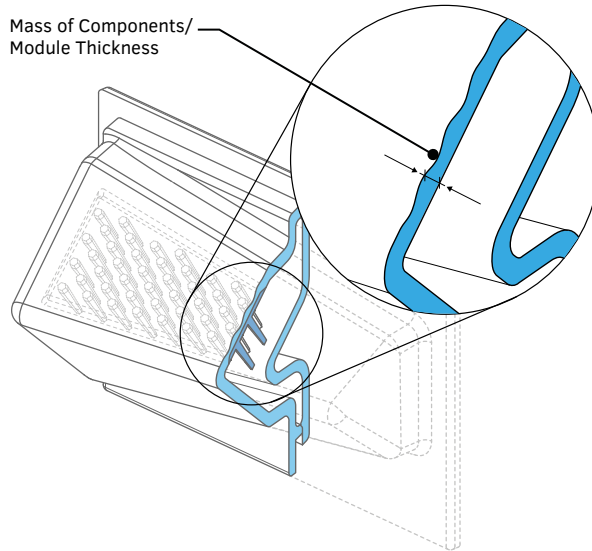


**FIG. 5.11** Diagram of pin connection showing variable mass. The simulation was run with several different masses for the pin plate to determine how much impact increased mass would have on the overall performance.

The upper transient conduction component, “Front Top Panel Transient Conduction” of the Modelica model, as shown in Figure 5.12 contains the physical attributes (e.g., thermal capacity, conductivity, etc.) for the top of the component. This study varied the thickness of the upper transient conduction component, as highlighted in Figure 5.12. By changing the physical amount of material; the thermal capacity was altered. The impact of mass on the performance of the MVP Prototype I model can be understood by the impact on the inlet and outlet port temperatures. The energy transfer component (e.g., the Pin and Pin Base) was kept a constant mass in order to isolate a single variable.

A cosine thermal ramp profile was set to range from 0-75°C (32-167°F) for one diurnal cycle, or 24 hours, and run with three different thicknesses for the upper transient conduction component. The model was set up to model the inlet and outlet port temperatures and record changes over the ramp period temperatures.

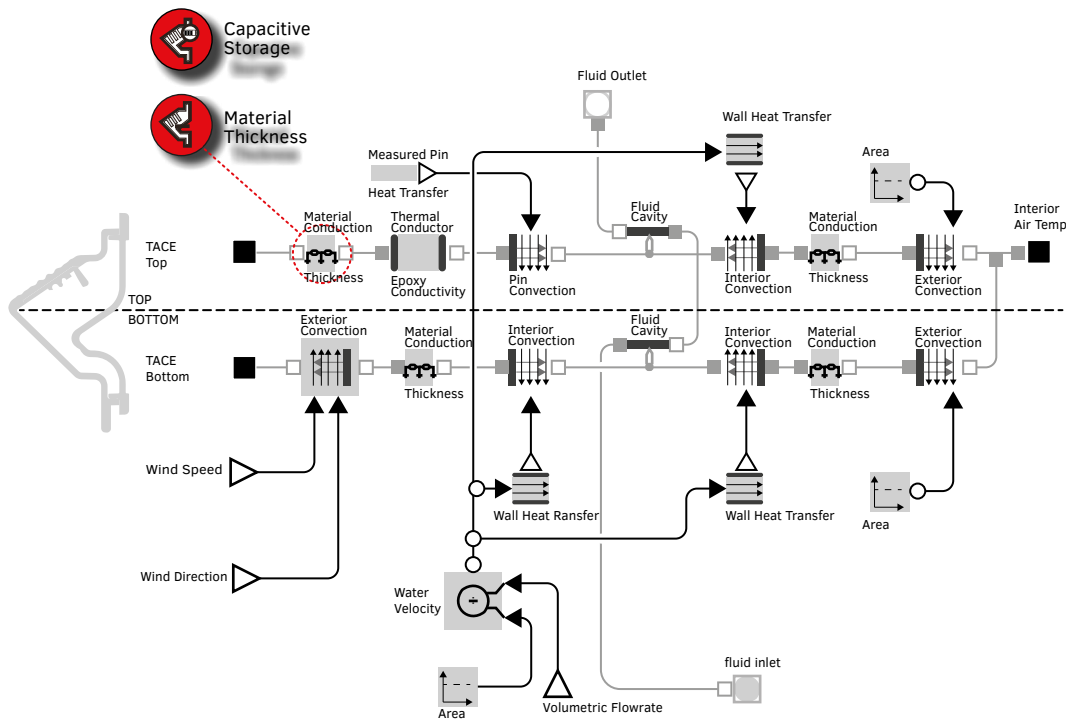


FIG. 5.12 The thickness of the plate, and thus the mass, was adjusted by the circled attribute.

The geometry for the energy transfer component of the MVP Prototype I module was studied to determine if the overall design attribute of the geometry of the energy transfer attribute and the arrangement of that attribute would have a significant effect on the thermal transfer performance. This study looked at determining what geometry and pattern of the design attribute would maximize the thermal transfer across the energy transfer component of the MVP Prototype I model. Thermal characteristics of thermal engineering have been studied in a range of fields for an array of goals, from fluid mechanics to thermodynamics, this study of possible energy transfer component design attribute geometries was limited to the geometries that could be manufactured with similar material forming constraints to the MVP Prototype I module, a hexagonal tapered pin.

The thermal transfer geometry of the energy transfer component was investigated in 2 studies. Study I investigated the design attribute of geometry in 3 flow conditions. Phase II studied the array, or pattern, of the geometry in 2 flow conditions. The purpose of Phase 1 was to observe if the geometry has a significant effect on the transfer rate.

The purpose of Phase II was to see what effect modifying an array of that geometry had on energy transfer.

The five thermal transfer attribute geometries studied, as shown in Figure 5.13 were: Flat, Spike, Sinusoidal, Fin and Pin. These specific geometries were chosen to represent two primary ways of creating additional surface area for the thermal transfer components of the module: point and ribbon. While the point options performed better, with hexagon pins creating the most turbulence and thus the most opportunity for exchange, the results are not optimized and could be investigated as part of a further study.

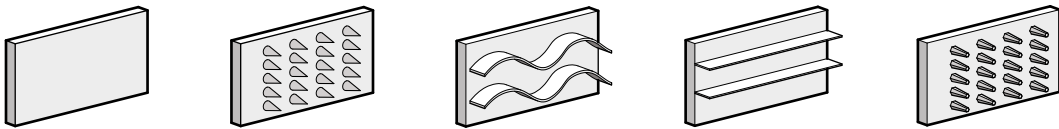


FIG. 5.13 Geometries of plate types initially identified for CFD simulation.

Ultimately the hexagonal tapered pins were used to move forward for testing of MVP Prototype I. Further, the geometry effect on the fin efficiency, part of the overall system efficiency, may be far outweighed by the proportion of surface areas to working fluid which was significantly reduced in the ASI Prototype III as discussed in Chapter 8.

The geometry was tested for four pin length cases, as shown in Figure 5.14, that corresponded to the pin lengths of the MVP and that were tested in the calibration experiment.

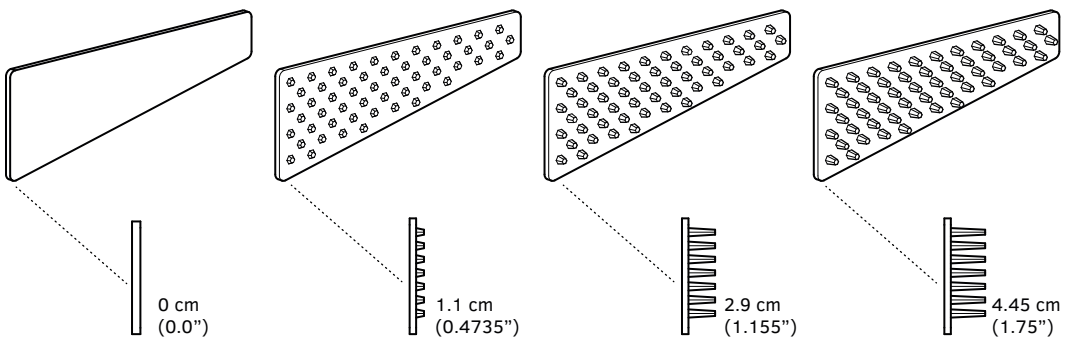


FIG. 5.14 Diagram of pin plates used for quantitative testing and simulations.

In Phase II, two types of arrangements were parallel and staggered, as shown in Figure 5.15. This simulation was conducted as a check against unexpected laminar flows that would derate the efficacy of the thermal transfer. Each geometry was simulated with three flow conditions: no flow, low flow – 1.25 l/min (0.33 gpm), and high flow – 2.50 l/min (0.66 gpm) flowrate.

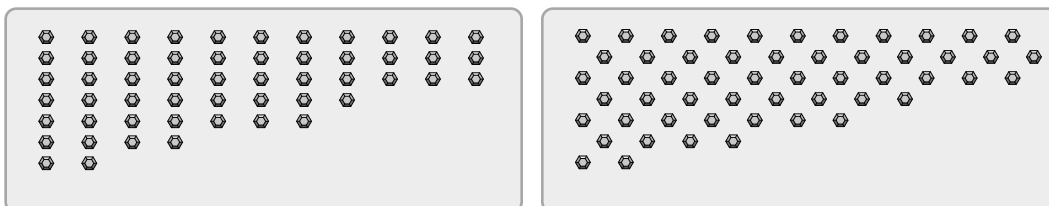
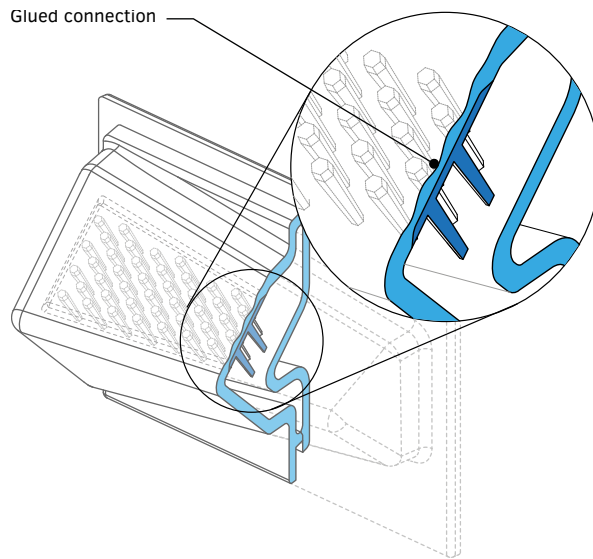


FIG. 5.15 1.75 inch hexagonal pins, staggered arrangement (Left) and parallel arrangement (Right)

As noted in Section 5.3.2.1, the thermal flux between the inlet port and outlet port was a key indicator of potential performance and was measured and compared to develop the analysis.

### 5.3.2.2 Assembly Techniques

Understanding the thermal flows across the across building envelope components was critical to being able to leverage conductivity as a design attribute. The method of assembling components and the understanding of the role that this plays in conductivity can give critical insight into the design of the manufacturing and assembly of a functional system and the proposed real world performance. Assembly techniques play a critical role in the development of the efficacy of the MVP Prototype I. MVP Prototype I used conductive epoxy to bond the exterior component with the energy transfer component as illustrated in Figure 5.16. The conductivity of the material of the TACE ceramic components was about  $20 \text{ W/m}^2/\text{K}$  ( $3.52 \text{ btu/hr/ft}^2/^\circ\text{F}$ ). The Conductive Epoxy has a thermal conductance of  $0.2 \text{ W/m}^2\text{K}$  ( $0.0352 \text{ btu/hr/ft}^2/^\circ\text{F}$ ) approximately 25% as conductive as the alumina oxide based ceramic material the TACE MVP was manufactured. As thermal energy flows from the exterior tile directly through the energy transfer component, it was assumed that maintaining conductivity for this component contact was critical to system performance. To support universal thickness and consistent contact, a wet bonding technique was applied on both surfaces and evenly compressed using a registration thickness that was built into the TACE module as a guide.



**FIG. 5.16** Diagram of conductive epoxy layer modelled. The simulation was run with and without the glued connection.

Using the same boundary conditions as the simulation in Section 5.3.2.1, a comparative simulation analysis was run that included and excluded the thermal conductor component of the TACE MVP Modelica model called “Glue: Conductance” as shown in Figure 5.17. As in Section 5.3.2.1, the thermal transfer rate can be observed by logging the difference between the inlet port and outlet port temperatures and the overall heat flux ( $Q$ ) can be observed at the peak of the cosine ramp profile which corresponds to the highest simulation temperature – representing noon.

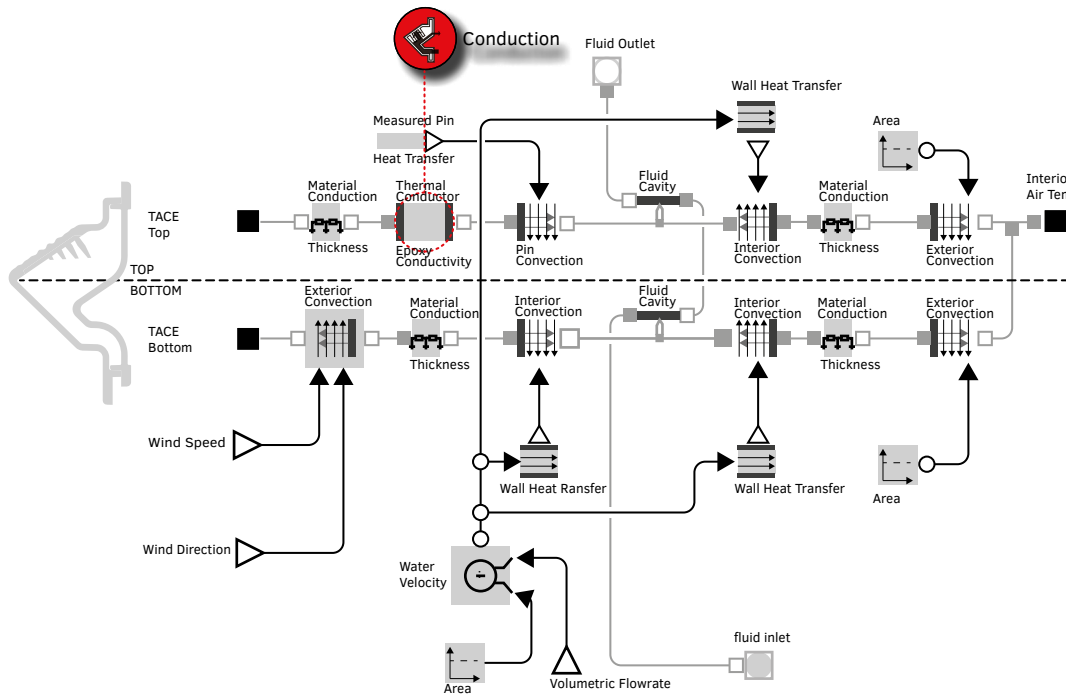


FIG. 5.17 The simulation used the following parameters for the conductive epoxy: conductivity of  $0.2 \text{ W/m}^2/\text{K}$ ; surface area of  $0.0249 \text{ m}^2$ , based on the area of the exterior top panel that comes into contact with the thermal energy component; thickness of  $0.001 \text{ m}$ , assuming a  $1 \text{ mm}$  thick layer of conductive epoxy.

### 5.3.2.3 Flowrates

As described in Chapter 4, the role of the working fluid was to move energy through mass transfer effect. Both advection, the movement of mass as a fluid body, and diffusion, the interaction of bodies at a molecular level, are the primary modes driven by thermal conduction in the TACE MVP module; convection was the result as a whole of diffusion and advection. The goal of the design attribute of the energy transfer component was to create a state of turbulence where one state of matter passes by the other in a way that enhances the overall convective effect. The geometry of the energy transfer component, as studied in Section 5.3.2.2, accounts for part of the overall convective effect, the other was the interaction of the fluid with the geometry. The flow rate of the working fluid was studied to understand the overall convective effective of the interaction of flow rate and pin geometry, as illustrated in Figure 5.18. The overall convective effect can be observed by the heat

flux between the inlet port and outlet port. A cosine ramp profile was used again to create a diurnal cycle.

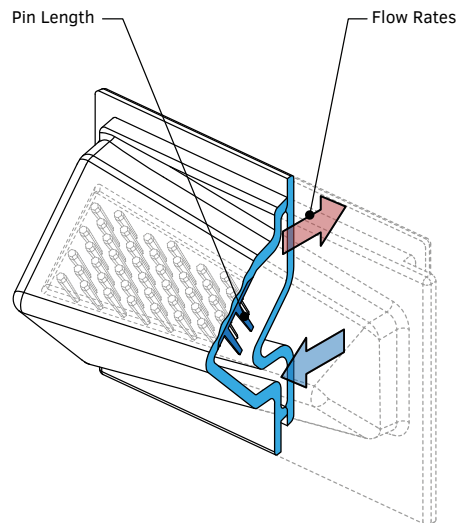


FIG. 5.18 Diagram showing pin length location. The simulations were run for multiple cases.

The pin length cases investigated were: no pins (see note below), 1.1, 2.9, and 4.4 cm (0.4375, 1.155, and 1.75 in). The working fluid flowrates investigated, as illustrated in Figure 5.19 were: no flow, 1.25 l/min (0.33 gpm), and 2.50 l/min (0.66 gpm). All simulations were conducted with the thermal epoxy adhesive thermal conductor component and again without the thermally conductive component, described in Section 5.3.2.3.

The flow rate may be considered a design attribute of the system, rather than a design attribute of any of the MVP Prototype I module components. Understanding the relationship of the flowrate to the performance of the TACE system was critical in developing the system design as a whole and simulating bay and zone scales.

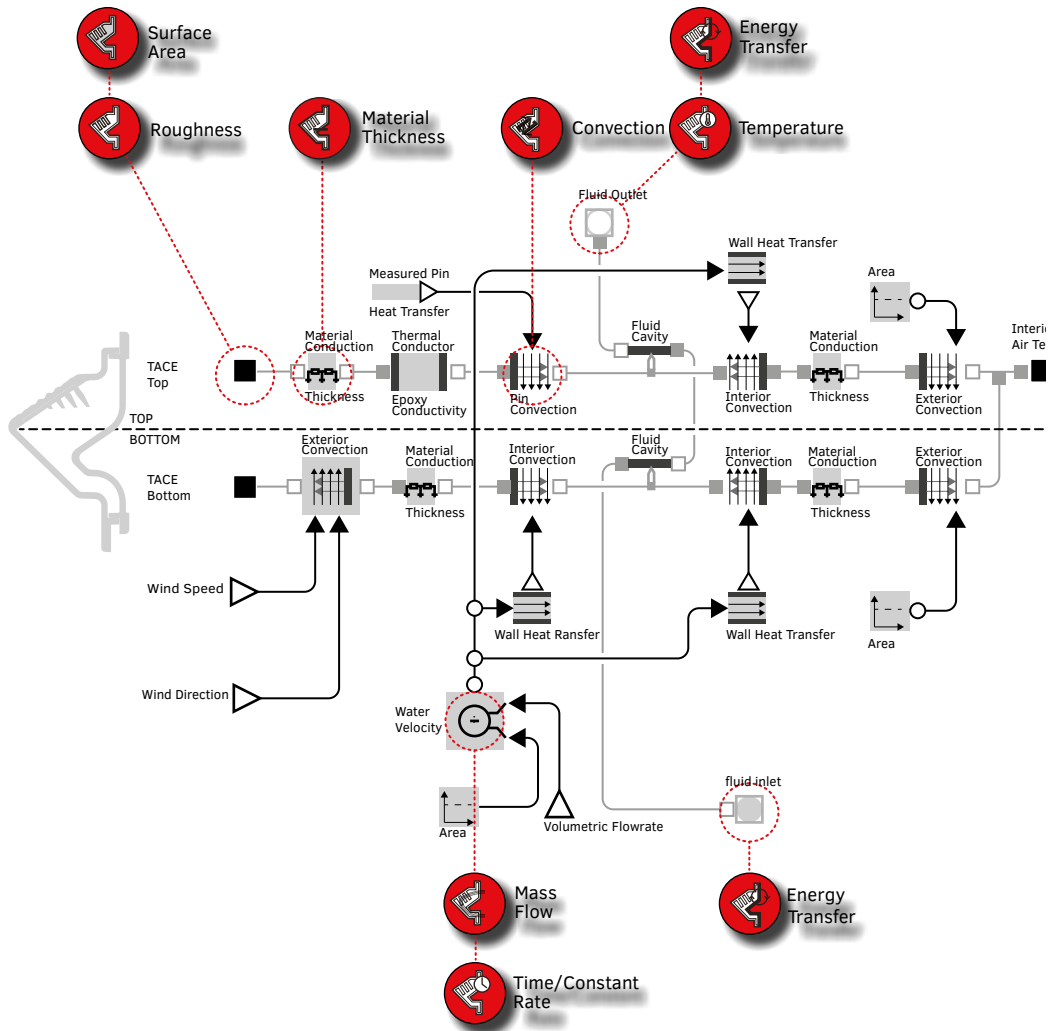


FIG. 5.19 Diagram of systems model showing flowrate and pin length components.

### 5.3.2.4 Insulation

Thermal transfer in the TACE module was designed to be captured in the working fluid and transported to a thermal storage and exchange section of the system. If the inside component of the module maintains contact with the working fluid,



it can be assumed that there will be significant thermal loss through the inside face of the module instead of being captured by the working fluid, reducing the dynamic insulation effect and performance potential. Therefore, there was a required insulative layer that must be placed to the inside of the working fluid to reduce thermal transport towards the interior of the building. This study investigated: 1) what effect if any adding an insulating layer to the inside of the working fluid would have on performance; where should the layer best be located, 2) as an insulative layer directly adjacent to the working fluid on the wet side of the TACE MVP module interior component or 3) as an insulative layer to the inside of the interior module component on the dry side of the TACE MVP module interior component.

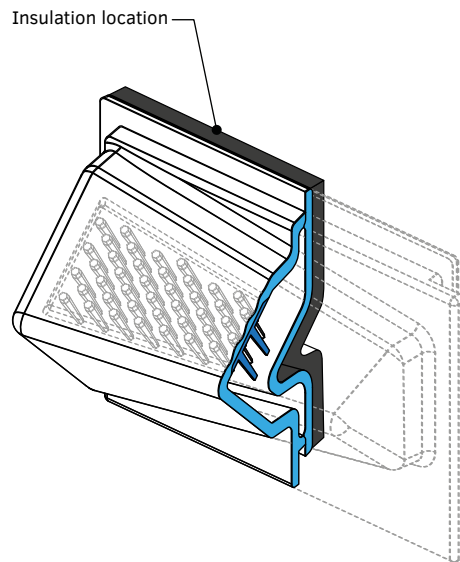


FIG. 5.20 Diagram of the location of the insulating layer.

In order to study the effect of adding insulation, a thermal conductor component was added, as shown in Figure 5.20 that contained the insulative properties equivalent to 1 inch thick polyethylene. Figure 5.21 shows the location of the insulative component in the Modelica model.

### Assumptions

- Thermal conductivity of polyethylene:  $0.4 \text{ W/m}^2/\text{°K}$  ( $0.0705 \text{ btu/hr/ft}^2/\text{°F}$ )
- Thickness:  $0.254 \text{ cm}$  ( $1 \text{ in}$ )
- Surface area:  $0.0275 \text{ m}^2$  ( $0.296 \text{ ft}^2$ )
- Thermal conductance:  $0.433 \text{ W/°K}$  ( $1.477 \text{ btu/hr}$ )

The effect of an insulative layer was analyzed by observing: 1) the temperature difference between the inlet port and outlet ports and 2) and maximum heat flux between the TACE MVP Modelica model and the interior of the building zone directly adjacent to the module. Both studies were simulated using pin lengths of 1.1, 2.9, and 4.4 cm (0, .4375, 1.155, 1.75 in) and flow rates no flow, low flow – 1.25 l/min (0.33 gpm), and high Flow – 2.50 LMP (0.66 gpm) per Section 5.3.2.2.

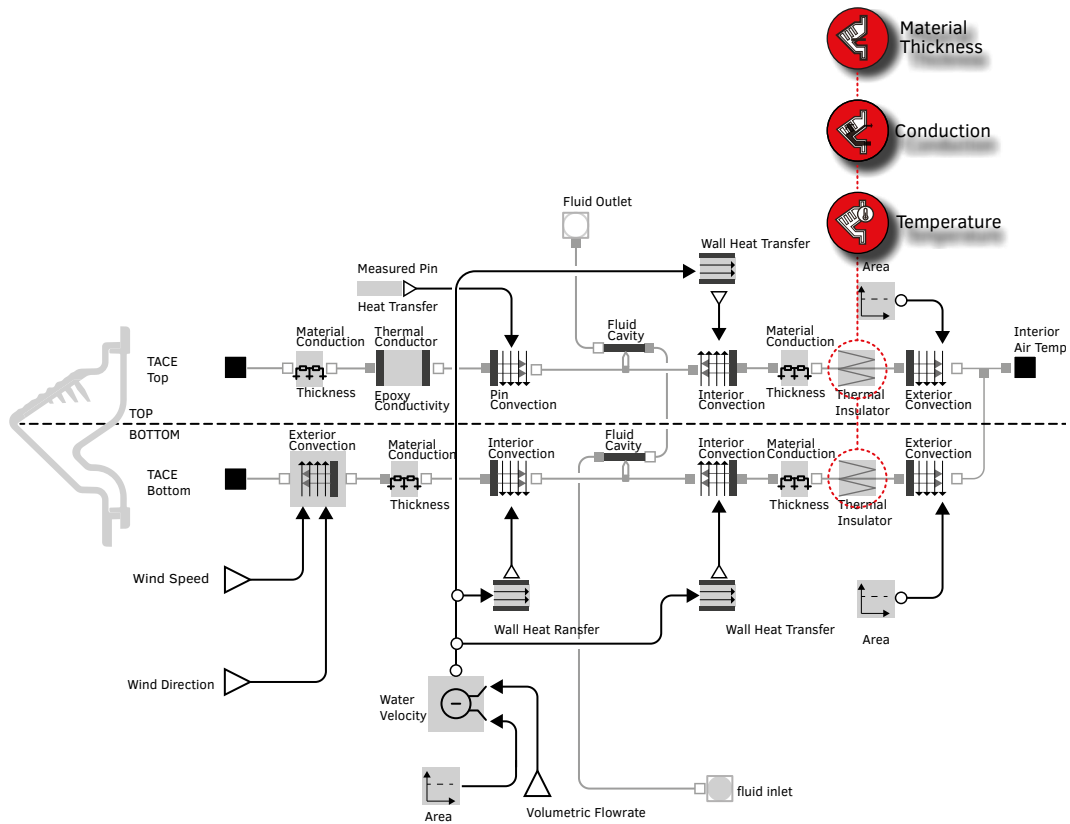


FIG. 5.21 Diagram showing the location of the insulation component.

### 5.3.3 Results

The results in this section affect two critical trajectories of the research discussed in Chapters 6 and 7, respectively. In Chapter 6, the results of this section are integrated

into the MVP Prototype I Modelica module model for the system performance simulations of the series array, as a bay, and as a zone of a building. The results are also used, in conjunction with the result of Chapter 6, in Chapter 7 to refine the design of the MVP Prototype I module and help develop module variations explored as Prototypes II and III as well as discuss the design development based on performance, simulations, and architectural integration limitations. The future work and a design proposal for a fourth prototype that evolved from these results are discussed in Chapter 8.

### 5.3.3.1 Design Attributes and Energy Use Intensity Reduction

---

The design attributes studied look at the various and relative effects of conduction and convection through the components of the MVP Prototype I module throughout the following section below. The overall goal of these results was a refinement of understanding of principals that appear to be making differences in performance and refinement of boundaries of modulation that should reasonably take place in the design attributes that impact EUI. Each section below tries to answer: 1) what design attributes may impact the EUI of the building with the TACE system, and 2) how much impact was possible at the module scale.

### 5.3.3.2 Impact of Mass on Energy Transfer

---

The purpose of this experiment was to determine that the increase in the mass of the energy transfer component pins was not the cause in changes in energy flow rate so the effect of the attribute of the increased surface area of the pins could be isolated against the increase in mass. As state in Section 5.3.2.1, The effect of thermal capacity as a function of mass can be observed by changing the thickness of the upper transient conduction component. The results showed that doubling the thickness of the panel from 0.3175 cm (0.125 in) to 0.635 cm (0.25 in) decreased the outlet port water temperature by 0.1°C (0.18°F). When making the thickness 1.5875 cm (0.625 in), the output port temperature decreased by 0.3°C (0.54°F), as shown in Figures 5.22 and 5.23. The T-Type thermocouples have a possible variation of 1°C (1.8°F) accuracy, more than five times the difference as simulated. So while there was a difference observed when increasing the mass, as expected, the difference was negligible and less than what can be measured and validated with the experiment set up. As to the performance of the module as a whole; there was not enough of a difference to be considered significant when compared to other design attributes targeting energy transfer rates.

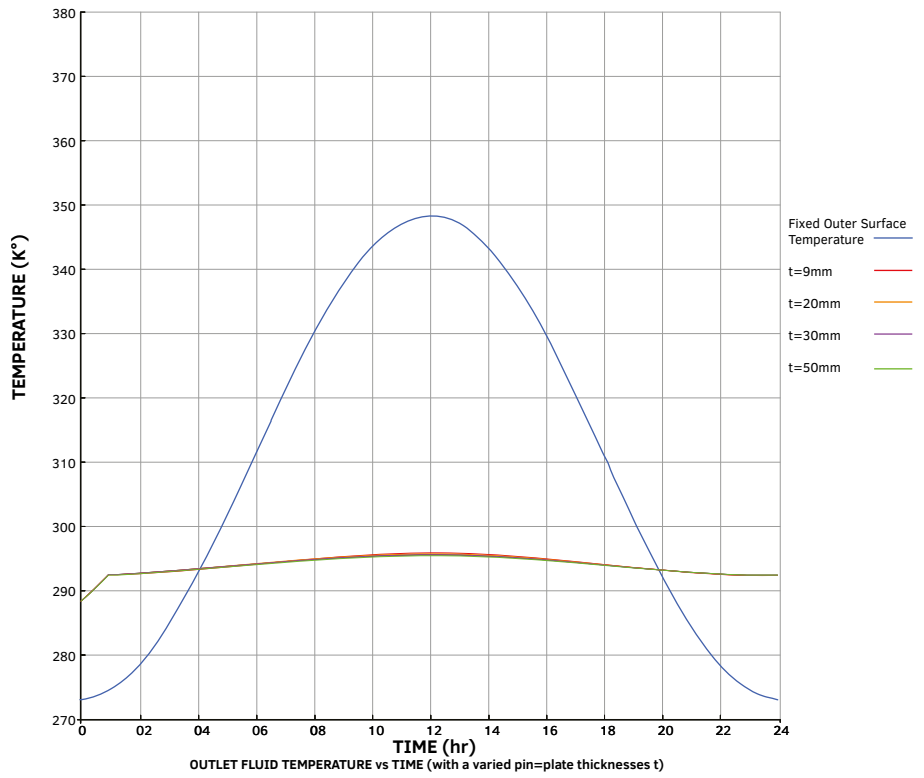


FIG. 5.22 Results graph showing the negligible impact of changing the mass of the collecting surface.

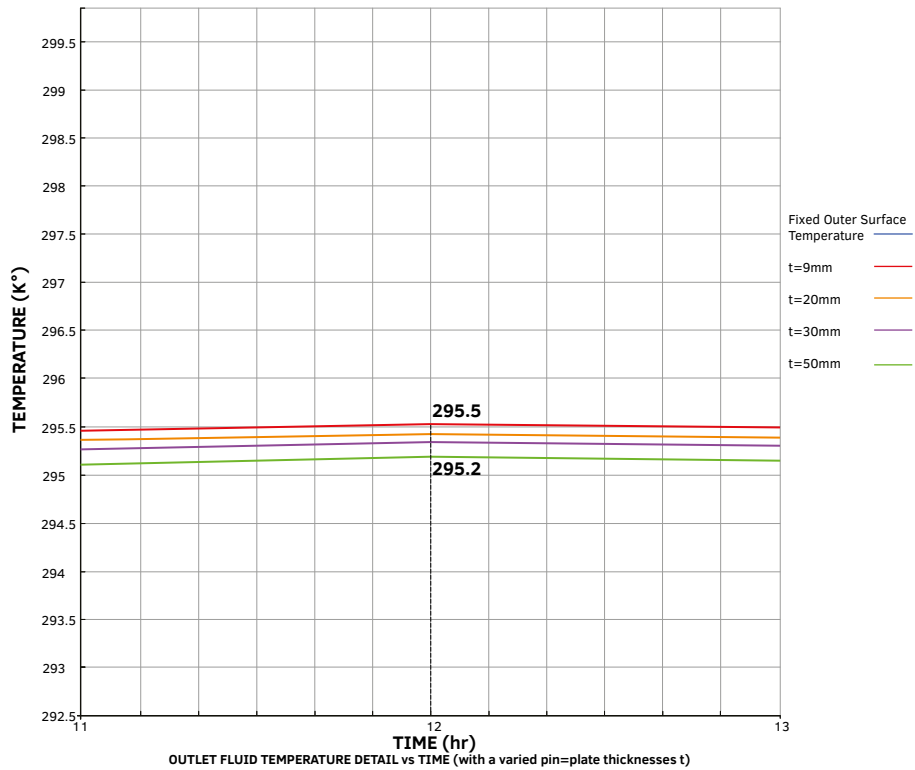


FIG. 5.23 Results graph showing the negligible impact of changing the mass of the collecting surface.

### 5.3.3.3 Impact of Geometry of Thermal Transfer Components on Energy Transfer

As shown in Table 5.3 and Figure 5.24, the pin length did not have a significant impact on the thermal flux as measured between the inlet port and outlet ports. While increased pin length showed an increase in temperature the actual heat flows rates, rose correspondingly, just not significantly in magnitude. The flow rate, discussed in more detail in Section 5.3.3.5, was the driving factor in energy transfer. The flow rate determines the amount of exposure time for the fluid and solid body to interact, and the turbulence of the fluid as it moves through the module. The CFD simulations corroborated the diminishing returns of pin length and indicated that the inlet and outlet position, as well as the array of the pins, was more critical than the proportion of surface area in a flowing state. The offset inlet port and outlet port configuration performed about 25% worse than the vertically aligned

parallel configuration. The CFD simulation suggested that the staggered array with parallel vertical port aligned allowed for more even distribution of fluid amongst the most pins, while maintaining a distributed turbulence, maximizing the convective exchange. The offset port alignment appeared to allow a short circuit of the pins.

**TABLE 5.3** Results are showing the impact of pin length and flowrate on temperature difference due to pin length and flowrates with and without glue layer, demonstrated graphically in Figure 5.24.

Case		Temperature Difference (°C)			
		No Flow	0.625 l/min (0.165 gpm)	1.25 l/min (0.33 gpm)	2.50 l/min (0.66 gpm)
1a	No Pins w/ glue	3.91	3.55	2.11	1.19
2a	1.1 cm (0.4375 in) w/ glue	5.12	3.88	2.24	1.23
3a	2.9 cm (1.155 in) w/ glue	6.83	3.95	2.25	1.23
4a	4.4 cm (1.75 in) w/ glue	7.90	3.95	2.25	1.23
1b	no pins w/o glue	4.02	7.96	6.19	4.59
2b	1.1 cm (0.4375 in) w/o glue	5.33	9.83	7.46	5.37
3b	2.9 cm (1.155 in) w/o glue	7.23	10.29	7.64	5.42
4b	4.4 cm (1.75 in) w/o glue	8.46	10.30	7.64	5.42

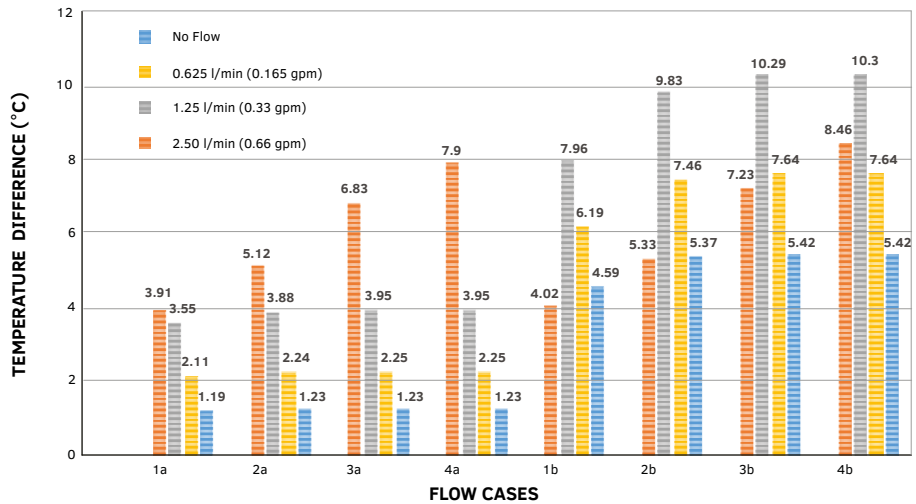


**FIG. 5.24** Results graph illustrating the temperature difference due to pin length and flowrates with and without glue layer.

**TABLE 5.4** Results showing impact of pin length and flowrate on heat flow due to pin length and flowrates with and without glue layer, demonstrated graphically in Figure 5.25.

Cases		Heat Flow Rate (watts)			
		No Flow	0.625 l/min (0.165 gpm)	1.25 l/min (0.33 gpm)	2.50 l/min (0.66 gpm)
1a	No Pins w/ glue	10.3	154.9	184.0	206.8
2a	1.1 cm (0.4375 in) w/ glue	13.5	169.0	195.1	214.7
3a	2.9 cm (1.155 in) w/ glue	18.0	172.0	196.5	215.1
4a	4.4 cm (1.75 in) w/ glue	20.9	172.1	196.5	215.1
1b	no pins w/o glue	10.6	346.9	539.5	800.9
2b	1.1 cm (0.4375 in) w/o glue	14.1	428.2	650.1	936.2
3b	2.9 cm (1.155 in) w/o glue	19.1	448.4	665.4	945.3
4b	4.4 cm (1.75 in) w/o glue	22.3	449.0	665.6	945.3

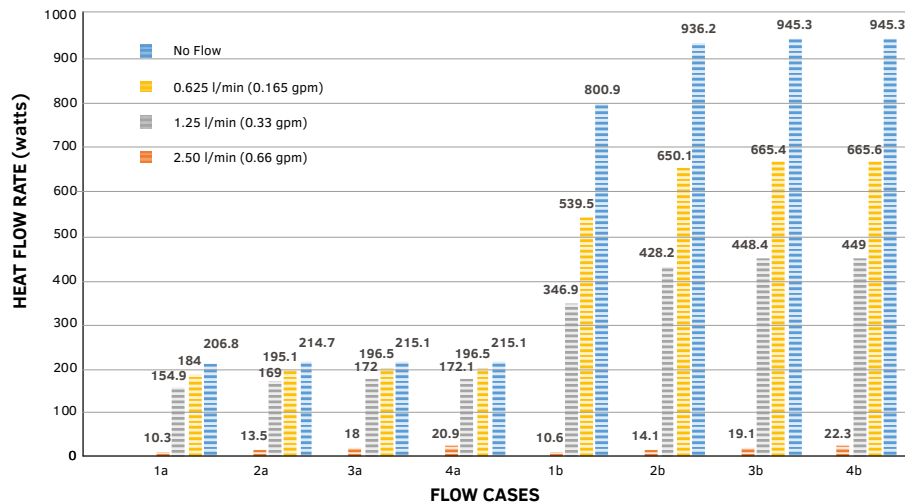


**FIG. 5.25** Results graph illustrating the heat flow due to pin length and flowrates with and without glue layer.

The CFD simulations showed that the most thermal exchange occurred at the base of the pins, as shown in Figures 5.6 and Table 5.2. It was concluded that other diving factors might govern the optimal pin length, such as manufacturability and the optimal amount of fluid in the system, which is discussed as part of the conclusions and future work in Chapter 8.

### 5.3.3.4 Impact of Assembling Components on Energy Transfer

---

The comparative analysis in the simulation observed a maximum thermal flux transfer rate ( $Q$ ) of 215.1 W for the simulation that included the thermal conductor component (representing the conductive epoxy layer) and 945.3 W for the simulations without the thermal conductor component, as shown in Table 5.4 and Figure 5.25. This heat flux was in proportion to the observed difference in inlet port and outlet port temperature between the two comparatives. As shown in Figure 5.24 and Table 5.3, the simulation with the thermal conductor component showed a 3.55°C (6.39°F) degree difference between the inlet port and the outlet port, whereas the simulation excluding the thermal conductor component showed a difference in temperature of 10.3°C (18.59°F) between the inlet port and the outlet port – a significant increase in impact.

These results indicated that the thermal conductivity of each layer had a significant effect on the outcome of the performance of a system that was dependent on thermal transfer. While the simulations in Chapters 5 and 6 continued to use the MVP Prototype I module Modelica model, based on the results of this section, the thermal conductor component was excluded from subsequent simulations. The ramifications of excluding the thermal conductor component are addressed in Chapter 7 where subsequent design iterations and evolutions were characterized and the Proof of Concept (POC) Prototype II was developed to test if the exterior component could be combined with the energy transfer component in the manufacturing process to eliminate the glued connection.

### 5.3.3.5 Impact of Flowrate on Energy Transfer

---

As shown in Table 5.3 and Figure 5.24, the no flow case showed the effect of the pins, with a heat flux of the longest pin was 8.46°C (15.228°F) more than twice that of the no-pin configuration which was observed at 4.02°C (7.236°F). In all flow cases, the difference between the pin length performance was minor, never more than 1°C (1.8°F), all performing better than the no pin case. It can be concluded that pins of any length perform better than no pins. The results also showed that the faster the flowrate, the more total energy was transferred to the working fluid, although at a significantly reduced heat flux than the low flow case. For example, the heat flux for the 4.4 cm (1.75 in) case at 2.5 l/min (0.66 gpm) was 5.42°C (9.756°F), and the corresponding heat flow rate was 945.3 W (3,225.btu/hr). Comparatively, using the same pin length, the low flow and no flow heat flux was 449.332 W and 22.3 W respectively.



The difference in heat flux in the no flow case was assumed to be because conduction was the governing principle and that there was a proportional relationship to the amount of heat flux in relation to the amount of surface area available for conduction. When flow was induced, it was assumed that convection was the driving energy transfer and that the turbulence created by the surfaces and enhanced by the pins – any length – has a far more significant effect than conduction alone. Convection creates a constant temperature differential. It can also be concluded that the turbulence and temperature differential rather than the surface area has a more significant effect on the total amount of energy transferred.

The results of the flowrate test suggested that a control algorithm that dynamically modulated the flowrate should be considered. Depending on how the system is integrated and configured, and the required need, it may, at times, be advantageous to have a higher heat flux, and at other times, a lower flux but significantly more energy transfer. It should also be noted that the data suggested that at faster rates, there were diminishing returns and that at flowrates greater than the 2.5 l/min (0.66 gpm), the temperature difference was so low that there would be little benefit to the other building systems.

In the no flow case, the assumption was that the sensible heat was being stored in the working fluid as latent heat, and the working fluid becomes the thermal storage module directly in contact with the thermal transfer component of the TACE module.

As the flowrate increased, the temperature difference decreased, and the power increased. For example, in the long pin case, the max temperature decreased by 54% and the max power increased by 217% between the low and high flowrates. Faster flowrates had more potential energy at lower grade temperatures. However, this study looked at a single MPV Prototype I module alone. Going forward this data suggests that aligning the modules in series rather than parallel, as shown in Figure 5.26 would begin to develop more energy and heat flux as the temperature was raised when the working fluid engages in each successive module. This alignment strategy is discussed in Chapter 6.

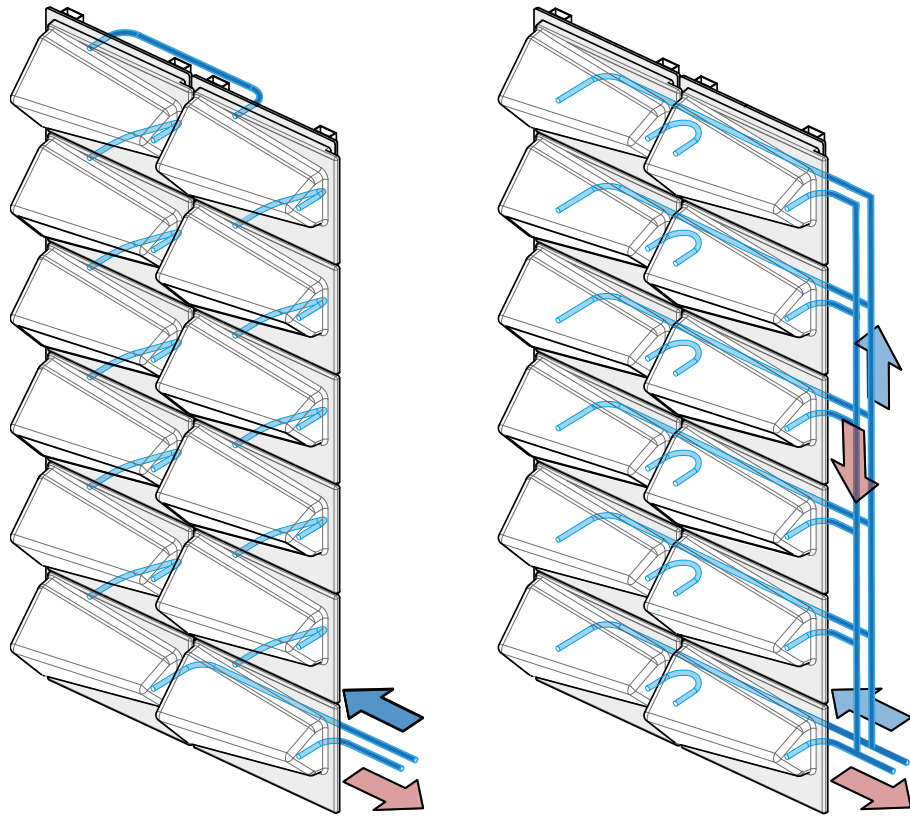


**FIG. 5.26** Diagram series and parallel arrangement. Results indicate that series may support the increased performance of the system as a whole.

### 5.3.3.6 Impact of Insulating Layer on Energy Transfer

The difference between the placement of the insulative layer on the wet side or the dry side of the MVP Prototype I Modelica model interior component showed no discernable difference in outlet port temperatures as shown in Table 5.5 and Figure 5.27 and detailed in Figure 5.28. Additionally, the heat flux temperatures showed the same values,  $-1.3434 \text{ W}$  ( $-4.58 \text{ btu/hr}$ ) at the peak of flux. The no insulation case showed a slightly higher peak flux of  $-1.4768 \text{ W}$  ( $-5.04 \text{ btu/hr}$ ). As these values are all within a very small range, the effect of insulation could be considered as negligible on the overall system performance. However, in real world operation, the impact of not having insulation has significant effects on the building envelope assembly,

and function (e.g., dew point calculation, weather profiles, weather extremes, etc.). Based on section 5.3.3.5, the operating profile of the TACE system may use dynamic flowrates, including no flowrate at times. No flow scenarios would increase conduction through the building envelop assembly, required additional insulation as part of the envelope assembly. Therefore, the conductive component was included on the dry side, or interior side, of the MVP Prototype I Modelica module as part of the bay and zone scale simulations, and as part of the design development going forward as an insulating layer as incorporated into Prototype III as shown in Chapter 7.

**TABLE 5.5** Results showing the negligible impact of the location of insulation within the TACE module assembly.

Case	Heat Transfer (W) At Highest Flux
No Insulation	-1.4768
Dry Insulation	-1.3434
Wet Insulation	-1.3434

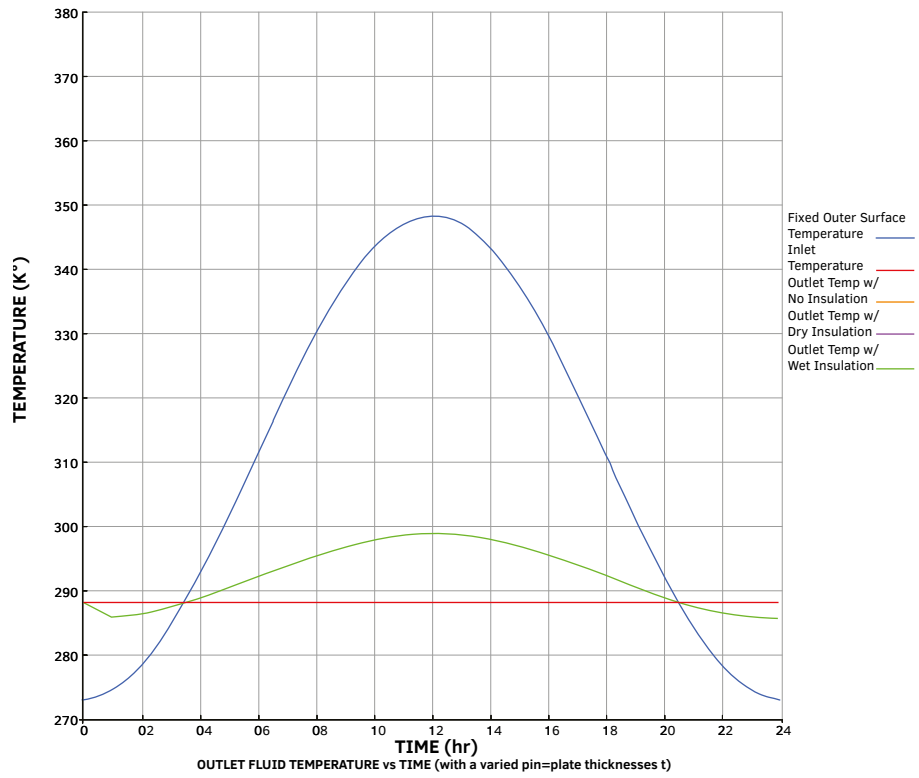


FIG. 5.27 Results showing the negligible impact of the insulation layer on the interior side of the MVP I module.

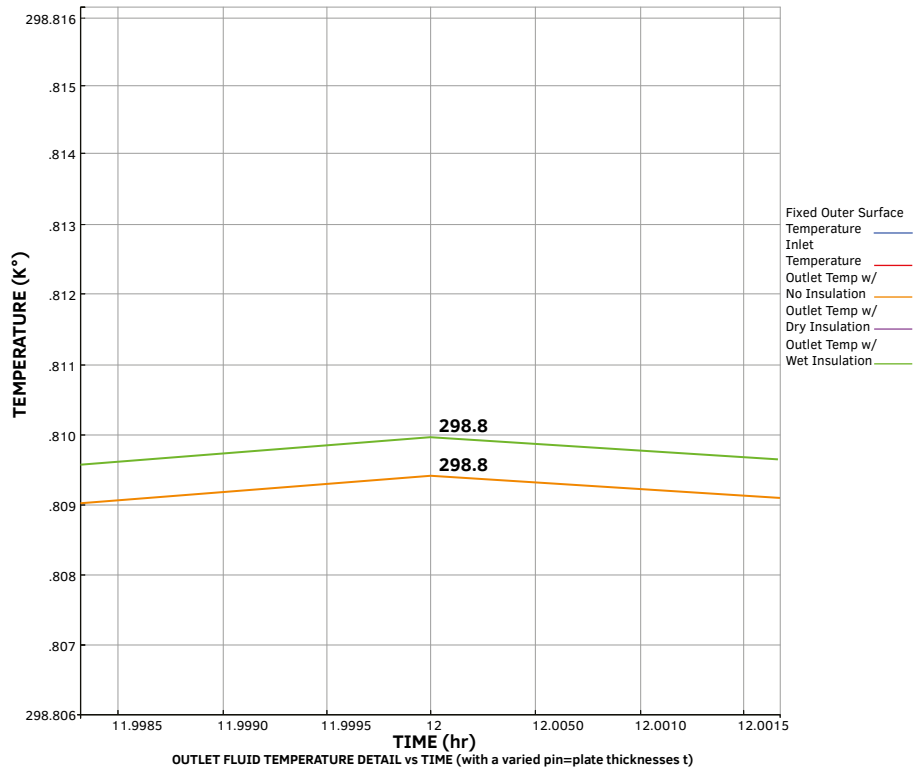


FIG. 5.28 Results showing the negligible impact of the insulation layer on the interior side of the MVP I module.

## 5.4 Summary: Energy Transfer Impacts of Design Attributes

The results of Chapter 5 are used to refine the TACE component in subsequent design prototypes that are modelled as assemblies to assess its impact on EUI in Chapter 6, and future design directions as noted in Chapter 4, developed in Chapter 7, and discussed in Chapter 8.

## Specifically

- While the geometry of the heat transfer component surface area appears to be important, the increased surface area created by the thermal transfer components appears to be the primary driver. Thus, an alternative heat transfer components geometry was explored in Chapter 6 and the refined ASI Prototype III.
- The method of assembly and specifically bonding was shown to have a significant impact on thermal transfer for both temperature difference and max power. Bonding of the thermal transfer component to the exterior tile components was avoided in POC Prototype II, as these components were designed and manufactured from a single piece. In ASI Prototype III, the thermal transfer component was bonded to the tile component using a material with similar conductive properties to that of the ceramics.
- The relationship of temperature flux and power based on differing flowrates was used in Chapter 5 to address cumulative power potential where both high and low flowrates were simulated for prototypes I and III.
- Further, based on the results of this chapter, the mass of the ceramic was not considered as a primary driver of energy transfer, and the location of insulation was placed according to the method of manufacture and assembly as the location had no discernable impact.

While these results directly influenced further design directions, they also alluded to potential operational control strategies, and while not explicitly explored in this dissertation, are nonetheless a critical area to consider as future work for countercurrent energy exchange building envelopes.

By testing the variables at the components scale, additional questions were developed to explore a focus around the type of thermal transfer component that was necessary to support the TACE system performance, and under what way was the thermal transfer components impacting transfer rates. It was determined to include with some surety parts of the building assembly that were not developed as a physical prototype but were necessary to include in the building level simulation which was delineated in detail in Chapter 6.

Perhaps most importantly, this chapter establishes a baseline from which to make evolutionary steps in design development based on the simulations due to a refinement of the hypothesis based on the results. The baseline established in this chapter established a heat transfer rate according to the key attributes identified in Chapter 4. This rate was used as a basis on which to develop the bay, zone and whole building energy model in Chapter 6. In this way, the prototype, developed as a physical prototype and as a model for simulation, was refined by answering each

research question, which was subsequently refined by the resulting prototypes in an iterative process. Chapter 6 integrates these observations into real world scenarios using climate data and building areas at multiple scales and the testing and refinement platform for the research and prototype iterative cycle.

## References

- Acusolve. (2019). Retrieved from <https://altairhyperworks.com/product/AcuSolve>
- ASTM International. (2012). Standard terminology for additive manufacturing technologies. Designation F2792-12a: ASTM International.
- Dassault Systemes. (2018). Dymola Systems Engineering. Retrieved from <https://www.3ds.com/products-services/catia/products/dymola/>
- Energy Plus. (2019). Retrieved from <https://energyplus.net/>
- Gindlesparger, M., Harrison, S., Shultz, J., & Vollen, J. (2018). Design Optimization Workflow for a Dynamic Mass Envelope System using Complementary Digital and Physical Testing Methods. ARCC Conference Repository. <https://doi.org/10.17831/rep:arcc%y560>
- Modelica. (2019). Retrieved from <https://www.modelica.org/>
- New York State Pollution Prevention Institute (NYSP2I). (2017). Performance Evaluation of EcoCeramics Active Thermal Building Envelope System. Research Report. Green Technology Accelerator Center (GTAC), Rochester Institute of Technology.

# 6 Performance and HVAC System Integration

---

Intercepting and redirecting the thermal energy through the building envelope has the potential to influence the size and configuration the building systems that affect thermal comfort. New construction, where great emphasis is placed on the performance and aesthetics of the building envelope and usable space is valued at a premium over the massing and orientation, has the potential to benefit from a more flexible or adaptable envelope and mechanical system integration. Deep Energy Retrofits, where both the building envelope and mechanical systems are being replaced, and the spatial conditions are often limited by the original structure, have the potential to take advantage of the same benefits. This chapter investigates the thermal potential of the TACE as a heating and cooling system and discusses possible building system configurations that leverage the TACE as an energy transfer function to aid in HVAC performance. The results of the MVP Prototype I as simulated in Chapter 5 were used to build the primary simulations for this chapter, and the results of simulations of ASI Prototype III show the potential evolution of the performance based on incorporating design enhancements that resulted from the experiments.

## 6.1 Introduction

---

To understand what potential impact, if any, the TACE system has on building systems, the following research question needs to be answered.

**What are the impacts of the Thermal Adaptive Ceramic Envelope on building systems?**



To answer these questions, it was essential to gauge the size of the potential contribution that the TACE system can make to the associated building systems. A multiscale modelling framework was used to assess the quantity of this potential. To understand how the TACE system may be integrated with other building systems, and therefore impact the size and configuration of these other systems that were related to thermal comfort, several scenarios were developed for comparison and discussion.

To answer the question of building systems impacts, multiple systems and integration configurations were explored, and the following sub research questions were discussed:

- What building systems are impacted by the Thermal Adaptive Ceramic Envelope?
- What is the impact of Thermal Adaptive Ceramic Envelopes on the sizing of HVAC systems?
- What are the most effective HVAC systems to combine with a Thermal Adaptive Ceramic Envelope?

To provide a baseline for comparison, an existing building was used as a case study to build comparisons for both deep energy retrofits and climate analysis from between the New York Metro Region, Phoenix Arizona and Amsterdam.

### 6.1.1 Case Study: Wesley J. Howe Center at Stevens Institute of Technology

---

The Wesley J. Howe Center at Stevens Institute of Technology was used to provide both a real world context and a basis for the modelling framework and system configuration exploration. A typical structural Bay and thermal Zone scales were modelled to provide the comparative analysis and architecture integration framework.

The Wesley J. Howe Center, as shown in Figure 6.1, is an administrative office building at the centre of the Stevens Institute of Technology campus in Hoboken New Jersey. The Howe Center has 14 above ground stories and tops out at 43.6 m (143 ft). Construction commenced in 1961 and was completed in 1962. The structure is a steel frame. The building envelope is a stick-built curtain wall with single pane glazing, with granite and limestone panels and maintains approximately a 40% Window Wall Ratio (WWR). A 10 cm (4 in) concrete block wall is layered behind the spandrel panels. The mechanical heating and cooling system are comprised of two pipe fan coil units.



**FIG. 6.1** The Wesley Howe Center at Stevens Institute of Technology is an example of first generation curtain walls buildings that need significant building systems upgrades.

The Howe Center is a candidate for building repositioning. The form and program also serve as a typical green field office typology in metro regions in the US. The original envelope is failing with both air and water infiltration. The two pipe fan coil system is unable to heat and cool the building adequately, especially during colder months when the diurnal temperatures swing from heating to cooling and back in the 24 hour cycle. In 2015, Tishman Construction had identified this building as an excellent value for repositioning due to its age and lack of repair and maintenance.

Perhaps most importantly, the Howe Center is representative of the first wave of curtain wall buildings that need deep energy retrofits around the world while whose massing can also be used to imagine a new construction Class A office building type.

## 6.2 Research Collaborations

---

As in Chapter 5, modelling in support of this chapter was funded by a \$44,000 grant from the Green Technology Accelerator Center (GTAC) as part of a program administered by the New York State Pollution Prevention Institute (NYSP2I)(NYSP2I, 2017). The funds were distributed to Rensselaer Polytechnic Institute to support research assistant Justin Shultz, who collaborated in translating the model design into a numerical model for the simulation framework in support of the objective of this chapter. Following the development of ASI Prototype III, Vollen, Gindlesparger, and Shultz developed the modelling scenarios to show a comparison between the MVP Prototype I and ASI Prototype III. The results of this Chapter was submitted for review for publication by the Technology | Architecture and Design (TAD) Journal.

## 6.3 Research Methods

---

In order to conduct a comparative analysis between the TACE system and comparable alternatives it was critical to establish a research framework that was: 1) capable of integrating enough resolution of the performance of the TACE module Modelica model into an energy model at the building system scale; 2) simulated in a framework that would give apple to apple comparative results through an industry standard energy model protocol.

Modelica has the advantage of being interoperable via object oriented packages such at the Functional Mockup Unit (FMU) with OpenStudio, the open source building system simulation environment developed by the National Renewable Energy Laboratory (NREL), Argonne National Laboratory (ANL), Lawrence Berkeley National Laboratory (LBNL), Oak Ridge National Laboratory (ORNL), and the Pacific Northwest National Laboratory (PNNL) (“OpenStudio,” 2014).

EnergyPlus by itself does not have the capability to account for the type of transient and dynamic thermal flows that define the operation of the TACE module, specifically at the component scale of the wall assembly. EnergyPlus is, however, capable of incorporating ‘modules’ developed on platforms more capable of modelling the dynamic thermal flows (Nouidui et al., 2014) similar to how the TACE components

operate. The process of co-simulation, as delineated in Figure 6.3 and described in Section 5.3.1.2, runs the two models together in a simulation giving a single result that incorporates the transient dynamic flows simulated in the Modelica environment within the EnergyPlus platform.

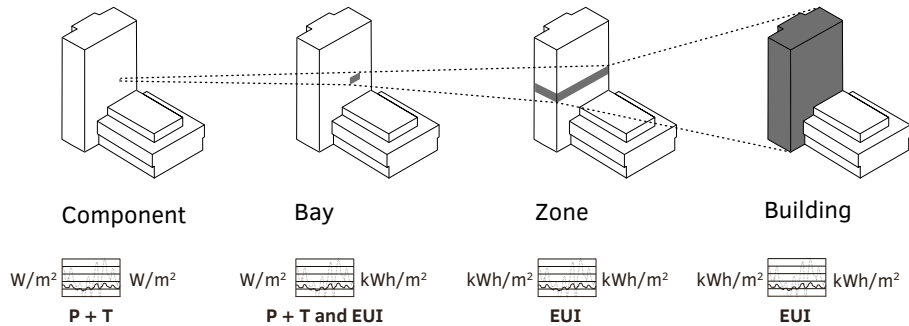


**FIG. 6.2** Diagram of scalar relationships studied in this chapter. The components, or module, modelling in Chapter 5 was developed into a model for a typical Bay, Zone and extrapolated to represent the impact of the TACE system on a whole building EUI in this chapter.

### 6.3.1 Modelling and Simulation

In this investigation, the model was developed using the TACE system and the Howe Center as a spatialized set of dimensional and performance parameters; whereas the simulation in this investigation was the implementation of the model of a set of the comparable scenarios of the Howe Center to produce a set of potential performance results. Accordingly, the model and simulation workflow as shown in Figure 6.3 was designed to create the comparative analysis between: the original Howe Center case study; the current ASHRAE recommended configuration; and the TACE system configuration. This comparative analysis showed the differences between the original and the TACE system and the TACE system and the ASHRAE recommended system in the context of the performance potential of deploying a new building envelope as part of a deep energy retrofit strategy.

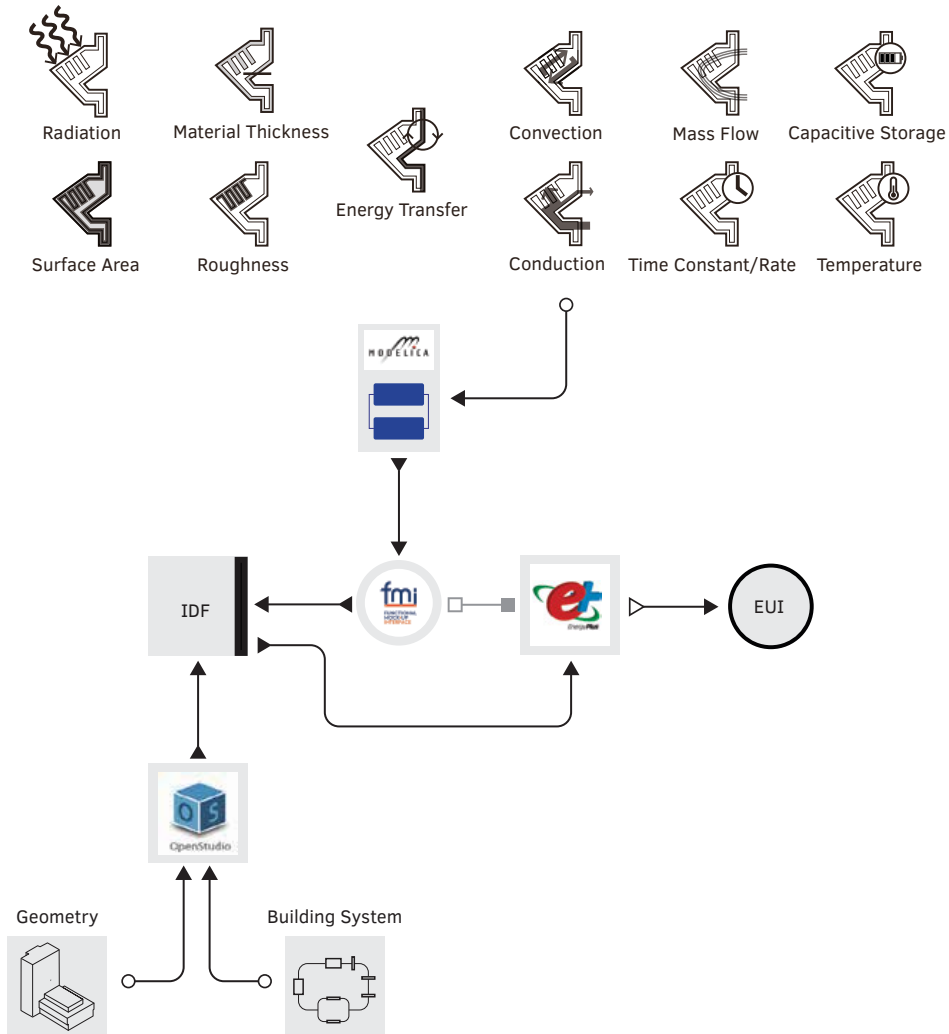


FIG. 6.3 Model in simulation workflow showing the flow of input and outputs of data to arrive at performance results.

### 6.3.1.1 Model and Simulation Design

The models were each built in two parts in two distinct platforms: the assembly of the physical spatial dimensions and the specification and parameters of the system. The data from the dimensional model component was exported into the system specification environment where the systems were modelled. The model workflow

was used as the basis for the comparative analysis and developed from dimensional measurements taken on site at the Howe Center. The mechanical systems of the model were specified in the model based on the observed specifications of the HVAC equipment. The envelope assembly was developed based on observed finishes, dimensional analysis and concurrent construction type details and construction photos available.

The simulation, as described in the following section was developed to see: if there were specific mechanical systems that could be deployed in a deep energy retrofit situation that would perform better than others; and under what circumstances or configuration of the TACE system would benefit the energy performance of the Howe Center. The simulation was designed using the parameters of the Typical Meteorological Year (TMY) data from the weather station log at Teterboro Airport located in Teterboro New Jersey. The location of the TMY3 data is 13.28 km (8.25 mi) north by north west of the Howe Center Site on the campus of The Stevens Institute. This location was chosen for the similarity to the outer New York metro area climatic conditions, except for the bluff condition overlooking the Hudson River unique to the Howe Center site and west Hudson locations. The simulations were run for the typical TMY3 year.

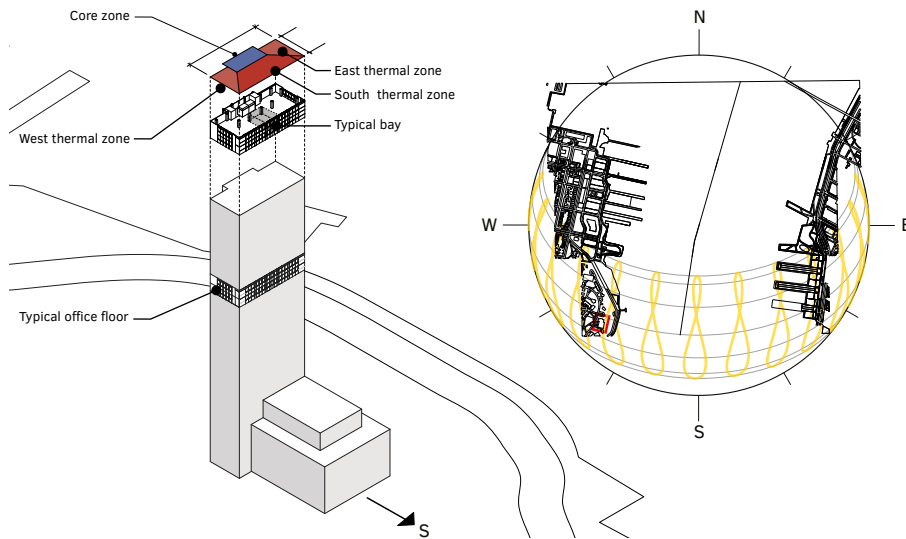


FIG. 6.4 Diagram of the Howe Center showing general orientation, geolocation and analemma.

#### 6.3.1.1.1 Bay Model Design

---

The dimensional component of the bay scale model framework was developed based on the Howe Center measurements. This dimensional model input was built as an energy model in Sketchup. The dimensions of the typical office floor bay in the Howe Center are 5.84 m deep by 8.23 m wide by 3.51 m tall (19.2 ft, 27 ft, 11.5 ft) as shown in Figure 6.5. These bay dimensions are typical and representative of mid century vintage office buildings in the US, and while they are somewhat smaller than a typical new construction, steel frame office building, the emergence of Mass Timber framing for office buildings has a smaller bay footprint that was similar. The bay is oriented south and uses a WWR of 40%. The exposed south face was set to expose all the interior boundaries, walls, floors, & ceilings, and was set as adiabatic boundary conditions. This file was exported as a Green Building Extensible Markup Language (gbXML) and imported into OpenStudio. Load conditions for the simulation parameters were added in OpenStudio based on ASHRAE 90.1 2013 (ASHRAE, 2013) which included demands for occupancy, lighting and plug load, etc.

OpenStudio was then used as a framework to develop models for the comparative scenarios by specifying HVAC configuration scenarios and the three envelope conditions described in this section. The baseline upgraded HVAC system used ASHRAE 90.1 Appendix F as the configuration to specify Variable Air Volume (VAV) with reheat terminal units, as shown in Figure 6.5.

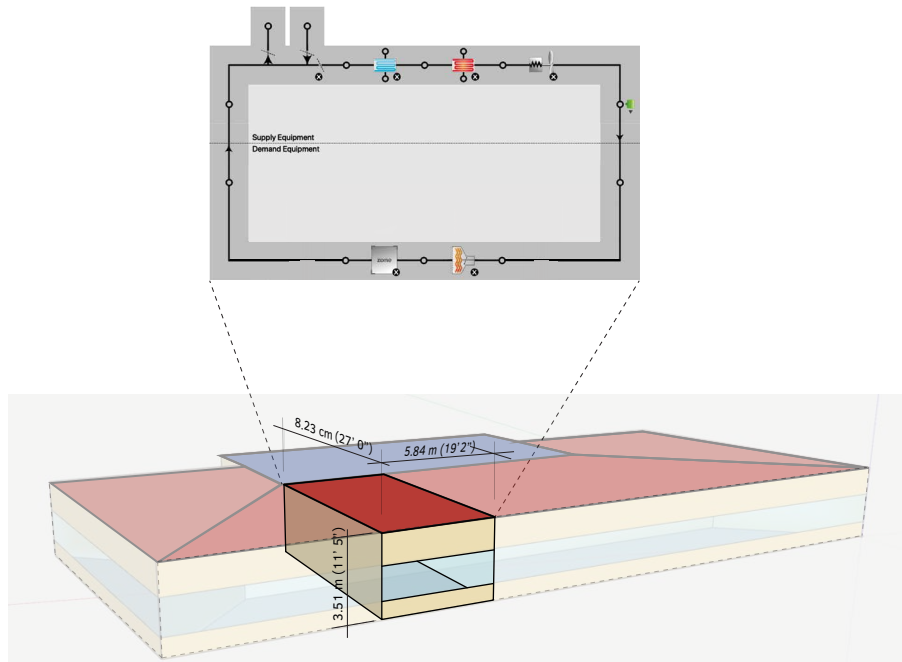


**FIG. 6.5** Bay-scale energy model geometry in Google SketchUp and OpenStudio model showing ASHRAE Recommended VAV with reheat.

Through all the studies on both the bay and floor scales, the HVAC system internal loads persisted as continual through each scenario supporting the reduction of variables required to create the comparative analysis.

### 6.3.1.1.2 Floor Model Design

The dimensional component of the floor scale model framework was developed based on the Howe Center measurements. This model represents a typical mid-tower office floor. This dimensional model input was again built as an energy model in Sketchup. The dimensions of the typical office floor are 32.66 m by 14.38 m by 3.51 m (107.15 ft by 47.18 ft by 11.52 ft), as shown in Figure 6.6. The floor is angled 12.8° to the southwest, as shown in Figure 6.4 and also has a window-to-wall ratio (WWR) of 40% as a continuation of the bay parameters. The extension on the north was built as the vertical transportation core contained elevator shafts and stairwells. All faces were set as exposed; the interior boundary of the core, floors, and ceilings were set as adiabatic boundary conditions as floors were above and below. As with



the bay scale, this file was exported as a Green Building Extensible Markup Language (gbXML) and imported into OpenStudio.

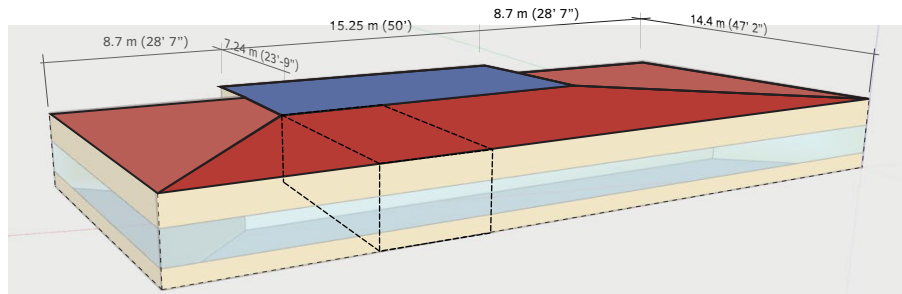


FIG. 6.6 Howe Center floor building energy model geometry created in Google SketchUp.

As in the bay model, load conditions for the simulation parameters were added in OpenStudio based on ASHRAE 90.1 2013, which included demands for occupancy, lighting and plug load, etc. As with the bay scale model, the floor scale model framework was designed to incorporate differing systems scenarios. As per ASHRAE 90.1, Appendix F, a VAV with Reheat HVAC terminal units were designated as the improved baseline HVAC system.

Zones were designated as North, South East, and West. Each zone used a setpoint manager that controlled the: thermostat, cooling coil, heating coil, and air distribution unit. Using a separate setpoint manager per zone allowed each zone to be controlled individually. Primary heating coils in the primary air handling unit (AHU) and the reheat coils located in the terminal units were routed to the remote central boiler. Similarly, the cooling coils in the main AHU were routed to a chiller. The chiller was routed to a remote condensing unit.

TABLE 6.1 Modelled building envelope U-value, Modelled building fenestration U-value, SHGC, and Visible Transmittance.

Building and Envelope Configuration	U-value w/ Air Film [W/m <sup>2</sup> K]	U-value w/ no Air Film [W/m <sup>2</sup> K]
Howe Center Existing Envelope	2.529	4.071
ASHRAE 90.1 – 2013 Curtain Wall CZ 4	0.306	0.321
TACE system	0.292	0.306

Building and Envelope Configuration	U-value [W/m <sup>2</sup> K]	SHGC	Visible Transmittance
Howe Center Existing Envelope	5.778	0.862	0.899
ASHRAE 90.1 – 2013 Curtain Wall CZ 4	2.559	0.352	0.442
TACE system	2.559	0.352	0.442

The envelope U-values used in the model and the fenestration U-values, SHGCs, and  $T_{vis}$  are shown in Table 6.1. The U-value of the envelope assembly not including the TACE modules was 0.292 W/m<sup>2</sup>K (0.0515 btu/hr/ft<sup>2</sup> °F) with the external air film resistance at the module surface and 0.306 W/m<sup>2</sup> K (0.0539 btu/hr/ft<sup>2</sup> °F) without the air film. The fenestration for TACE was modelled using the same as the ASHRAE fenestration. This comparison shows the relative similarity in a U-value build up between the ASHRAE recommended curtain wall performance (used as the contemporary standard) and the TACE system, and the striking difference of both to the original Howe Center, which is representative of buildings of this age. Table 6.6 also illustrates that both the ASHRAE and TACE glazing inputs were kept the same with similar U-Value build-ups in order to isolate the dynamic performance of the TACE system.

The envelope and fenestration criteria for both the bay and floor scale are detailed in Section 6.4 for each case.

### 6.3.1.2 Modelica and EnergyPlus Co-Simulation

The OpenStudio and Modelica models were used to create the basis for the co-simulations in EnergyPlus. As described in Section 5.2.2.1-2, EnergyPlus was used as the industry recognized established standard comparative modelling framework that will give results in Energy Use Intensity (EUI), representing the key comparative indicator of building system performance. OpenStudio was used to model the building system configurations and export an IDF file. In order to construct the framework for the co-simulation, the TACE module was exported as a Functional Mock-Up Interface (FMI) from Dymola, the Modelica modelling environment as described in Section 5.2.1.3-4. The TACE module FMI was used to replace the code

that described the building envelope within the Intermediate Data Format (IDF) that was exported from the OpenStudio model for use in the EnergyPlus Building Energy Simulation Environment. The modified IDF, therefore, contains parameters from both model scales for the simulation (Nouidui et al., 2014). This co-simulation, therefore, provides more comprehensive results than can be achieved by running and analyzing the models separately as well as have more potential to accurately account for the interactions that were taking place from a building physics perspective.

## 6.4 Model and Simulation of Envelope Types with Deep Energy Retrofit Scenarios

---

Once the envelope and system parameters were set in the OpenStudio models, several modifications were developed in preparation for the co-simulation. These modifications created connection points to the Modelica model as inputs and outputs that interacted with the TACE modules – effectively operating as one system that bridged the co-simulations.

The research study originally planned to connect the TACE system directly to multiple types of HVAC systems. Once the outlet temperatures of the TACE systems were simulated, it was determined that the temperature differential was not adequate to support existing system temperatures. For example, the hot water supply for the ASHRAE recommended VAV with reheat is typically in 82.2°C (180°F) and more recently based on better efficiency and energy savings is now 60°C (140°F). The outlet temperature of the TACE module was simulated to reach a potential of 37.7°C (100°F) – not enough temperature to support existing system heating requirements, but enough to affect the thermal conditioning of the space. While cooling temperatures were slightly different, supply was delivered typically around 7.2°C (45°F), it was determined that for the sake of developing the comparative analysis the TACE system would use a radiant panel decoupled from the HVAC system to augment the simulated HVAC system (Marshall, 2016). It was possible that the system based on a lower diffuse source would benefit from the lower temperature gradient of the TACE system output as proposed in Chapter 8 for a fourth prototype design.

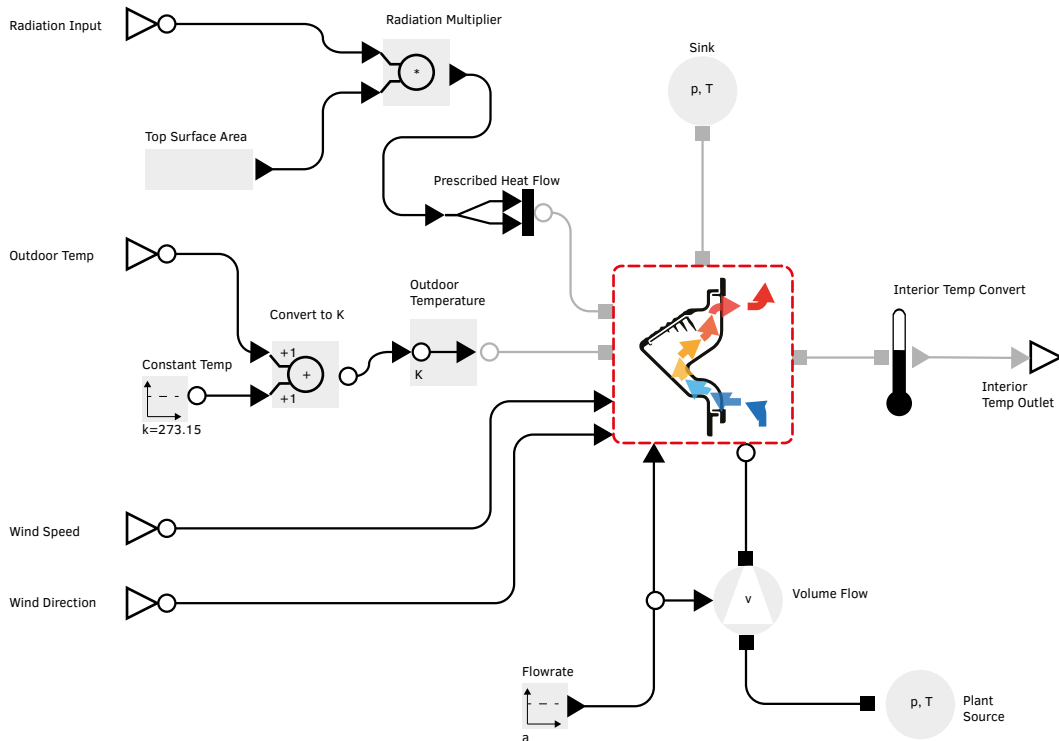


FIG. 6.7 Diagram of visual programming interface in Dymola showing working fluid integration.

In Modelica, a hot water circuit with input and output nodes was created to characterize the thermal energy captured in the working fluid collected from the TACE module array. In the OpenStudio environment, a hot water circuit was created as shown in Figure 6.8 that included a Plant Component: Temperature Source node on the hot water supply side and a Thermal Storage Tank on the hot water demand side. The working fluid temperature and mass flowrate output from the Modelica model was set up to control the temperature and working fluid mass flowrate of the Plant Component: Temperature Source during the co-simulation.

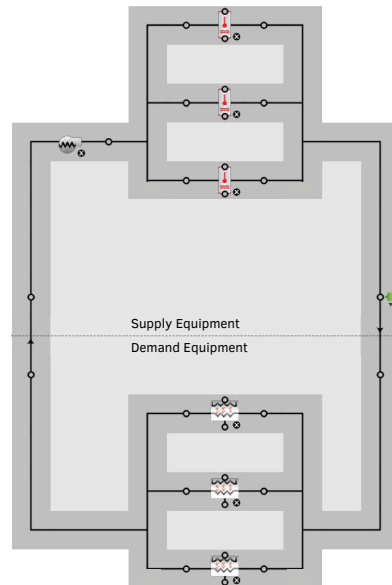


FIG. 6.8 OpenStudio Diagram of Hot Water Circuit.

In the OpenStudio model the Plant Component: Temperature Source node characterized a concentrated point source of hot working fluid that delivered energy to the Thermal Storage Tank, which collected the heat for use in achieving thermal comfort. The Thermal Storage Tank node supply side was coupled to a Zone HVAC: Baseboard: Convective: Water node to model a hot water based convective radiant panel source located adjacent to the inside of the building envelope in the bay, and in each bay of the floor model. The convective radiant source in each bay included a setpoint that activated the thermal circuit when the temperature in the Thermal Storage Tank was 2°C (3.6°F) higher than the zone setpoint.

The system as a whole was programmed with the priority on the convective radiant source to provide all possible heat before the building heat source was signalled. Thus, the remote central boiler and the reheat loops in the VAV terminal units were only turned on when there was insufficient thermal capacity from the TACE system.

It should be noted that additional cooling could be provided by the TACE system, amounting to further potential reductions in the whole building EUI. The effect of cooling from TACE would be used when the thermal storage could charge coolth in the shoulder months where it was cooler at night and warmer in the day than the indoor thermal comfort zone. In the NYC Metro area, for example, this particular condition occurs more than five months of the year as shown in the weather profile in

Figure 6.9 The study of the potential of using coolth collected from the TACE system was proposed as future work.

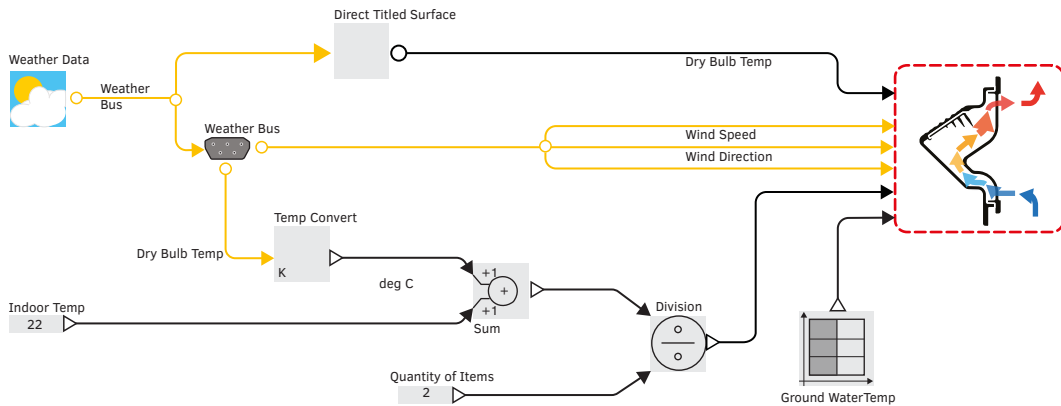


FIG. 6.9 Diagram of visual programming interface in Dymola showing weather and climate data integration and fluid inlet.

The co-simulations were combined with exterior data as boundary conditions from both the Modelica model and the OpenStudio model. Exterior air temperature, wind exposure and insolation were taken into consideration to the envelope area where the TACE modules were present in the Modelica model, introduced as a node in the Dymola interface and exported as part of the FMI code. The same climate conditions from the TMY3 data set were accounted for on the fenestration in the OpenStudio model.

The thermal transfer from the TACE module was represented as a surface temperature output in the FMI and used as a new outdoor dry bulb temperature modelled as the exterior surface of the envelope in OpenStudio.

With these modifications to the base files, the IDF was exported from OpenStudio to EnergyPlus. The FMI was exported from Dymola as an External Interface: Functional Mockup Unit Import. The FMI code was then placed into the IDF connecting the inputs and outputs between the TACE FMI and OpenStudio model – once completed, the IDF was ready for simulation in EnergyPlus.

EnergyPlus 8.7.0 was used for the co-simulation. Results were generated when the EnergyPlus simultaneously simulated the IDF and TACE FMI, which referenced each other as part of the simulation timescale every 10 minutes.

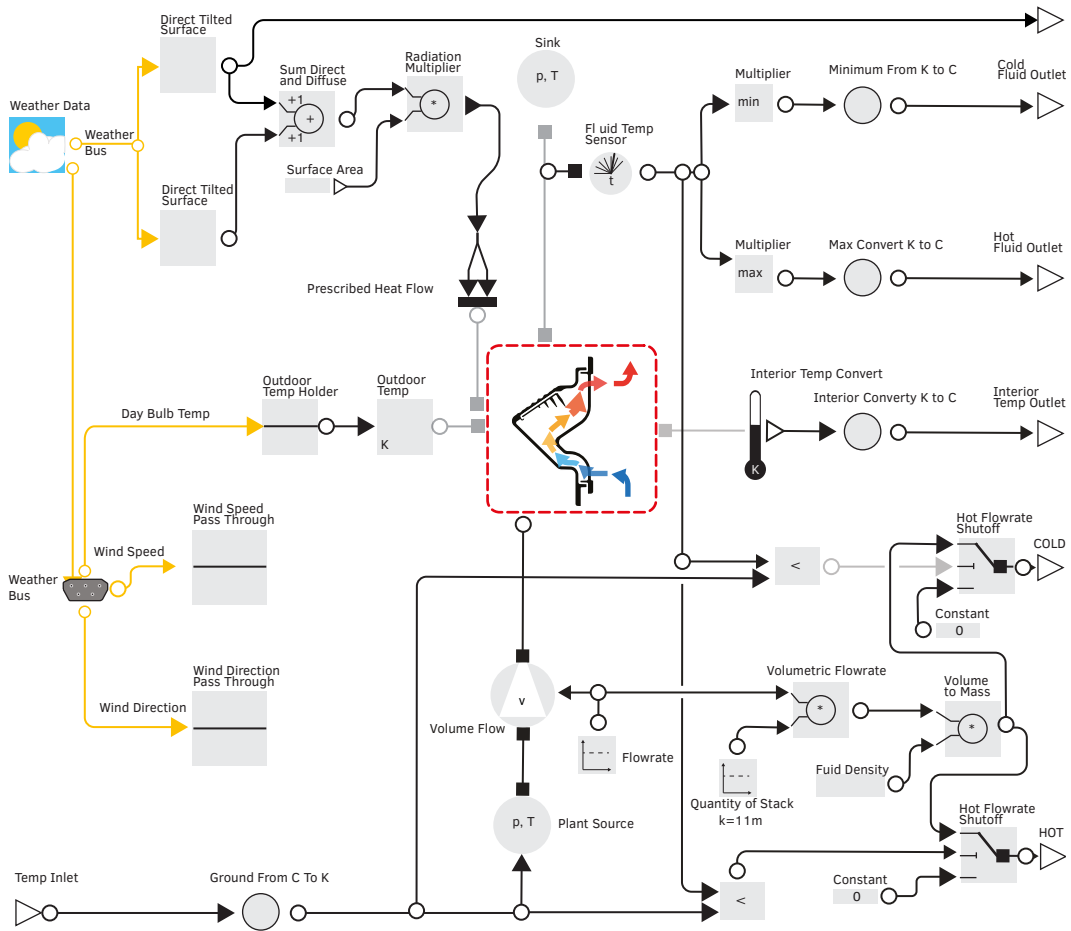


FIG. 6.10 Module array in Dymola interface highlighting the multiplier node that creates a simulation of the module in series.

Prior to running the co-simulation at the Bay and Floor scales, a simulation was created in Modelica for a sequentially linked array of 12 TACE modules, as shown in Figure 6.9. The number of sequentially linked modules was chosen based on two factors: 1) 12 modules could be arrayed on a typical bay 5 times using a 40% window to wall ratio, as shown in Figure 6.10, therefore, a simple scaling factor was used in the bay and floor zone simulations; and 2) after 12 modules in sequence the initial simulation showed diminishing returns as the input and output temperatures were not significant to harvest additional energy from extending the sequential array beyond 12. On other climate conditions or geographic locations, the co-simulation could be developed in other length sequential arrays. Additional

numbered sequential arrays were not investigated; however, other types of modules with different module to performance variables were investigated in Chapter 7.

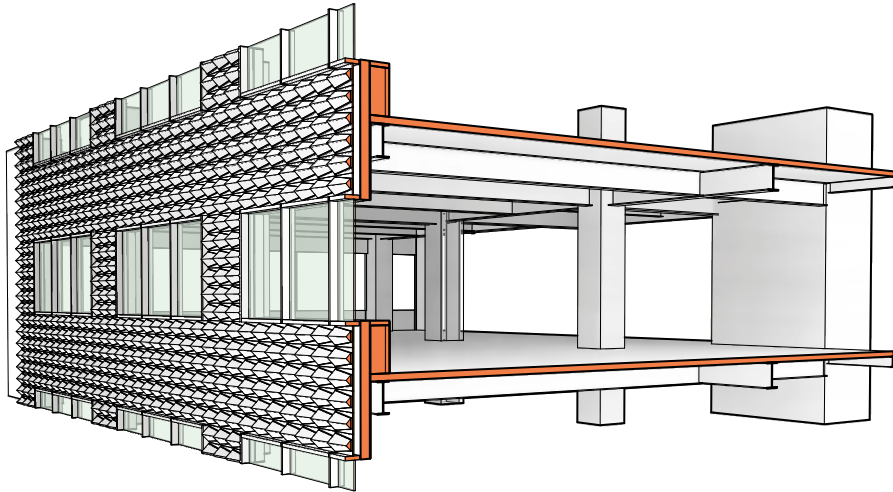


FIG. 6.11 Diagram of Modules in Stacks on a typical Bay.

The TACE FMI sequential array configuration was exported from Dymola as an FMI module. As noted a multiplier node as shown in Figure 6.10 created the output port for the 12 modules in sequence. This FMI was exported using FMI Version 1.0 (32 and 64-bit). The packaged FMI included environmental conditions as noted by the integration of the weather data.

The FMI input conditions were specified as Insolation ( $\text{W}/\text{m}^2$ ), Outside Dry Bulb Temperature ( $^{\circ}\text{C}$ ), Wind Speed ( $\text{m}/\text{s}$ ), Wind Direction ( $\text{rad}$ ), and Fluid Inlet Temperature ( $^{\circ}\text{C}$ ). The Output condition was specified as the Outlet Port from the 12 modules sequential array as calculated within the FMI. It included Cold Fluid Outlet Temperature ( $^{\circ}\text{C}$ ), Cold Fluid Mass Flowrate ( $\text{kg}/\text{s}$ ), Hot Fluid Outlet Temperature ( $^{\circ}\text{C}$ ), Hot Fluid Mass Flowrate ( $\text{kg}/\text{s}$ ), and Interior Wall Surface Temperature ( $^{\circ}\text{C}$ ). Within the FMI a condition statement node was used to shift the mass flowrate between the Cold Fluid or Hot Fluid outputs (depending on the outlet port temperature to be used in the appropriate system) as inputs in the IDF model during the simulation.



## 6.4.1 Simulations

---

Three series of co-simulation were run: 1) 12 module sequential array facing south; 2) single south facing bay zone on the Howe Center; 3) full building floor zone on the Howe Center. All simulations used the TMY3 data from the Teterboro Airport weather monitor. The 12 modules sequential array used the ordinal orientation of the Howe Center to establish a baseline platform for comparison. The Bay and Floor Zone simulations used the Stevens Institute Howe Center as the baseline for the model and the orientation. The Floor simulation used module stacks that were calculated for each sub zone, specifically, East South, and West directions, as part of the aggregation for the inputs and outputs. While the building contained a dining hall, common areas, and meeting spaces, the primary program for the Tower floors was as offices. Built in 1962 the Howe Center has had minimal facade and HVAC upgrades. As detailed in Chapter 2, this building represents both an opportunity for a Deep Energy Retrofit and serves as a stand-alone office building that can serve as a model of a new construction office tower in a metro region.

The simulations serve to investigate the performative impact on a building with the TACE System. Specifically, as a dynamic insulation system that changed the effective surface temperature of the building envelope, and as a thermal collector to capture, store and redistribute heat and coolth gathered from the envelope.

### 6.4.1.1 TACE 12 Module Array Simulations

---

It was established in Chapter 3 that the thermal energy capture or rejection potential of any passively configured TABS was dependent mainly on the flowrate of the working fluid, as long as there was some increase in surface area and articulation to create turbulent flow. In order for that thermal energy to be useful, the temperature boundaries of the working fluid must support the heating and cooling for indoor comfort. These boundaries were set mainly by the inlet port temperature of the module array. Using the 12 modules sequential array, various working fluid inlet port temperatures were studied. These simulations were run for the TMY3 data at Teterboro, NJ. The results were logged as an aggregation energy potential of a typical year. Heating energy was added when the outlet port temperature was above the inlet port temperature. Coolth energy was added when the outlet port temperature was below the inlet port temperature.

Thermal energy was attained as the heat was collected from insolation raising the exterior top surface temperature of the TACE modules and ambient heat transfer from the exterior conditions. Cooling was attained when the working fluid temperature was at a higher temperature at the inlet port than the exterior air temperature. It was assumed that both the heat and coolth capacity of the TACE system would offset either the use or the size of the zone associated mechanical heating and cooling systems.

These simulations attempted to quantify the heat and coolth potential per annum when simulated with both various inlet port working fluid temperatures and flowrates.

#### 6.4.1.2 Bay Zone Simulations

---

The bay zone model, as shown in Figure 6.5 was developed into three comparison simulations where the variable was the envelope: 1) the Howe Center's existing envelope, 2) against an ASHRAE recommended curtain wall envelope and 3) the TACE System. Glazing performance values for all cases are summarized as the following.

1) Howe Center Envelope: The existing Howe Center building envelope was constructed prior to the ASHRAE recommended standards. As shown in Figure 6.12 the Howe Center uses an assembly indicative of the first generation of stick built curtain wall assemblies – the same basic layering – and performance – found in the Lever House (SOM, 1952) Seagram's Building (MVD R, 1958). The opaque portion of the curtain wall layers from the exterior 6.35 cm (2.5 in) of Granite, 2.54 cm (1 in) of mortar, 10.16 cm (4 in) solid concrete block, and 1.27 cm (.5 in) of gypsum board on the interior. This results in a U-value of 2.529 W/m<sup>2</sup>-K (0.446 btu/hr/ft<sup>2</sup> F) with window film and 4.071 W/m<sup>2</sup> K (0.717 btu/hr/ft<sup>2</sup> F) without air film. The glazing was a single 6.35 mm (0.25 in) pane with an assumed U-value of 5.778 W/m<sup>2</sup> K (1.018 btu/hr/ft<sup>2</sup> F), SHGC of 0.862, and visible transmittance of 0.899. The assembly was not thermally broken or insulated.

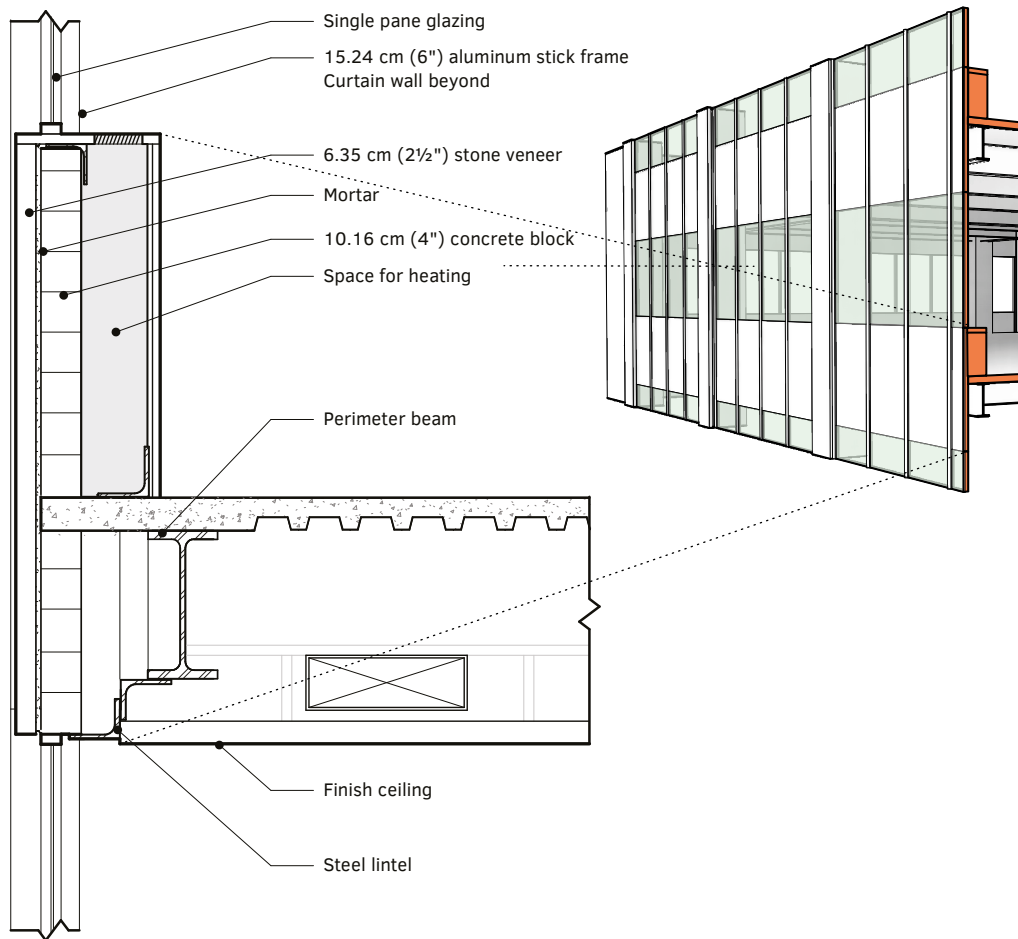


FIG. 6.12 Existing Assembly of the Howe Center building envelope as typical of office buildings of this vintage.

2) ASHRAE Recommended Curtain Wall noted as current standard: The ASHRAE curtain wall recommendation was used as the universal baseline for measuring and upgrading building envelope performance. The industry expects that a new curtain wall or repositioned curtain wall will meet or exceed this performance standard. As shown in Figure 6.13 the ASHRAE recommended standard layers from the outside, 2.54 cm (1 in) of stucco, 10.16 cm (4 in) of stone wool insulation and 1.59 cm (0.625 in) gypsum board on the interior. This assembly results in a U-value of 0.306  $W/m^2 K$  (0.717  $btu/hr/ft^2 F$ ) (0.054  $btu/hr/ft^2 F$ ) with air film and a U-value of 0.321  $W/m^2 K$  (0.717  $btu/hr/ft^2 F$ ) (0.056  $btu/hr/ft^2 F$ ) without film. The ASHRAE recommended exterior glazing is prescribed in ASHRAE 90.1-2013 where the glazed

pane has a U-value of 2.559 W/m<sup>2</sup> K (0.717 btu/hr/ft<sup>2</sup> F) (0.47 btu/hr/ft<sup>2</sup> F), an SHGC of 0.352, and a visible transmittance of 0.442.

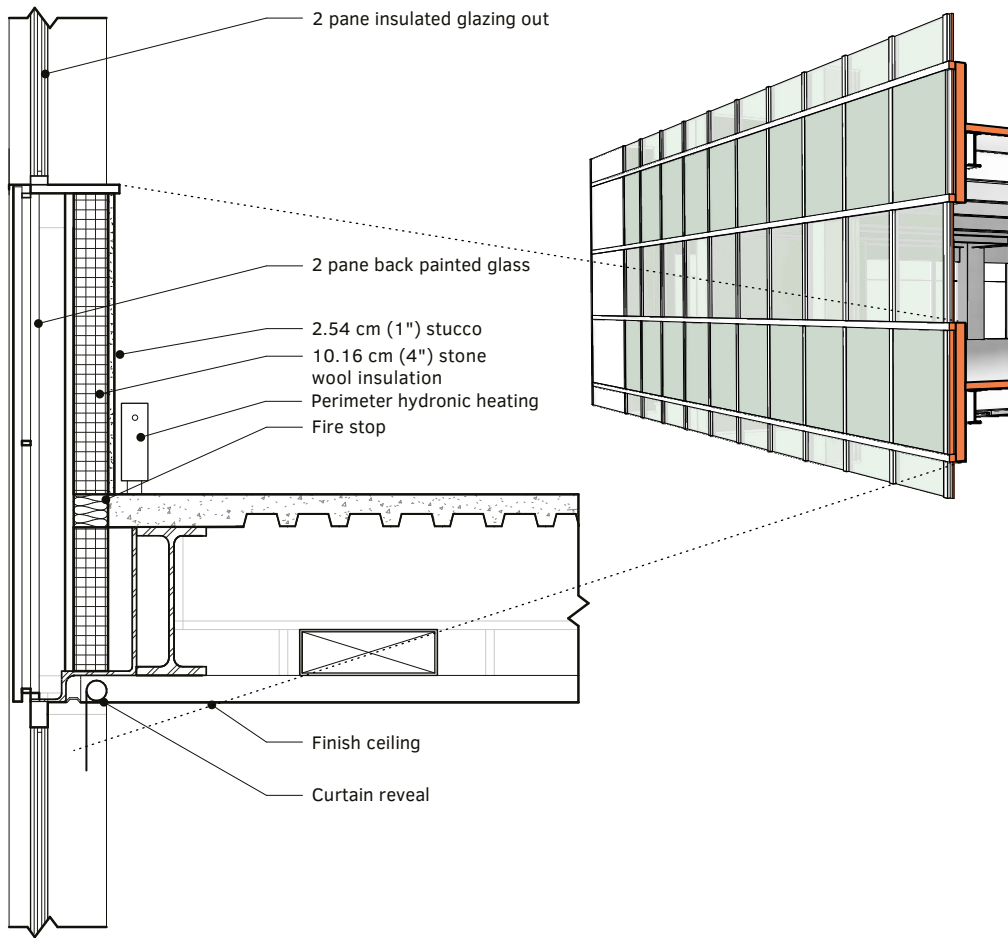


FIG. 6.13 Example Assembly of ASHRAE Recommended Standard for Climate Zone 4

3) TACE System: In comparison, as shown in Figure 6.14 the TACE system was assembled from the exterior with TACE modules, an air gap, a 10.16 cm (4 in) stone wool insulation, and a 1.59 cm (0.625 in) type X gypsum board on the interior. With the exclusion of the TACE module, the remaining wall assembly has a U-value of 0.292 W/m<sup>2</sup>-K (0.051 btu/hr/ft<sup>2</sup> F) with the film and 0.306 W/m<sup>2</sup> K (0.054 btu/hr/ft<sup>2</sup> F) without the film. The exterior glazed pane has a U-value of 2.559 W/m<sup>2</sup>-K (0.47

btu/hr/ft<sup>2</sup> F), an SHGC of 0.352, and a visible transmittance of 0.442, the same as the ASHRAE 90.1-2013 recommended standard.

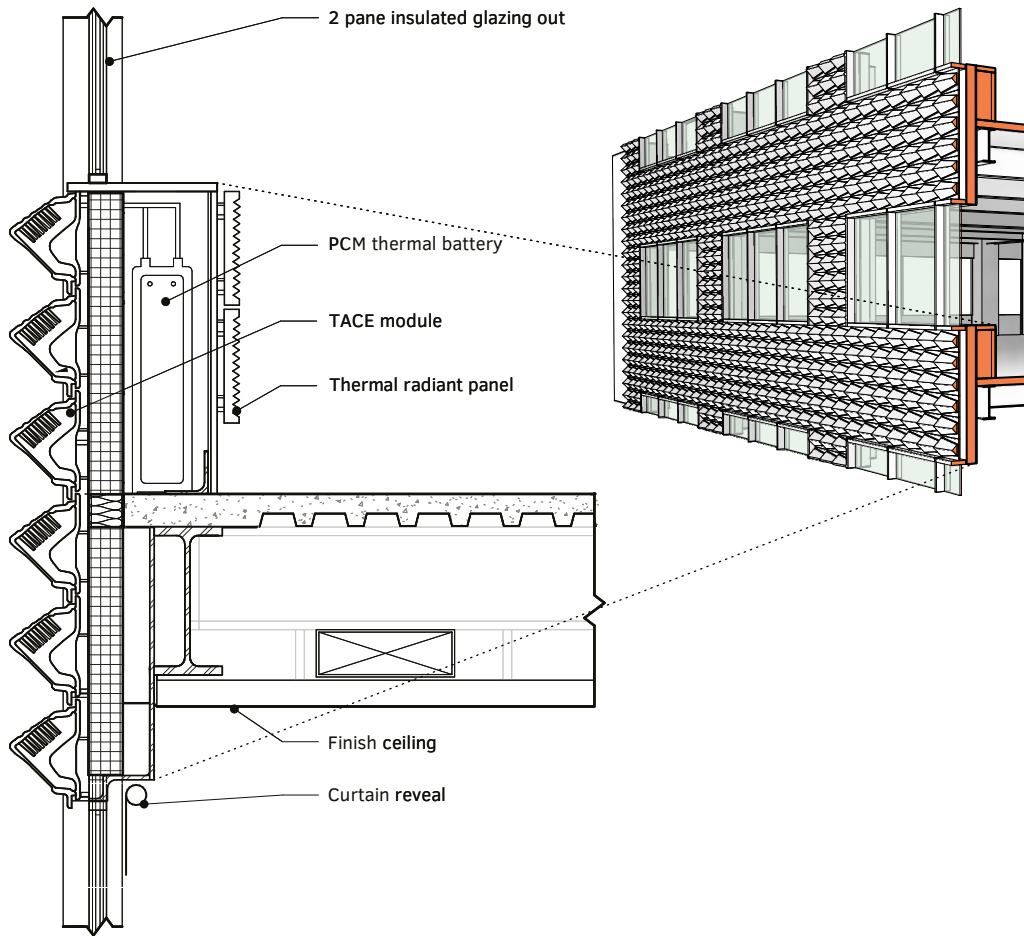
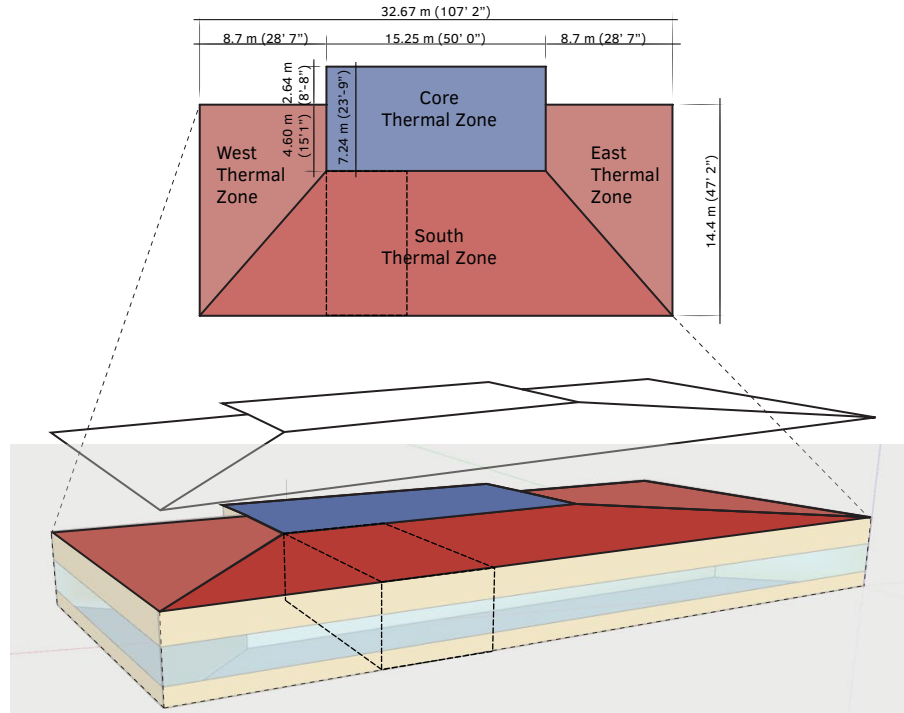


FIG. 6.14 Example TACE building envelope applied at the spandrel panel.

### 6.4.1.3 Floor Zone Simulations

The Floor Zone simulations used the model, as shown in Figure 6.15 were developed based on the Bay Zone simulations. The Floor Zone was based on the office floor plate of the Howe Center. The total area of 517.8 m<sup>2</sup> (5,575 sf) was divided into three

discrete sub zones, East, South and West. The southern face was oriented 12.8° to the southwest as per the existing Howe Center orientation. All simulations used a window to wall ratio of 40%.



**FIG. 6.15** Representative model of Floor Zone used for the EnergyPlus model. The model was divided into thermal zones and most closely reflects the modern office space where there was the complexity of having multiple zones open to one another where at times some zones may be in heating and other in cooling modes.

The boundary conditions at the exterior wall were modified to substitute the TACE system for the exterior envelope input linked to thermal storage similar to the bay zone simulations. The following floor zone simulations were initially designed to link the thermal capacity and management of TACE system to augment various HVAC systems by directly tempering the working fluid of the HVAC systems. The following HVAC configurations, as shown in Figure 6.16-6.19, were examined for addressed potential integration strategies between systems.

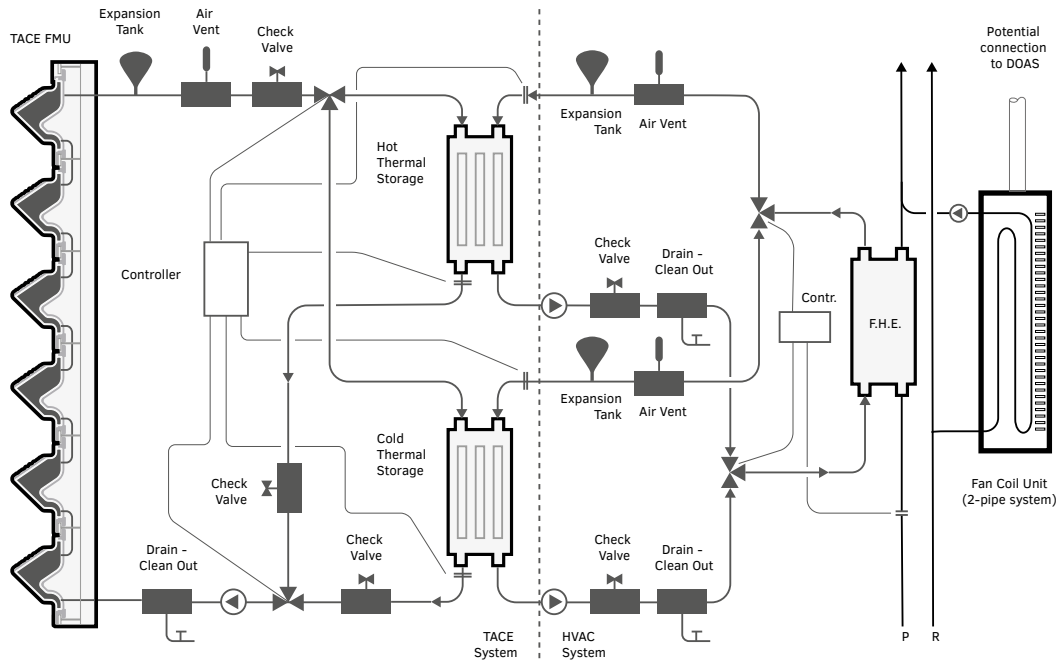


FIG. 6.16 Pipe Fan Coil in the current Howe Center using a seasonal switch with return and potential connection to DOAS.

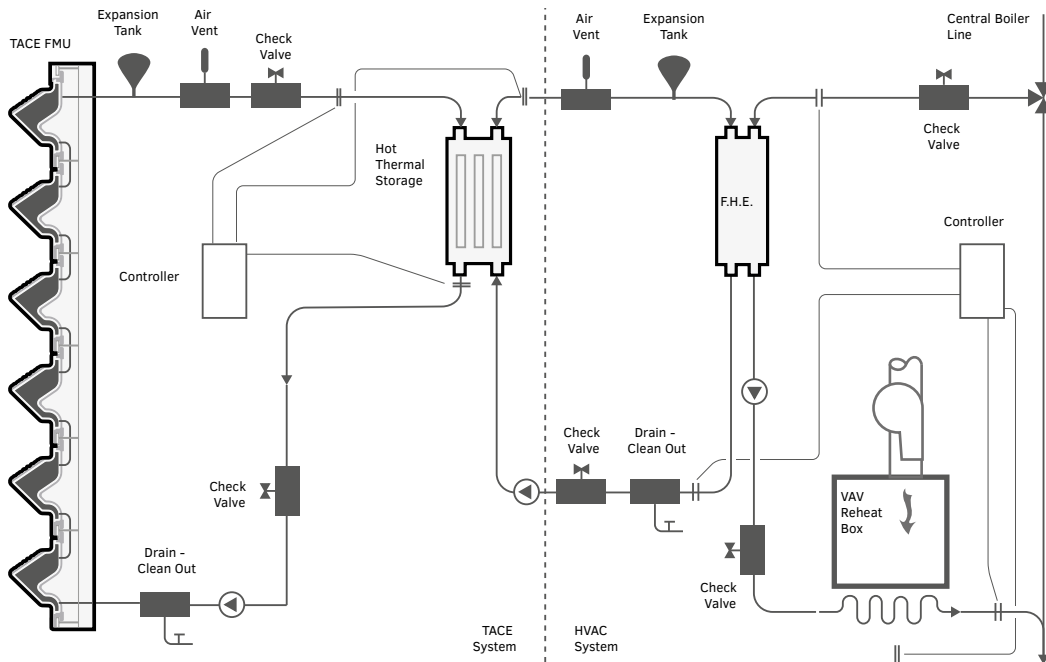


FIG. 6.17 Variable Air Volume (VAV) with Reheat (ASHRAE Baseline).

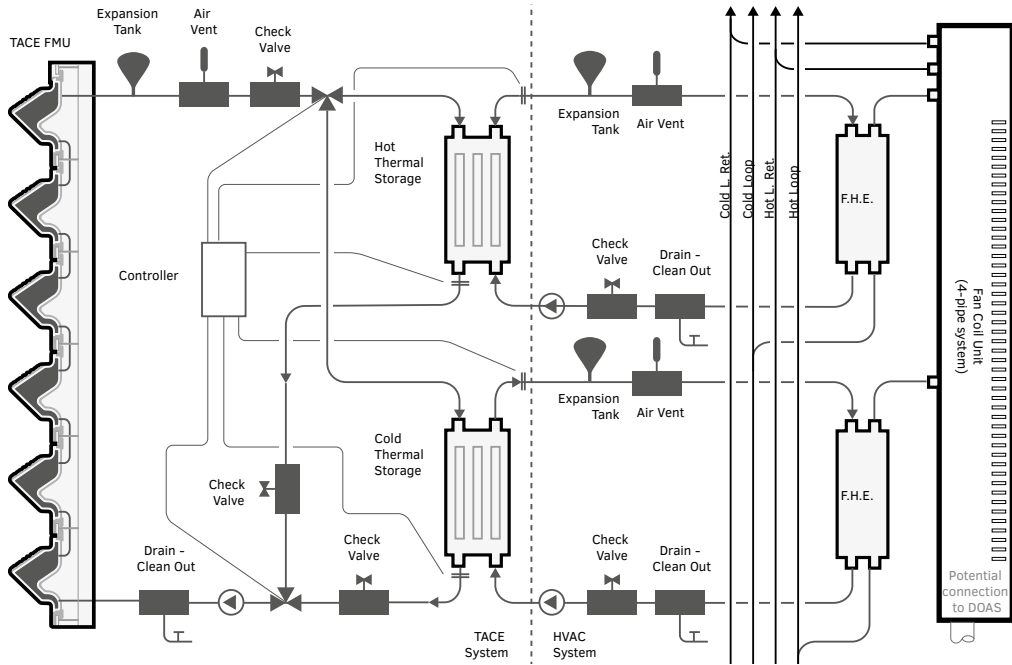


FIG. 6.18 4-Pipe Fan Coil with DOAS.

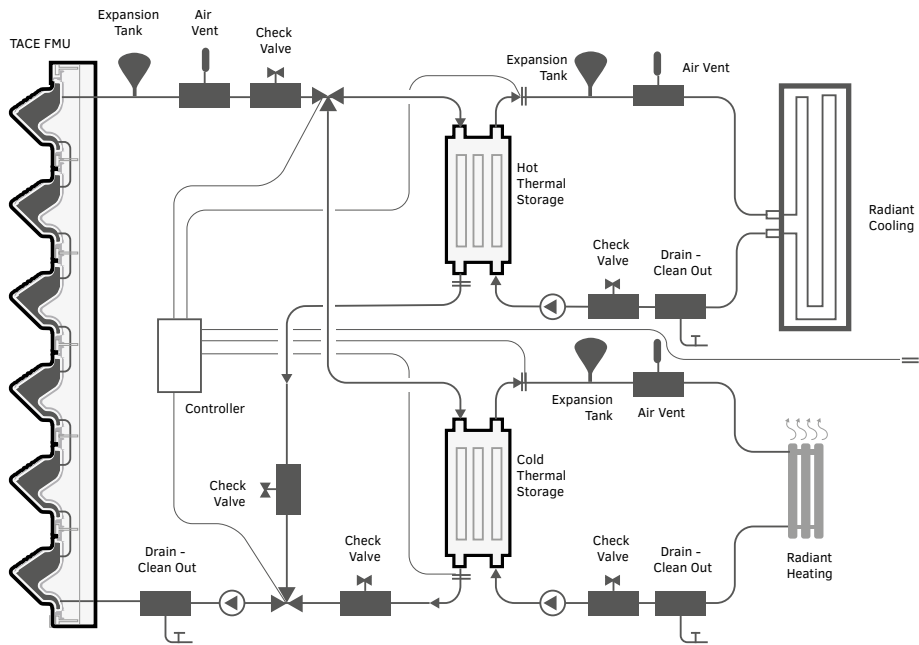


FIG. 6.19 Direct Radiant System decoupled from the primary heating and cooling system.



The simulations, as shown in Figures 6.16-6.18, were run as a direct augmentation to the various HVAC systems and as a radiant baseboard heater, as shown in Figure 6.19 to offset an ASHRAE compliant system.

To independently isolate and operate the subzones of the Floor Zone Simulation three water plant loops were added to the model – as distinct Plant Component: Temperature Source and Hot Water Heater: Mixed – for individual bay assemblies of the TACE. As the loops were independent, the components of the thermal storage and radiant baseboard system could be optimized for each façade facing subzone. The Hot Water Heater: Mixed system components provided exclusive thermal storage for allocated TACE system zones. Each zone was connected using a countercurrent thermal exchanger which were then connected to the subzone radiant baseboard heater. The individual control of the subzones was linked directly to the subzone heating demand as specified dynamically by the radiant baseboard heater. These plant loops were interconnected so that the heating demand in one subzone could be serviced by the thermal capacity of another zone if required. The radiant baseboard heater in the East subzone, for example, based on heating demand of this subzone, could be serviced by heat collected and stored on the south and the west subzones.

Cooling was not explored at the Floor Zone Simulation; however, there could be significant energy savings if coolth was considered similar to the heating. Energy saving from cooling could be investigated by including a more complex feedback controller that could modulate between heating and cooling demand that could prioritize thermal demands of heat or coolth loops based on a combination of the requirements of the thermal comfort, energy utilization, external weather conditions, and stored thermal resource harvested by the TACE system.

#### 6.4.1.3.1 Original Building Envelope with HVAC Scenario

---

The following describes the input for the OpenStudio model and simulation of the Existing Howe Center Envelope:

- Envelope: Existing Building Envelope
- Building: 517.93 m<sup>2</sup> (5,575 ft<sup>2</sup>) rectangular building, one floor, 12.8° oriented southwest
- Heating: Forced Air, Natural Gas Boiler
- Cooling: Central Air, Chiller and Condensing Tower
- Location: Hoboken, NJ
- Construction: Concrete Block, R-Value of 7.844 W/m<sup>2</sup> K (1.4 btu/hr/ft<sup>2</sup> F)
- Window-to-Wall: 40%

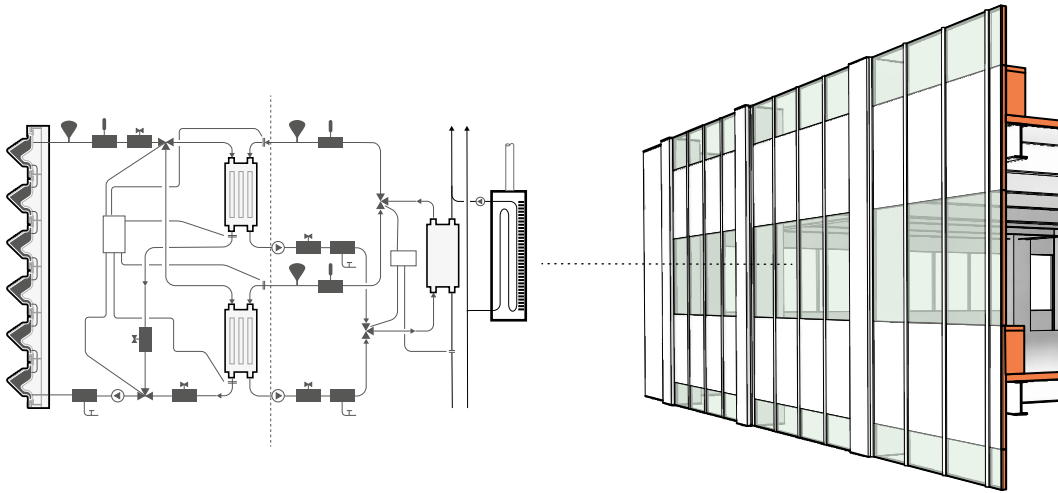


FIG. 6.20 Alignment of existing heating and cooling type with existing façade.

#### 6.4.1.3.2 Improved Building Envelope with HVAC Scenario

The following describes the input for the OpenStudio model and simulation of the AS HRAE improved envelope on the Howe Center:

- Envelope: ASHRAE Recommended Curtain Wall
- Building: 517.93 m<sup>2</sup> (5,575 ft<sup>2</sup>) rectangular building, one floor, 12.8° oriented southwest
- Heating: Forced Air, Natural Gas Boiler
- Cooling: Central Air, Chiller and Condensing Tower
- Location: Hoboken, NJ
- Construction: Spandrel stone wool insulation, R-Value 100.44 W/m<sup>2</sup> K (17.7 btu/hr/ft<sup>2</sup> F)
- Window-to-Wall: 40%

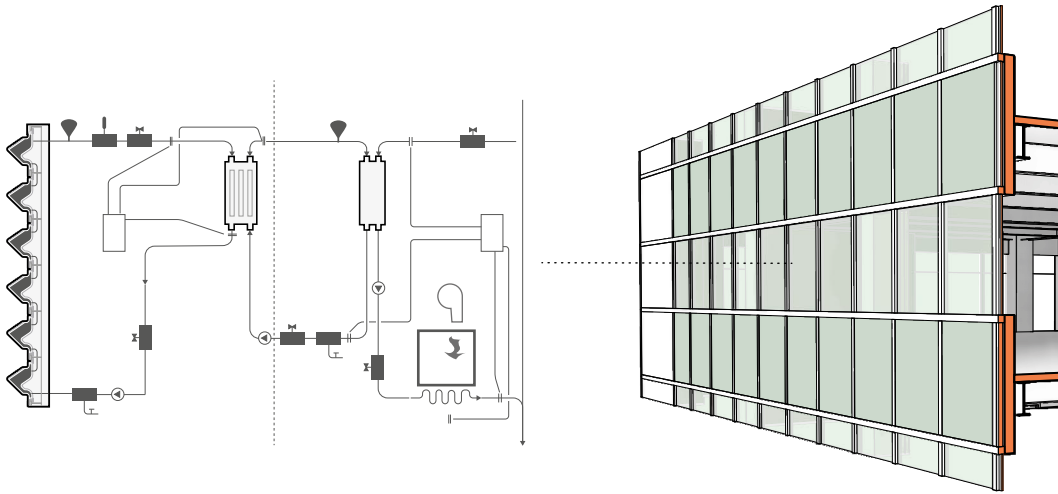
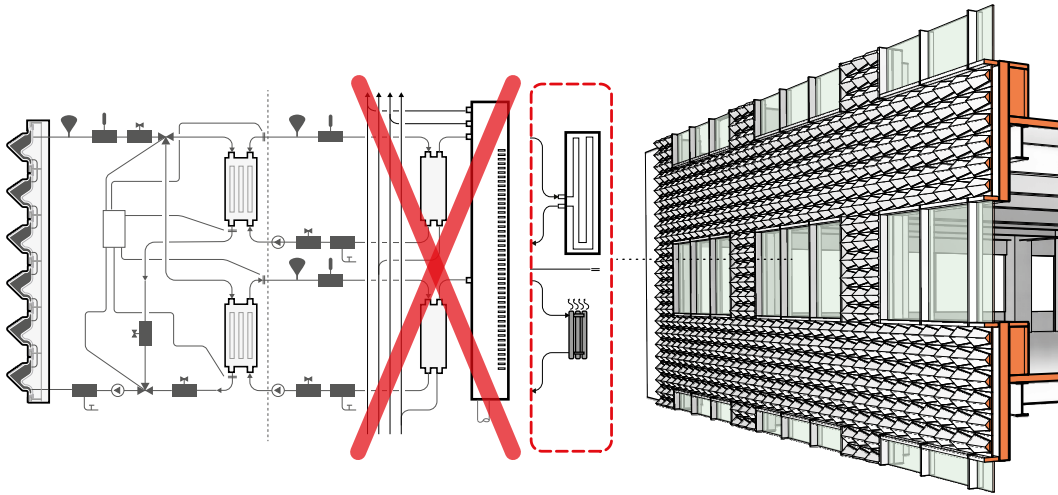


FIG. 6.21 Alignment of ASHRAE recommended heating and cooling type with recommended façade.

#### 6.4.1.3.3 TACE with HVAC Scenario

The following describes the input for the OpenStudio model and simulation of the TACE system envelope on the Howe Center:

- Envelope: EcoCeramic Envelope System
- Building: 517.93 m<sup>2</sup> (5,575 ft<sup>2</sup>) rectangular building, one floor, 12.8° oriented southwest
- Heating: Forced Air, Natural Gas Boiler,
- Cooling: Central Air, Chiller and Condensing Tower
- Location: Hoboken, NJ
- Construction: stone wool insulation, Air gap, R-Value 105.55 W/m<sup>2</sup> K (18.6 btu/hr/ft<sup>2</sup> F)
- Window-to-Wall: 40%
- TACE: 3 Walls, 128 m<sup>2</sup> (1,377.78 ft<sup>2</sup>) of envelope area -deployed as radiant heating and cooling panel decoupled from central HVAC



**FIG. 6.22** Alignment of the initially proposed TACE system and heating and cooling system, and diagram of system design modified based on simulation results that were used for final EUI studies for Prototypes I and III.

## 6.4.2 Results using MVP Prototype I

The results covered in this Chapter fall into two primary categories: 1) the potential for the TACE system to harvest heat or coolth as shown by the 12 module array simulations, and, 2) the potential the TACE systems to lower the EUI of an existing space, explored in the bay and floor zone scale.

### 6.4.2.1 Results of TACE 12 Module Array Simulations

The results of the 12 Module Array Simulations using MVP Prototype I were focused on two studies: 1) system performance output as a function of input temperatures, and 2) power output as a function of temperature differential according to flowrates. The matrix of complete results is summarized in Table 6.2. The results of the per annum simulation and normalized values were used for other energy harvesting building systems, as discussed in Section 8.1.1.1.

**TABLE 6.2** Summary results showing the impact of system inlet temperatures on annual energy potential and maximum temperature flux for MVP Prototype I.

Inlet Water Condition (°C)	Flowrate (l/min)	Mode	Annual Energy (kWh/yr)	Annual Energy Normalized (kWh/m <sup>2</sup> /yr)	Max Temp Difference (°C)
Ground 2.0 m	0.625 l/min (0.165 gpm)	Heating	686.98	410.81	16.43
		Cooling	-268.03	-160.28	-8.54
	2.50 l/min (0.66 gpm)	Heating	959.68	573.88	7.4
		Cooling	-373.41	-223.29	-3.17
22°C (71.6°F)	0.625 l/min (0.165 gpm)	Heating	211.5	126.48	9.79
		Cooling	-1228.46	-734.61	-14.54
	2.50 l/min (0.66 gpm)	Heating	291.38	174.25	3.89
		Cooling	-1728.52	-1033.65	-7.35
Average Between Indoor and Outdoor	0.625 l/min (0.165 gpm)	Heating	203.27	121.55	8.23
		Cooling	-540.57	-323.26	-7.47
	2.50 l/min (0.66 gpm)	Heating	285.57	170.77	5.5
		Cooling	-786.42	-470.28	-3.75

#### 6.4.2.1.1 Results of Inlet Temperature

Inlet temperatures were explored in three conditions: 1) daily varying groundwater temperature as over the year as inlet temperature; 2) consistent 22° C (71.6°F) inlet temperature; 3) average temperature between indoor and outdoor temperatures for inlet temperature. Ultimately inlet temperatures were a function of the outlet temperature of the thermal exchange loop in the TACE system and were not modelled as part of this simulation, but were accounted for in the whole building model using EnergyPlus. These comparative results, as shown in Figures 6.23-6.26, were intended to illustrate the potential of the system and provide a starting point for Bay and Zone calculations for EUI reduction potential. Chapter 8 discusses the recommended approach for further refinement of results.

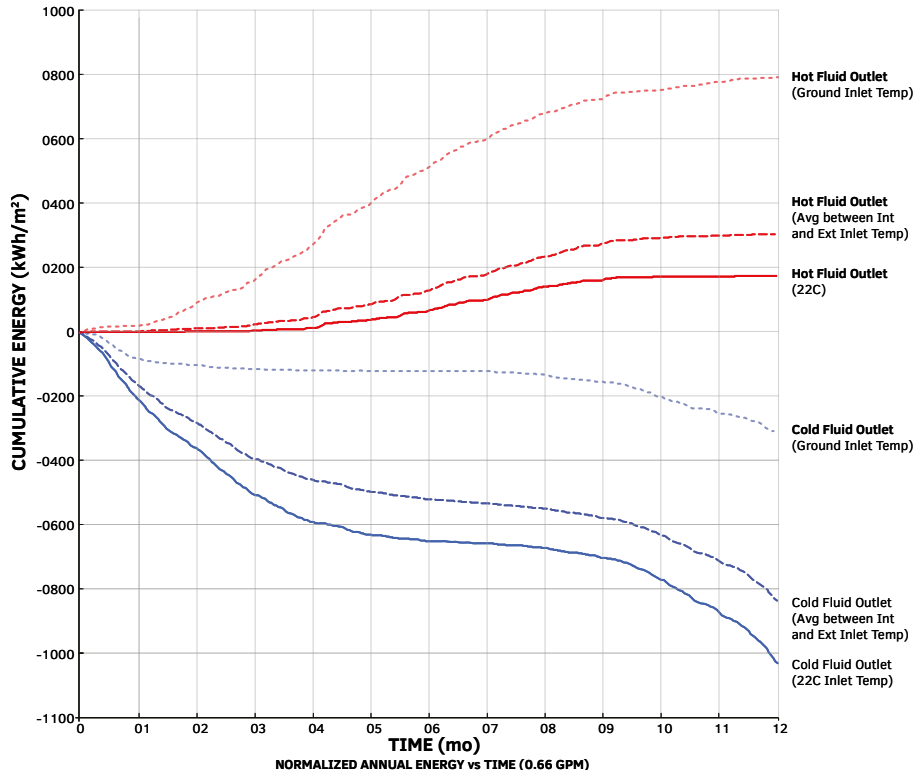


FIG. 6.23 MVP Prototype I comparison of normalized annual energy with 2.50 l/min (0.66 gpm) using system inlet temperatures of: groundwater temperature; 22° C (71.6° F) temperature; average between indoor and outdoor temperatures.

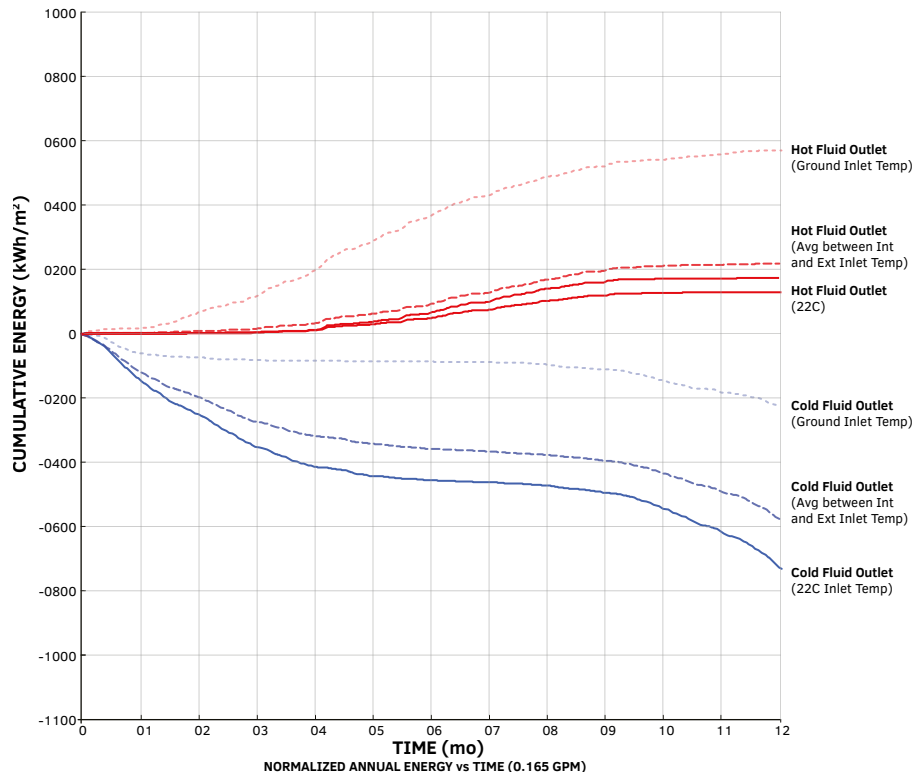
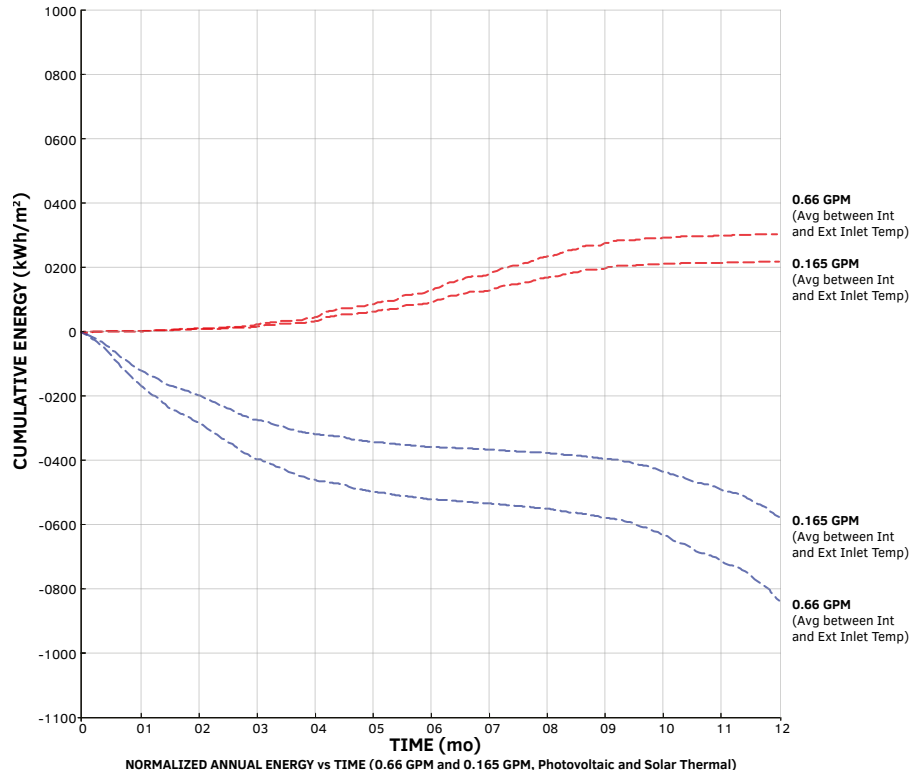
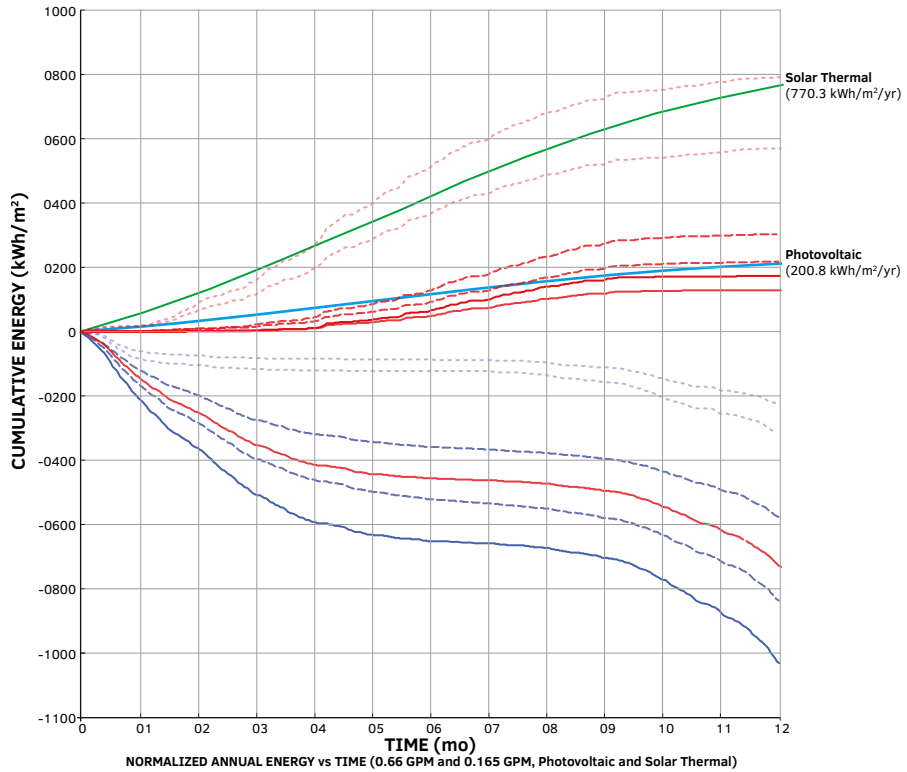


FIG. 6.24 MVP Prototype I comparison of normalized annual energy with 0.625 l/min (0.165 gpm) using system inlet temperatures of: groundwater temperature; 22° C (71.6° F) temperature; average between indoor and outdoor temperatures.



**FIG. 6.25** MVP Prototype I comparison of normalized annual energy using 2.50 l/min (0.66 gpm) vs 0.625 l/min (0.165 gpm) using the system inlet temperature of an average between indoor and outdoor temperatures.





**FIG. 6.26** MVP Prototype I comparison of normalized annual energy using 2.50 l/min (0.66 gpm) vs 0.625 l/min (0.165 gpm) compared to Photovoltaic and Solar Thermal outputs.

While cumulative power is one measure of system efficacy, the access to available power is a better real world measure of how much the TACE system can impact EUI. As shown in Figures 6.27 and 6.28, Heat and Coolth were simulated for a year using: 1) daily varying groundwater temperature over the year as inlet temperature; 2) consistent 22° C (71.6° F) inlet temperature. These cases represent both a varying and static inlet temperature, and while they do not reflect real world performance, they illustrate the impact of the inlet temperature and its importance. Ultimately, to characterize the real work performance, the inlet temperature was simulated as a function of the outlet temperature after the working fluid has transferred energy with the thermal battery through the countercurrent heat exchanger and was captured in the results of the Bay and Floor and Building energy simulations.

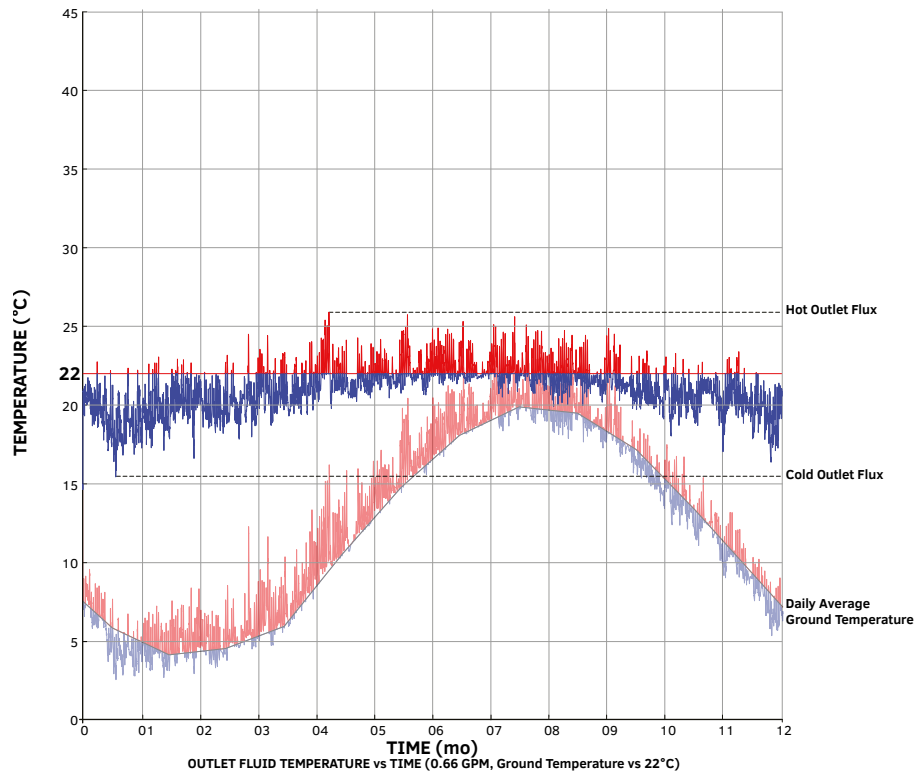


FIG. 6.27 MVP Prototype I comparison of temperature flux at 2.50 l/min (0.66 gpm) flowrate using ground temperature and 22°C (71.6° F) as inlet temperatures.

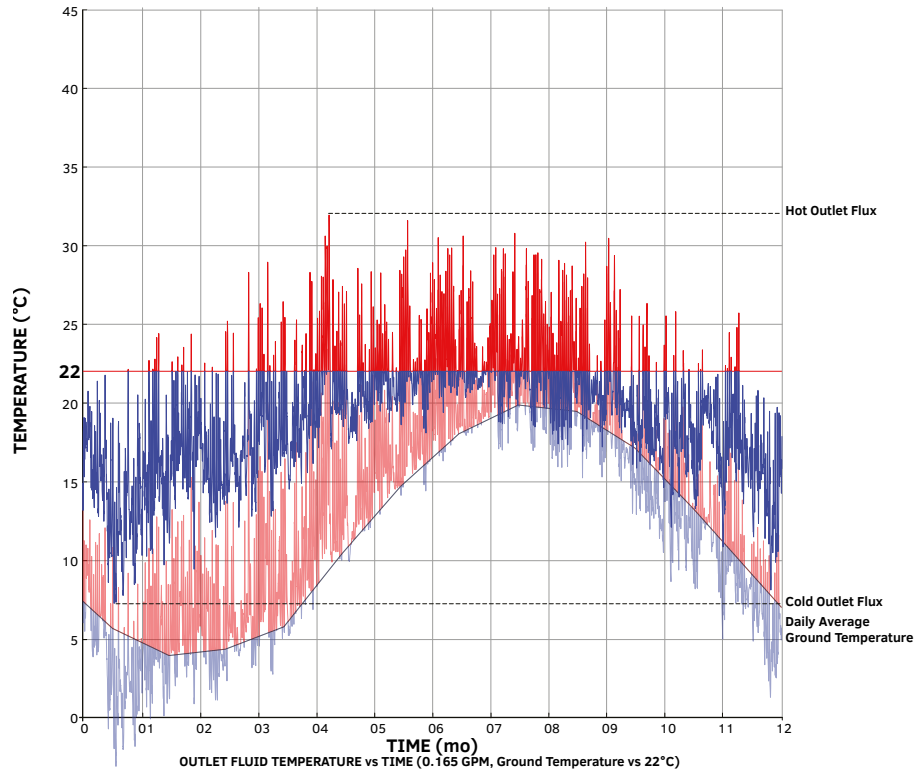


FIG. 6.28 MVP Prototype I comparison of temperature flux at 0.625 l/min (0.165 gpm flowrate using ground temperature and 22°C (71.6° F) as inlet temperatures.

The results of the inlet temperature simulations indicated:

- That using average groundwater temperature yields the most heating potential of all three cases
- That using 22° C (71.6° F) yields the most cooling potential of all three cases
- The inlet temperature should be determined according to the heating and cooling demands required for achieving thermal comfort if it can be controlled outside of the outlet temperature for the thermal cycle of the TACE system
- That although hot water systems or radiant systems could not be replaced based on these results, one form of integration could be to precondition the water that was feeding domestic hot water or radiant system, whereas the TACE systems become a thermal preconditioner.
- That there appear to be diminishing returns for the ability to provide hot water as the inlet water temperature increased, while conversely, the cooling potential improves as the inlet water temperature increased.

Although the cooling potential of the TACE system was not investigated initially as part of this thesis, conditions exist that suggest that the TACE system can provide free cooling to the building under certain conditions – as shown in Table 6.2, there was more cooling energy available than heating energy in the New York climate zone. In order to provide cooling with TACE, the outside air temperature must be lower than the comfort range within occupied space while the temperature in the space with additional cooling would naturally be higher than the comfort zone. This condition was actually quite common and happens routinely on warmer winter days and predominantly during shoulder months, as shown in Figures 6.27 and 6.28. As a means to compare the New York results, several cases have been simulated for the Phoenix, Arizona and Amsterdam, Netherlands climates. These comparative cases are detailed in Section 6.4.3.1.

#### 6.4.2.1.2 Results of Heat and Coolth Harvesting by Flowrates

---

The results as shown in Table 6.2 compare flowrates in the functional mode as heating or cooling measured in terms of annual energy captured measure in kWh/yr. The 0.625 and 2.50 l/min (0.165 and 0.66 gpm) cases were simulated. The 2.50 l/min (0.66 gpm) flowrate case can produce more energy, 272.70 kW/hr heating energy more than the 0.625 l/min (0.165 gpm) case – but at a reduced temperature, 9.03° C (16.25° F) lower than the 2.50 l/min (0.625 gpm) case. The same behaviour was observed from the simulation of Coolth, where 2.50 l/min (0.66 gpm) case stored 105.38 kWh/yr more Coolth than the 0.625 l/min (0.165 gpm) case, though again at a lower temperature, 5.37 kWh/yr. As shown in Figures 6.29 and 6.30, the power available daily shows diurnal and seasonal energy availability. Understanding the pattern of potential Heat and Coolth was critical to developing the system design to be able to access the energy as well as in developing the control logic in the EnergyPlus simulation.

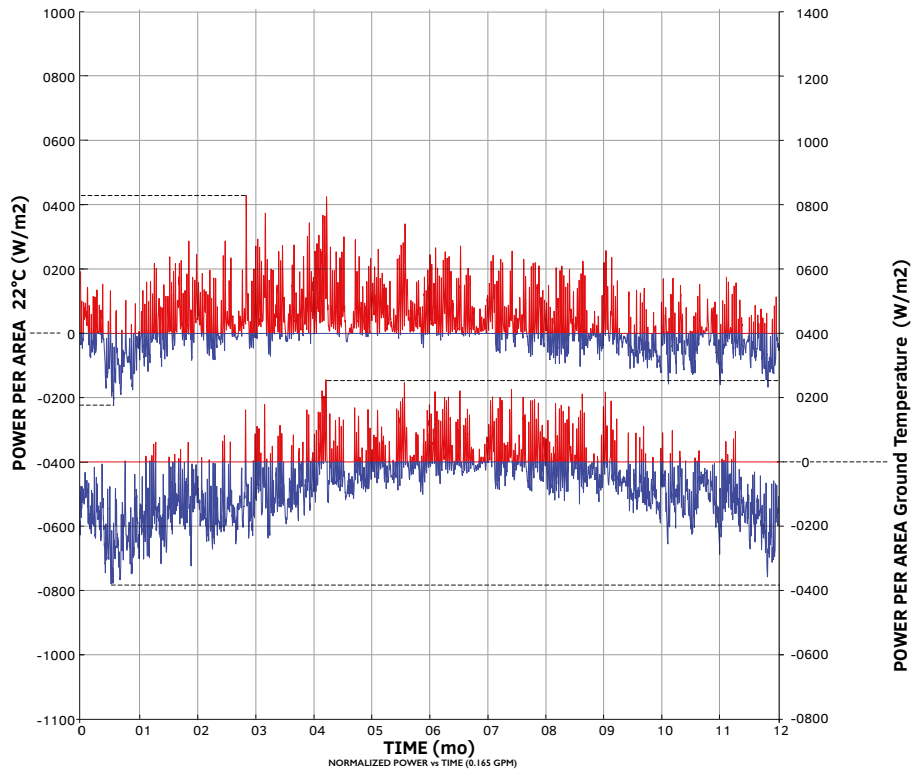


FIG. 6.29 MVP Prototype I comparison of power per area at 0.625 l/min (0.165 gpm) flowrate using ground temperature and 22°C (71.6° F) as inlet temperatures.

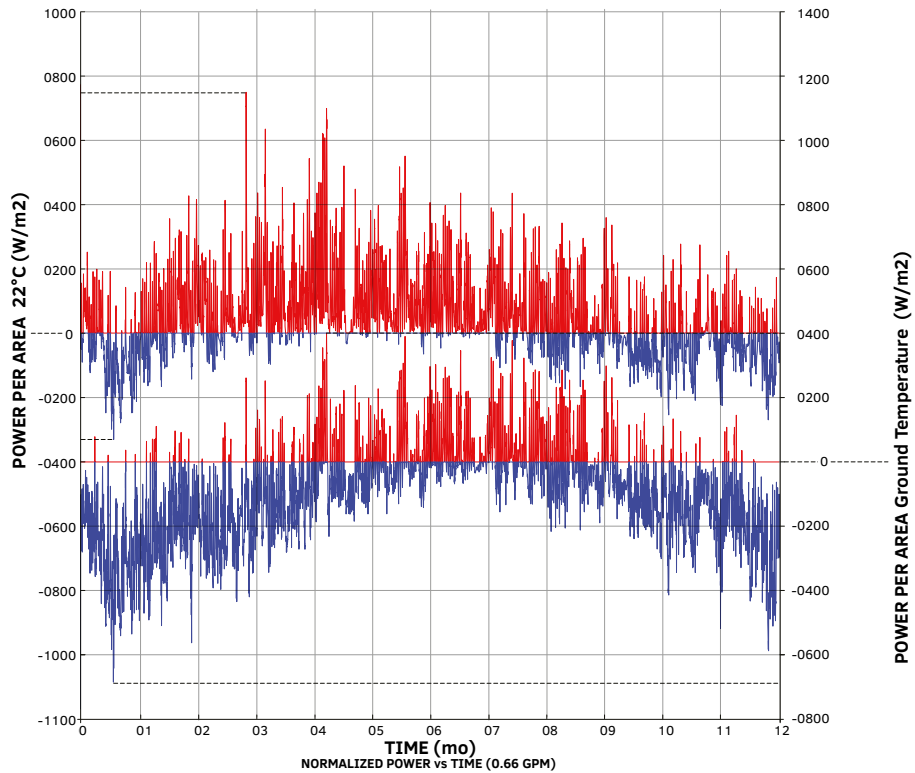


FIG. 6.30 MVP Prototype I comparison of power per area at 2.50 l/min (0.66 gpm) flowrate using ground temperature and 22°C (71.6° F) as inlet temperatures.

While power per unit area appears to be significant as shown in Figures 6.29 and 6.30, in both cases, the low simulated temperature differentials, when including the energy needed to move the fluid, reveals a system that cannot compete with contemporary highly concentrated energy used in current efficient systems that use electricity and natural gas as primary sources. Depending on the application, or end use, one could modulate the flowrate depending on the most impactful use towards a particular demand. Where more temperature but less energy was desired, for example, the lower flow might be warranted, wherein other conditions, the high flow with lower temperatures but more energy might be warranted.

### 6.4.2.2 Analysis of HVAC Scenarios at Multiple Scales

---

The sub question addressed in this chapter was initially directed towards understanding what HVAC system could best be integrated with the TACE system and was intended to find the supportive synergies in system combinations. Initially, it was the intention of this study to offset the energy use of a variety of HVAC systems by directly augmenting the heating and cooling loops at the terminal delivery of the heating and cooling systems. Based on the initial results of the 12 Module Array, the fluid temperatures as demonstrated in the simulation in Figures 6.27 and 6.28, were significantly more moderate than those which were used by conventional HVAC systems (e.g., Fan Coil Unit, Variable Air Volume Unit, Chilled Beam, etc.) which operate at temperature ranges from 12.8° C (55° F) for cooling and 60° C (140° F) for heating.

In the observed simulated temperature in the standard HVAC systems, it quickly became apparent that the temperatures that could be captured and stored from the TACE system were not enough to impact existing heating and cooling systems; therefore a new approach was needed to make use of the harvested energy. In the round of simulations used for generating the following results at the Bay and Zone scales, the TACE system used radiant heating and cooling panels as the terminal delivery for heat and coolth. This radiant system was decoupled from the primary building heating and cooling system, which remains as described in Section 6.4.1.3 and as shown in Figure 6.19.

### 6.4.2.3 Energy Use Intensity Reduction Potential MVP Prototype I: Bay Scale

---

The bay-scale energy model simulations were run using the three different building envelopes, as described in Section 6.4.1.2. The Bay Scale Simulation 1 was established as the baseline for EUI improvement from which results of the other two cases were compared.

The results are shown in Table 6.3 of the Bay Scale Simulation 1 of the Howe Center with the existing envelope show an annual average total EUI for the Bay Zone of 870.0 MJ/m<sup>2</sup> (76.6 kBtu/ft<sup>2</sup>).

**TABLE 6.3** MVP Prototype I EUI comparative simulation case results for a typical south facing bay installation in three cases: Simulation 1 Existing Envelope, Simulation 2 ASHRAE Curtain Wall, and Simulation 3 TACE System.

EUI Per Building Area - Bay					
Case	[MJ/m <sup>2</sup> ]	[kWh/m <sup>2</sup> ]	[kBTU/ft <sup>2</sup> ]	Savings	
Existing Envelope	870.03	241.68	76.61	0.0%	
ASHRAE CW	587.21	163.11	51.71	32.5%	
TACE System	561.84	156.07	49.47	35.4%	
Savings Comparison					
Case	Existing	ASHRAE	TACE	Difference	Difference Savings
Existing Envelope	0.0%	-48.2%	-48.2%	0.0	0.0%
ASHRAE CW	32.5%	0.0%	-4.5%	282.8	32.5%
TACE System	35.4%	4.3%	0.0%	25.4	9.0%
HVAC Savings					
Case	[MJ/m <sup>2</sup> ]	Savings	Difference [MJ]	Difference Savings	[kBTU/ft <sup>2</sup> ]
Existing Envelope	615.99	0.0%	0.0	0	54.24
ASHRAE CW	333.17	45.9%	282.8	45.9%	29.34
TACE System	307.79	50.0%	25.0	8.8%	27.10
End Use Comparison Typical South Bay Zone					
End Uses	Existing (GJ)	ASHRAE (GJ)	Savings	TACE (GJ)	Savings/ASHRAE
Heating	9	4.43	50.8%	3.69	16.7%
Cooling	11.11	6.19	44.3%	5.92	4.4%
Fans	0.78	0.49	37.2%	0.46	6.1%
Pumps	5.25	2.93	44.2%	2.84	3.1%
Heat Rejection	3.47	1.98	42.9%	1.89	4.5%
Total End Uses	41.83	28.23	32.5%	27.02	4.3%

The ASHRAE recommended building envelope in the form of a curtain, Bay Scale Simulation 2, showed an annual total EUI of 161.11 kWh/m<sup>2</sup> (51.7 kBtu/ft<sup>2</sup>). This 78.5 kWh/m<sup>2</sup> (24.9 kBtu/ft<sup>2</sup>) differential represents a 32.5% savings from the existing Howe Center baseline.

The results of the Bay Scale Simulation 3, which featured the TACE system, showed a total annual EUI of 156.07 kWh/m<sup>2</sup> (49.47 kBtu/ft<sup>2</sup>). The EUI difference of 85.6 kWh/m<sup>2</sup> (27.13 kBtu/ft<sup>2</sup>) represents a 35.4% energy density reduction than as Shown in Bay Scale Simulation 1, and a reduction in EUI of 7 kWh/m<sup>2</sup> (2.23 kBtu/ft<sup>2</sup>) represents a 4.3% saving from the ASHRAE recommended enveloped as shown by Bay Scale Simulation 2.

Bay Scale Simulation 1, which used the Howe Center’s existing building envelope, as expected underperformed the both the ASHRAE recommended envelop in



Bay Scale Simulation 2, and the TACE system in Bay Scale Simulation 3. The enveloped assembly as it exists had limited ability to resist thermal transfer – it was constructed of highly conductive components with few if any insulating layers and thermal breaks.

Lighting and Plug Loads were modelled as consistent across all three Bay Scale simulations to isolate the envelope performance as measure by the performance of the HVAC system. These loads accounted for 70.6 kWh/m<sup>2</sup> (22.37 kBtu/ft<sup>2</sup>) of the total annual EUI. When isolating the EUI to HVAC, it is possible to see the impact more clearly for the EUI that was attributed to the building envelope – creating a clearer picture of comparison and efficacy.

As shown in Table 6.3, the results of the Bay Scale Simulations with the lighting and plug loads removed showed the larger and scaled impacts of the envelopes in comparison. The HVAC in Bay Scale Simulation 1 utilized 616.99 MJ/m<sup>2</sup> (29.34 kBtu/ft<sup>2</sup>), a 45.9% saving from the baseline as shown in Bay Scale Simulation 1. The TACE system simulation showed an annual HVAC consumption of 307.8 MJ/m<sup>2</sup> or 85.5 kWh/m<sup>2</sup> (27.1 kBtu/ft<sup>2</sup>), a 50.0% saving from the baseline simulation and a 7.6% reduction in consumption from the ASHRAE recommended curtain wall as shown in Bay Scale Simulation 2.

As shown in the breakdown of the component of energy usage as shown in Table 6.3, energy savings through the TACE system was accomplished through reductions of energy use of 16.7% in heating, 4.4% in cooling, 6.1% in fans, and 3.1% in pumps when compared to the ASHRAE curtain wall. It is important to note that Coolth was not applied in this system; the potential of Coolth to further reduce energy usage by using the TACE system is discussed in Section 6.4.3.1 and interpolated in Chapter 8.

#### 6.4.2.4 Energy Use Intensity Reduction Potential MVP Prototype I: Floor Zone Scale

---

The floor-scale building energy model simulations were run for the same comparative cases of building envelopes as described in Section 6.2.1.2. The Howe Center was used as a framework and Floor Zone Scale Simulation 1; the existing Howe Center was used to develop the baseline.

As in the Bay Scale Simulations, the Floor Zone Simulations energy models for case 1 and 2 were both simulated in OpenStudio, while Floor Zone Simulation 3, the

TACE system model, used the co-simulation methodology as described in Chapter 5 between EnergyPlus and the TACE FMU.

As in the Bay Scale Simulation results, the TACE system performed better than the other two Floor Zone Simulation cases. The energy use intensity results from each simulation are shown in Table 6.4.

**TABLE 6.4** MVP Prototype I EUI comparative simulation case results with TACE System contributing heating only for typical Floor Zone.

EUI Per Building Area - Floor					
CASE	[MJ/m <sup>2</sup> ]	[kWh/m <sup>2</sup> ]	[kBtu/ft <sup>2</sup> ]	Savings	
Existing Envelope	1275.7	354.3	112.3	0.0%	
ASHRAE CW	717.3	199.2	63.2	43.8%	
TACE System	676.8	188.0	59.6	46.9%	
Savings Comparison					
Case	Existing	ASHRAE	TACE	Difference [MJ]	Difference Savings
Existing Envelope	0.0%	-77.8%	-88.5%	0.0	0.0%
ASHRAE CW	43.8%	0.0%	-6.0%	558.4	43.8%
TACE System	46.9%	5.6%	0.0%	40.5	7.2%
HVAC Savings					
Case	[MJ/m <sup>2</sup> ]	Savings	Difference [MJ]	Difference Savings	[kBtu/ft <sup>2</sup> ]
Existing Envelope	1064.1	0.0%	0.0	0	93.7
ASHRAE CW	505.7	52.5%	558.4	52.5%	44.5
TACE System	465.2	56.3%	93.1	16.7%	41.0
End Use Comparison Typical Floor Zone					
End Uses	Existing (GJ)	ASHRAE (GJ)	Savings	TACE (GJ)	Savings/ASHRAE
Heating	286.4	116.5	59.3%	99.4	14.7%
Cooling	134.1	73.6	45.1%	68.8	6.6%
Fans	9.4	6.1	35.8%	5.7	6.3%
Pumps	80.3	42.8	46.7%	46.2	-8.0%
Heat Rejection	40.9	22.9	43.9%	20.9	9.0%
Total End Uses	660.8	371.5	43.8%	350.6	5.6%

The Floor Zone Simulation 1, the baseline case, shows an annual EUI of 1275.7 MJ/m<sup>2</sup> or 354.3 kWh/m<sup>2</sup> (112.33 kBtu/ft<sup>2</sup>). Lighting and power density accounted for 211.6 MJ/m<sup>2</sup> or 58.7 kWh/m<sup>2</sup> (18.6 kBtu/ft<sup>2</sup>) of the total energy usage. For Floor Zone Simulation when isolated for the energy used for HVAC the results show 1064.1 MJ/m<sup>2</sup> or 295.5 kWh/m<sup>2</sup> (936.99 kBtu/ft<sup>2</sup>).

The Floor Zone Simulation 2, which utilized the ASHRAE recommended curtain wall assembly showed a reduction in energy use by 43.8% from the baseline in Floor Zone Simulation 1 for an annual EUI of 717.3 MJ/m<sup>2</sup> or 199.2 kWh/m<sup>2</sup> (63.16 kBtu/ft<sup>2</sup>). When isolating the HVAC energy, the results showed a 52.5% reduction in HVAC energy use when compared to Floor Zone Simulation 1 for an annual EUI of 505.7 MJ/m<sup>2</sup> or 140.4 kWh/m<sup>2</sup> (44.52 kBtu/ft<sup>2</sup>).

In Floor Zone Simulation 3, the TACE system showed an annual energy use of 676.8 MJ/m<sup>2</sup> or 188.0 kWh/m<sup>2</sup> (59.59 kBtu/ft<sup>2</sup>) for a reduction in energy over the baseline of 46.9% and when isolating the HVAC energy consumption, 56.3% savings in HVAC energy consumption using 465.2 MJ/m<sup>2</sup> or 129.2 kWh/m<sup>2</sup> (40.963 kBtu/ft<sup>2</sup>). These quantities resulted in a 5.65% reduction in total annual EUI% from Floor Zone Simulation 2 and only reduction of 8 % in HVAC load.

In more detail, the Floor Zone Simulation 3 showed a reduced heating energy consumption of 14.7% from Floor Zone Simulation 2, as well as reduced energy consumption for cooling energy of 6.6% and heat rejection of 9.0%.

The TACE system reduced CO<sub>2</sub> emissions by 453 metric tons per year when compared to the existing envelope and 21.5 metric tons when compared to the ASHRAE curtain wall envelope. Water usage for heat rejection in the cooling tower was reduced by 3,570,302 litres (943,174 gallons) with the TACE system, compared to an ASHRAE recommended curtain wall envelope. These metrics are reviewed in more detail in Chapter 8.

### 6.4.3 Results using ASI Prototype III

---

The following comparative results as shown in Figure 6.31 for ASI Prototype III were generated using the Modelica model and the same co-simulation frameworks developed for MVP Prototype I. The dimensions in the model were updated to Prototype III and the following simulations were re-run. As a reference check on expected performance, two additional weather files were added to the Modelica model, Phoenix, Arizona and Amsterdam, the Netherlands. The summarized results are shown in Figures 6.32-6.37.

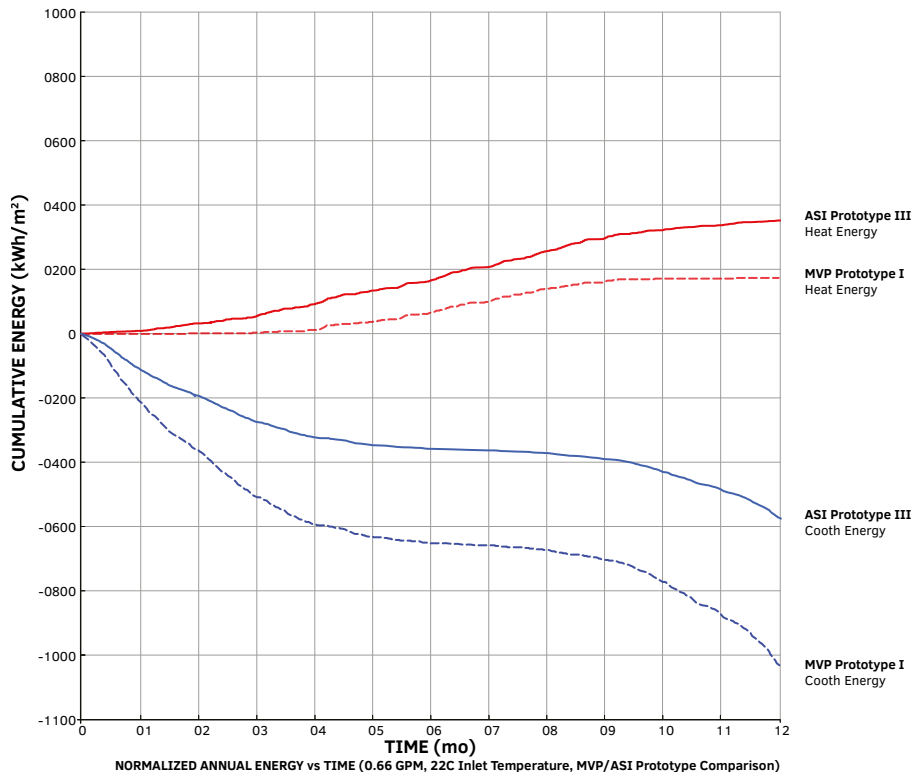


**FIG. 6.31** Normalized cumulative energy comparison for MVP Prototype I and ASI Prototype III showing MVP Prototype I outperforming ASI Prototype III in coolth, where ASI Prototype III outperforms MVP Prototype I in heating.

### 6.4.3.1 Results of TACE 12 Module Array Simulations Comparison

The two primary points of comparison for the simulations were: 1) to compare heating and cooling potential of the TACE system array between MVP Prototype I and ASI Prototype III, and 2) to assess the possible impact that the TACE system may have on building Energy Use Intensity (EUI). The comparison as shown in Figures 6.32-6.37 was made between TACE modules I and III and applied to three climates: 1) New York, NY, 2) Amsterdam, Netherlands, and 3) Phoenix, AZ. In each of the climate locations: two working fluid flow rates, 2.50 l/min (0.66 gpm) and 0.62 l/min (0.165 gpm), were simulated; and two heat transfer working fluid inlet temperatures, 22° C (71.6° F) and local ground temperature, were simulated, creating 24 quantities for comparison. Each simulation provides results as total heat or coolth

energy from the TACE array, and those results were normalized to the surface area of the building envelope and provide the total normalized heating and cooling energy (kWh/m<sup>2</sup> yr) for the system.

### New York (40.7° Collector Inclination Angle)

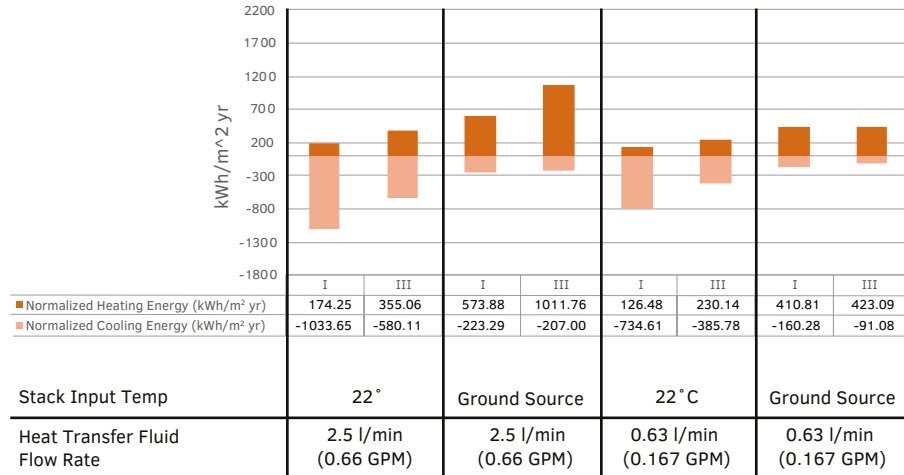


FIG. 6.32 Normalized thermal energy comparison for New York climate (40.7° Collector Inclination Angle). MVP Prototype I outperforms ASI Prototype III in coolth, where ASI Prototype III outperforms MVP Prototype I in heating.

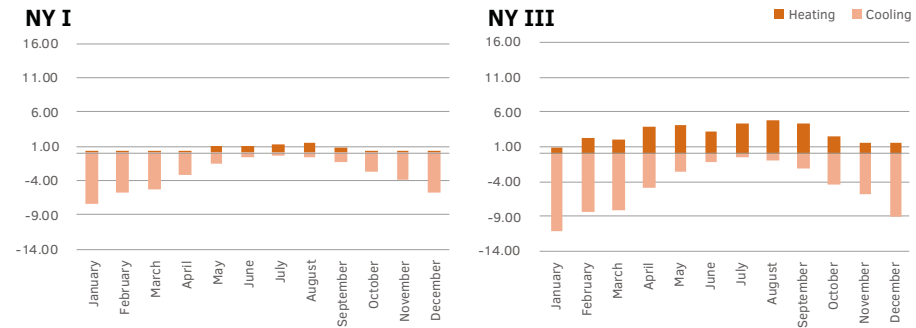


FIG. 6.33 Average monthly fluid temperature rise per stack using 22°C inlet temperature and 0.63 l/min flow rate for NY. ASI Prototype III outperforms MVP Prototype I in both average high and low temperatures.

## Netherlands (50.2° Collector Inclination Angle)

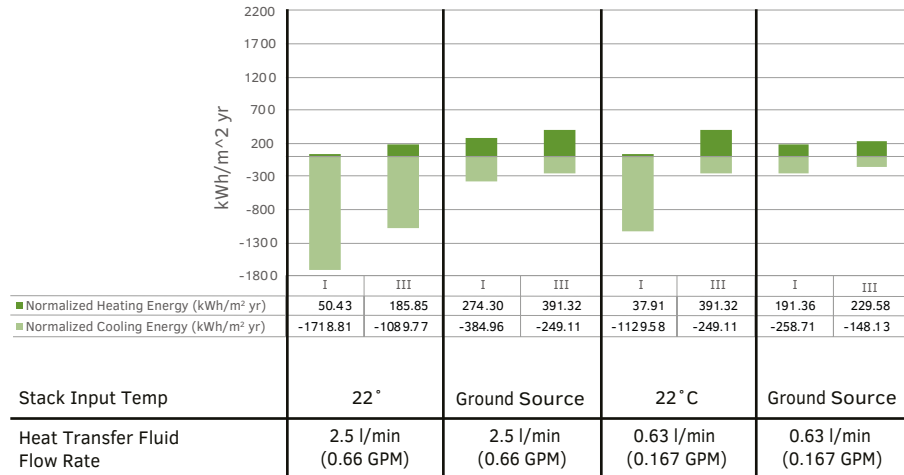


FIG. 6.34 Normalized thermal energy comparison for the Netherlands climate (50.2° Collector Inclination Angle). MVP Prototype I outperforms ASI Prototype III in coolth, where ASI Prototype III outperforms MVP Prototype I in heating

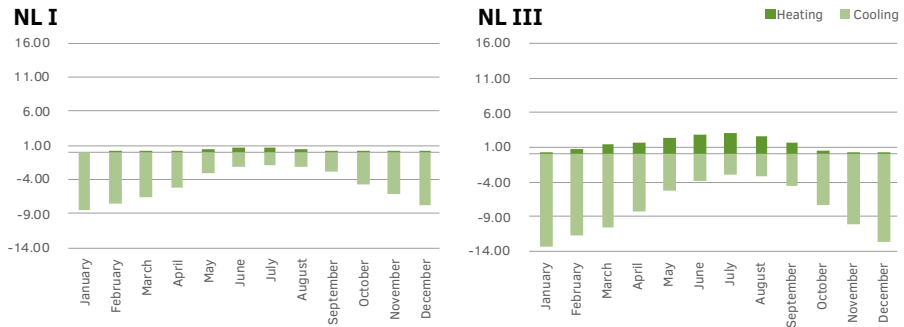
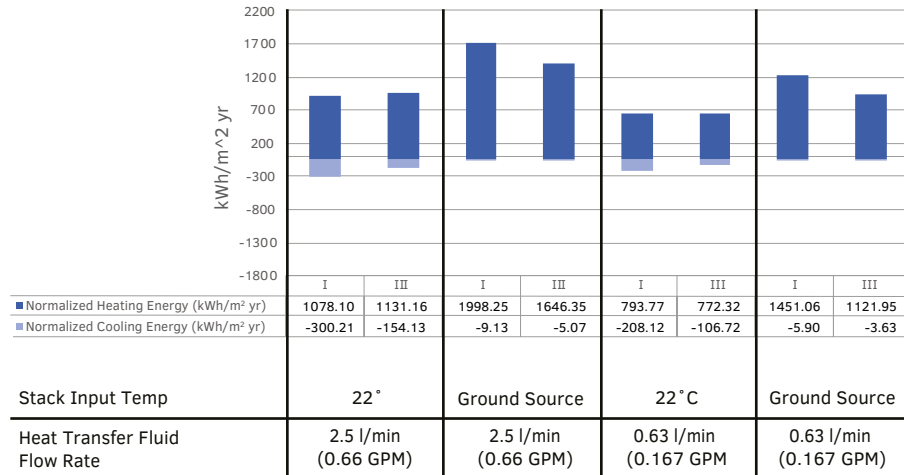
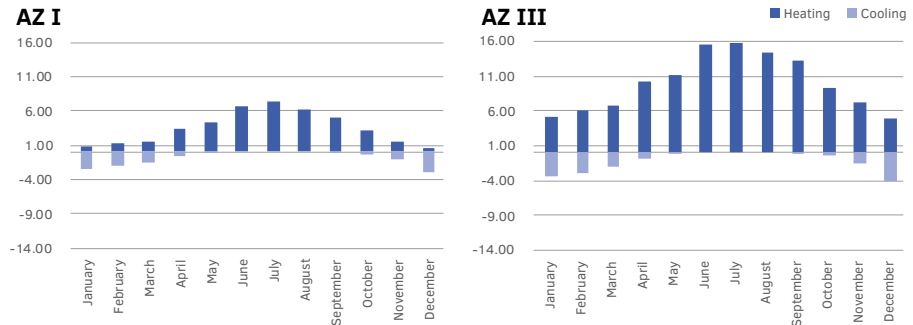


FIG. 6.35 Average monthly fluid temperature rise per stack using 22 °C inlet temperature and 0.63 l/min flow rate for NL. ASI Prototype III outperforms MVP Prototype I in both average high and low temperatures.

## Phoenix (33.4° Collector Inclination Angle)



**FIG. 6.36** Normalized thermal energy comparison for Phoenix climate (33.4° Collector Inclination Angle). MVP Prototype I outperforms ASI Prototype III in coolth. ASI Prototype III outperforms MVP Prototype I in heating in only 22°C inlet temperature and 0.66 gpm, in all other cases I outperforms III.



**FIG. 6.37** Average monthly fluid temperature rise per stack using 22 °C inlet temperature and 0.63 l/min flow rate for Phoenix. ASI Prototype III outperforms MVP Prototype I in both average high and low temperatures.

The results show there was significant improvement in normalized heating energy from prototypes I to III for all conditions in New York and the Netherlands with the greatest improvement (1032%) seen in the Netherlands with a flow rate of 0.625 l/min (0.165 gpm) and using an inlet temperature of 22° C (71.6° F). There was also a consistent reduction in normalized cooling energy for the same cases, creating a more balanced result between heating and cooling for III than I. Results from Phoenix, however, showed a small reduction in both normalized heating energy and cooling energy when comparing I and III TACE arrays. The improvements in New York and the Netherlands are likely attributable to a reduction in fluid volume between I and III, moving from the module fluid chamber to embedded heat transfer pipes, respectively. The consistent reduction in normalized cooling energy was likely attributable to the elimination of heat transfer fluid in contact with the shaded surface of the façade. Heat transfer fluid in I was in direct contact with a shaded surface, increasing cooling potential by offloading heat. Heat transfer fluid in III was limited to the embedded piping in the collector surface.

The simulations of the arrays are valuable to compare to one another in relative performance only. The input and output temperatures of these simulations are unrelated to how the TACE system would work as an integrated building system. To understand the performance as an integrated system, a whole building energy model using Prototype III would need to simulate the differences in EUI between the two prototypes and geographies. In Chapter 8, a direct comparison was made between the results of the stacks of Prototypes I and III and extrapolated to indicate the performance differences.

## 6.5 Summary: Architectural Integration Impacts of HVAC Retrofit Scenarios with TACE

---

The impact of architectural integration can be considered in two ways: 1) the localized impact of deploying the TACE system components at the building envelope; 2) the impact of how and what building systems are integrated with the TACE system as a whole building system strategy and specifically as a system design.



Due to the limitation of temperature ranges when comparing the TACE to conventionally HVAC working fluid temperatures, there was a relative localized impact of integrating the TACE system, especially when using the data from MVP Prototype I. When decoupled, the essential components of the full TACE system outside of the envelope components, and the ones required for energy storage and any possible integration are not significant. Based on the dimensional analysis as shown in Figure 6.38, the required volume per bay for these components should fit within  $0.1 \text{ m}^2$  ( $3.5 \text{ ft}^2$ ) per linear  $0.3 \text{ m}$  ( $1 \text{ ft}$ ) of façade, which accounts for the approximate space available to integrate the system components. Depending on the system configuration, the components take up 50% of the available space in a typical curtain wall as visualized in Figure 6.38. These components could be arranged with the spandrel section from below or adjacent to the fenestration height. The architectural integration and the impacts are studied in greater depth in Chapter 7.

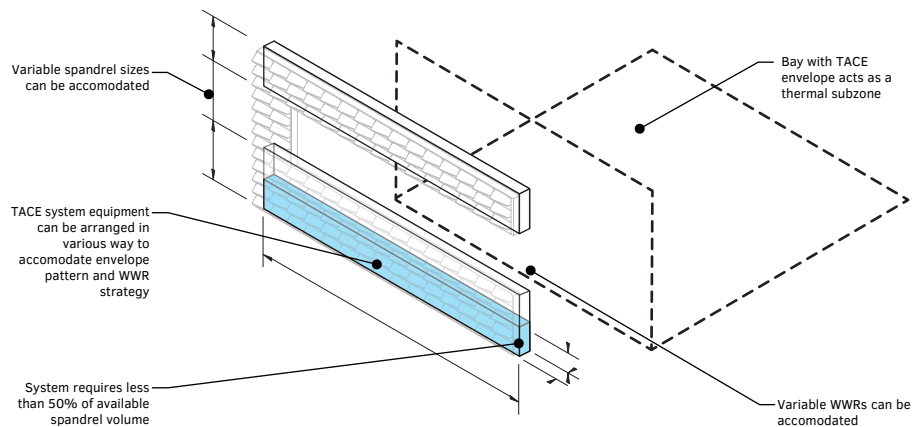


**FIG. 6.38** Volume identified required to house the integrated system components.

The impacts on whole building mechanical system are focused on: 1) reduction in size of primary mechanical system heating and cooling in the decoupled scenario explores in Chapter 4; 2) integration of a fluid-based system, such as a geo-exchange heat pump as the primary building heating and cooling system integrated with the TACE system, which is discussed in depth in Chapter 7.

Based on the reduction in EUI due to the TACE system and the decoupling of the TACE system and the primary mechanical heating and cooling system, resulted in a reduction in equipment sizes of almost 15% in heating equipment and almost 7% in cooling equipment rated sizes for MVP Prototype I. For ASI Prototype III, based on percentage differences only for the stack comparison at  $22^\circ \text{ C}$  ( $71.6^\circ \text{ F}$ ) inlet temperature, a reduction in heating equipment of 30% and a 3.5% in cooling

equipment rated sizes for the New York climate could be extrapolated. While equipment sizes for primary mechanical heating and cooling will significantly vary from manufacturer and equipment type, the specification of which for both is outside of this research, based on the EUI it was reasonable to estimate a reduction in central and terminal equipment units. This potential reduction is discussed in more detail in Chapter 8.

## References

- ASHRAE. (2013). ASHRAE/IES Standard 90.1-2013 Energy Standard for Buildings Except Low-Rise Residential Buildings.
- Kelly W., Vollen, J., & Dyson, A. (2012). Re-Framing Architecture for Emerging Ecological and Computational Design Trends for the Built Ecology Association for Computer-Aided Design in Architecture (pp. 251-258). ACADIA. San Fransisco, California.
- Marshall, G. (2016). Evaluating low-temperature water-heating options. Retrieved from <https://www.csemag.com/articles/evaluating-low-temperature-water-heating-options/>
- New York State Pollution Prevention Institute (NYSP2I). (2017). Performance Evaluation of EcoCeramics Active Thermal Building Envelope System. Research Report. Green Technology Accelerator Center (GTAC), Rochester Institute of Technology.
- Nouidui, T., Wetter, M., & Zuo, W. (2014). Functional mock-up unit for co-simulation import in EnergyPlus. *Journal of Building Performance Simulation*, 7(3), 192-202.
- OpenStudio. (2014). Retrieved from <https://www.energy.gov/eere/buildings/downloads/openstudio-0>



# 7 Design Iterations

---

One of the critical aspects of deploying a new building system is the often fractured nature of the multiple stakeholders within the decision-making process to adopt or deploy the system. The architects, engineers and speciality consultants, the owners and project managers, and the contractors and installers all have a stake in the outcome of any project, but each has different criteria, especially when integrating a new building system. In an architectural construct energy effectiveness is a criterion in the system development process that must be tested against other design drivers: availability of materials; manufacturability of components; ease of installation; maintenance, etc., In order to assess the potential of the TACE system it was critical to investigate the other criteria that could affect system performance in building integrated conditions.

Thus, while this dissertation is not focused on the commercialization or deployment of the TACE system, understanding how the performance of the system and the roadmap towards a realistic instance of a viable commercial product was critical to evaluating its viability to perform under real world conditions. Therefore, it was necessary to understand the possible limits of the forming methodology of the components, the module design, and the method of assembly, the method of installation, and how maintenance of the system may affect the design instantiations.

## 7.1 Introduction

---

In Chapter 6, we discussed the thermal energy potential and systems configuration options. Acknowledging the performance criteria developed in Chapter 6, Chapter 7 explores design limitations on both the module and the assembly. The objective of the design iterations was threefold: to explore the potential of different forming techniques for the TACE components; to understand the morphological limits of module design based on the forming techniques; to understand the potential methods of system assembly using the optimal module design.

In order to meet these objectives, the following research question needs to be answered:

**What are the potential design limitations for the Thermal Adaptive Ceramic Envelope system?**

In order to answer this question, the following sub questions are investigated in this Chapter:

- What are the possible forming techniques of the Thermal Adaptive Ceramic Envelope components, and how would these forming techniques affect the component design?
- What are the design limitations for the Thermal Adaptive Ceramic Envelope module based on the forming techniques and method of assembly?
- What are the potential envelope system configurations to assemble the Thermal Adaptive Ceramic Envelope system?

## 7.2 Methodology

---

The methodology for developing design iterations follows a quasi-experimental method of looking at ranges of the quantitative potential of optimal architectural integration scenarios. The quasi-experimental design method employed in this chapter uses three primary approaches: empirical design investigations resembling the underlying impacts of interventions on non-random circumstances; critical variable identification based on limitations; design based pre-testing to

identify potential system behaviors to advise the future design development and experimental design of the system (Shadish, Cook, & Campbell, 2002).

Within this methodology framework, typical contemporary and future potential fabrication processes were explored to catalogue the distinct and limiting characteristics of each process. Maximum material, fabrication and installations limits were catalogued within ranges, and taxonomy of potential morphologies was developed as a means to refine the TACE components. These options were explored as three investigations to look for combinations that met performance and buildability criteria.

### A Fabrication Process and Morphology Exercise

Multiple fabrication processes for the ceramic components were explored to frame the potential of development for the TACE systems, including current and developing techniques.

### A Construction Typology Exercise

Building envelope typologies were explored to capture a range of contemporary assembly and installation techniques, specifically for unit masonry type, window wall type, rainscreen type, curtain wall types as both stick-built and unitized assembly subtypes.

### A Design Integration Exercise

Finally, systems were matched with assemblies and components to understand potential architecture integration potential of the TACE systems in New and Retrofit scenarios.

## 7.3 **Critical System Design Drivers**

---

The TACE component assembly, as discussed in Chapter 3, consists of a collecting surface, a thermal transfer component, a working fluid, and an insulation layer. The TACE system beyond the TACE components includes the heating loop, cooling loop, pumps, controllers, heat exchangers, thermal storage components, and the radiant

cooling and heating surfaces, as shown in Figure 7.1. These components each have critical roles to play in the performance and integration potential of the TACE system. The critical design drivers for the development of the TACE system were governed by:

- Manufacturing method which regulates the total build size and weight of the component;
- Size limitations of each manufacturing method to produce components that promote energy exchange;
- Assembly methods that promote efficient energy exchange at scale and support architecture and systems integration.

It was critical to understand that these design drivers were only the major categories: the variables were myriad and each contributed limiting factors to the decision making for the development of the system as delineated in Chapter 6. The relative value of each design driver is discussed throughout this Chapter.

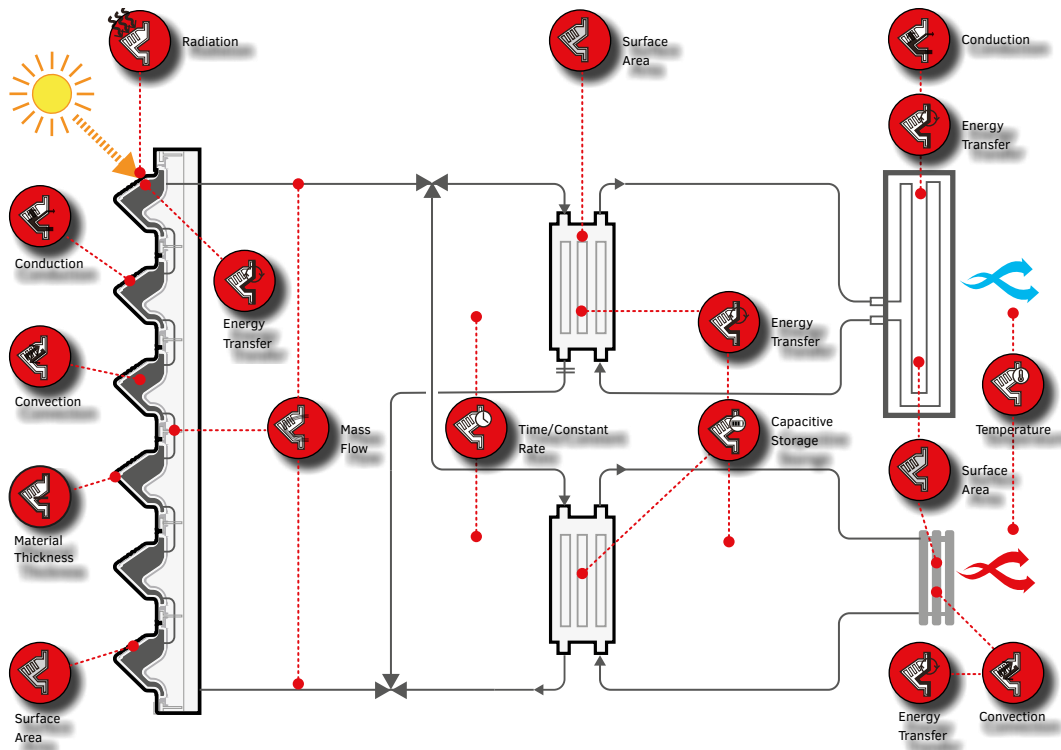


FIG. 7.1 Critical drivers as part of the TACE module and system.

### 7.3.1 TACE System Service Area

The driving variables that impact the TACE System Service Area were the exterior collecting surface, the associated system configuration that can be reasonably and economically integrated as part of the envelope assembly, and the installation of the envelope on the construction site. Based on the system configuration discussed in Chapter 4, where the TACE system was decoupled physically from the base building HVAC system, the focus for the implementation of the system was on the development of the method of assembly and construction for the building envelope and discussed in terms of appropriate thermal zones that would support the performance integration with a heating and cooling system.



The System Service Area (SSA) as shown in Figure 7.2 for this research, was defined as the area that includes the length of façade per bay, as determined by column spacing width, and the floor area serviced by the thermal exchange combined with the Heating and Cooling (HC) system boundaries that service the floor area of the bay. This floor area was delineated by the area between the two exterior columns and the core or two inner columns; essentially one structural bay. This area limits system integration potential. Multiple SSAs may make up the typical thermal zone. The thermal zone was serviced by the HC and multiple TACE bay scale systems deployments.

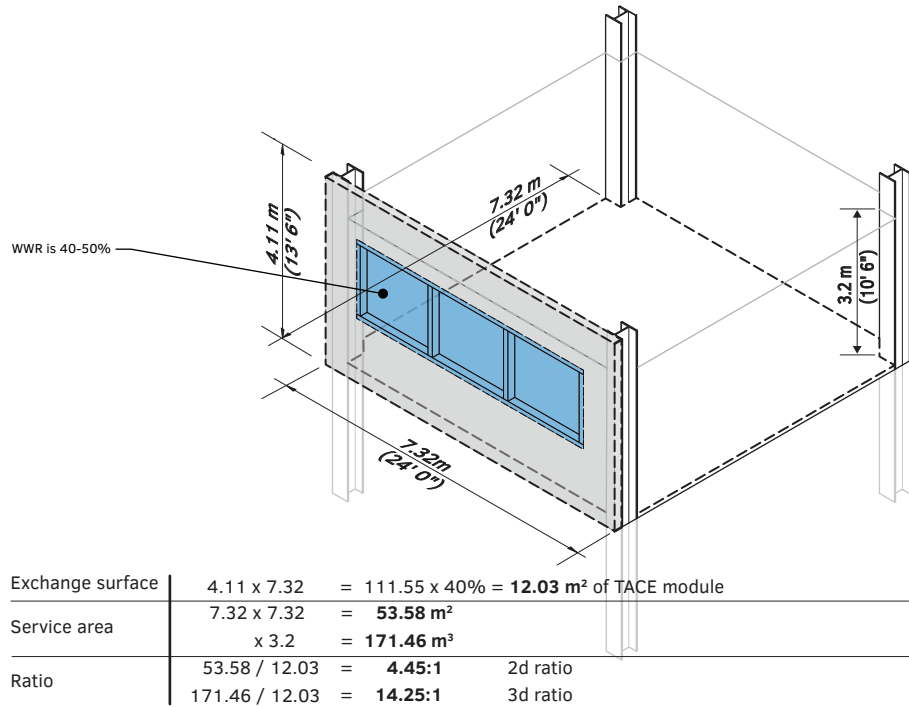


FIG. 7.2 Diagram of typical bay showing surface area to volume ratio.

### 7.3.1.1 Minimum TACE Service Area

To determine the minimum TACE SSA, it is appropriate to discuss the determination of the ideal thermal zone. The thermal zone in an office building is based on four factors: 1) Climate and Weather Factors; 2) Building Envelope Design; 3) Internal

Demands; 4) Space Programming and Layout (Haglund, 2014). To limit this study, the Howe Center was used as the model for a typical office layout. As shown in Figure 6.4 the core of the Howe Center is located on the north side of the building leaving one core zone and two small zones on the northeast and northwest of the floorplate (subsumed in this part as East and West zones). The remaining and primary zones were East, West and South.

This thermal zoning is typical and based on column grids that create the bay subzones. The Howe Center is based on a lease span of 8.23 m (27 ft) and column space of 5.84 m (19.2 ft) resulting in a bay subzone of 48 m<sup>2</sup> (517 ft<sup>2</sup>). This is smaller than the typical modern office floorplate layout that would have a lease span ranging from 9.15-13.72 m (30-45 ft) and an ideal column spacing of 9.15-13.72 m (30-45 ft), with typical bay subzone area ranging from 83.61-188.13 m<sup>2</sup> (900-2025 ft<sup>2</sup>), though typically remaining on the lower end of the range for modern office buildings (CROSBY et al., 2008). Three issues allow the Howe Center Bay Zone size to be relevant for study: 1) the program of open office space was the new standard for the majority of Class A office space, making the traditional thermal zoning less relevant and modern thermal zoning more fluid; 2) the Howe Center bay size is typical of midcentury office building layouts in both steel and concrete construction and thus provides a model for retrofit scenarios; 3) the rise in mass timber framing for office construction will privilege smaller bay size to limit the depth of the structural members.

### 7.3.1.2 Exterior Surface Area

---

The exterior surface area of the MVP Prototype I, as described in Chapter 4, was indicative of the surface of the typology. This surface, termed the Thermal Collecting Surface (TCS), was designed to maximize exposure from external thermal resources, derived from an insolation exposure (Winn, 2014). There was an ostensibly parametric relationship to the power output potential of the TACE system of the surface area exposed to insolation, and the surface area of the transfer component, along with the thermal capacity and flowrate of the working fluid.

This chapter assumes the basic ratio of performance of potential power output of 19.8 m<sup>2</sup> (213.5 ft<sup>2</sup>) Exterior to 174.25 kWh/m<sup>2</sup>/yr (22° C inlet temperature and 2.5 l/min flowrate) output as modelled in Chapter 5 and 6 as results of the MVP Prototype I testing. The refinement of the design based on the architecture integration was as stated above to optimize for the method of manufacture, assembly and installation of the TACE system that would maximize the exterior surface area ratio within this

context, thus improving the potential power output of the system and integrating into the building systems matrix as the building envelope. Further, while the focus of this research was not on the offloading of excess thermal load from the interior, the same original reasoning perseveres; increased surface area on the exterior will enhance the ability of the TACE system to act as conduit to the exterior as a heat sink that uses local external environment to offload excess thermal loads in the building – providing coolth for thermal comfort.

As shown in Figure 7.3 the exterior surface area can be defined as the collecting area ratio on multiple scales: the total vertical surface (TVS) area of the system service area (SSA), the total thermal transfer surface area (TTSA) of the total vertical surface area, and the collecting surface area per square meter of TACE components. In envelope adjacent to a habitable program, the Window Wall Ratio (WWR) was a critical driver for the surface area ratios and ultimate real-world performance that impacts both occupants and system efficacy.

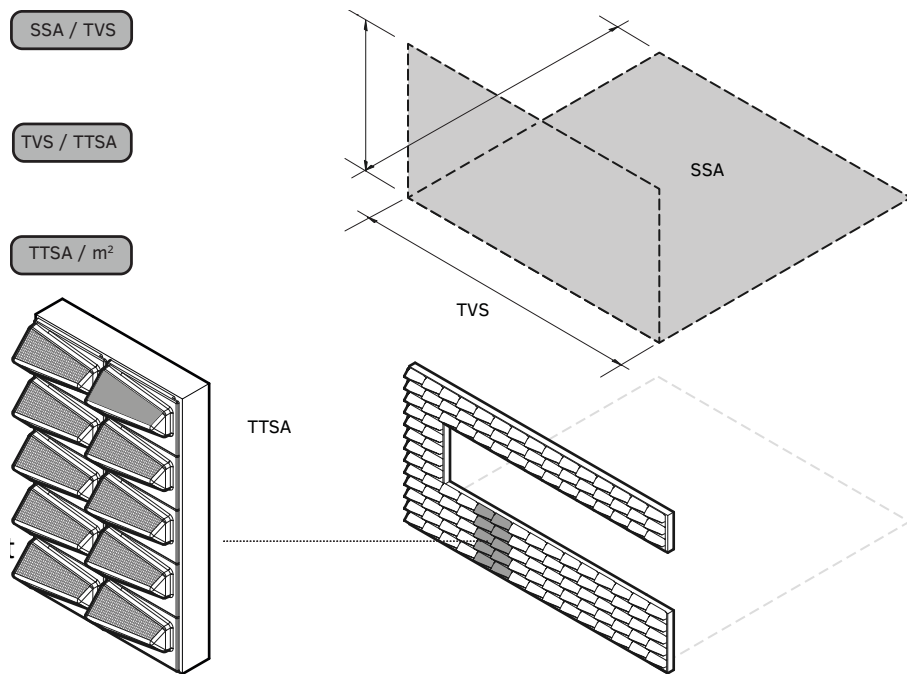


**FIG. 7.3** Surface areas at multiple scales showing the proportion of actual collection surface to total façade surface to the service area.

### 7.3.1.3 Window Wall Ratios

---

In a typical new construction or façade repositioning project, the development of the optimal WWR understood as the Effective Aperture (EA), is well established. The EA is derived from a combination of the WWR and Visible Transmission (VT) and on whole results in the Penetration Depth (PD) for daylight in the bay scale subzones (O'Conner, et al., 1997). The PD is related to the height of the window in the VT. Removing any obstruction factors (i.e., trees, adjacent buildings, etc.), one can calculate the WWR for the typical bay by taking the window area and removing all building related obstructions (i.e., mullions, floor structure, superstructure, etc.) to get the initial WWR ratio. The EA is calculated as WWR multiplied by the VT (Selkowitz, 2013).

In modern office building design, it is critical to take into account the factors of daylight sensing lighting and automatic shading systems. Both of which manage the use of natural light and control glare and have been used to increase the WWR percentage in office buildings. The drive to increase the WWR percentage emanates from the notion that more glass has been historically, if not colloquially, thought to be more attractive to tenants of developer led building projects who hold a long held belief that more glass brings a higher lease price, often at the expense of energy efficiency.

When the envelope system is a countercurrent heat exchanger, however, developing the optimal WWR and EA, must take into account the balance of market pressures, thermal management and TACE system efficiency. When factoring in need to maximize an opaque surface on the building envelope to improve the overall energy effectiveness of the building system matrix, a narrower range of effective WWR ratios can be developed. Further, because the TACE system has physical constraints (e.g., maximum component sizes, the weight of units, the orientation of surfaces, etc.), the optimal arrangement of the morphology of the fenestration of the WWR should be optimized according to the matrix of variables. The design balance was explored in Section 7.6.1 of this chapter and discussed in Chapter 8.

A limiting range that balances performance and market forces for the WWR can thus be described for both new constructions and serve as a goal for deep energy retrofits with building envelope replacements. In these situations, the efficiency of the building structural system, the PD, the height of the window, WWR and EA and thermal bay subzone and thermal zone were looked at to provide a balance of performance and integration potential in order to delineate the next steps in systems development towards a real world building integrated prototype. In modern office design, access to quality, glare free, daylight, viewsheds and thermal comfort were

as equal stakeholders to energy management – and together they drive the decision trade offer with WWR, productivity enhancements, and project costs.

The optimal WWR was thus targeted at 40%, with a PD to 9.15 m (30 ft), with a lease depth of 9.15-13.72 m (30-45 ft), and a lease span from 7.32 or 9.15 m (24 or 30 ft). The restriction 7.32 or 9.15 m (24 or 30 ft) was based on best practices of contemporary open office layout modules that utilize a standardized 1.52 and 1.83 m (5 and 6 ft) modular furniture module and aligned with most historic and modern steel structure office build structural bay dimensions. (Ko, et al., 2008; Goia, 2016).

Alternatively, one possible delineation was to see if the TACE system can provide enough energy benefits to increase the WWR allowing for more daylight penetration and viewshed aperture while keeping the energy expenditure the same as measured by the overall EUI as shown in Figure 7.4.

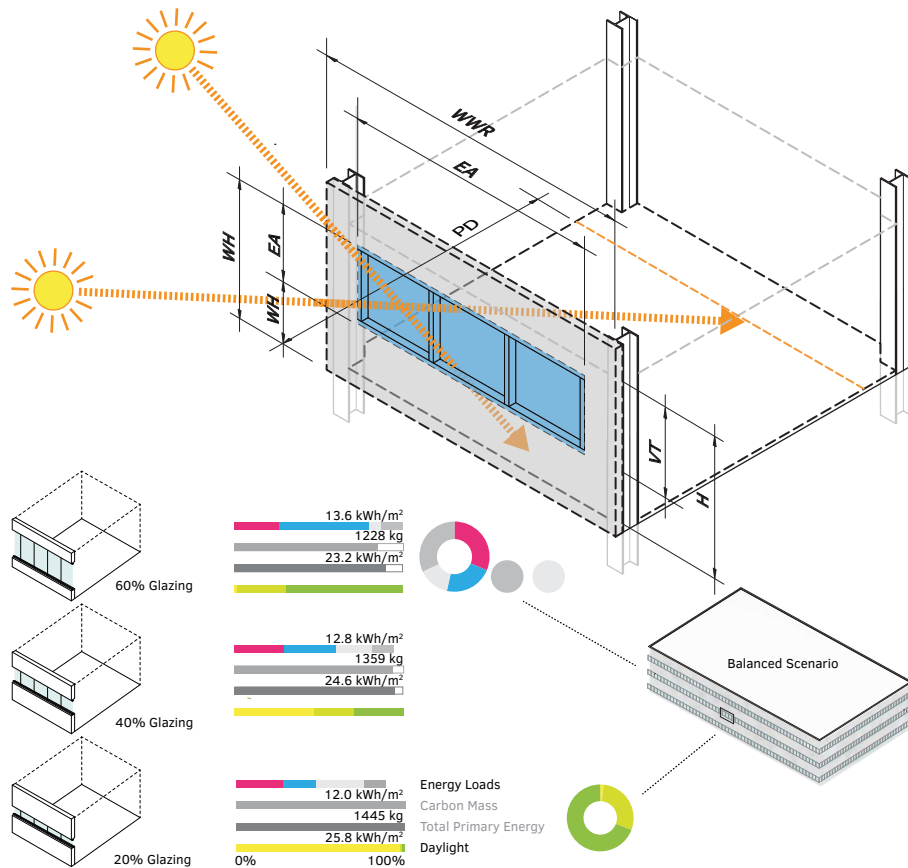


**FIG. 7.4** Relationships of critical metrics of the façade design and energy impacts. Multiple scenarios can privilege most energy reduction to no loss in energy efficiency while increasing daylight and access to viewsheds.

### 7.3.2 Fabrication Techniques

The Fabrication techniques of architectural ceramics have remained relatively un-evolved for centuries. Hand packed bricks can easily be traced back to early Mesopotamian culture and mould making, pressing and casting were highly developed techniques in ancient Roman and Greek cultures. The development of modern architectural ceramics has mostly been dependent on the development of two critical aspects: the advent of material science as a distinct discipline in the

20<sup>th</sup> century and the refining of the clay body recipe and modernized production techniques of forming and firing the clay into a purposeful ceramic object. Both of these aspects directly affect the size and performance limitations and directly correlate to how one assembles the modern ceramic envelope and what the assembled performance would be (“A Brief History of Ceramics and Glass,” 1990).

This section of the investigation looks at the ceramic components fabrication techniques in terms of the optimal exterior surface area as defined in Section 7.3.1.2 of the system alongside the ability of that fabrication technique to integrate the TACE System into the architectural envelope assembly. Ultimately, for each fabrication technique and assembly method, there was a combination that optimizes TACE performance based on a decision-making framework that includes both integration and market-based criteria (i.e., increased glazing percentage of a higher WWR, optimized fenestration morphology, etc.)

The focus of comparison was on dimension potential and stability and overall manufacturing, fabrication and assembly and installation throughput. Current and next generation fabrication techniques were noted with a focus on the design limiting factors of two primary criteria: the capacity of the fabrication technique (i.e., throughput of units per annum, dimension and weight limitations) and the potential limits of the assembly and installation methods (i.e., two vs four hand object limitations, stick built vs factory prefabrication limitations, etc.).

Hand assembled objects are, for all intents and purposes, limited in the US by the National Institute for Occupational Safety and Health (NIOSH) mathematical model for Recommended Weight Limit (RWL). While multiple variables determine the limitations of what a healthy worker may safely lift for a sustained period of time (i.e., an 8 hour work shift)(Waters, et al., 1994). Using these equations, we can safely target the weight limit of objects for hand assembly to 22.68 kg (50 lb) for a two hand and 45.36 kg (100 lb) for a four hand object, both in the factory and on the construction site. As a note of comparison, a 20 x 30 x 40 cm (8 x 12 x 16 in) common two core Concrete Masonry Unit (CMU) weighs 23.59 kg (52 lbs) per unit, effectively the limit for a two hand construction object.

Therefore, depending on the type of assembly, unit masonry, stick built rainscreen or unitized curtain wall, it may be more or less advantageous to use different forming techniques shown in the manufacturing process cladogram in Figure 7.5 to match to the different assembly techniques. The following sections further discuss the potential and limitations of matching the forming technique to the appropriate assembly technique to investigate which combination yields the most effective performance.

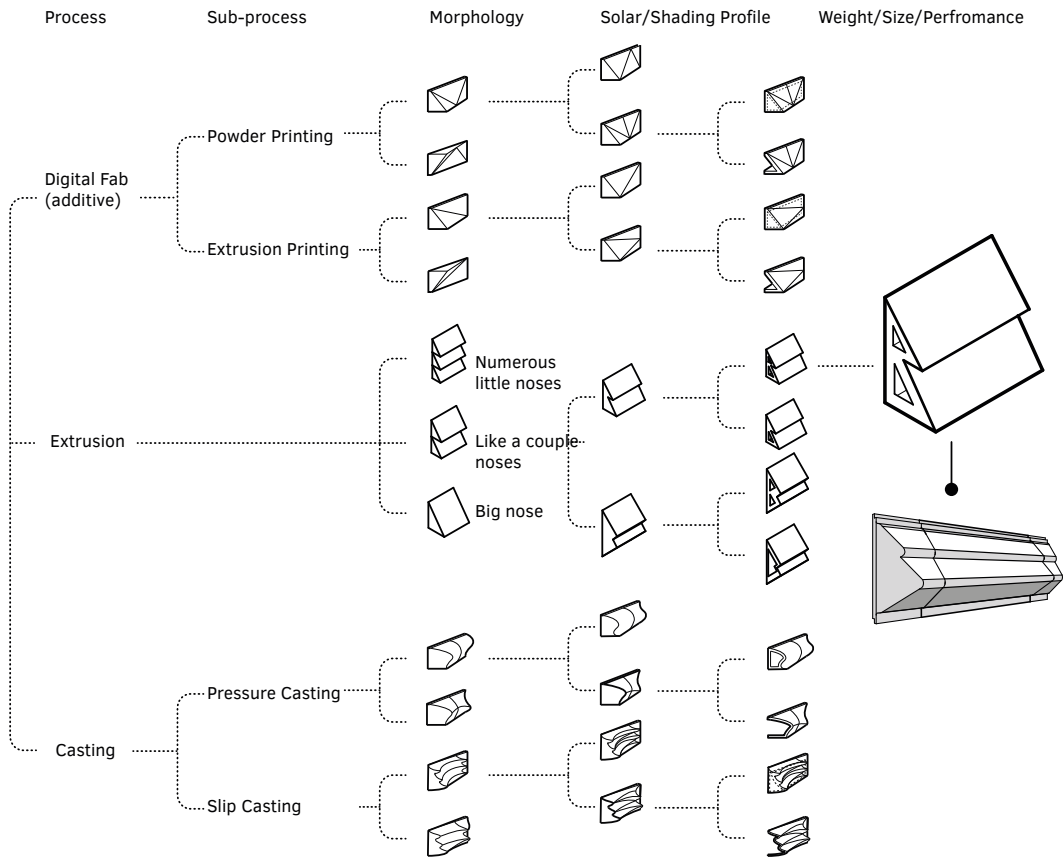


FIG. 7.5 Taxonomy of shape logics based on manufacturing methods.

### 7.3.2.1 Current Fabrication Techniques

While the modern fabrication techniques of Pressing, Casting and Extruding have been used relatively unchanged for centuries, the industrial revolution and the modernization of production processes have provided avenues for architectural ceramics to proliferate and recently enter the foray of contemporary architecture as a distinctive and plastic material. The specific manufacturing technique primarily limits the morphology, precision of the product, and the speed of production. The TACE system has the potential to take advantage of the plasticity of the material. As a set of related performance variables, it was possible to develop the TACE components using any of the modern forming techniques. Each



fabrication technique, having its own design limitations, would ultimately form the TACE into different morphologies that have relative performance and assembly potentials – resulting in a lexicon of the total morphological guidelines of the TACE system components and ultimately a recommendation for how to fabricate components now as well as frame a roadmap for future development into emerging fabrication processes.

#### 7.3.2.1.1 Pressing

---

The earliest and likely the first technique for clay forming was pressing the clay together between the fingers first to make figurines and pinch pots. Mass produced pressed ceramics date back thousands of years, having developed in Asia, South America, and the Mediterranean cultures, for example, independently. The earliest examples can be traced to 24,000 BC, using the pinching technique and the use of moulds for forming ceramics can be traced back to 10,000 BC. Now heavily engineered, the basic principles still apply, and the modern process for ceramic pressing is based on the development of the RAM press, called RAM casting. In this process, the raw clay body is pressed in between two dies, known anachronistically as a female and male die. A typically industrial production RAM press is rated between 18.5 to 272.2 t (200 to 300 tn), depending on the bed size, translates to 0.69 to 3.45 MPa (100 to 500 psi) depending on the bed or mould size. This high working pressure assures that the clay is evenly distributed, with excess water and air forced out of the mould/die/clay assembly. Developed in the 1940's the industrial RAM process of today remains mostly unchanged. The reinforced plaster dies are cast into metal restraining rings. The plaster is porous to absorb water and includes a pressurized air breather tube cast into the die to aid the quick release of the clay piece once pressed and the drying of the mould between pressing. Dies typically have a lifespan between 1000 and 5000 repetitions, most averaging around 2500 uses. The RAM process can press up to 6 pieces per minute as part of an industrial workflow. (Pelleriti, 1998)

The benefit of the components that were manufactured using the RAM press process was that the compression compacts the clay particles evenly strengthening the finished ceramic component by producing a denser clay body and ultimately a more robust finished ceramic piece. The limitations of RAM pressing were in the amount of direct labour required and limitation on production speed that limits throughput.

POC Prototype II used RAM pressing as the manufacturing method, visualized in Figure 7.6.

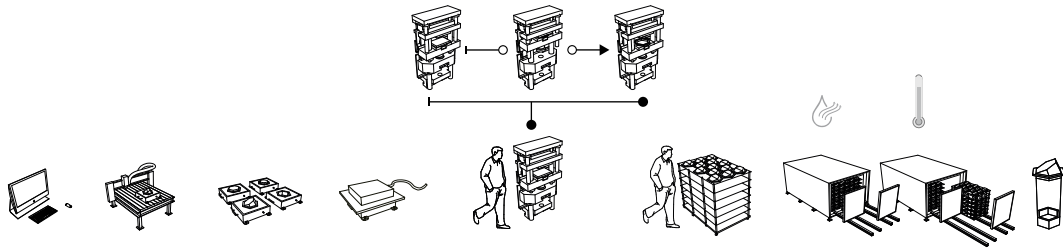


FIG. 7.6 Process diagram of RAM pressing manufacturing steps.

The following limitations on pressing ceramics show a range which is governed by many factors. The intention here was to provide a comparison to other fabrication types.

### Limitations of the Ram press process

- Size limitation: typical maximum 45.7 x 76.2 x 20.3 (18 x 30 x 8 in)
- Weight limitation: 45.36 to 68.04 (100 to 150 lbs) fired
- Throughput limitation: 50-100 pieces per day
- Status as architectural ceramics: currently used for restorative work

While there are emerging and alternative pressing technologies such as Ceramic Powder Compaction, these techniques are currently used primarily for flat tiles (i.e., flooring) and speciality precision ceramic components in the medical and aerospace industry and were not targeted for components for the building envelope at this time. Therefore, Ceramic Powder Compaction and other similar and relatively emerging pressing techniques were not discussed in this dissertation at length. Notwithstanding, future work could involve the investigation of Ceramic Powder Compaction as a possible forming technique.

#### 7.3.2.1.2 Casting

Slip-Casting, in its modern form, was developed in the mid 18<sup>th</sup> century in Europe, with industrialization occurring in the mid 18<sup>th</sup> century. The process uses a clay slurry cast into a porous mould where the water is wicked away from the component through capillary action of the model materials, typically some derivative of Plaster of Paris (and similar in most regards to the mould material used for RAM press moulds), consolidating the clay particles at the exterior of the component where it is

adjacent to the form. The advantages of slip-casting are the uniform consolidation of particles without excessive pressure (which can stretch clay particles away from the centre of the mould) and the ability, assuming (as in press moulding) a draft angle of fewer than 90 degrees, can have a significantly higher degree of detail compared to pressing. It is possible to slip both plastic and non-plastic clay slips (Adams, 1971). Slip casting is primarily used to create dinnerware, and prior to Pressure Casting was the primary manufacturing technique sanitaryware.

Ceramic Pressure Casting was developed into an industrialized process in 1982. A typical slip cast mould could be used for about 100 cycles. Slip casting uses the pressure of the slip in the mould, which is limited to about .2 Mpa (29 psi). Industrialized Pressure casting reduces mould time from days to hours, and as poly materials replaced plaster-based mould materials production cycle per mould now often last over 10,000 cycles with a working pressure of 3 Mpa (435 psi), 15 times that of manual slip casting. As shown in Figure 134, pressure casting is now commonly automated, and throughput for gang or batch moulds can easily achieve over 100,000 pieces per year of architectural scale components. Beyond the throughput, pressure casting lowers the initial water content of the slip from between 1.5 and 3% from traditional factory ready slips reducing drying and firing cycles. There is an increase in warpage and shrinkage observed with pressure casting during the drying and firing stages; however, the reduction in labour, increase in productivity, efficient use of factory and factory automation has made pressure casting the primary industrial process for ceramics.

While high quality and highly intricate shapes can be produced, and wall thickness can vary within a single component, structural and building envelope components are not currently made using pressure casting. For the most part, the pressure casting process is currently used to mass produce sanitaryware.

MVP Prototype I was developed using the slip-casting techniques. The slip-casting process is visualized in Figure 7.7.

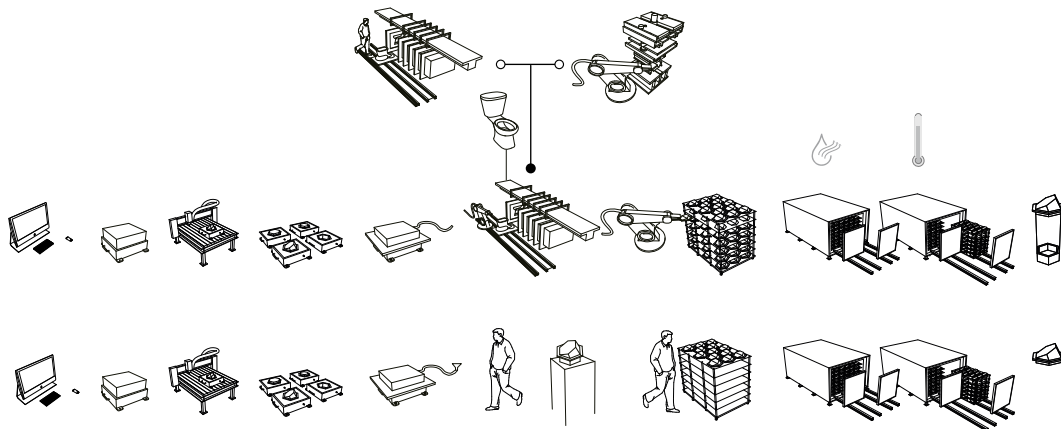


FIG. 7.7 Process diagram of Pressure Cast (above) and Slip Cast (below) manufacturing steps.

### Limitations of Slip Casting/Pressure Casting process

- Size limitation: typical maximum 91.4 x 20.3 x 30.5 cm (36 x 8 x 12 in), however, a more efficient size for production is 45.7 x 76.2 x 20.3 cm (18 x 30 x 8 in), about the same as the Ram Press.
- Weight limitation: 100 fired
- Throughput limitation: 1 piece per mould per day for slip casting, where pressure casting often gangs eight or more moulds per cycle with a short cycle time allow for the production of hundreds and even thousands of pieces per day depending on size and complexity.
- Status as architectural ceramics: currently not used or used for restorative work.

#### 7.3.2.1.3 Extruding

The extrusion process relies on a three-stage process: the force mechanism to move the material; a die to shape the material, and a cutter to size the material. In modern architectural ceramics, a post finishing computer numerically controlled process of measuring and cutting is utilized post firing to create a level of precision in the lengths and the cuts needed for attachments to architecture facades. The pressure mechanism may take the form of a ram, similar to the RAM press described in 7.3.2.1.1, a pellet mill roller, and screw type auger.

Industrial production typically uses screw type auger systems that allow a high rate and continuous feed of material. The screw type auger system can be traced

back at least to the 1600s in Holland and England for the mass production of pipes. The modern extruder can be traced back to the machinery manufacturer Carl Schlickeysen in 1855 with the “Universal Brickmaking Machine”. Schlickeysen continued to develop the extruder technology, focusing on the die and die technology, ultimately forming what we can still observe in modern brick making factories. While extruders are used for producing the base pieces of architectural terra cotta or restorations, modern terra cotta rainscreens are almost exclusively produced on modern extruder lines. Today, modern extruder lines use rheological simulation to design the dies, pressure sensing heads to make adjustments to the material flow directly at the die, and Computer Numeric Control (CNC) wire cutters as part of the typical architectural terra cotta production line.

The benefits of using an extruder are the scale and consistency of the units that are produced. The limitations are the anisotropic qualities of the material and the limitations on the morphology and surface that comes from a single direction shaping process. (Händle, 2007; Schweizer, 2008)

Stick built Terra cotta rainscreens produced from extruded ceramic units have grown in popularity in the 1990s. In the 2010s unitized curtain walls have been developed using extruded ceramic units, which will be showcased in One Vanderbilt Place, 57-floor, 150,000 m<sup>2</sup> (1,600,000 ft<sup>2</sup>) when completed in 2020. The scale of One Vanderbilt was a testament to the opportunity for widespread deployment of unitized ceramic curtain walls.

ASI Prototype III was developed using extruding technology. The extruding process is visualized in Figure 7.8.

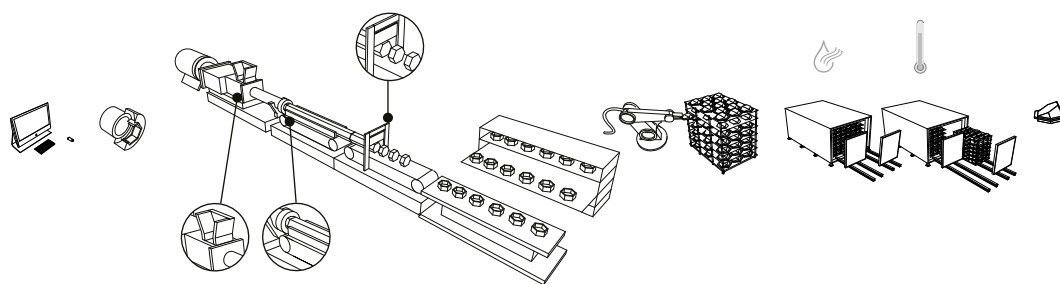


FIG. 7.8 Process diagram of Extrusion manufacturing steps.

Typical size of piece – 18” x 10 x 60” 150-250 lbs fired. – throughput average about 50-75 60” pieces per day.

## Limitations of Slip Casting/Pressure Casting process

---

- Size limitation: typical maximum 45.7 x 25.4 x 152.4 cm (18 x 10 x 60 in)
- Weight limitation: 68 to 113.4 kg (150 to 250 lbs) fired
- Throughput limitation: 50 to 75 152.4 cm (60 in) pieces per day
- Status as architectural ceramics: well established and currently used for façades

### 7.3.2.2 Future Fabrication Techniques

---

Future Fabrication techniques in ceramics focus primarily on Additive Manufacturing (AM). A range of technologies has been in development since the 1980s that focus on powder deposition and CNC extruder type manufacturing.

#### 7.3.2.2.1 Computer Numerically Controlled Ceramic Additive Manufacturing

---

Computerized additive manufacturing in ceramics was developed as a commercialized process in 1987. Soligen Technologies Inc. licensed direct shell production casting (DSPC) for ceramics technology based on inkjet printing developed at MIT in 1993 (“Three Dimensional Printing,” 1989-1999). Modern ceramic additive manufacturing in ceramics can be broadly categorized into three buckets based on feedstock: powders, pastes and suspensions.

The advantages of AM allow for the direct-to-part production and the ability to produce parts on-demand, as visualized in Figure 7.9. The equipment needs are smaller and more flexible than traditional ceramic manufacturing methods. The ability to free form parts unrestricted by the directional requirements of pressing, casting, and extruding provide unparalleled flexibility and this flexibility allows for full use and translation of digital design tools to create complex parts.

AM in ceramics is already in use in a variety of industries including aerospace and medicine. However, the current AM technologies of ceramics are primarily focused on porous structures. Monolithic structures, those required for robust architectural components, are currently challenging to produce with computational additive processes. This difficulty is particularly true for prototype designs that require the working fluid to be held directly by the ceramic component. Future designs based on ongoing technology advances with AM are discussed in more detail in Chapter 8.

For the purposes of understanding the potential impact that AM may have on the architectural components of the building envelope, the focus is with the processes where their limitations of production in throughput and morphology as it related to the architectural scale at the time of this research investigation. Powder-based 3D Printing (P-3DP) where a flowable powder is deposited in layers, Slurry-Based 3DP (S-3DP) where the ceramic powder is suspended in a liquid, and Robocasting, Direct Ink Writing (DIW) where a paste is printed through an extruder building layer upon layer, all have the capacity to produce architectural sized components in the single meter scale. Using this assumed limitation, the focus was on the performance potential of an AM ceramic component for the TACE system, specifically what was the potential to create surface area and which method of assembly was most suited for deploying an AM TACE component at scale. While the advent of automation for assembly of components in the factory and on site robotic installation has been focused on speed and accuracy for developing the final product, inherently the automation process supports an increase the sizes of units that could be used, and thus allows for a reduction of both parts and points of system failure. For future development, other limiting factors may apply and are discussed in Chapter 8 (Zocca, et al., 2015).

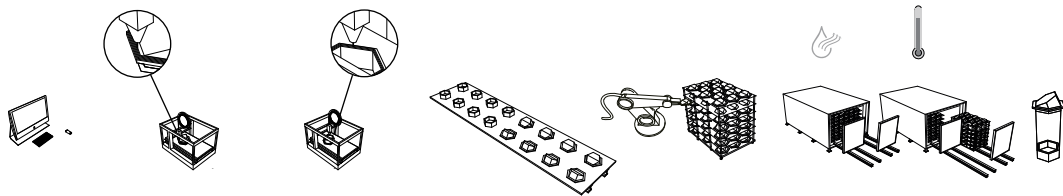


FIG. 7.9 Process diagram of Digital Fabrication manufacturing steps.

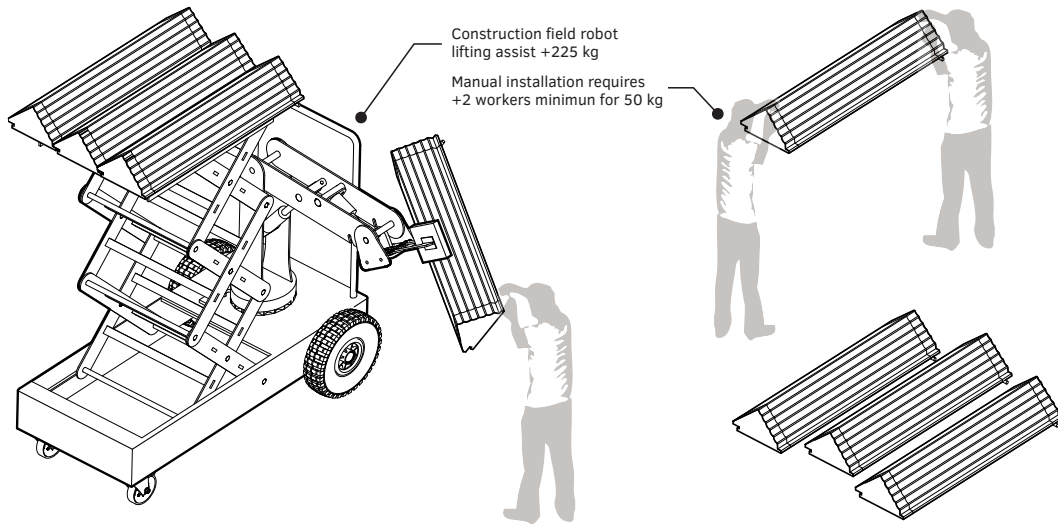


FIG. 7.10 Diagram of typical unit size limitation and increased limitations with robotic lifting support.

## 7.4 TACE Module Options

The TACE module options are developed based on the limiting criteria discussed in Section 7.3. These options are representative of a lexicon of TACE component shapes based on cardinal and ordinal orientation and fabrication technology. While each different orientation of the building envelope could be clad with a specific TACE module optimized for energy transfer, the basic morphology can be described by a simple lexicon of modules based on polar coordinates to develop the geometry. Each instance was simulated for annual solar exposure based on TMY3 data from New York Metro Area, Tucson, Arizona and Delft, NL. Ratios of directly exposed surface area to the indirect surface area to annual insolation values are used for comparison.

While the module design concept for prototypes I, II and III are discussed in Chapter 4, The following was a development for use in developing the module for architectural integration and basic quantification.



## 7.4.1 TACE Morphology Based on Cardinal and Ordinal Polar Coordinates

---

The following morphology guide assumes a 40° North latitude (representing New York, US) as a baseline and expands to 30° North (representing Tucson, US) and 50° North (representing Delft, NL) Latitude. Solar analysis for the development of the thermal transfer surface ratio as a comparative measure of potential effectiveness. The ratio was derived by the Direct Transfer Surface (DTS) divided by Indirect Surface (IS) multiplied by the annual solar insolation. While this ratio was used only to analyze the comparable morphologies, it forms part of the foundation of developing possible energy transfer coefficient for countercurrent heat exchanging building envelope systems as discussed as part of future work in Chapter 8. The North morphology was not explored, though its development and deployment are also discussed as future work in Chapter 8.

### 7.4.1.1 South Component Morphology

---

The South component morphology, as shown in Figure 7.11, assumed a direct southern cardinal orientation. Annualized solar exposure was based on atmospheric and climatic phenomena as included in the TMY3 data for all locations. The inclination angles were adjusted between locations to match the latitude of that geolocation to maximize exposed transfer surface and thermal transfer potential.

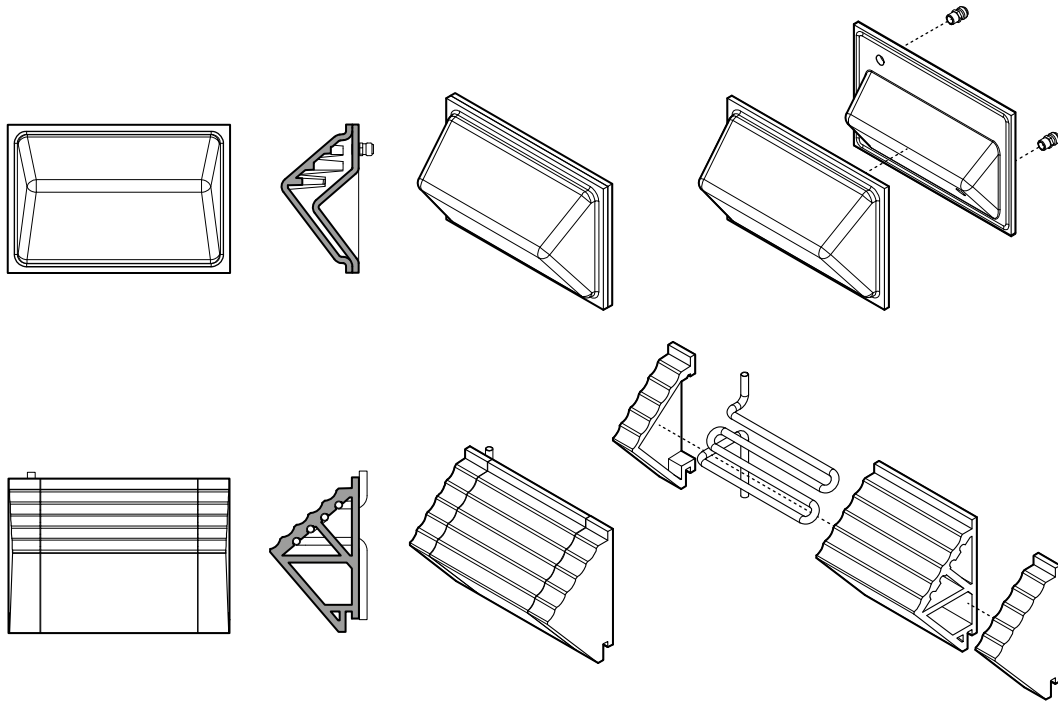


**FIG. 7.11** Diagram of South facing component geometries for prototype POC Prototype II (above) and ASI Prototype III (below).

#### 7.4.1.2 East and West Component Morphology

The East and West TACE component morphology, as shown in Figure 7.12, assumed symmetrical vertical inclination between the two and as such are developed as a single morphology for both cardinal directions. Annualized solar exposure often differs on the East and West faces based on atmospheric and climatic phenomena. These differences were not investigated here, however the methodology to develop site specific and differing East and West oriented morphologies follow the same method: based on the annual exposure of a surface on the East and West, the inclination angle could be adjusted to maximize exposed transfer surface by aligning the surface to the highest average inclination of that direction.

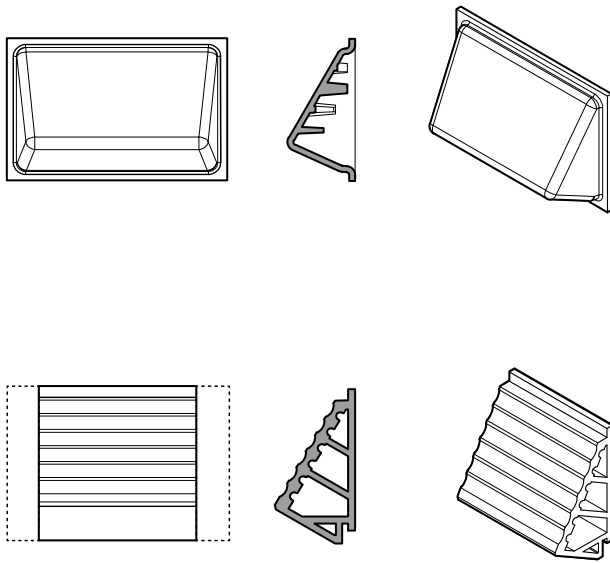


FIG. 7.12 Diagram of East and West facing component geometries for Prototype POC II (above) and Prototype ASI III (below).

### 7.4.1.3 Southeast and Southwest Component Morphology

Similar to Section 7.4.1.2, the Southeast and Southwest component morphology are treated as symmetrical morphologies. This ordinal morphology was used as a transition example between the cardinal direction morphologies. The varying inclination angles represent the potential for the TACE system to maximize output based on morphology that is related to local massing and orientation.

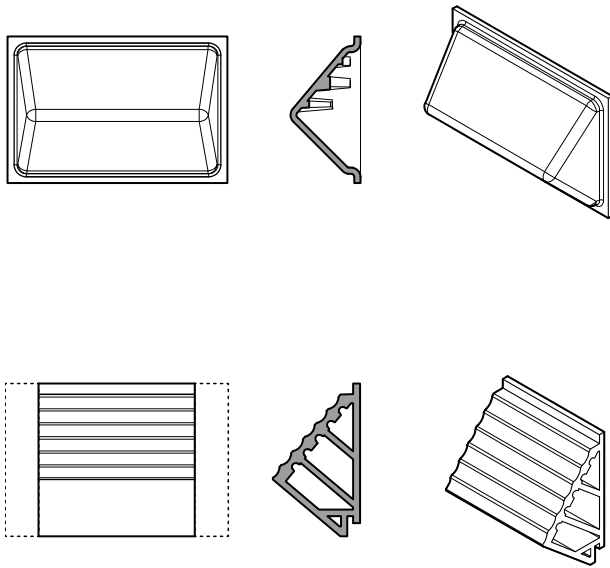


FIG. 7.13 Diagram of Southeast and Southwest facing geometries for POC Prototype II (above) and ASI Prototype III (below).

#### 7.4.2 Design to Minimize System Loss

A system that relies on multiple lengths of fluid transfer has the potential to experience efficacy loss (loss of thermal potential) in multiple areas of the system. As shown in Chapter 5, the TACE components were insulated to reduce the loss on the interior side of the external component – the back side of the tile. Care must be taken to insulate the working fluid loops, heat exchangers and phase change thermal storage batteries to maximize efficacy and minimize loss. System loss was also directly related to length and time that the working fluid was not actively transferring energy (i.e., collected or offloading in the TACE components). While this loss could be minimized with insulation, minimizing the length and required connections outside of the transfer components directly affects the TACE system performance, the system complexity, and the system cost.

Therefore, the approach to minimizing system loss was to reduce the amount of length that the working fluid must pass through. The governing criteria of these lengths were twofold: 1) the distance the working fluid must travel from the end of the collection or offloading sequence to the storage transfer sequence, and 2) the number of connections between TACE components during the collection sequence.

Criteria 1 is addressed in Chapter 8. Criteria 2 suggested that the system maximize the size of components and minimize connections to increase energy transfer efficacy and decrease system losses. This position of using larger components further suggested the development of the system as a factory automated manufacture where possible with factory assembly as a unitized system, as discussed in Section 7.5.3.

#### 7.4.2.1 Surface to Working Fluid Ratio

---

Another critical aspect of the TACE system was the Surface Area and Working Fluid ratios; described as the surface area of the direct and indirect collecting surface the surface area of the transfer surface of the transfer components, and the volume and average cross section of the working fluid as shown in Figure 7.14. It was shown in Chapter 6 that there was a significant benefit in the transfer of energy when there was an increased ratio from the exterior surface to the interior transfer surface. In MVP Prototype I the water volume and average thermal transfer area of the transfer chamber was 5.69 litres (1.5 gal) and 0.206 m<sup>2</sup> (2.2 ft<sup>2</sup>), with a heat transfer surface area to fluid volume ratio of 1.08. POC Prototype II was developed to showcase a full-scale working prototype and utilized a similar set of ratios. ASI Prototype III was developed to address the challenges of the Prototypes I and II design, showcasing a significantly reduced ratio of surface area to water volume: 0.12, where the water volume and average thermal transfer area of the transfer chamber was 0.2214 litres (0.0585 gal) and 0.074 m<sup>2</sup> (0.79 ft<sup>2</sup>), respectively.

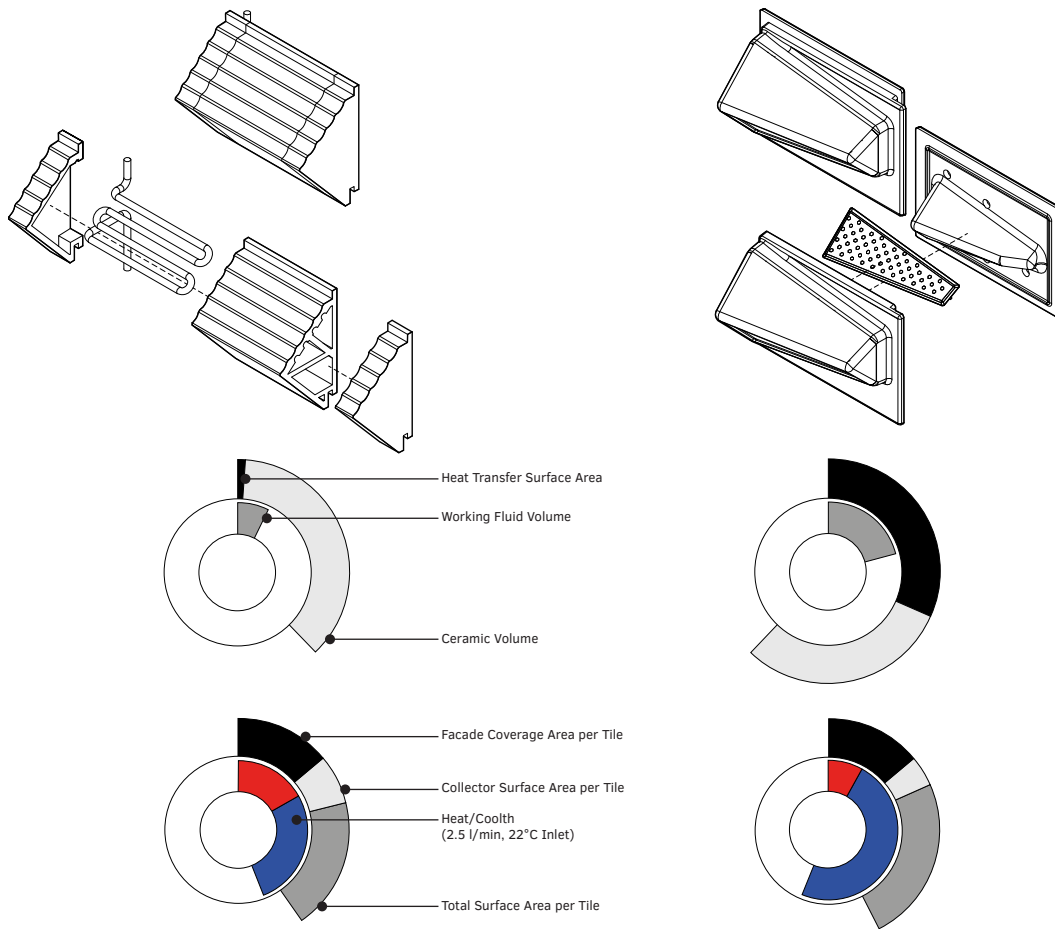


FIG. 7.14 Comparison of Prototypes I and III by working fluid volume, surface areas and power output.

### 7.4.3 Module Size Limitations

As noted in Section 7.3.2, the TACE modules were limited by the fabrication process and the method of assembly. Factory assembly affords larger units; thus, the module size is governed by the assembly method. Site assembly is governed by the weight and size of labour assembly standards as also discussed in Section 7.3.2. Emerging site assembly technologies like robotic field assembly may have future potential to assemble the TACE system on site. This might create the possibility of larger units for site assembly where the factory fabrication limits then govern the

component dimensions. However, the TACE system as a whole needed mechanical electrical and plumbing assemblies requiring a complexity that would likely put robotic field assembly out of reach for the foreseeable future for automated site assembly methods.

Maximizing the size of the TACE modules will have different limitations depending on the method of assembly and installation.

## 7.5 TACE Assembly and Installation Options

---

Three types of façade assemblies and installations were explored as visualized Figure 7.15: Site Assembled Rainscreen (noted as an updated form of unit masonry construction), Stick Built Curtain Wall Rainscreen assembly and Unitized Curtain Wall assembly. The summary comparison was based on relative assembly time, relative cost factors, performance potential and integration potential.

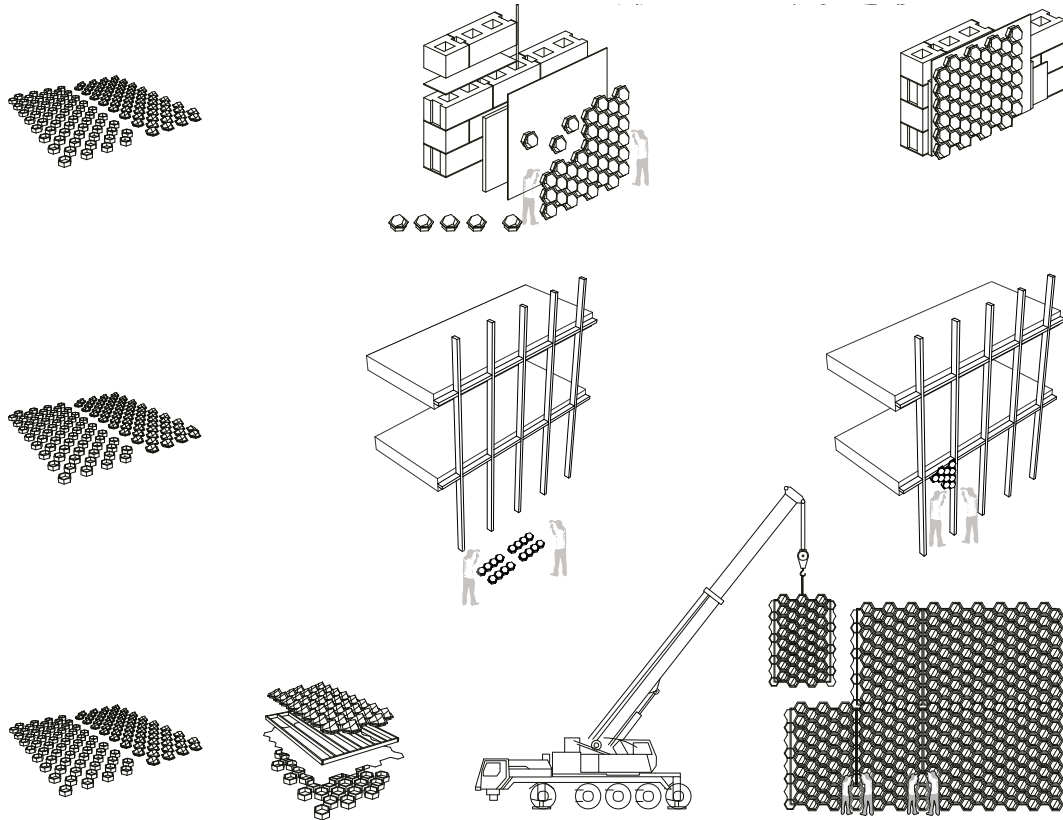


FIG. 7.15 Assembly methods diagram for: masonry cavity or traditional rainscreen (top); stick build rainscreen curtain wall (middle); unitized curtain wall (bottom).

### 7.5.1 Rainscreen Assembly

The design of the rainscreen façade in principle goes back almost 1000 years. The modern terra cotta rainscreen façade is a tile hung, open joint rear ventilated system that is site assembled. The rainscreen approach to Terra Cotta is currently ubiquitous and well established in the industry. The ceramic components remain the exterior side of the building envelope demarcation line. The advantages of using a rainscreen type of assembly for TACE was the ability to have vast expanses of field installed systems using smaller punched windows. The disadvantages were the site time, labour expense and testing required. Boston Valley Terra Cotta provided the system attachment for all assembly systems explored.



ASSEMBLY TIME – site assembled with labour and testing in situ, however field adjustments readily achievable.

RELATIVE COST – site time, labour and system testing drive higher cost when compared unitized curtain wall, comparable to stick systems.

PERFORMANCE POTENTIAL – structurally sound, as the primary wall support was a structural component continuously supported. Penetration through the building envelope is limited to the working fluid pathways that cross the building envelope demarcation line.

INTEGRATION POTENTIAL – mainly depending on site labour expertise and ability to site install and test, the high degree of skilled labour and design planning to integrate the systems required.

---

### 7.5.2 **Stick Build Rainscreen Curtain Wall**

Stick built curtain walls are the precursor of the unitized curtain wall system and are assembled in several ways to create the building envelope. The system relies on site assembly with some factory prefabrication of components (e.g., cutting lengths of primary vertical members, rainscreen units, etc.) with the option of field adjustments, unlike unitized systems. In these scenarios, the TACE system was assembled and tested in the field similar to the rainscreen process, and it constrained by the arrangement of the stick framing.

ASSEMBLY TIME – Factory limited, primarily assembled on site with substantial time and labour commitment, field adjustments are readily achievable.

RELATIVE COST – time and labour on site drive the cost to be comparable or more than unitized system.

PERFORMANCE POTENTIAL – settlement and deflection could compromise TACE system or require robust support to ensure the soundness of the working fluid pathways.

INTEGRATION POTENTIAL – ability to install alongside ladder and stick type of curtain wall site assembled was improved over traditional rainscreen assembly as the trades can more easily be integrated; however, testing was required on site potentially limited integration.

### 7.5.3 **Unitized Curtain Wall**

---

A unitized curtain wall system was investigated using the Schüco Façade USC (Unitized System Construction) 65. Unitized curtain walls such as the Schüco 65 system are factory assembled where much of the assembly is automated. As such, the factory assembled option allows for several advantages that distinguish it from the typical RainScreen assembly and Stick Built Curtain Wall Assembly detailed above. Unitized systems can typically be fabricated in less time and assembled as a building envelope with less time and labour. There are significant advances to factory assembly when it comes to reducing connections and integrating what would be separate trades for onsite installation.

**ASSEMBLY TIME** – Factory extensive, reduced on site labour and time; however, field adjustments are limited.

**RELATIVE COST** – Factory assembly increases initial manufacturing cost, though this was offset by reduced onsite labour and time.

**PERFORMANCE POTENTIAL** – accepts building settlement and deflection better than stick built and rainscreen assembly methods, limited joints for thermal and moisture leakage support the TACE system increasing overall performance.

**INTEGRATION POTENTIAL** - ability to factory install supports efficiency in testing and control of penetrations through the building envelope demarcation line.

### 7.5.4 **Assembly Limitations**

---

Based on the analysis in the previous sections, the limiting factors of assembly are the complexity of the installation. Onsite labour could limit the size of the TACE modules and requires multiple trades for assembly and installation. At the same time, without the benefit of automation processes to reduce errors due to poor craftsmanship, the assembly of the TACE system could prove prohibitive. While the unitized system has some limitations, the ability to preassembly and factory test and certify the mechanical components of the system create a clear advantage over site assembled options.

## 7.6 Results

---

The results of Chapter 7 were delineated by a proposed design for a complete system based on the design exercises and analysis of the preceding sections. The proposed design was developed using the Howe Center as the baseline model. A conceptual overall system performance efficacy for this proposed design is discussed in Chapter 8.

### 7.6.1 Deployment Potential

---

Based on the design exercises in this Chapter, the following deductions are interpolated as results of the design iteration study. System deployment was governed by multiple factors: System Efficacy, System Complexity, Deployment Potential and Return on Investment (discussed in Chapter 8). System Efficacy was determined for this exercise as the performance potential based on transfer surface area. System complexity was based on the quantification of components, fabrication and assembly steps. Deployment Potential - and Limitations - was based on the steps to install, system integration, and design potential.

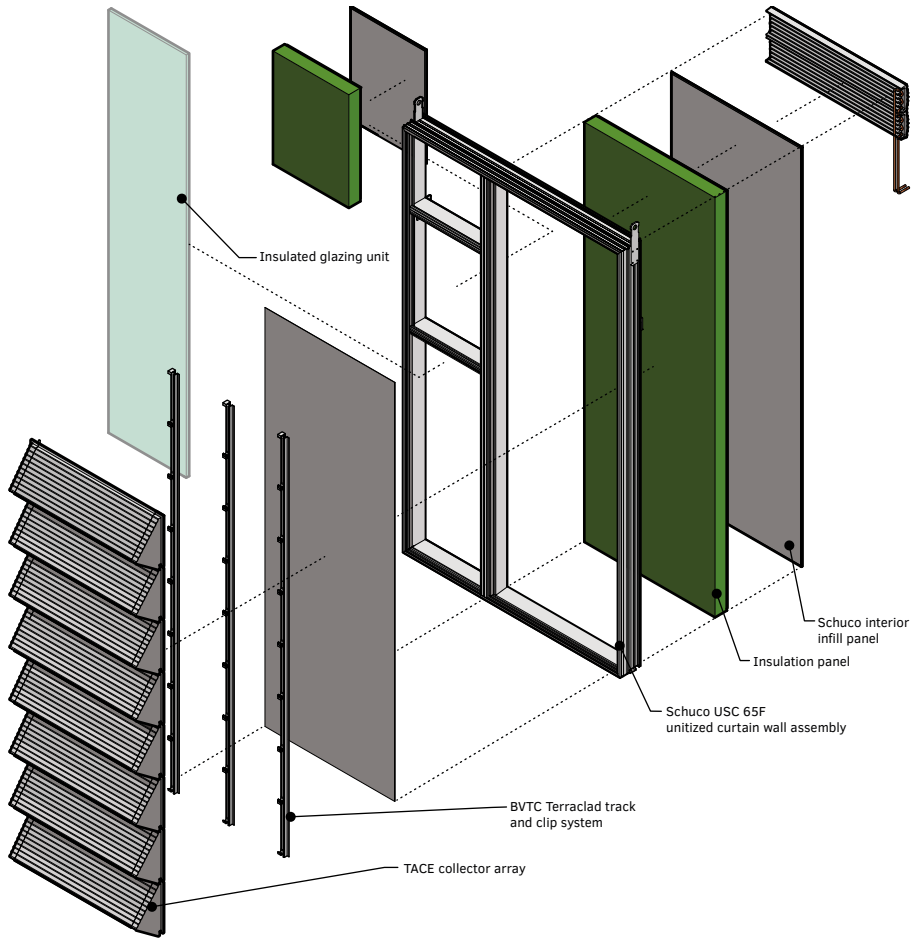


FIG. 7.16 Diagram of the component parts showing rainscreen attachment system integrated with Unitized Curtain Wall components.

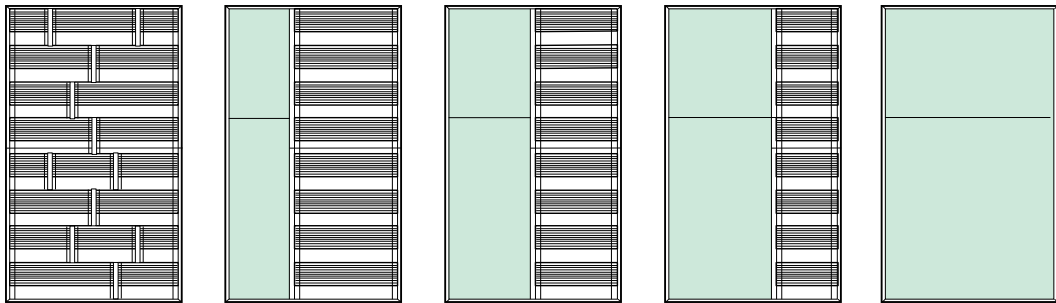


FIG. 7.17 Example of Unitized Curtain Wall assembly options.

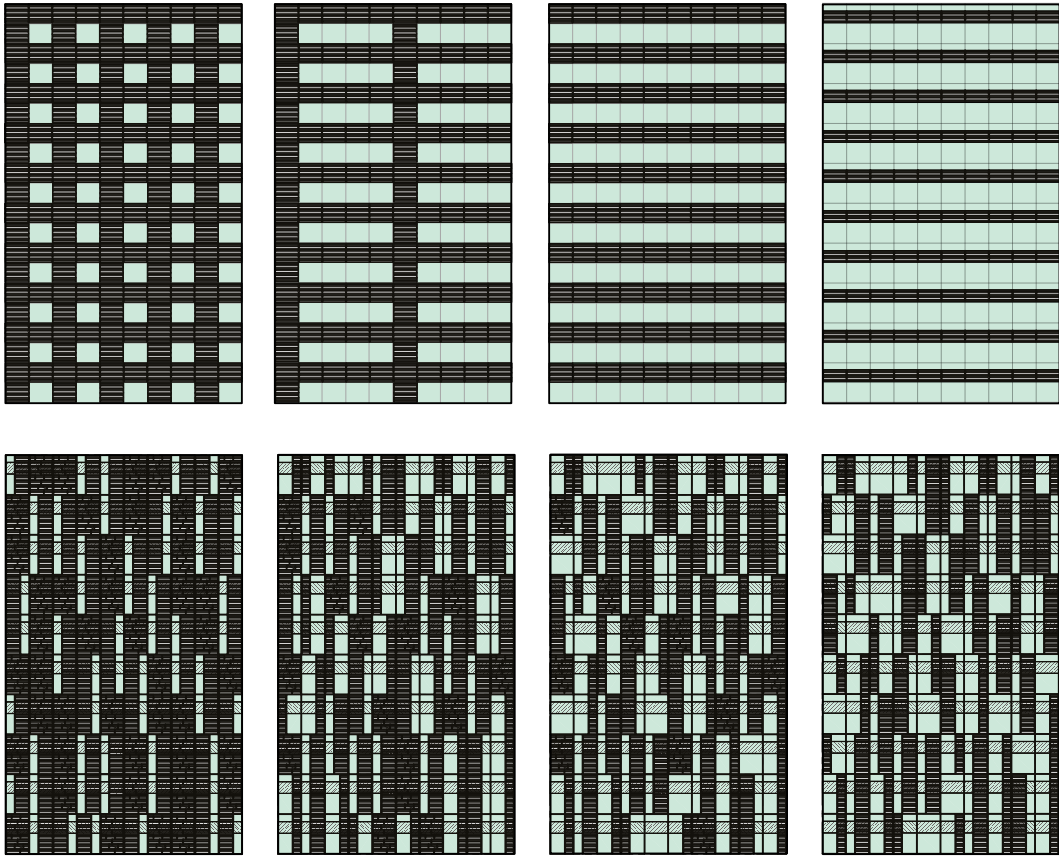


FIG. 7.18 Example of potential facades with corresponding WWR and TCS areas.

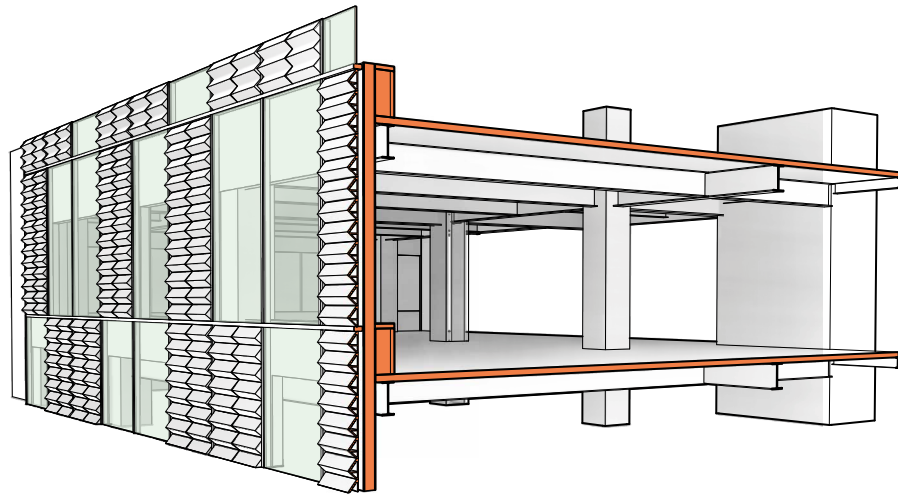


FIG. 7.19 Example of typical bays showing UCW examples from Figure 7.17.

The deployment potential of the Unitized Curtain Wall TACE system iteration, as shown in Figures 7.16-9, offers a composite of efficiency for manufacturing and assembly, as well as flexibility of design within the high performance office space context. The ability to modularize and preassemble the mechanical componentry addresses multiple design drivers and potential critical points of failure.

The reduction of parts and the controlled environment of the factory assembly combined with the reduction in onsite labour and speed of installation suggest that the Unitized Curtain Wall iteration should be developed. The development of a fourth prototype would be used to understand the limits of the unitization of a curtain wall that includes the energy exchange and integrated mechanical system.

## 7.6.2 Deployment Limitations

The weight of the TACE system was a limiting factor and based on the need to reduce parts and limit connections as each is contributing points of possible failure. The move towards integrated thermal transfer tubing with reduced connections, a reduction in weight by reducing the amount of working fluid, and the ability to factory install the system supports the development of the TACE system as a unitized factory assembled module using extruded ceramic components.

Under current construction processes, stick-built and field installed ceramics facades are limited by the size of the object and the logics of the on site install. This limitation was further compounded when considering the ceramics as part of the façade integrated HC system. Discussed in more detail in Chapter 8, the unitized assembly has many advantages over site assembled system. The TACE system, in the end, should be thought of as an appliance, and one would not in current construction processes assemble a refrigerator from its individual pieces on a construction site.

## 7.7 Summary: Design Limitations

---

The physical limitations of the manufacturing and assembly of the TACE system and the process for installation must be weighed against system performance and ultimately the aesthetic drivers that will limit the viability for the deployment of any product that was so distinctly visible. Therefore, while it was critical to understand the variability of integration into the architectural systems of the envelope, it was equally critical to understand the range of design aesthetics that provide effective system performance. Ultimately when considering the viability for deploying a new building envelope system, the concerns of the various stakeholders must be addressed:

- The design architect has a twofold vested interest in performance and aesthetic design. The design of a new building envelope system must be sufficiently flexible, aesthetically, to allow for creative visioning – within a led framework that supports the performance of the system.
- The design engineer has the responsibility of assuring the performance of the building and as such, will require validated data to support a new building envelope technology that demonstrates a reduced need for mechanical heating and cooling.
- The project manager has to navigate the relationships of the various entities tasked with delivering the building systems as an integrated whole; thus the need to develop precoordinated products, such as the unified curtain wall, will support the decision to integrate a new system typology.
- The specialist consultant (i.e., sustainability, energy code consulting, etc.) will drive the design narrative for the engineers and set the approach for achieving performance goals in the early stages of the project and thus require an adequate early understanding of a product well ahead of the normal process of the product specification.

- The contractor is both concerned with the robustness of building systems, the schedule for procurement and installation, and the availability and ability of installers to install a new building envelope system.
- The installer closes the loop between the design intent and the physical manifestation of the project and thus requires a comfort level of installing
- Ultimately the owner must drive the vision that requires the multiple stakeholders to work towards a common vision and support the risk of deploying a new system that may be considered, at least at first, unconventional to the mainstream AEC industry.

Chapter 8 recaps the research questions as a whole and discusses the design and systems integration and limitations in more detail.

## References

- A Brief History of Ceramics and Glass. (1990). Retrieved from <https://ceramics.org/about/what-are-engineered-ceramics-and-glass/brief-history-of-ceramics-and-glass>
- Adams, E. (1971). 7 - Slip-Cast Ceramics. In A. M. Alper (Ed.), *Refractory Materials* (Vol. 5, pp. 145-184): Elsevier.
- Crosby, B., Ely, B., Hickey, J., Hoang, L., Johnston, M., Orlando, S., & Veliz, E. (2008). Office Building Northeastern University School of Architecture ARCH G691 Graduate Degree Project Studio. Retrieved from [https://issuu.com/neuarchitecture/docs/office\\_building\\_issuu](https://issuu.com/neuarchitecture/docs/office_building_issuu)
- Goia, F. (2016). Search for the optimal window-to-wall ratio in office buildings in different European climates and the implications on total energy saving potential. *Solar Energy*, 132, 467-492. DOI:<https://doi.org/10.1016/j.solener.2016.03.031>
- Haglund, B. (2014). Thermal Zones. Arch 463 [PowerPoint Presentation]: University of Iowa.
- Händle, F. (2007). *Extrusion in Ceramics. Engineering Materials and Processes*. Springer, New York, New York.
- Ko, D., & Elnimeiri, M., & Clark, R. (2008). Assessment and prediction of daylight performance in high-rise office buildings. *The Structural Design of Tall and Special Buildings*. 17. 953 - 976. 10.1002/tal.474.
- O'Conner, J., Lee, E., Rubinstein, F., & Selkowitz, S.. (1997). Tips for Daylighting with Windows: The Integrated Approach. Retrieved from <https://eta-publications.lbl.gov/sites/default/files/tips-for-daylighting-1997.pdf>
- Pelleriti, R. (1998, July). History of the RAM Process. *Ceramic Industry Magazine*.
- Schweizer, J. (Producer). (2008). Extrusion Basics. Retrieved from <https://www.ceramicindustry.com/articles/87808-extrusion-basics>
- Selkowitz, S. (2013). *Tips for Daylighting with Windows*. Berkeley, California: Lawrence Berkeley National Laboratory.
- Shadish, W., Cook, T., & Campbell, D. (2002). *Experimental and Quasi-experimental Designs for Generalized Causal Inference*: Houghton Mifflin.
- Three Dimensional Printing. (1989-1999, June 28, 2000). Retrieved from <http://www.mit.edu/~tdp/index.html>
- Waters, T., Putz-Anderson, V., Garg, A. (1994). Applications manual for the revised NIOSH lifting equation. (Publication No. 94-110). Cincinnati, OH: U.S. Department of Health and Human Services, Public Health Service.
- Winn, K. (2014). *Inter-scalar Multivariable Decision Making Framework for the Architectural Envelope*. (PhD), Rensselaer Polytechnic Institute, ProQuest LLC.
- Zocca, A., Colombo, P., Gomes, C., & Günster, J. (2015). Additive Manufacturing of Ceramics: Issues, Potentialities, and Opportunities. *Journal of the American Ceramic Society*, 98(7), 1983-2001.





# 8 Conclusions and Future Directions

---

The motivation behind the research presented in the preceding chapters was to develop an understanding of the potential efficacy of a countercurrent heat exchanger integrated into the building envelope. This motivation was investigated as design, development, testing and simulation of the TACE system as a design instance of a countercurrent heat exchange system typology. The research hypothesis and questions were answered as part of the design and development process of the TACE system, where the results of the questions had direct impacts on the developed design iterations. In this way the research questions and design iterations were linked in a feedback loop where research and design supported the development of a novel building system, providing proof of concept for a potential class of building systems that provide an energy transfer function across the building envelope demarcation line. As such, the research conducted in this dissertation was supported by: the design and testing of a Minimum Viable Product (MVP) Prototype I; the demonstration of energy transfer with the design fabrication and assembly of Proof of Concept (POC) Prototype II; the design and demonstration of an architectural and systems integration (ASI) Prototype III; and the proposed design for a Unitized Curtain Wall (UCW) Prototype IV TACE iteration.

## 8.1 Introduction

---

The dissertation followed several threads to validate the efficacy potential of the proposed countercurrent heat exchanging envelope; the development of a range of prototypes, quantitative testing, performance simulations, and design iterations based on the results. The following discussions in this chapter are focused on four primary categories: 1) answers to the research questions; 2) review of the TACE prototypes; 3) valuation of the research proposition; 3) propositions and future work 4) impacts on the discipline.

## 8.1.1 **Answers to the Research Questions**

---

The research questions were addressed in detail in Chapters 5, 6, and 7. The following discussion reviews the driving hypothesis, research objectives, and results to the research questions.

### 8.1.1.1 **Review of the Hypothesis and Research Objectives**

---

A review of the research hypothesis and research objectives is necessary to frame the results and discussion of the research questions.

The hypothesis of this dissertation, as stated in Chapter 1, was:

**Countercurrent Heat Exchange Building Façade using ceramic components reduces the peak energy loads that contribute to the Energy Use Intensity of existing commercial buildings.**

Based on the results of the modelling and simulation in Chapters 5 and 6, as shown in Table 8.1, the TACE system improves the building energy profile over the ASHRAE baseline to maintain equal occupant thermal comfort by 5.6% in total end use energy calculations. Heating was reduced by 14.7% and cooling by 6.6%; thus, it is reasonable to deduce that the peak for heating could also be reduced proportionally. It can be reasoned based on the correlated simulations for the ASI Prototype III that the proposed design development can increase the load shifting potential by at least two times more than MVP Prototype I, suggesting further development and validation testing as discussed in Section 8.1.4.1. This magnitude of improvement may reduce the operating costs, discussed in this section. Furthermore, if peak energy pricing was used as part of the measure of energy costs, one can reasonably project that the impact of reducing the peaks and filling the valleys of the energy demand profile would indeed also be magnified and aligned to the current trajectory of utility and regulatory bodies.

TABLE 8.1 Results comparing the performance of MVP Prototype I and ASI Prototype III.

EUI Per Building Area Extrapolation Comparison- Floor					
Case	EUI (MJ/m <sup>2</sup> )	EUI (kWh/m <sup>2</sup> )	EUI (kBtu/ft <sup>2</sup> )	EUI Additional Savings	
MVP Prototype I	676.8	188.0	59.6	<b>7.7%</b>	
ASI Prototype III	624.7	173.5	55.0		
ASI Prototype III Extrapolated End Use Comparison Typical Floor Zone					
End Uses	Existing (GJ)	ASHRAE (GJ)	Savings	TACE (GJ)	Savings/ASHRAE
Heating	286.4	116.5	59.3%	84.5	27.5%
Cooling	134.1	73.6	45.1%	63.7	13.5%
Fans	9.4	6.1	35.8%	5.1	16.3%
Pumps	80.3	42.8	46.7%	46.2	-8.0%
Heat Rejection	40.9	22.9	43.9%	19.4	15.6%
<b>Total End Uses</b>	<b>660.8</b>	<b>371.5</b>	<b>43.8%</b>	<b>328.5</b>	<b>11.6%</b>
MVP Prototype I End Use Comparison Typical Floor Zone					
<b>Total End Uses</b>	<b>660.8</b>	<b>371.5</b>	<b>43.8%</b>	<b>350.6</b>	<b>5.6%</b>

The research objectives were met by answering the research questions.

- Evaluate Energy Use Intensity reduction using a countercurrent heat exchanging envelope with ceramic components

The evaluation of EUI reduction was conducted and demonstrated in the results in a potential EUI reduction of the MVP Prototype I as discussed following in Section 8.1.1.2. Based on observations of the system as demonstrated and reasoned correlations, the ASI Prototype III can be expected to provide a significant reduction in EUI based using The Howe Center as the test case. The reductions of whole building EUI suggested more detailed examination of the impact a countercurrent energy exchange building envelope has on the overall EUI of a building.

- Test various combinations of design attributes including surface area, flow rate and flow direction of the Thermal Adaptive Ceramic Envelope prototype for the most effective performance

The physical tests and simulated results from Chapter 5 using the MVP Prototype I revealed several observations: 1) the difference in surface area did make a significance in the thermal transfer rate, with diminishing returns as the ratio grew, 2) lower flow rates were able to capture higher temperature, and faster rates captured more energy, 3) thermal transfer worked bidirectionally creating a countercurrent heat pump. The design iterations based on the results of Chapter 5 and Chapter 6 provided further insights that alongside the correlated results

of the ASI Prototype III suggested further critical factors in determining optimal performance for future study.

#### — Assess architecture integration and impacts for the Thermal Adaptive Ceramic envelope

Modern Office Spaces, have spatial demarcations between the mechanical systems responsible for thermal comfort and the systems responsible for weather tightness. It is typical, though not exclusive that commercial office developments are most often delivered as a core and shell that limits complete system integration as the incomplete mechanical heating and cooling system remains as a ring around the core. Tenants, through the Tenant Improvement (TI) process, are typically responsible for completing and outfitting the distribution and terminal systems for the heating and cooling of the spaces included in the tenancy. However, OVG Real Estate, for example, has deployed at scale across their portfolio a novel approach that challenges this traditional demarcation line between developer or owner and tenant by providing all components for the heating and cooling system equipment for both the base building and the tenancy; still an emerging approach generally, and specifically in the United States where these types of projects are outliers to standard commercial development practice.

The TACE system challenges this traditional demarcation line that was in the spirit of the examples, as shown in Chapter 3. These systems effectively used the envelope to assist in the heating and cooling. In the UCW Prototype IV, the primary heating and cooling system was linked directly to the envelope as described in Figure 8.1.2.5.2.

Chapter 7 delineated the design drivers and impacts the architectural integration of the TACE system. Ultimately, the version of the TACE as a unitized curtain wall and an integrated system as described for the design of the UCW Prototype IV leveraged the performance and installation requirements necessary for reimagining the placement of the heating and cooling systems within modern office spaces.

While not studied in detail in this research, cost impacts can be discussed in two primary ways; as capital cost and as operating costs. Capital costs are understood as the total costs of deploying the system including: materials, transport, labour, and are assessed in net present value as a premium cost above a baseline system. Operating costs are assessed as the cost of energy in net present value per year as well as a percentage of operating cost savings over the lifecycle of the building. Operating costs are looked at in both net present value and as an escalation of energy costs over time. These cost impacts are discussed for future research in Section 8.1.4.1.

While attempting to craft a system that would be viable for widespread deployment in the modern office design it was thus critical to address the following criteria: 1) demarcation of the core and shell and mechanical system by developer, owner and tenant, 2) manufacturing, assembly and installation methods, and 3) valuation of the system in terms of capital cost premium and operating cost reduction.

The research question and results that were developed to support achieving the research objectives are discussed in the following sections. Based on the results of the research questions, specific design decisions were made and discussed in the following Section 8.1.2.5.1-8.1.2.5.2. In many cases, as noted in the following subsections, the results of the research question either confirmed the hypothesis, helped develop and pose new questions and illuminated a new and unexpected result that led to unanticipated conclusions and possible new directions for development and design of the TACE system.

### 8.1.1.2 Review of the Research Questions

---

The primary research question was stated:

**What is the energy use intensity reduction potential of the Thermal Adaptive Ceramic Envelope using ceramic components for commercial office projects?**

Based on the simulation results for end use detailed in Section 6.4.2.4 the energy use intensity reduction for the MVP Prototype I was 5.6% over the ASHRAE recommended baseline and 49.2% reduction over the case study example of The Howe Center. Using the ASI Prototype III, it is reasonable to expect a reduction of an additional 15% over the ASHRAE recommended baseline and 75% reduction over the case study example of The Howe Center. These figures assume the NYC climate; energy reduction potential will vary by location. Additional reduction potential can also be reasonably assessed when integrating the TACE system with a working fluid-based system such as a geo-exchange heat pump. Geexchange heat pumps are shown to reduce EUI on high performance buildings attributed to the mechanical heating and cooling over the ASHRAE comparative VAV system by an average of about 50% (Maor, 2019). The potential additive value was that both the geo-exchange loop and the TACE system could use the same radiant terminals for heat and coolth delivery; an essential part of the heating and cooling infrastructure was shared in the hybrid system scenario.

The following sub questions were stated:

## – What design attributes of the Thermal Adaptive Building Envelope impact the Energy Use Intensity reduction?

Chapters 2 and 4 delineated the attributes that impact EUI reduction. Chapter 5 tested and simulated these attributes, the results of which were used to refine POC Prototype II and more significantly for ASI Prototype III. The impacts of varying the amount of mass, the geometry of the thermal transfer components, fabrication techniques, working fluid flowrates, and location of insulating layers were all explored. Several explicit and actionable observations resulted from these tests: 1) increased surface area of the transfer components appeared to augment energy transfer 2) modulating flowrates allowed higher temperature capture or more energy capture. Based on these observations, it was critical to discuss why the increased surface augmented transfer and how the modulation of flowrates could be used to augment the system performance.

The simulated performance of ASI Prototype III sits in stark contrast to the performance of MVP Prototype I. While there are multiple physical and design differences between the two prototypes, Chapter 5 established, at least in general terms, that the mass of the ceramic material and the location of the insulation either had little effect on performance or in the case of the insulation layer, remained in the same location within the module assembly of the components on both prototypes. Furthermore, the overall morphology was similar, enough to direct a more focused discussion on what was different between the two prototypes. MVP Prototype I used a specialized ceramic pin plate as the thermal transfer component with a ceramic to working fluid volume ratio of 0.1%. ASI Prototype III used a specialized thermal transfer tube and had a ratio of 3.1%, significantly higher than the MVP Prototype I. What was common between what appears to be quite different thermal transfer components, was that both the pin plate and Vipertex thermal transfer tube disrupted laminar flow and created turbulent flow in the working fluid. We can reasonably conclude that at least one of the corresponding causes of the augmentation in energy transfer was the increase in turbulent flow of the working fluid along the transfer surface, due to an increase in surface area of specialized surface geometry, as this was the common attribute between otherwise dissimilar thermal transfer components.

The ability to modulate working fluid flowrates in mechanical heating and cooling equipment is in everyday use in typical fluid based systems (Siegenthaler, 2004). In the TACE system, while typically the increased temperature capture of the slower working fluid would be more useful, the ability to move more energy at reduced temperature rise could also be valuable. The best-case scenario would be the ability to modulate the flow rates on the TACE module, and in the case of ASI Prototype

III, modulate that flowrate into the interior radiant tile as well. This type of dynamic control was not used in the simulations and was recommended for inclusion in future simulations to determine if the dynamically modulating flowrates make a significant difference in performance, and if so, under what conditions.

#### – What are the impacts of the Thermal Adaptive Building Envelope on building systems?

Chapter 6 integrated the results of the design attributes testing with the aim of interpolating the performance of the TACE modules as a part of heating and cooling systems. Initially, architectural impacts were investigated as to how the TACE systems could be directly integrated into the heating and cooling system to reduce the system usage and sizing. The results of the initial simulations showed that the system impact based on thermal gradient would not cause a significant difference in operation or sizing of traditional mechanical heating and cooling equipment. Thus, the primary impact was that the system works best as a decoupled system, directly adding and removing heat from an associated space.

The results of Chapter 6 also lend the system to being distributed, scalable and either independent of the primary mechanical heating and cooling systems or linked to a system that runs at similar temperature gradients such as a geo-exchange system. These observations directly influenced the design iterations and recommendations for the assembly type in ASI Prototype III as detailed in Chapter 7 and the UCW Prototype IV discussed in Section 8.1.2.4.

#### – What are the potential design limitations for the Thermal Adaptive Building Envelope system?

As delineated in Chapter 7, the impacts on building systems can be discussed in several ways: 1) the method of fabrication and installation of the TACE system, 2) the design of the integration and the design of the type of the mechanical heating and cooling systems, 3) the design of the façade as an architectural system.

The inquiry into the methods of fabrication and installation was primarily focused on reducing the amount of labour and parts while increasing the amount of exchange surface of the TACE exterior module. The impacts of the reduction of connections by maximizing the size of the TACE module was in the locations where working fluid leakages could occur and reduced thermal leakages due to uncovered or uninsulated connections between units. The reduction in parts through maximizing the TACE module size also suggested that factory installation into a unitized curtain wall system would reduce installation time and significantly reduce onsite labour.



As the TACE system included mechanical, plumbing and electrical components it was suited to factory assembled systems with integrated – and pretested – transportable units. The unitized curtain wall version allows for a more straightforward onsite install and aligns with the results of Chapter 4 that suggested a decoupling of the TACE system from the primary heating and cooling system being the most effective way for the TACE system to lower EUI. This conclusion was based on the simulated operating temperatures of the TACE system, and the normal ranges for operating temperatures for mechanical systems, including the ASHRAE recommended mechanical systems. This direct output of the TACE system and indirect integration into the mechanical system through prioritization of these systems based on available energy was shown to be the most effective use of energy, at least for the results of MVP Prototype I simulations. As a decoupled system configuration, multiple options for the primary heating and cooling system could be utilized. On the other hand, as proposed in UCW Prototype IV system design, having unitized modules with factory installed connection locations allows for an orderly integration of a geo-exchange loop in predetermined zones based on the structural and design bay that is easily mapped to thermal zones. This geo-exchange loop could be integrated into the TACE system at the thermal storage location to fill gaps in energy availability from the envelope or indoor environment resource.

As an architectural system, the envelope assembly also impacts daylight and viewsheds. As shown in Figures 8.1-8.3, the various methods of assembly, from rainscreen to unitized curtain wall, each trend towards a different architectural language of the façade. Each language addresses access to daylight and views in a different way. Considerations include the ease in which each system can modulate the WWR and its' customized based on geographical location or orientation.

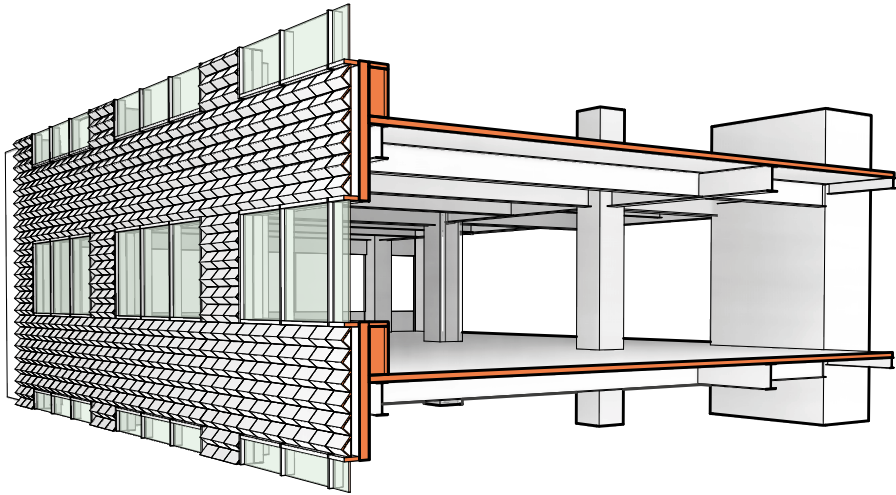


FIG. 8.1 Rainscreen and punched window deployment for the TACE system.

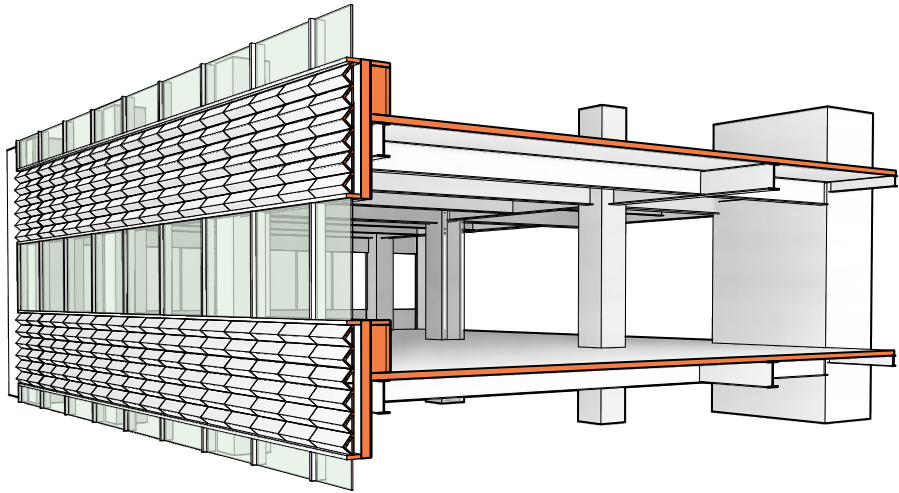


FIG. 8.2 Stick Built curtain wall deployment of the TACE system.

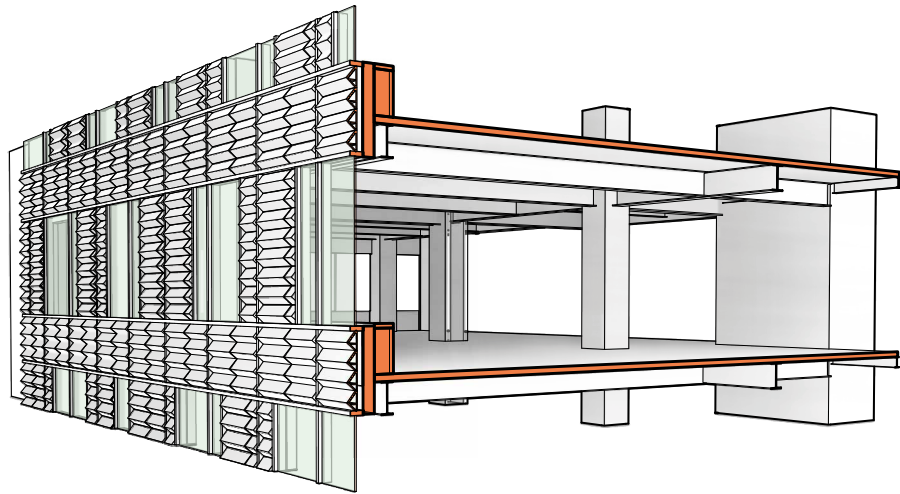


FIG. 8.3 Unitized Curtain Wall deployment of the system.

While not explicitly addressed as a research question in this dissertation, a discussion of the capital and operation cost impacts are critical when seeking to evaluate a new system and by extension, the impact of this research.

The capital costs can be looked at from two perspectives, the differences in installation methods and the differences in manufacturing technology. A rough order of magnitude (ROM) estimate of the TACE system indicates an approximate 85-95% performance upgrade cost over the typical ASHRAE recommended curtain wall envelope without TACE system integration. Based on the cost of a typical bay, the total per area cost was €2,305/m<sup>2</sup> (\$236/ft<sup>2</sup>) of TACE area in 2019 costs. The total cost of the envelope must factor in WWR as well as the overall complexity of the façade. When factoring in the increased heating and cooling potential of the TACE building, the size of the ASHRAE recommended VAV mechanical system may be reduced. The potential follow on impacts of reducing the size of the mechanical system may include: 1) additional floor space through size reduction or reduced footprint of alternative system type due to more efficient design (i.e., perimeter based Ground Source Heat Pump (GSHP) TACE system integration as described as part of UCW Prototype IV); 2) reduced size of supporting electrical equipment and associated reduced capital costs; 3) reduced size or removal of perimeter heating system in climates that might typically require it.

The complexity of the assembly of the TACE system and the desire to develop a reasonable ROI suggested that the path forward to development and deployment was to use a unitized curtain wall system as described in Section 7.5.3 and 7.6.1. The increased cost for a unitized factory assembled units may be offset by the reduction in onsite labour, field alterations, and overall construction time. In geographic regions where unions control the labour market, such as the NY Metro region, this reduction in onsite labour cost may become even more pronounced.

Three other factors are important to consider: 1) the rising price of energy over the building lifecycle; 2) the implementation of potential peak demand pricing for energy; 3) the location of the project.

Energy costs have been traditionally expected to rise on average about the same as the consumer price index, about 2.5% per year escalation. There was enough uncertainty in the forecast of energy markets that it was impossible to predict: the impact of climate change; the impact of renewable growth; deployment of smart microgrids; the impact of oil reserves; political and social dynamics, etc. What can be said for sure was that if the cost of energy exceeds the consumer price index, the payback period for deploying energy efficient building systems will reduce.

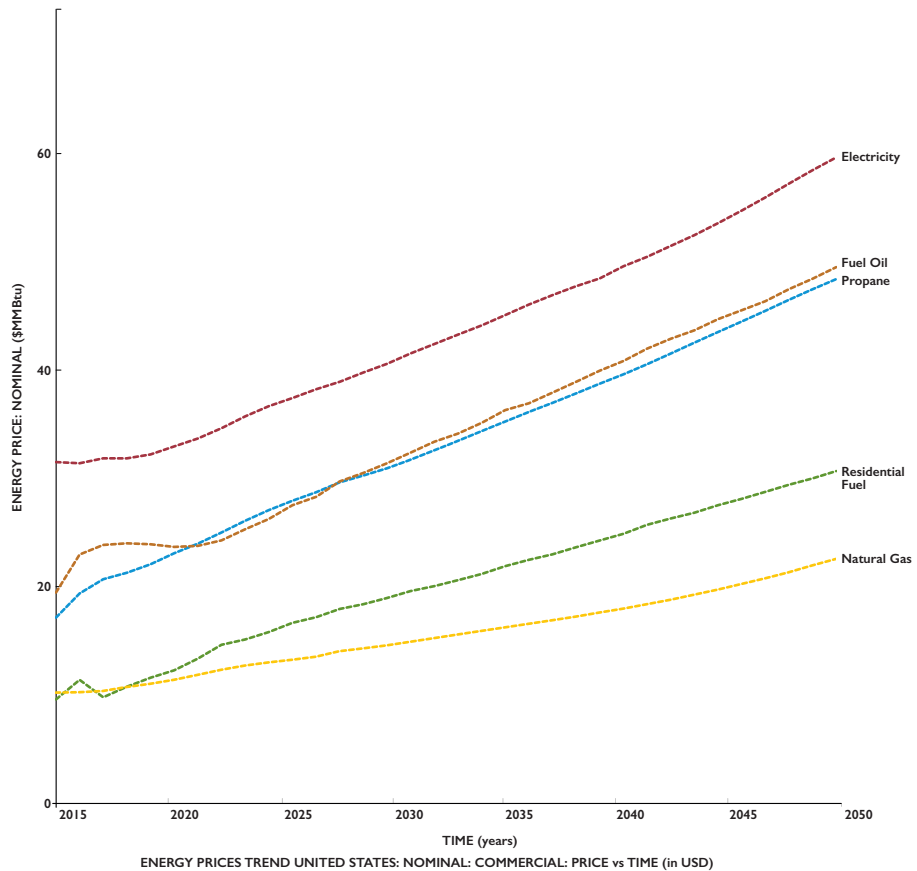


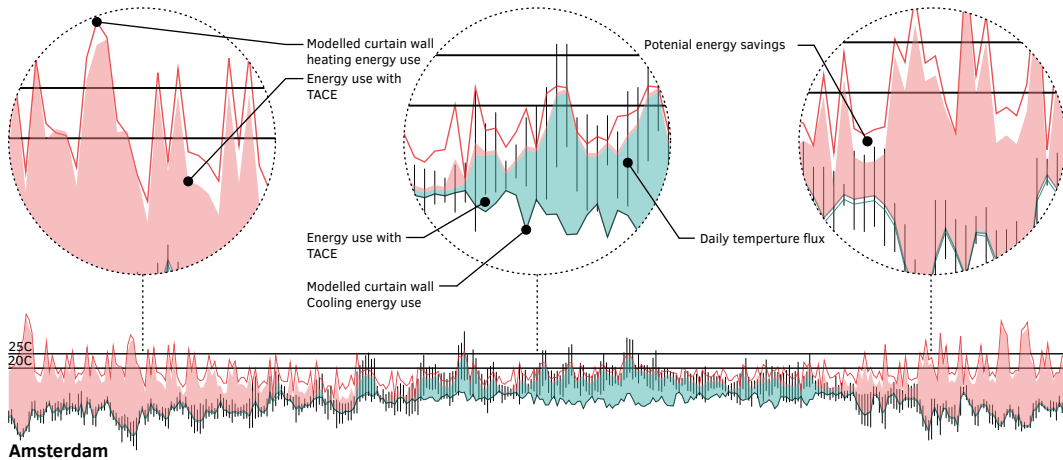
FIG. 8.4 Energy Information Administration 2019 Outlook and Trends for Commercial Energy Cost in USD (“Annual Energy Outlook 2019,” 2019).

What is expected to become more prevalent is peak pricing for energy and programs that support peak energy load shifting. While the EUI is a critical indicator of system efficacy, energy costs may actually drive adoption of systems that load shift energy demand out of peak demand time windows. Notably, several California utilities require users to load shift energy demand away from peak times to take advantage of reduced rates overall (Statewide Joint IOU Study

of Permanent Load Shifting, December 1, 2010). This policy incentive that is driven by utilities both serves to keep average energy costs down while promoting the adoption of building systems that have the capacity to load shift (Dyson, August 2015). Therefore, systems like the TACE system that can shift loads to non-peak time windows may compound savings by allowing the operational costs of the

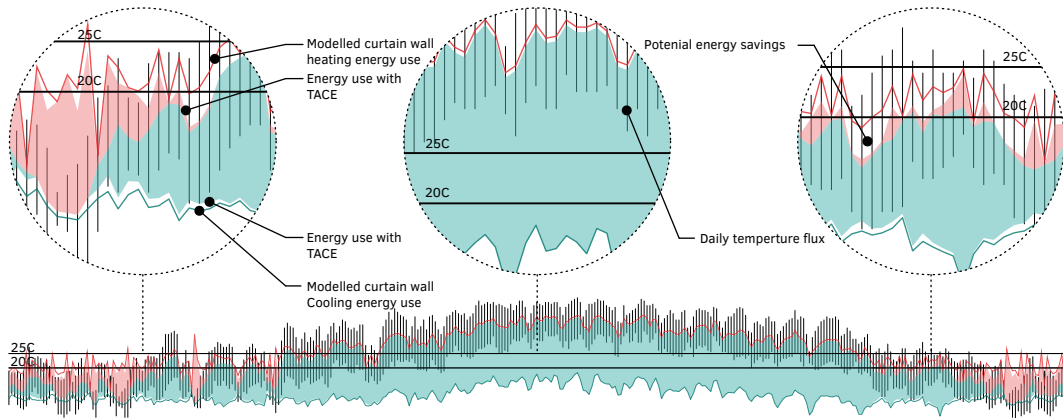
building due to energy costs to be reduced. So, while the EUI shows potential for operational savings, the load shifting potential would have the opportunity to make the energy shifting systems desirable choices for owner operators with an invested interest in the long term costs of operating their facility.

A third critical factor was the performance of the TACE system in different climate types. The analysis in Figure 8.5 showed how the TACE system might perform in Phoenix, Arizona and the Netherlands as compared to the New York Metro climate. These preliminary results indicate that the system works best in climates with a quality good solar resource.



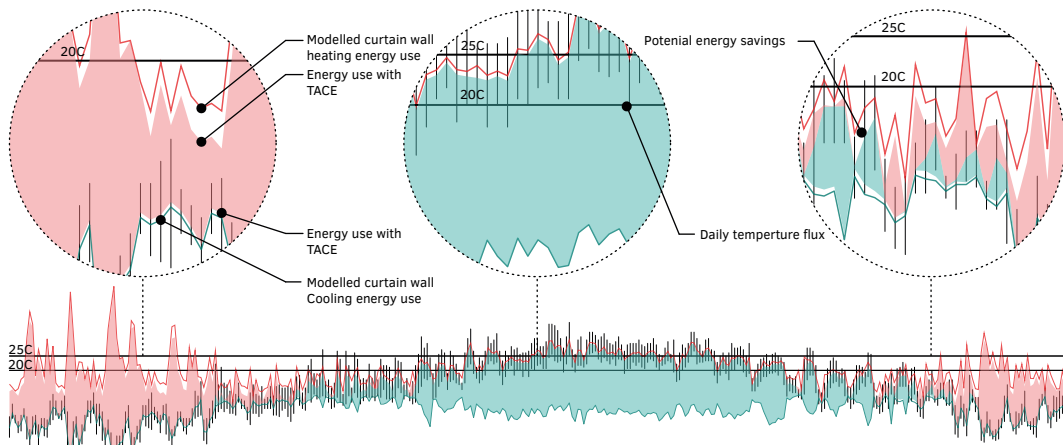
**Amsterdam**

**FIG. 8.5** Comparison of Amsterdam showing projected energy reduction impact due to TACE system. The graph is defined by correlating ASI Prototype III simulation data applied on the South, East, and West facades at 40% WWW with the modelled energy use of a 300,000 m<sup>2</sup> office tower.



**Phoenix**

**FIG. 8.6** Comparison of Phoenix showing projected energy reduction impact due to TACE system. The graph is defined by correlating ASI Prototype III simulation data applied on the South, East, and West facades at 40% WWW with the modelled energy use of a 300,000 m<sup>2</sup> office tower.



**New York**

**FIG. 8.7** Comparison of New York showing projected energy reduction impact due to TACE system. The graph is defined by correlating ASI Prototype III simulation data applied on the South, East, and West facades at 40% WWW with the modelled energy use of a 300,000 m<sup>2</sup> office tower.

## 8.1.2 Review of the TACE Prototypes

---

As discussed in Chapter 4, three physical TACE prototypes were developed during the research, each focused on different hypothetical aspects of the dissertation. MVP Prototype I focused on concatenating the hypothetical design principles of the TACE system into the ceramic components that were used for testing and calibration. POC Prototype II focused on demonstrating the viability of energy exchange between the exterior and interior TACE assemblies as part of a countercurrent energy exchange using industry standard ceramic production casting and pressing techniques. ASI Prototype III focused on demonstrating the potential of energy capture, storage and redistribution validating the hypothesis that thermal energy can be harvested and stored for load shifting. The fourth prototype, UCW Prototype IV, was a design proposal based on the analysis of ASI Prototype III and the review of system integration and assembly methods in Chapter 7. UCW Prototype IV was fabricated for the 4<sup>th</sup> annual Advanced Ceramics Assembly Workshop (ACAW) as shown in Section 8.1.2.6.

### 8.1.2.1 MVP TACE Prototype I

---

The first prototype, detailed in Chapter 4, was used for a series of tests to showcase a typical morphology and create the baseline to calibrate of the computational model used for simulation as delineated in Chapter 5. It was developed as part of the NEXUS-NY technology accelerator Grant. Several key observations resulted from the design, testing, modelling and simulation of MVP Prototype I:

- It was assumed that the most effective flow through the thermal transfer chamber would be where the working fluid entered through the lower rear of the chamber on one side and exited on the upper part of the opposite side. Preliminary CFD results as shown in Chapter 5 show that there was a better mixing and therefore more thermal transfer when the working fluid entered front the lower centre and excited from the upper centre of the TACE module. At the same time, it became clear through the CFD results that an optimal turbulent flow state was not achieved consistently throughout the thermal transfer chamber.
- It was assumed at the outset of the research that a greater surface area of the thermal transfer component would result in a corresponding increase in thermal transfer. While the increase in the thermal transfer was related to the amount of surface area, the length of the pins had a diminishing effect on thermal transfer as they grew longer in a nonlinear relationship. It can be reasoned that a more



significant effect of the increase in surface area, especially in flow conditions, was the turbulence in the flow that created the maximum thermal transfer. The flow rate, the geometry and the amount of working fluid appeared to be driving the thermal transfer ability of the thermal transfer component. This observation was corroborated with ASI Prototype III, which used the Rigidized Metals ViperTex product as the thermal transfer component, as discussed in Section 8.1.2.5. Prototype I showed that while that flow was important, modulating the speed of flow was also important, and an increase in surface area with specific patterns to create turbulent flow all had a relationship to modulating thermal transfer.

- While the results showed improvement over the ASHRAE recommended curtain wall, they were incremental and challenged how the unit was constructed and what components had the most effect and whose principles should be preserved in the next round of prototypes. During the testing process, it was challenging to keep the module assembly from leaking or weeping water. The challenges of creating a ceramic body that could hold fluid in an assembly would require using a porcelain grade ceramic, similar to bathroom fixtures. More research needs to be conducted on whether there is a viable pathway for development where the thermal transfer component and working fluid are in direct contact with one another.

### 8.1.2.2 POC TACE Prototype II

---

The second prototype was developed in collaboration with Boston Valley Terra Cotta to coincide with the 2<sup>nd</sup> Annual ACAW. Where the first prototype was used to determine that relative value of particular design decisions and build a baseline performance model for the system, the POC Prototype II was used to demonstrate the ability to transfer energy from an exterior TACE module to an interior TACE module. Key observations from the POC Prototype II were:

- While the attempt to merge the thermal transfer components and the exterior tile as developed in prototype I was achieved, the forming process of RAM pressing the component was incapable of providing the desired articulation of the thermal transfer forms to replace the pin plate in MVP Prototype I. Therefore, a significant amount of post processing work was required for significantly less final articulation. Further development of this morphology used in MVP Prototype I, which used slip casting, and POC Prototype II, which used RAM pressing, could evolve in the future using more sophisticated processes to achieve the required amount of detail, reduce production and post production time, and control warpage during the forming and firing process.

- As with MVP Prototype I, there was moisture moving through the faces of the ceramic over time. While moving to a terra cotta exterior clay body for prototype II significantly reduced seepage, terra cotta was designed to keep moisture out of the clay body, not hold liquids. This situation could be addressed in the design of the ceramic body. However, during the assembly of the front tile component with the back tile component, the exterior unit had multiple leaks which required many attempts to seal adequately. The propensity for leaks was due to several factors: 1) warpage of the tile components do the RAM press process and firing process; 2) assembly workmanship, which may have been better controlled in a factory environment, but may always present an issue.
- Direct energy transfer was achieved by pumping water through the exterior TACE module into a storage container, then pumping the water from the storage container through the interior TACE module. Using a thermal imaging camera, it was clearly observed that energy was transferred from the exterior tile to the storage container and into the interior tile. However, this set up proved challenging to control as the two loops formed an open system and created potential weak points in the system design, including maximizing energy transfer while attempting to load shift. MVP Prototype I used 40.8 l/m<sup>2</sup> or 5.69 litres per module (1 gal/ft<sup>2</sup> or 1.5 gallons per module) where POC Prototype II had 26 l/m<sup>2</sup> or 3.74 litres per module (0.64 gal/ft<sup>2</sup> or 1 gallon per module) and ASI Prototype III had 1.5 l/m<sup>2</sup> or 0.22 litres per comparable module (0.036 gal/ft<sup>2</sup> or 0.058 gallons per module). This larger volume of working fluid appeared not to be as useful in energy transfer as a smaller volume of working fluid. These issues were addressed in ASI Prototype III.

### 8.1.2.3 ASI TACE Prototype III

The third prototype was developed with Boston Valley Terra Cotta for the 3<sup>rd</sup> annual ACAW, similarly to POC Prototype II, but utilized an industry standard ceramic extruder for production. ASI Prototype III was designed to incorporate several observations from the previous prototypes: 1) reduction in working fluid volume; 2) reduction in seepage and reduced risks of workmanship errors, 3) isolated working fluid loops and a separate thermal storage loop. Key observations from ASI Prototype III are:

- The ratio of surface area to water volume appears to be a significant factor of system efficacy. Prototype III significantly reduced the volume of water from the previous prototypes and showed a significant improvement that was observed in the physical prototype and corroborated in the computational model and simulations when compared to prototype I. Future work should be conducted to isolate the effect of changing this ratio.

- A key aspect of understanding the behaviour of fluid flow and thermal transfer with the TACE model was understanding the flow rate through the working fluid chamber where the Nusselt number and Reynolds number intersect showing an increase in thermal transfer at the optimal turbulent flow. In this prototype, the Vipertex product used was designed to balance the flow rate in the zone at the intersection of the Nusselt and Reynolds numbers to control the rate of transfer by controlling turbulence within the thermal transfer chamber.
- The Vipertex product had increased surface area over a comparable smooth tube and a pattern designed to induce turbulence in the working fluid. While the increase in surface area was less proportionately than the MVP Prototype I, thermal transfer component pin plates, the volume of working fluid was significantly less. It can be reasoned that there was near constant turbulent mixing throughout the thermal transfer chamber unlike in the MVP Prototype I, which, along with a reduced volume of working fluid accounts for a significant amount of the increase in thermal transfer.
- Overall this prototype design appears to be most promising for further development from a module and systems perspective. Prototype III: reduced failure points and removed seepage issues; can be developed into a unitized curtain wall assembly as described in UCW Prototype IV design in Section 8.1.2.6 and can integrate as a system into other mechanical heating and cooling working fluid based systems.

#### 8.1.2.4 UCW TACE Prototype IV Design Proposal

---

UCW Prototype IV, as shown in 8.8, was conceived as a conceptual design exercise that incorporated the observations and lessons learned from each of the three preceding prototypes. Based partially on the corroborated computational modelling and simulation results and the design analysis in Chapter 7, prototype IV was viewed as the evolution of the design based on a combination of physical testing, industry standard approaches and best practices. Fundamentally, prototype IV acknowledged the benefits and drawbacks of the TACE system and attempted to overcome the barriers to the acceptance of a countercurrent energy exchanging building envelope in the marketplace.

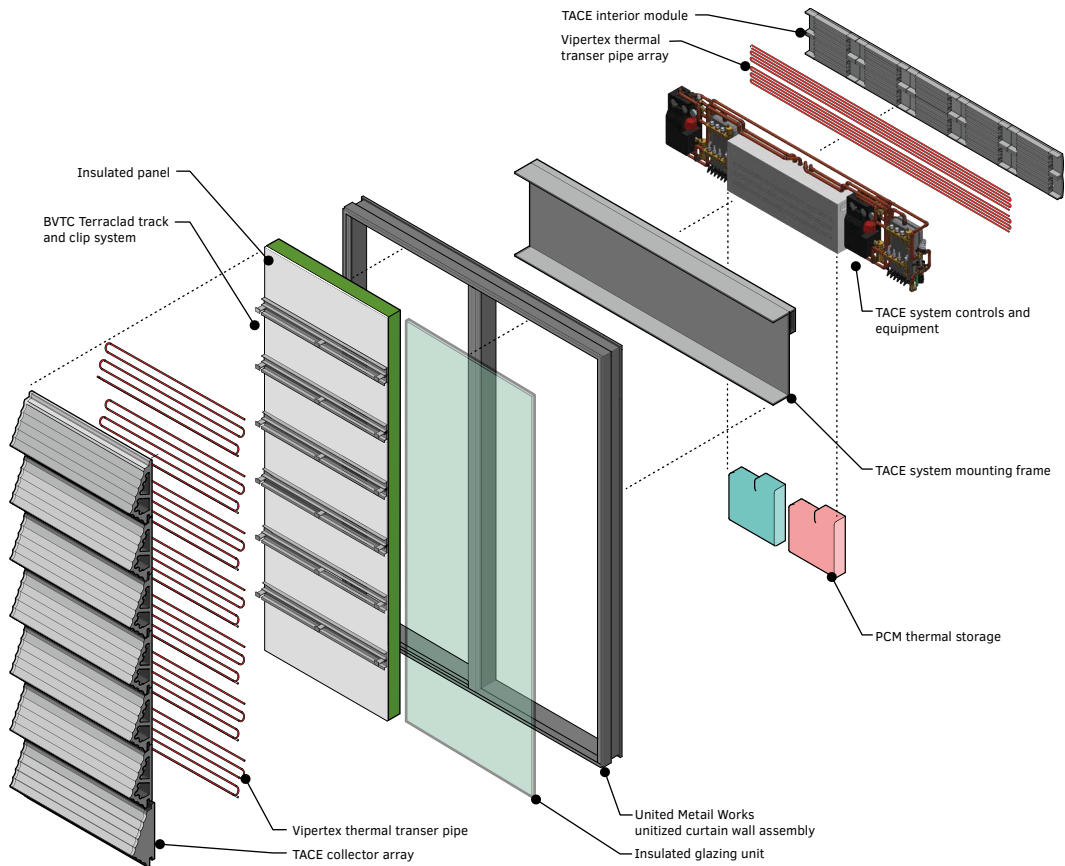
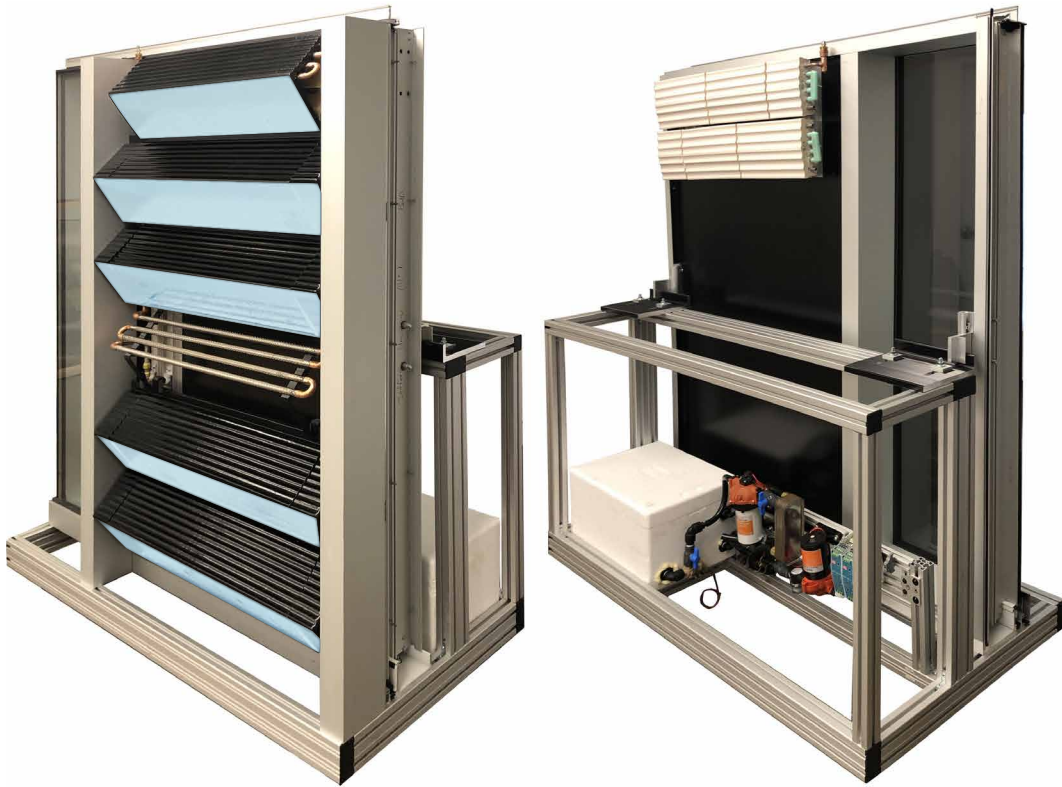


FIG. 8.8 Analytique of UCW Prototype IV Design.

### 8.1.2.5 Design Recommendations

The following design recommendations framed the design decisions for UCW Prototype IV, as shown in Figure 8.9, as a building envelope, as a system, and as designed in an architectural design language.



**FIG. 8.9** UCW Prototype IV developed for the 4<sup>th</sup> annual ACAW in August of 2019. The prototype was developed with direct support from United Architectural Metals, Rigidized Metals, and Boston Valley Terra Cotta.

#### 8.1.2.5.1 Component and Module Design Recommendations

The primary components of the ASI Prototype III were the extruded exterior tile, the thermal transfer pipe and the interior radiant tiles. These three components were carried over to the UCW Prototype IV design proposal with the following recommendations:

- The success of integrating the Vipertex thermal transfer component was carried over to the unitized curtain wall version. The relative weak points of prototype III were the multiple joints at the thermal transfer components. As shown in Figure 8.10, the thermal transfer tubing could be formed as a single pipe each time, significantly reducing joints, and thus reducing weak points, material and labour costs.

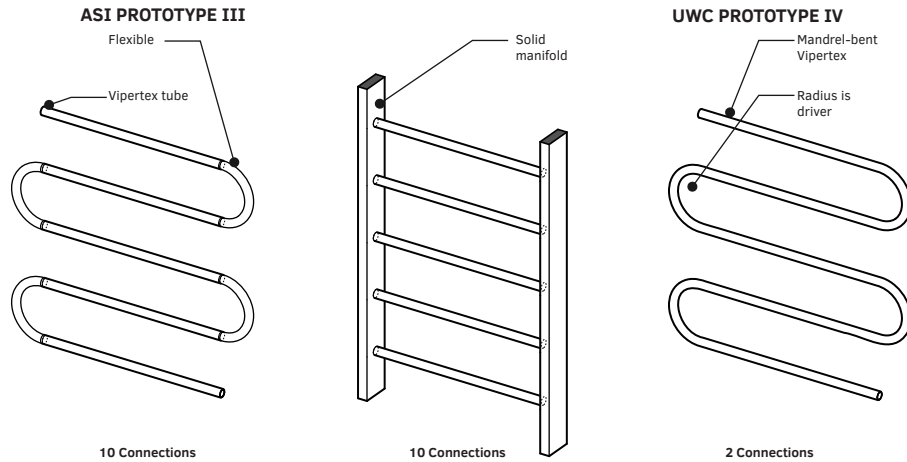


FIG. 8.10 Reduction of connections as developed from prototype III to IV.

- The exterior tile was based on the geometry of ASI Prototype III; however, in the UCW Prototype IV design, the exterior tile was maximized for production and factory assembly. The resultant tile was  $0.766 \text{ m}^2$  ( $8.3 \text{ ft}^2$ ), where ASI Prototype III was  $0.139 \text{ m}^2$  ( $1.5 \text{ ft}^2$ ), a 551% increase over prototype III, further reducing joints and weak points. As per Section 7.4.1, the tile absorbing face could be adjusted in altitude based on cardinal direction facade of the building envelope for which it was designed.
- The interior component was designed as a radiant tile in ASI Prototype III. In UCW Prototype IV, two radiant tiles were proposed; 1) a perimeter heating tile, and 2) and perimeter cooling tile. Both have been integrated, and in the TACE Prototype IV fully integrated system proposal, the geo-exchange loop was linked directly to the distributed storage (SunAmp) and indirectly to the radiant panels of the TACE system. As shown in Figure 8.11, the radiant heating panel was located at floor level. The vertical location within the office space allowed for the rising heat to address the load directly at the source first, (i.e., fenestration), creating a mixed temperature air that could be pulled through the office space to be either recirculated or to the return location. The absorbing panel (i.e., radiant cooling panel) was located vertically at the top of the bay section where the cooled air flowed down across the load (i.e., fenestration) and mixed into the occupied office space before either recirculating or going into the return air plenum.

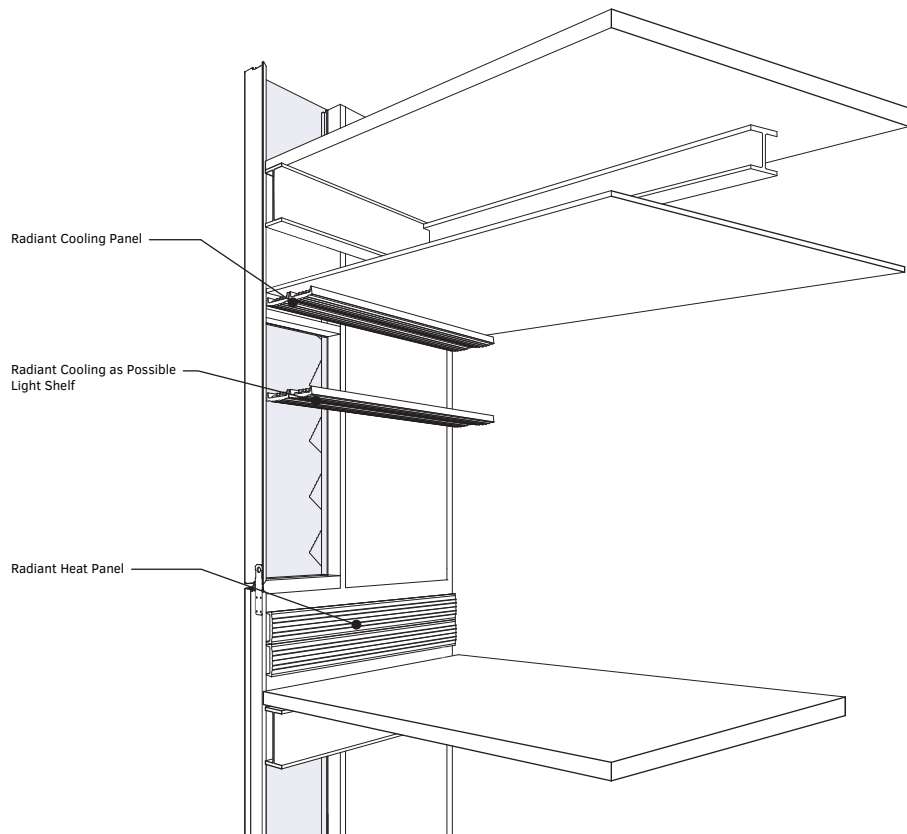
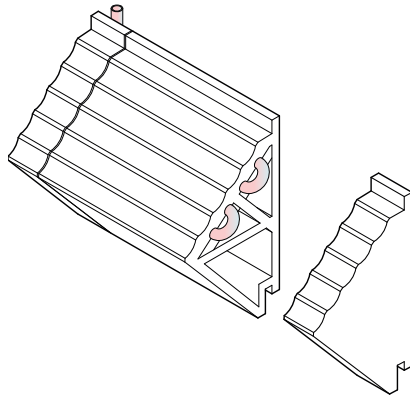


FIG. 8.11 Diagram of radiant panel locations for future work.

- The radiant cooling panel can adopt the form on the ceiling or serve as an integrated light reflector, as shown in Figure 8.11, and should be investigated as part of future research. The cooling, or absorbing panel, can be factory installed and was the same as installing a radiator type fixture for heating. In the case of the geo-exchange loop integration, labour was already required to be onsite for the connection of the loop to the TACE system; thus the lift to install a separate cooling panel can be partially absorbed by the same labour team.
- For assembly and access, ceramic end caps were required, as shown in Figure 8.12. These end caps allowed access from the exterior envelope without disassembly from either the inside or the structure and framing components of the Schüco 65 system.



**FIG. 8.12** Endcaps required for extrusion design. This assembly as the prototyped and modelled current version either must capture or offload thermal energy, restricting the adaptive potential of the TACE system.

- The thermal performance of ASI prototype III, designed and assembled to be similar for prototype IV, showed a more balanced heating and cooling capability than prototype I. While the cooling capacity for the NY climate, for example, was reduced in prototype III, heating capacity was significantly improved. To improve the cooling capacity of prototype III, two alternative designs were proposed as shown in Figure 8.13: 1) adding a cooling loop on the shaded side of the tile; 2) separating the single TACE tile into two separate tiles. The expectation of these potential options was twofold: 1) there would be a significant increase in performance; 2) as there was an increase in complexity, the first cost would increase necessitating an in-depth ROI study.



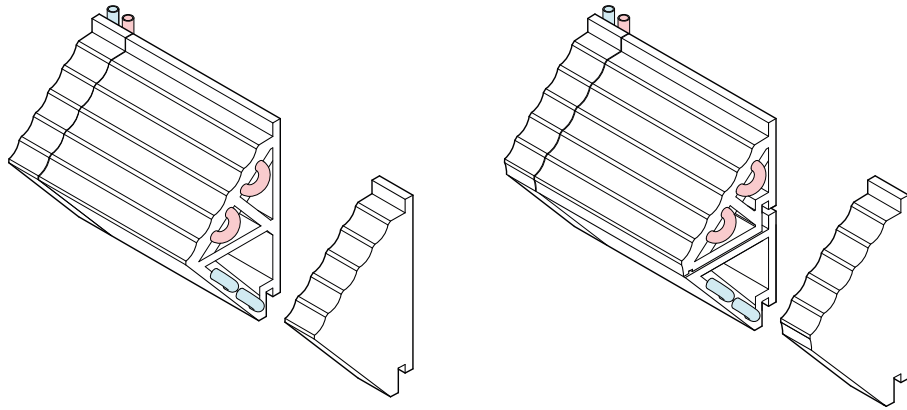


**FIG. 8.13** Diagrams of thermally improved prototype proposals for future study. The left arrangement separated cold and hot loops, and the right arrangement separated the tiles into a cold loop tile and a hot loop tile creating 1) a thermally broken assembly, and 2) the ability to simultaneously capture and offload thermal energy in that same assembly.

#### 8.1.2.5.2 System Design Recommendations

While the TACE system, based on the weather files in New York, Amsterdam and Phoenix, appeared to work effectively for extensive periods of the year as shown in Figure 8.14 the same Figure also showed gaps on an apportioned annual basis where the available thermal resources in, on, and around the building envelope did not significantly contribute to lowering the energy required to achieve occupant thermal comfort. The identification of these gaps in usability was perhaps the most significant finding coming from the investigation in Chapter 6 from a systems perspective and helped formulate the hypothesis for the system design proposal for the UCW Prototype IV that linked the heating and cooling mechanical systems directly to the energy transfer function of the building envelope. While it was reasoned in Section 6.4.1.3 that linking the thermal energy captured by TACE directly to the mechanical system was not practical due to the normal operating temperature ranges being outside of the TACE system temperature ranges, the equipment for delivering heating and cooling at the perimeter of the façade was nevertheless already in place for the times of year that the system was simulated to work. Therefore, it was reasonable to propose a mechanical system that could be integrated into the existing TACE infrastructure to fill the gaps.

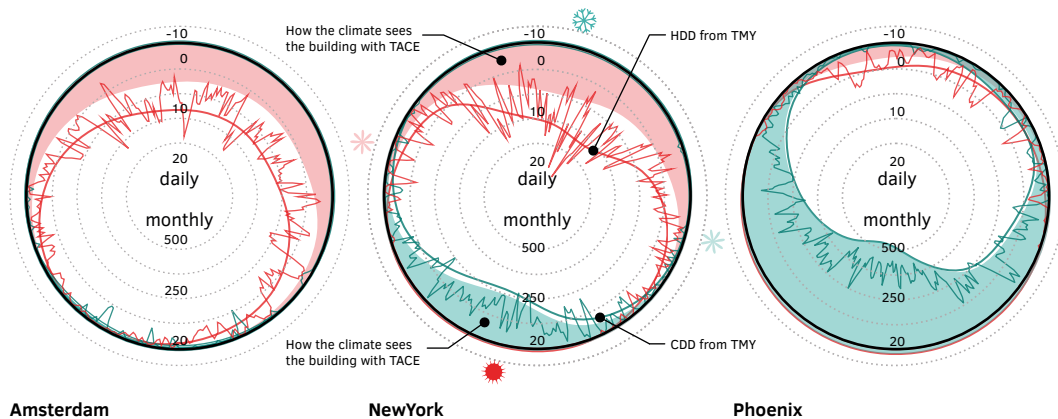


**FIG. 8.14** Climate diagrams showcase available resources and should play a role in determining how the TACE system should function to be most effective in local conditions

While the temperatures that were available from the TACE system working fluid were neither hot nor cold enough to link directly into a traditional HVAC system, other fluid based systems could link into the façade integrated radiant heating and cooling panels to provide thermal exchange outside to fill the gaps that face the TACE system. Geo-exchange or Ground or Water Source Heat Pumps where feasible based on site availability, for example, could cover short term (i.e., day to day weather anomalies) and long term (i.e., seasonal shifts) to make the TACE system fully utilized for the annual cycle. Leveraging a heat pump with distributed terminals at the exterior of the building could further reduce the size of the primary heating and cooling system, perhaps even reducing it to an auxiliary or secondary system that provides cold required make-up air, and most certainly would reduce the annual energy use intensity overall. This hybridized system then addressed the entirety of the year from a normal and peak loading perspective.

ASI Prototype III showed that heating and cooling were both viable modes of operation, and with further development, the TACE module could be shown to be more effective based on recommendations for development as discussed in Section 8.1.2.3. When integrated into a multizone geo-exchange system as described previously, it may be possible to deploy TACE modules that are optimized for heating, cooling and combination arrays, as shown in Fig. 8.15 to improve overall system efficiency.

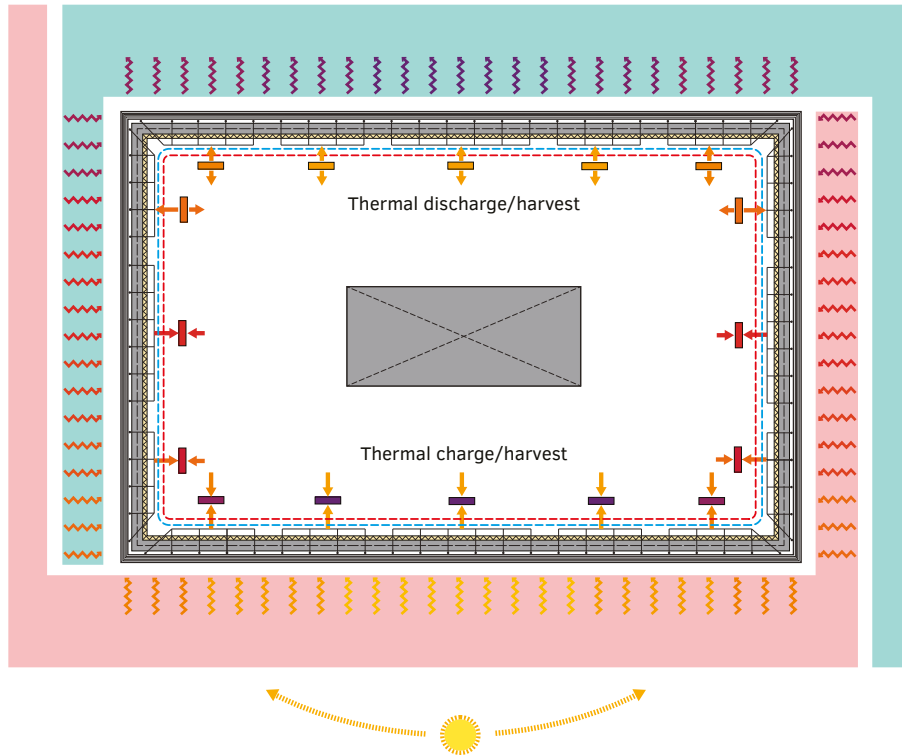


**FIG. 8.15** Multizone TACE system array showing TACE module arrays biased for heating on the south, cooling on the north, or in combination on the East and West faces of the floorplate. This diagram also shows a connection to a geo-exchange loop. This arrangement, when deploying the TACE modules in Figure 8.12, can heat, cool, and store thermal potential simultaneously.

The TACE system specifically targets the heating and cooling functions of the HVAC system, it does not address directly ventilation and indoor air quality. In a similar way to how the TACE system would work in concert with GSHP to reduce energy use, it should also be matched with appropriate on demand ventilation systems. The Fresh-r smart indoor air system developed by Jón Kristinsson is a distributed envelope integrated on demand ventilation and heat recovery system that could serve as a parallel system to further support energy savings and improve indoor air quality (Maack & Gunnarsson, 2016). As both envelope integrated systems, TACE and Fresh-r together could be arranged to work together and is worthy of further modeling and integration studies in order to build a more comprehensive systems approach to reimagining HVAC.

### 8.1.2.5.3 Assembly Type Recommendations

The complexity of assembling mechanical systems and the integration of required trades as part of the assembly labour for an onsite installation suggest that factory assembly of the TACE system would be the preferred method. Delivering the building envelope packaged as a façade reduces potential field errors and addresses regional labour policies, requiring that the complexity of integrating the TACE system as akin to plugging in an appliance. To illustrate the potential of factory installation UCW Prototype IV was developed on a largely unmodified Schüco 65 unitized curtain wall system.

### 8.1.2.5.4 Design Language Position

Differing methods of assembly lend themselves to differing architectural aesthetics. Typical modern terra cotta rainscreens can take many differing aesthetic positions but tends towards a rain screen aesthetic typology, privileging punched windows, for example, and in many ways represents, visually, a modern evolution of the traditional masonry and masonry cavity walls. Curtain wall typologies are equally as distinct as the rain screen design, regardless of whether it is stick built or unitized type. The unitized aesthetic becomes distinct when the traditional curtain wall aesthetic is challenged by having to integrate substantial portions of opaque thermal exchange surface and integrate an active mechanical system into the unit. The aesthetic precedent, as applied in Figure 8.3, was developed in the 2000s as a flexible and modular façade design approach, applied to projects with programs ranging from institutional, multifamily residential and commercial office space. Regardless of the particular aesthetic approach, the reality is that opaque facades will always exist, whether that is due to program (i.e., data centres) or locations (i.e., infill projects), or as a means to reduce WWR, in each instance giving an opportunity for the opaque elements to contribute meaningfully and actively in the performance of the building.

## 8.1.3 Valuation of the research proposition

While valuation can be in terms of capital and operating cost reductions as discussed in Section 8.1.1.2, there are several other viewpoints with which to support the research proposition: greenhouse gas emissions; comparison to other façade integrated energy harvesting technologies.

### 8.1.3.1 Greenhouse Gas Emissions Reduction Potential

---

Another critical method of understanding the value of any TABS system as part of an overall energy reduction strategy is to value the savings in greenhouse gas emissions. The reduction in greenhouse gas emissions was a key driver in the regulatory framework that is driving plans such as California's Title 24 and New York City's 80/50 Plan. Consequently, the Zero Net Energy rating system was used to drive a reduction in greenhouse gas emissions. While this study does not take into account cradle to gate emissions, greenhouse gas reduction is a valued assessment for new technologies in the market.

As part of the GTAC grant, initial greenhouse gas savings were calculated by the granting agency based on the modelled savings from the simulated results using the MVP Prototype I. The calculations were conducted using the Howe Center as the basis for comparison.

Potential Carbon dioxide emissions for the existing Howe Center Envelope, the ASHRAE recommended curtain wall envelope and the TACE system were developed from the energy utilization as shown in Table 6.3. As Figure 6.4 showed a single floor energy utilization only, each calculated result was multiplied by the total number of floors to achieve the calculation for the entire building. This calculating method was a gross approximation, while many floors repeat, there are multiple programs in an office building; however, the model can still be used for an apples to apples comparison.

It was important to note that emissions impacts will also vary due to geographical location as per the local ratio of various fuels used to make electricity. The US national average ( $7.44 \times 10^4$  t CO<sub>2</sub> / kWh) are shown in Table 8.2, and for localized comparison, the New York State 2015 average ( $2.35 \times 10^4$  t CO<sub>2</sub> / kWh) are shown in Table 8.3. The emissions attributed to natural gas are developed from the United States Environmental Protection Agency (EPA) estimates of 0.0053 t CO<sub>2</sub>/btu, equivalent to 0.05025 t CO<sub>2</sub> / GJ (EIA; EPA, 2017).

The following are the results based on the calculations for the MVP Prototype I as shown in Table 8.2 and 8.3:

- 453 t CO<sub>2</sub> (38%) reduction for the existing Howe Center building envelope based on US average electricity emissions.
- 21 t CO<sub>2</sub> (2.8%) reduction as compared to an ASHRAE curtain wall as applied to the Howe Center building envelope.

TABLE 8.2 Annual CO<sub>2</sub> emissions based on US average electricity fuel mix.

EPA US Avg Emissions (t CO <sub>2</sub> )	Existing	ASHRAE	TACE	TACE Reduction from Existing	TACE Reduction from ASHRAE
Electricity	1005.6	685.1	674.8	32.9%	1.5%
Natural Gas	187.1	76.1	65.0	65.3%	14.7%
Total	1192.9	761.2	739.7	38.0%	2.8%

TABLE 8.3 Annual CO<sub>2</sub> emissions based on New York State electricity fuel mix.

New York State Avg Emissions (t CO <sub>2</sub> )	Existing	ASHRAE	TACE	TACE Reduction from Existing	TACE Reduction from ASHRAE
Electricity	318.3	216.8	213.5	32.9%	1.5%
Natural Gas	187.1	76.1	65.0	65.3%	14.7%
Total	505.4	292.9	278.5	44.9%	4.9%

Based on the reasoned improvement in performance from the stack test that appeared to be demonstrated by ASI Prototype III, would result in a TACE system reduction (in heating cycle only) in an apples-to-apples comparison of:

- 564 Metric Tons CO<sub>2</sub> (30%) reduction for the existing Howe Center building envelope based on US average electricity emissions using Prototype III.
- 132 Metric Tons CO<sub>2</sub> (8%) reduction as compared to an ASHRAE curtain wall as applied to the Howe Center building envelope using Prototype III.

To develop a more accurate account of greenhouse gas emissions savings, a more robust calibration, model and simulation should be conducted based on the ASI Prototype III and the proposed integrated design for the UCW Prototype IV.

### 8.1.3.2 Comparison to Photovoltaic Systems

There are several notable differences between the TACE system and an integrated photovoltaic façade. While the output of an integrated photovoltaic panel and the output of the TACE system may be comparable, the energy from the photovoltaic system is directly converted to electricity and thus can be used for a variety of energy needs, included powering air or ground source heat pumps. It can be reasoned that the flexibility of energy conversion to an electrical source is preferably

in an apples to apples comparison. The equivalent area of PV ( $1 \text{ m}^2$ ) energy results in  $1369 \text{ kWh/Kwp}$  or  $207 \text{ kWh/m}^2$ . The annual heating and cooling capacity of the MVP Prototype I at  $2.50 \text{ l/min}$  ( $0.66 \text{ gpm}$ ) was  $959.68 \text{ kWh/yr/m}^2$  generated for heating and  $-373.41 \text{ kWh/yr/m}^2$  for cooling. When powering a ground source heat pump, for example, building integrated PV can reasonably be expected to produce heating production of  $622 \text{ kWh/yr/m}^2$  or  $-933 \text{ kWh/yr/m}^2$  of cooling in the NYC metro region climate as shown in Table 8.4.

Taken as a comparison between PV generation, Solar input of a typical panel is  $1000 \text{ W/m}^2$  on average with an efficiency factor of 17% resulting in  $170 \text{ W}$  of production. The average solar insolation for three comparable locations for PV production, as shown in Table 8.4, which shows the apple to apples comparison for the TACE system and an integrated PV façade linked to GSHP and Water Source Heat Pump (WSHP).

**TABLE 8.4** Comparison using PV powering GSHP (COP 3 heating, 4.5 cooling) or WSHP (COP 2.5 heating, 3.5 cooling) and TACE ASI Prototype III at 2.5 l/min (0.66 gpm) and 22 °C inlet ground temperature.

MODE	New York (4.3 kWh/m <sup>2</sup> /day)		Amsterdam (3.3 kWh/m <sup>2</sup> /day)		Phoenix (7.1 kWh/m <sup>2</sup> /day)	
	1369	kWh/kWp	902	kWh/kWp	1717	kWh/kWp
	207	kWh/m <sup>2</sup> PV	137	kWh/m <sup>2</sup> PV	260	kWh/m <sup>2</sup> PV
PV GSHP (kWh/yr/m <sup>2</sup> )	Cooling	933	615	1171		
OR						
PV GSHP Heating (kWh/yr/m <sup>2</sup> )	Heating	622	410	780		
PV WSHP Cooling (kWh/yr/m <sup>2</sup> )	Cooling	726	478	911		
OR						
PV WSHP Heating (kWh/yr/m <sup>2</sup> )	Heating	519	342	650		
TACE ASI Prototype III (kWh/yr/m <sup>2</sup> )	Cooling	1011	391	1646		
AND						
TACE ASI Prototype III (kWh/yr/m <sup>2</sup> )	Heating	207	249	5		

When looking beyond an apples to apples comparison, there are several key distinctions in the functional design of the TACE system that created potential differentiating values: 1) low energy heating and cooling in shoulder months, 2) architectural aesthetics, positive or negative, of the building envelope façade, 3) ability to work in cooling mode without a solar resource and heating mode when ambient temperatures are high or low without direct sunlight, 4) temperature driven has potential to extend beyond the typical solar day based on weather and seasonal conditions, 5) nighttime operation based on weather and seasonal climate conditions.



## 8.1.4 Propositions for Future Work

---

The results of the research suggested a series of propositions for future work. Further research and development should advance a more resolute understanding of how the countercurrent heat exchange function of the building envelope using terra cotta components may offset mechanical heating and cooling energy in either time or length scales (i.e., load shift or reductions/augmentations).

### 8.1.4.1 Testing Recommendations for TACE

---

An integrated systems computational model that links the TACE system and the mechanical heating and cooling system are suggested to look for further refinements and sizing characteristics for the mechanical heating and cooling system. This should include an analysis of fresh air intake requirements and energy effective ways to provide fresh air that works in conjunction with the systems' fluids.

To achieve enhanced understanding of the TACE system, the following modelled as part of an integrated mechanical heating and cooling system as described by UCW TACE Prototype IV Design Proposal, 2) reduce the capital and operations costs, 3) model the controls of variable flow rates, 4) investigate integration in a working fluid based mechanical heating and cooling system.

There is currently no direct physical comparative test conducted between MVP Prototype I and ASI Prototype III; this should be conducted to confirm the corroborated and simulated performance differences.

In ASI Prototype III, no comparison was conducted between smooth heat transfer tubes and the Vipertex product. While the simulation used the Vipertex to develop a ROM for performance, Vipertex claims a rough order of magnitude performance increase of up to 10 times comparable products under certain conditions.

It was essential to develop a more robust comparison for thermal transfer efficiency that compares thermal transfer component geometry, flow rates, associated Nusselt and Reynolds numbers and the role of the volume of water and the shape of the thermal transfer chamber.

While the issue of make-up air has not been investigated and assumed as a component of the base building mechanical system, make up air can be delivered in a similar countercurrent flow as demonstrated by Schuco system 65 as part of the

fenestration and should be investigated in future work as part of the development of the UCW Prototype IV.

It is critical to investigate in greater detail the premium cost for equipment and of the TACE system and how this may be offset by lowering of operating costs and the potential to support efforts in ZNE and High Performance Office designs. It is worth investigating the TACE system as part of a deep energy retrofit or new construction as part of an Energy Savings Performance Contract that average operating savings to afford higher performing systems in the capital stages of a project.

#### 8.1.4.2 Heat Balance and Advection

---

The heat balance equation is referenced in Section 2.3.1.2 and describes the heat flow through the building envelope. One way to begin to evaluate TABS as envelope systems would be to create a performance metric as a quotient on which to make comparisons for system development. Future work should include developing this advection quotient and could be phased:

$$\dot{Q}_{advection} = \frac{1}{AU(T_{inside} - T_{outside}) - W_{captured}}$$

Thus to derive an advection quotient, first calculate the heat balance equation and second subtract the amount of captured work energy per area, then create a percentage of efficiency for TABS in an envelope configuration.

#### 8.1.5 Potential Impact on the Discipline

---

The trajectory of technological innovation in the disciplines of architecture, sciences and engineering related to buildings has been towards the increased compartmentalization of knowledge (i.e., the separation of systems to be distinct from one another). For architecture, there has been an intense pressure for specialization within the discipline often at the behest of economic expediency rather than disruptive innovation; current advances often address that which can be made faster and cheaper by the reduction in labour and materials, though the construction

industry as a whole architecture remains the only modern industry that is trending towards lowered productivity (“Efficiency eludes the construction industry,” 2017).

In the steep face of these economic pressures, the AEC industry as a whole has struggled for a clear roadmap towards increased productivity that supports environmental stewardship while architectural design has found some traction in exuberant expressions of form without the constraints of forces; a decidedly biotic aesthetic without the biotic performance. On the other hand, for the science and engineering disciplines engaged in building specialization has been necessary for the more profound understanding of the part; its quantities, weights and measures, investigated most often without the complexity of interdependence with design, and construction and finance. Without performance and interdependence, it is impossible to engage the advantages of ecology-based or performance-based paradigms in impactful ways. The differing approaches among architects and scientists and engineers have exacerbated a significant rift in the process of making highly performative architecture based on systemic integration with a few notable exceptions. The processes of designing, making, and operating a building have become by-in-large independent pursuits (rather than interdependent, biotic and ecology-based) that have not significantly advanced in the last half century concurrent with construction industry at large (Vollen, 2009).

Following this trend, contemporary building technology practice dictates the development of systems in isolation (i.e., closed loop) subsequently precluding the possibility of multiple systems working synergistically (e.g., linked through advection) to extend the available resources at the building envelope. To be a truly disruptive green building innovation, a novel system must address multiple conflicting factors, coupling thermal and electrical resource for heating, cooling, and lighting, while adopting a distributed and systems-integrated approach. For next generation envelope systems to be developed as truly energy effective with the potential for widespread deployment they will require: 1) a comprehensive multi-modal approach for thermal and electrical simulations, 2) integration of specific material properties with parameters relevant to gradients across the building enclosure, and 3) an economic model for the valuation of the envelope that has the potential to affect policy that encourages deployment. The research developed for this dissertation is an example of an approach that views locally available and transient energy flow as significant resources that are encouraged to flow through the building envelope usefully instead of being rejected from it. To effectively engage these flows with the constant and fluctuating nature of occupant demand, the next generation of building envelopes will be required to be both adaptive and capable of controlling the multiple energetic resources on a variety of scales across the building systems matrix. A potential foothold then for the position of the architect - and the

AEC industry at large - is to view these resources as the primary driver of building envelope design as incorporated into design frameworks and energy simulations that responds to the institutional drivers of policy and valuation.

From a conceptual perspective, the conventional approach to the design of the building envelope is largely based on the First Law of Thermodynamics, that energy is neither gained nor lost – it is conserved. Based on the First Law approach, buildings use energy to mitigate energy (e.g., mechanical systems use external sources of energy to mitigate climate and interval energy loads), where efficiency is increased by increasing the resistance to energy in passing through the building envelope at a set rate, the R-Value. The Second Law of Thermodynamics states that entropy always increases towards a state of equilibrium – it transfers. The 2<sup>nd</sup> Law approach to building envelope design manages the increase in entropy to more effectively use the already available resource – and in doing so, proposes to merge the traditional disciplinary silos. Thermo Active Building Systems – and the TACE system are Second Law approaches to thermal management to manage entropy production, and offer a multidisciplinary opportunity to increase energy effectiveness of the building envelope as a matter of practice.

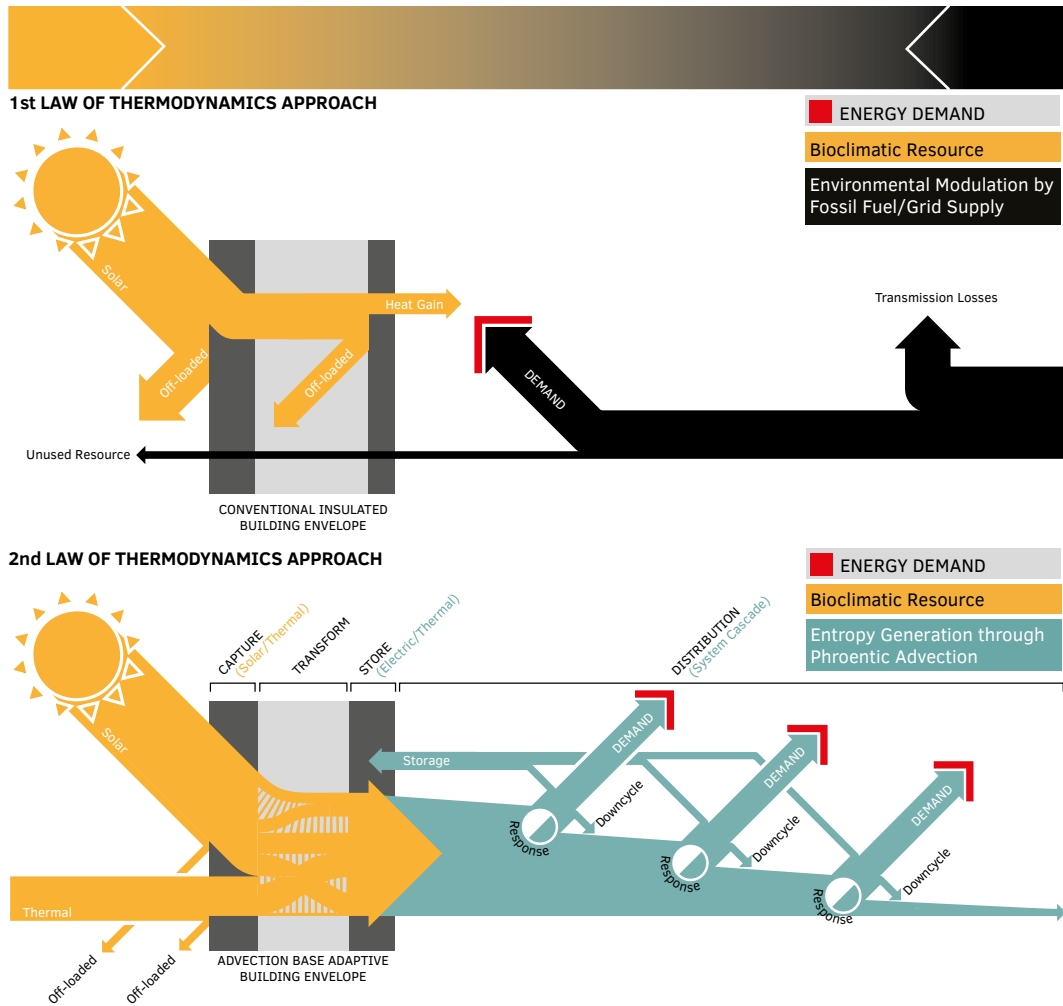


**FIG. 8.16** Diagram of the First Law and Second Law of Thermodynamics in relation to the building envelope. The First Law approach encourages disciplinary segregation, whereas the Second Law may encourage disciplinary cooperation. Adapted (Vollen & Shen, 2015).

## 8.2 Reflections on the Research

---

The philosophical underpinnings of the methodology and research design were based on the quasi-experimental method that supports the acts of discovery through causal inference. While this method provides an excellent framework to develop evidenced based designs, I found that this method can also be unruly if not precisely planned out. Researching across many disciplinary boundaries and workflows created unplanned challenges. If I had employed a more rigorous traditional scientific method, in the experimental validation phase, for example, the research might have proceeded in a more regimented and orderly process.

At the same time, the value that the Advanced Ceramics Assembly Workshop supported the research as a whole and specifically the development of the TACE system, cannot be overstated. The conference brought together architects, façade engineers, manufactures and academics into multidisciplinary teams with a focus on developing a prototype in a short amount of time. Having access to this group of diverse experts in one place at one time was invaluable to the iterative design of the prototypes and allowed design innovations to take place rapidly. A drawback was that the speed of the design outpaced the ability to conduct further experimental validation supporting the later simulations.

In retrospect, I would more precisely plan the process of moving between the scientific and the intuitive to develop a more rigorous and fruitful framework; one that could be more easily replicable to support future research, as well as serve as a framework for other research threads.

## 8.3 Final Remarks

---

The awareness that homeostasis should be an essential principle of architecture, at least with some theoretical clarity, emerged as two ideologies in the first half of the 20th Century from the works and writings of Frederick Kiesler and Siegfried Giedion; Correalism and Equipoise, respectively. Correalism and Equipoise are perhaps the first persistent theoretical conceptions of ecology and technology in architecture; both deal with dynamic balance and technology (Braham, 1999). While both theories

promote a universal approach to architecture, they each diverge significantly from one another, the former in terms of expression, and the latter in terms of performative response (Vollen, 2013).

Reimagining the building envelope as an energy transfer function was the result of a natural evolution of TABS and advances in technology, manufacturing and production in the construction industry. One speculative future for architecture is the merging of Kiesler and Giedion – that the performance and the expression are the same and that the design of the building envelope, and the meaning of the building as an object in the world, radiates the value of solving fundamental problems. The development of the TACE system may address this future as one example of the evolution of the role of the building envelope as part of a broader strategy to increase comfort and reduce energy expenditure in buildings.

## References

- Braham, W. (1999). Correalism and Equipoise: Observations on the Sustainable. *Architectural Research Quarterly*. 3. 57 - 64.
- Dyson, M. & Mandel, J. (August 2015). The Economics of Demand Flexibility: How “flexiwatts” create quantifiable value for customers and the grid. Retrieved from [http://www.rmi.org/electricity\\_demand\\_flexibility](http://www.rmi.org/electricity_demand_flexibility)
- Efficiency eludes the construction industry. (2017). Retrieved from <https://www.economist.com/business/2017/08/17/efficiency-eludes-the-construction-industry>
- Energy Information Agency State Electricity Profiles, (2015). Summary Statistics. Retrieved from <https://www.eia.gov/electricity/state/newyork/>
- Energy Information Agency Annual Energy Outlook. (2019). Table: Energy Prices by Sector and Source. Retrieved from <https://www.eia.gov/outlooks/aeo/data/browser/>
- Environmental Protection Agency (EPA). (2017). Greenhouse Gases Equivalencies Calculator - Calculations and References. Retrieved from [www.epa.gov/energy/greenhouse-gases-equivalencies-calculator-calculations-and-references](http://www.epa.gov/energy/greenhouse-gases-equivalencies-calculator-calculations-and-references).
- Maack, S., & Gunnarsson, A. (2016) The Physics of Architecture: Jón Kristinsson, pioneer in sustainable architecture. Retrieved from <https://hadesignmag.is/2016/02/28/edlisfraedi-arkitekturs-jon-kristinsson-frumkvodull-a-svidi-sjalbbaers-arkitekturs/?lang=en#menuopen>
- Maor, I., (2019). Evaluation of Factors Impacting EUI from High Performing Building Case Studies Retrieved from <http://www.hpomagazine.org/Case-Studies/Evaluation-of-Factors-Impacting-EUI/>
- Siegenthaler, J. (August 31st, 2004). A New Approach to Variable Flow Hydronic Systems. Retrieved from <https://www.pengineer.com/articles/84466-a-new-approach-to-variable-flow-hydronic-systems>
- Statewide Joint IOU Study of Permanent Load Shifting. (December 1, 2010). Retrieved from <https://www.ethree.com/wp-content/uploads/2017/02/PLS-Final-Report-with-Errata-3.30.11.pdf>
- Vollen, J. & Winn, K. (2013). Climate Camouflage: Advection Based Adaptive Building Envelopes. Paper presented at the 8th Energy Forum Conference Proceedings, Advanced Building Skins, Bressanone, Italy.
- Vollen, J. (2015). Environmental Parametrics: Prototyping Climate Camouflage and Adaptive Building Envelopes. *Time + Architecture*. Vol 2. Translated by Xiaofei Shen.

# Curriculum Vitae

---



## Jason Oliver Vollen

- 1971** Born in Brooklyn, New York, USA
- 1989-1994** Bachelor of Architecture  
The Cooper Union Institute for the Advancement of Science and Art
- 1994-1996** Master of Architecture II  
Cranbrook Academy of Art
- 1996** Teaching Assistant, Department of Architecture  
Cranbrook Academy of Art
- 1996-1998** Designer, Fabricator  
Cranbrook Architecture Office



- 1998-01      Visiting Assistant Professor, School of Architecture  
Mississippi State University
  
- 2002-2003    Principal, Private Practice  
Seville, Spain
  
- 2003          Assistant Adjunct Professor, School of Architecture and Design  
New York Institute of Technology
  
- 2003-08      Assistant Professor, College of Architecture, Planning and Landscape Architecture  
University of Arizona
  
- 2004-          Principal, Co-Founder  
Binary Design
  
- 2008-14      Associate Professor, School of Architecture (with Tenure)  
Rensselaer Polytechnic Institute
  
- 2009-10      Sponsored Visitor/Research Affiliate, Arizona Research Institute for Solar Energy  
The University of Arizona Department of Material Science and Engineering  
Department
  
- 2010-14      Associate Director  
Center for Architecture Science and Ecology
  
- 2012-14      Director, M. Arch. II Environmental Parametrics: Performance Design of the Built  
Ecology  
Rensselaer Polytechnic Institute
  
- 2014-2017    Principal, High Performance Buildings Group  
AECOM
  
- 2017-          Vice President, High Performance Buildings Practice Leader Americas  
AECOM
  
- 2018-          Director of Architecture, Northeast Region  
AECOM

## **Book Chapters**

---

Vollen, J. & Clifford, D. "Porous Boundaries" invited book chapter, *Matter: Material Processes in Architectural Production*, edited by Gail Peter Borden, Michael Meredith, Routledge Press, Taylor and Francis Group, 2011

Vollen, J. "Laboratory," invited essay and presentation for *Ineffable: Architecture, Computation and the Inexpressible* edited by Bradley Horn, Loft Publications. 2011

Vollen, J. "The Built Ecology," invited essay for *Material Evidence: New Designs for Architectural Practice* edited by Matt Burgermeister and Rhett Russo, NJIT, 2011

Lovell, J. "High Performance Masonry System", featured projects in *Building Envelopes: An Integrated Strategy*. Princeton Architectural Press. 2010

Klooster, T. "High Performance Masonry System" featured projects in *Smart Surfaces and their Application in Architecture and Design*. Birkhauser, 2009

Laver, J., Clifford, D. & Vollen, J. "Cacti, Termite Mounds and Performance Masonry Systems," *Design and Nature IV*, WIT Press. 2008

## **Journal Articles and Major Proceedings**

---

Menicovich, D., Lander, D., Vollen, J., Amitay, M., Letchford, C. & Dyson, A. "Improving aerodynamic performance of tall buildings using Fluid based Aerodynamic Modification," *Journal of Wind Engineering and Industrial Aerodynamics*, Volume 133, October, Pages 263-273, ISSN 0167-6105, 2014

Menicovich, D., Vollen, J., Amitay, M., Letchford, C., DeMauro, E., Rao, A. & Dyson, A. "A Different Approach to the Aerodynamic Performance of Tall Buildings," *CTBUH Journal*, Issue IV 2012

Dyson, A., Vollen, J. & Ngai, T. "BIM: Bioenergetic Information Modeling," *The Yale BIM Symposium*, 2011

Dyson, A., Ngai, T. & Vollen, J. "Active Modular Phytoremediation System," *SOM Journal*, Vol 6, 2010

Vollen, J. & Clifford, D. "The Peculiar Nodal Generator: a speculation," *International Journal of Architectural Computing*, Issue 2 Volume 4, pages 2-15, 2006

Van de Riet, K., Vollen, J. & Dyson, A. "Investigation Of Mangrove Compliant Structural Systems In Association With Human Coastal Development." (RE)building: Flood Architecture. ACSA Proceedings. March, 2010

Van de Riet, K., Berger, U., Dyson, A., Gowdy, J., Parks, S., Proffitt, E., Zeghal, M. & Vollen, J. "Multidisciplinary Modeling of Coupled Mangrove and Urban Ecosystems." Conference Proceedings of SubTropical Cities 2011, Florida Atlantic University, March 8-11, 2011.

Vollen, J., Winn, K., Laver, J. & Clifford, D. "Digital Production of High Performance Masonry Units," Material Matters: making architecture, ACSA West Fall Conference, with Winn, K., Jed Laver, and Clifford, D., , 2008

Vollen, J. "EcoCeramics" Deep Matter: The path to a meaningful and provocative architectural research, Association of the Collegiate School of Architecture (ACSA) Teachers Seminar, Bloomfield Hills, MI, 2008

Vollen, J., Laver, J., Winn, K. & Clifford, D. "Digital Material: Ecological Response in Parametric Modeling" Architecture in the Age of Digital Reproduction, ACSA West Central Fall Conference, 2008

Vollen, J. "Algorithmic Design: Past and Futures," Proceedings: the 94th Annual ACSA Conference, Salt Lake City, Utah, 2006

Vollen, J. "Digital and Analogue Modeling: Heliotrope," Proceedings: ACSA Central Regional Conference, Detroit, Michigan, 2005

## **Conference Proceedings**

Gindlesparger, M., Harrison, S., Shultz, J. & Vollen, J. (2018). Design Optimization Workflow for a Dynamic Mass Envelope System using Complementary Digital and Physical Testing Methods. ARCC Conference Repository. DOI: <https://doi.org/10.17831/rep:arcc%y560>

Dyson, A., Phillips, K., Shultz, J., Vollen, J., Gindlesparger, M. & Novelli, N. "High Efficiency Solar Building Envelopes for Integrated Delivery of Environmental Control Systems," in CLEO: 2014, OSA Technical Digest (online) (Optical Society of America, 2014) 2014

Aydogan, A., Dyson, A. Vollen J., Nyman, M. & Bird, J. "Building-Integrated Active Modular Phytoremediation System." Proceedings of The American Institute of Chemical Engineers (AIChE) Annual Meeting, San Francisco,CA, 32d, 2013

Vollen, J. & Winn, K. "Climate Camouflage: Advection-based adaptive building envelopes," Energy Forum: Advanced Building Skins, Conference Proceedings, Bressanone, Italy, 2013

Puerto, C., Dyson, A., Comodromos, D. & Vollen, J. "Exploring the Potential for Simultaneous Energy Production + Wave energy dissipation through applications of Architecturally-Integrated Reverse Electrodialysis [RED]," 2013 ACSA Fall Conference: Subtropical Cities, Fort Lauderdale, Florida, 2013

Wilson, N., Vollen, J., Menicovich, D., Rao, A. & Dyson, A. "Distributed Subtropical Coastline Emergency Energy: Generation using Building Integrated Wind Technology," 2013 ACSA Fall Conference: Subtropical Cities, Fort Lauderdale, Florida, 2013

Winn, K., Dyson, A. & Vollen, J. "Thermo-regulating Future City Envelopes with Multivalent Surfaces," 2013 ACSA Fall Conference: Subtropical Cities, Fort Lauderdale, Florida, 2013

Winn, K., Vollen, J. & Dyson, A. "ReFraming Architecture for Emerging Ecological and Computational Design Trends for the Built Ecology, " 2012 ACADIA Conference, San Francisco, California, 2012

Menicovich, D., Gallardo, D., Bevilaqua, R. & Vollen, J. "Generation and Integration of an Aerodynamic Performance Data Base within the Concept Design Phase of Tall Building," 2012 ACADIA Conference, San Francisco, California, 2012

Steinfeld, K., Vollen, J. & Dyson, A. "Graphic Evaluative Frameworks," 2010 ACADIA Conference, New York, NY, 2010

Domin, C., Clifford, D., Medlin, L. & Vollen, J. "Homeostasis and Perpetual Change," ECO Architecture: Harmonization between Architecture and Nature, WIT Press: Wessex, UK, 2010

Domin, C., Juarez, M., Medlin, L., Clifford, D. & Vollen, J. "Ecologically Sound: Public / Private Partnerships," ConnectED Proceedings, 2010

Clifford, D., & Vollen, J. "Smart and Sustainable Built Environments," SASBE 2009, Delft, The Netherlands, 2009

Vollen, J. "Local Complexities: A Tale of Two Rats," Assembling Architecture, Building Technology Educators Society 2009

Vollen, J. "The End Of The Line: An Elder Hostel For Water Colorists To Paint The Sunset," Translations: From Understanding to Misreading and Back Again, edited by Conrad Rathmann, Savannah College of Art and Design Press, 2007

Vollen, J. & Clifford, D.. "Digital Fabric: Generating Ceramic Catenary Networks," Expanding Bodies, Association for Computer Aided Design in Architecture (ACADIA) 2007, Halifax, Nova Scotia, 2007.

Vollen, J. & Folan, J. "Phenomenological Negotiations: Integrated Systems," Intersections: Design Education and Other Fields of Inquiry - 22nd National Conference on the Beginning Design Student, Iowa State University, Ames, Iowa, 2006

Vollen, J. & Clifford, D. "Digital Building Technology: Composite Paper Shells," Proceedings: SSTA 8th Annual Conference, Jurata, Poland, 2005

Vollen, J. & Clifford, D. "Parametric Shells: Experimental Methods of Form Generation," Proceedings: SSTA 8th Annual Conference, Jurata, Poland, 2005





20#05

# Countercurrent Heat Exchange Building Envelope Using Ceramic Components

**Jason Oliver Vollen**

Research and development in building envelope design have promoted the convergence of two system types, Thermo-Active Building Systems and Adaptive Building Envelopes, that re-conceptualize the envelope as a distributed energy transfer function that captures, transforms, stores, and even re-distributes energy resources.

The widespread deployment of Thermo-Active Building Systems as a building envelope will depend on several factors. These factors include the value of the design attributes that impact energy transfer in relation to the performance of the building envelope assembly and the return on investment that these attributes individually or in the aggregate can provide as a reduction in Energy Use Intensity. The research focus is on the design development, testing, and energy reduction potential of a Thermo-Active Building System as an adaptive countercurrent energy exchange envelope system using ceramic components: the Thermal Adaptive Ceramic Envelope.

**A+BE | Architecture and the Built Environment | TU Delft BK**